

NASA Conference Publication 3223

Computational Methods for Crashworthiness

(NASA-CP-3223) COMPUTATIONAL
METHODS FOR CRASHWORTHINESS (NASA)
261 p

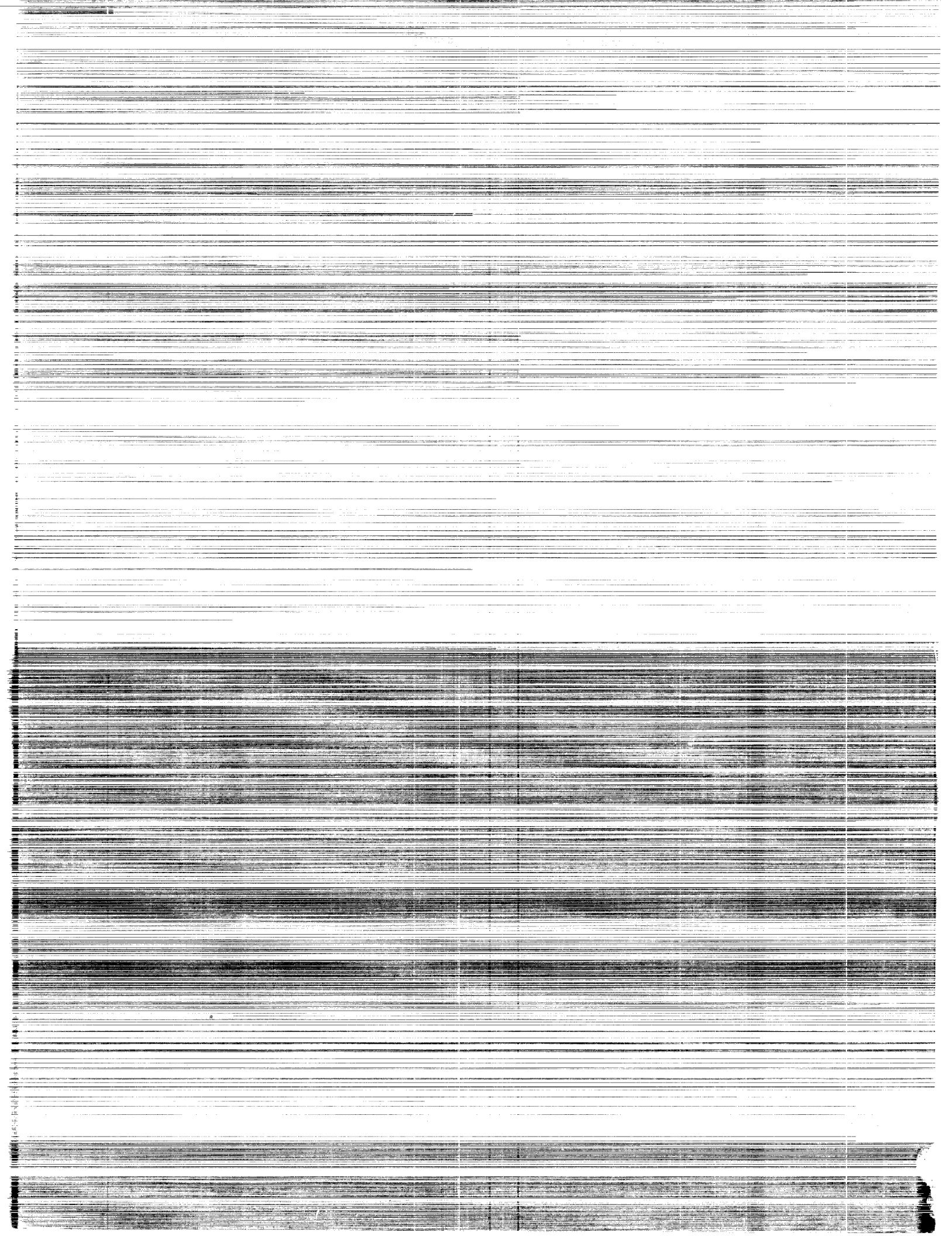
N94-19465
--THRU--
N94-19476
Unclas

H1/39 0187831

Available from
NASA

June 2, 1989

NASA



NASA Conference Publication 3223

Computational Methods for Crashworthiness

*Compiled by
Ahmed K. Noor
University of Virginia Center for
Computational Structures Technology
Hampton, Virginia*

Huey D. Carden
*Langley Research Center
Hampton, Virginia*

Proceedings of a workshop sponsored by the
National Aeronautics and Space Administration,
Washington, D.C., and the University of Virginia
Center for Computational Structures Technology,
Hampton, Virginia, and held at
Langley Research Center
Hampton, Virginia
September 2-3, 1992



National Aeronautics and
Space Administration
Office of Management
Scientific and Technical
Information Program

1993

PREFACE

This document contains the proceedings of the Workshop on Computational Methods for Crashworthiness held at NASA Langley Research Center, September 2-3, 1992. The workshop was jointly sponsored by the University of Virginia Center for Computational Structures Technology and NASA. Workshop attendees came from government agencies, the aerospace and automotive industries, energy laboratories, and universities. The objectives of the workshop were to assess the state-of-technology in the numerical simulation of crash and to provide guidelines for focused future research leading to an enhanced capability for numerical crash simulation.

Certain materials and products are identified in this publication in order to specify adequately the materials and products that were investigated in the research effort. In no case does such identification imply recommendation or endorsement of products by NASA, nor does it imply that the materials and products are the only ones or the best ones available for the purpose. In many cases equivalent materials and products are available and would probably produce equivalent results.

Ahmed K. Noor
University of Virginia Center for Computational Structures Technology
Hampton, Virginia

Huey D. Carden
NASA Langley Research Center
Hampton, Virginia

PRECEDING PAGE BLANK NOT FILMED

ii

CONTENTS

PREFACE	iii
ATTENDEES	vii
INTRODUCTION	xi
HIGHLIGHTS OF THE WORKSHOP	1
Ahmed K. Noor	
ADAPTIVE METHODS FOR NONLINEAR STRUCTURAL DYNAMICS AND CRASHWORTHINESS ANALYSIS	7-1
Ted Belytschko	
COMPOSITE IMPACT DYNAMICS RESEARCH AT NASA LaRC -- A REVIEW	37-2
Huey D. Carden	
IMPACT ANALYSIS OF COMPOSITE AIRCRAFT STRUCTURES	65-3
Allan B. Pifko and Alan S. Kushner	
DEVELOPMENT AND USE OF COMPUTATIONAL TECHNIQUES IN ARMY AVIATION R&D PROGRAMS FOR CRASH RESISTANT HELICOPTER TECHNOLOGY	95-4
LeRoy T. Burrows	
EXPLICIT SOLUTION TECHNIQUES FOR IMPACT WITH CONTACT CONSTRAINTS	105-5
Robert E. McCarty	
NUMERICAL SIMULATION OF VEHICLE CRASHWORTHINESS AND OCCUPANT PROTECTION	125-6
Nripen K. Saha	
DIRECTIONS FOR COMPUTATIONAL MECHANICS IN AUTOMOTIVE CRASHWORTHINESS	141-7
James A. Bennett and T. B. Khalil	
EFFICIENCY AND BIOFIDELITY OF OCCUPANT SIMULATORS	155-8
Walter D. Pilkey	
CURRENT CAPABILITIES FOR SIMULATING THE EXTREME DISTORTION OF THIN STRUCTURES SUBJECTED TO SEVERE IMPACTS	165-9
Samuel W. Key	
CRASH DYNAMICS WITH DYNA3D: CAPABILITIES AND RESEARCH DIRECTIONS	185-10
Robert G. Whirley and Bruce E. Engelmann	
TRANSIENT DYNAMICS CAPABILITY AT SANDIA NATIONAL LABORATORIES	207-11
S. W. Attaway, J. H. Biffle, G. D. Sjaardema, M. W. Heinstein and L. A. Schoof	
LIST OF BOOKS, MONOGRAPHS, SURVEY PAPERS AND REPORTS ON COMPUTATIONAL TECHNIQUES FOR SIMULATING CRASH	251
Howard S. Levine and Ahmed K. Noor	

PRECEDING PAGE BLANK NOT FILMED

Attendees

Mr. Mark Anstey
Micro Craft, Inc.
3130 North Armistead Avenue
Hampton, VA 23666
(804) 865-7760; Fax (804) 865-7487

Dr. Steven W. Attaway
Division 1425
Sandia National Laboratory
P.O. Box 5800
Albuquerque, NM 87185
(505) 855-9288; Fax (505) 844-9297

Dr. Roshdy Barsoum
Code 1132SM
Office of Naval Research
800 North Quincy Street
Arlington, VA 22217-5000
(703) 696-4306; Fax (703) 696-0934

Prof. Ted Belytschko
Department of Civil Engineering
Northwestern University
Evanston, IL 60208
(708) 491-7270; Fax (708) 491-4133

Dr. James A. Bennett
Engineering Mechanics Department
General Motors Research Laboratories
Warren, MI 48090
(313) 986-2031; Fax (313) 986-0446

Dr. Johnny H. Biffle
Applied Mechanics III, Div. 1523
Sandia National Laboratory
P.O. Box 5800
Albuquerque, NM 87185
(505) 844-5385; Fax (505) 844-9297

Dr. Charles P. Blankenship
Mail Stop 118
NASA Langley Research Center
Hampton, VA 23681
(804) 864-6005; Fax (804) 864-8088

Dr. Richard L. Boitnott
Mail Stop 495
NASA Langley Research Center
Hampton, VA 23681
(804) 864-4161; Fax (804) 864-8547

Dr. Akif Bolukbasi
Bldg. 530, MS B337
McDonnell Douglas Helicopter Company
500 East McDowell Road
Mesa, AZ 85205
(602) 891-5111; Fax (602) 891-7671

Mr. James R. Branstetter
Mail Stop 250
FAA Engineering Field Office
NASA Langley Research Center
Hampton, VA 23681
(804) 864-6396

Mr. LeRoy T. Burrows
Aviation Applied Technology Directorate
Attn: SAVRT-TY-ASV
Fort Eustis, VA 23604-5577
(804) 878-5875; Fax (804) 878-3108

Mr. Huey D. Carden
Mail Stop 495
NASA Langley Research Center
Hampton, VA 23681
(804) 864-4151; Fax (804) 864-8090

Mr. Frank Chang
The MacNeal-Schwendler Corp.
7529 Standish Place, Suite 105
Rockville, MD 20855
(301) 424-9590; Fax (301) 424-9589

Mr. Charles W. Clarke
MS S314A2
Sikorsky Aircraft
6900 Main Street
Stratford, CT 06601
(203) 386-3515; Fax (203) 386-3717

Mr. Paul Conley
Department of Mechanical and
Aerospace Engineering
University of Virginia
Charlottesville, VA 22903
(804) 924-3291; Fax (804) 982-2037

Mr. James D. Cronkhite
MS 81/14
Bell Helicopter Company
Box 482
Fort Worth, TX 76101
(817) 280-5597; Fax (817) 280-8688

Mr. Barry Dombek
LME, Inc.
444 Jacksonville Road
Warminster, PA 18974
(215) 674-5881; Fax (215) 674-5883

Dr. Wolf Elber
Aerostructures Directorate
Mail Stop 266
NASA Langley Research Center
Hampton, VA 23681
(804) 864-3957; Fax (804) 864-3970

Dr. Edwin L. Fasanella
Mail Stop 495
NASA Langley Research Center
Hampton, VA 23681
(804) 864-4159; Fax (804) 864-9601

Mr. Dave Fenton
Department of Mechanical and
Aerospace Engineering
University of Virginia
Charlottesville, VA 22903
(804) 924-3291; Fax (804) 982-2037

Mr. Howard Fleisher
Aviation Division
Galaxy Scientific Corporation
71 Cantillion Blvd., Suite 100
Mays Landing, NJ 08330
(609) 645-0900; Fax (609) 645-2881

Mr. David C. Fleming
Department of Aerospace Engineering
University of Maryland
College Park, MD 20742
(301) 405-1931; Fax (301) 314-9001

Mr. James C. Garman
MS Z101A
Sikorsky Aircraft
6900 Main Street
Stratford, CT 06601
(203) 383-3491; Fax (203) 383-3492

Dr. Gerald L. Goudreau
L-22, Bldg. 131, Rm 2153
Lawrence Livermore National Laboratory
Livermore, CA 94550
(510) 422-8671; Fax (510) 422-2085

Dr. O. Hayden Griffin
Department of Engineering Science
and Mechanics
Virginia Polytechnic Institute
and State University
Blacksburg, VA 24061
(703) 231-5018; Fax (703) 231-4574

Dr. Steven Hooper
Department of Aerospace Engineering
Wichita State University
Box 44
Wichita, KS 67208
(316) 689-3410; Fax (316) 689-3853

Dr. Jerrold M. Housner
Mail Stop 240
NASA Langley Research Center
Hampton, VA 23681
(804) 864-2906; Fax (804) 864-8318

Dr. Karen Jackson
Mail Stop 495
NASA Langley Research Center
Hampton, VA 23681
(804) 864-4147; Fax (804) 864-8547

Dr. Eric Johnson
Department of Aerospace and
Ocean Engineering
Virginia Polytechnic Institute
and State University
Blacksburg, VA 24061
(703) 231-6611; Fax (703) 231-9632

Ms. Lisa E. Jones
Mail Stop 495
NASA Langley Research Center
Hampton, VA 23681
(804) 864-4148; Fax (804) 864-8547

Dr. Rembert F. Jones, Jr.
David Taylor Naval Ship Research
and Development Center
Code 1720
Bethesda, MD 20084
(301) 227-1534; Fax (301) 227-1230

Mr. Sotiris Kellas
Mail Stop 495
Lockheed Engineering & Science Corp.
NASA Langley Research Center
Hampton, VA 23681
(804) 864-4150

Dr. Samuel W. Key
Key Associates
1851 Tramway Terrace Loop NE
Suite 410
Albuquerque, NM 87122
(505) 292-1971; Fax (505) 292-1971

Mr. Mike Kleinberger
NHTSA
Department of Transportation
400 7th Street, S.W.
Washington, D.C. 20590
(202) 366-4726; Fax (202) 366-5670

Dr. Alan S. Kushner
Department of Mechanical Engineering
State University of New York
at Stony Brook
Stony Brook, NY 11794
(516) 632-8493; Fax (516) 632-8544

Mr. James Mack
Mail Stop 918
Micro Craft, Inc.
3130 North Armistead Avenue
Hampton, VA 23666
(804) 865-7760; Fax (804) 865-7487

Mr. Robert E. McCarty
Aircrew Enclosures Group
WL/FIBRE, Bldg. 255, Area B
Wright Patterson Air Force Base, OH 45433
(513) 255-5060; Fax (513) 476-4275

Dr. John Morton
Department of Engineering Science
and Mechanics
Virginia Polytechnic Institute
and State University
Blacksburg, VA 24061
(703) 231-6051; Fax (703) 231-4574

Mr. Mark Muller
Aviation Division
Galaxy Scientific Corporation
71 Cantillion Blvd., Suite 100
Mays Landing, NJ 08330
(609) 645-0900; Fax (609) 645-2881

Prof. Ahmed K. Noor
Center for Computational Structures Technology
Mail Stop 210
NASA Langley Research Center
Hampton, VA 23681
(804) 864-1978; Fax (804) 864-8089

Dr. Allan B. Pifko
Mail Stop A08-35
Research Department
Grumman Corporation
Bethpage, NY 11714
(516) 575-1965; Fax (516) 575-7716

Prof. Walter D. Pilkey
Department of Mechanical and
Aerospace Engineering
University of Virginia
Charlottesville, VA 22903
(804) 924-3291; Fax (804) 982-2037

Ms. Martha Robinson
Mail Stop 495
NASA Langley Research Center
Hampton, VA 23681
(804) 864-4149; Fax (804) 864-8547

Dr. Nripen K. Saha
MD-4, ECC
Ford Motor Company
Dearborn, MI 48121
(313) 845-9341; Fax (313) 390-4565

Mr. Mike Schultz
Mail Code 6034
Naval Air Development Center
Warminster, PA 18974
(216) 441-2469

Dr. John A. Tanner
Mail Stop 497
NASA Langley Research Center
Hampton, VA 23681
(804) 864-1305; Fax (804) 864-8090

Dr. Robert K. Thomas
Org. 1562
Sandia National Laboratories
P.O. Box 5800
Albuquerque, NM 87185
(505) 844-7450; Fax (505) 844-9297

Ms. Danniella Thompson
Department of Engineering Science
and Mechanics
Virginia Polytechnic Institute
and State University
Blacksburg, VA 24061
(703) 231-7428; Fax (703) 231-4574

Mr. Joe Tilson
AFSA/SESO
Norton Air Force Base, CA 92409
(714) 382-6844; Fax (714) 382-2777

Dr. Anthony J. Vizzini
Department of Aerospace Engineering
University of Maryland
College Park, MD 20742
(301) 405-2376; Fax (301) 314-9001

Dr. Robert G. Whirley
Methods Development Group
Lawrence Livermore National Laboratory
P.O. Box 808
Livermore, CA 94550
(510) 423-0907; Fax (510) 422-2085

Dr. Todd Wieland
Department of Engineering Science
and Mechanics
Virginia Polytechnic Institute
and State University
Blacksburg, VA 24061
(703) 231-4655; Fax (703) 231-4574

Mr. Tony Wilson
Mail Code ACD 210
FAA Technical Center
Atlantic City International Airport, NJ 08405
(609) 484-4500; Fax (609) 484-4005

Mr. Marshall Woodson
Department of Aerospace and Ocean Engineering
Virginia Polytechnic Institute
and State University
Blacksburg, VA 24061
(703) 231-6611; Fax (703) 231-9632

INTRODUCTION

The numerical simulation of the nonlinear response of aircraft structures and other components subjected to large impact loads has been the focus of intense efforts because of the pressing needs for collision protection, or crashworthiness, of transportation vehicles (aircraft, cars, trains and ships), and nuclear reactors and containment vessels. Several software systems are currently available for impact analysis of structures (e.g., KRASH, DYNA, MSC/DYTRAN, NIKE, DYCAST, SUPERWHAMS, PAMCRASH, PRONTO and McALOG/RADIOSS).

Crashworthiness is already a design requirement for many vehicles and is likely to become more important with increasing demands for safety considerations in structural design. Major advances are needed in our analysis capabilities for predicting the structural response of vehicles subjected to impact loads and the subsequent response of human occupants. To this end, there are a number of technology needs and related tasks that must be addressed by the research community to enhance the state-of-the-art in computational methods for crashworthiness.

The joint NASA/University of Virginia workshop held at NASA Langley Research Center, September 2-3, 1992 focused on the status of computational methods for crashworthiness and the current and future needs for further development of this technology. The list of the pacing items given in this introduction was compiled from a number of participants. Research efforts to address these needs can guide the design of future transportation vehicles in the following two ways: 1) by providing better understanding of the phenomena associated with crash, thereby identifying the desirable energy-absorbing design attributes; and 2) by verifying and certifying crashworthy designs, and making low-cost modifications during the design process.

COMPUTATIONAL NEEDS FOR CRASHWORTHINESS

The technology needs identified by the participants can be grouped into the following five major headings: 1) understanding the physical phenomena associated with crash; 2) high-fidelity modeling of the vehicle and the occupant during crash; 3) efficient computational strategies; 4) test methods, measurement techniques and scaling laws; and 5) validation of numerical simulations. For each of the aforementioned items, attempts should be made to exploit the major characteristics

of high-performance computing technologies, as well as the future computing environment. The five primary technology needs and related tasks are described subsequently.

1. Understanding the Physical Phenomena Associated with Crash

This includes understanding a) the mechanics of large dynamic deformations of structures, including the effects of frictional contact; b) the effects of inertia forces and of material strain-rate sensitivity on the dynamic response; and c) damage initiation and progression during crash. For the occupant, the factors that can be correlated with the level of injury or death (e.g., dynamic response index, head injury criteria, force in the lumbar spinal region) need to be identified. The modeling details required to capture the different phenomena associated with the structural response during crash need to be identified.

2. High-Fidelity Modeling of Vehicle and Occupant

The reliability of the predictions of the response of the structure and occupant during crash is critically dependent on: a) the accurate characterization and modeling of material behavior; b) high-fidelity modeling of the critical details of the vehicle and occupant (e.g., seat, fasteners, and the human anatomy); and c) modeling of the frictional contact between the vehicle and the impactor, as well as between the different parts of the vehicle, including the need for accurate material constitutive models and properties for foam, padding, and textile composites, especially the strain rate sensitivities, for modeling of the seat/occupant interaction.

3. Efficient Computational Strategies

The effective use of numerical simulations for predicting the vehicle response during crash requires strategies for treating phenomena occurring at disparate spatial and time scales, using reasonable computer resources. The strategies are to be based on using hierarchical (multiple) mathematical models in different regions of the vehicle to take advantage of the efficiencies gained by matching the model to the expected response in each region. To achieve the full potential of hierarchical modeling there should be minimum reliance on *a priori* assumptions about the response. This is accomplished by adding adaptivity to the strategy. The key tasks of the research in this area are the following:

- a) Rational selection of a set of nested mathematical models for different regions of the vehicle and discretization techniques for use in conjunction with the mathematical models. The mathematical models should include damage models.
- b) Efficient numerical algorithms for simulating frictional contact and other local phenomena, such as stiffness reduction due to damage and redistribution of load paths in damaged components.
- c) Automated (or semiautomated) coupling of different mathematical/discrete models.
- d) Sensitivity analysis to assess the sensitivity of crash response to each of the material and geometric parameters used in the computational model.
- e) Criteria for adaptive refinement (or derefinement) of the mathematical and discrete models.
- f) Stable and efficient iterative procedures and numerical algorithms for use in conjunction with adaptive model refinement.

4. Test Methods, Measuring Techniques and Scaling Laws

The effective coupling of numerical simulations with experiments requires a high degree of interaction between the computational analysts and the experimentalists. This is done at three different levels, namely: 1) laboratory tests on small specimens to obtain material data; 2) component tests to verify computational models and to determine empirical structural properties which can be used in hybrid experimental/numerical models; and 3) full-scale (or scale model) tests to validate the computational model and assess the need for model improvements.

New test methods and measurement techniques are needed to study progressive failure, as well as soil and water impact. The influence of specimen size or scale factor on structural response is not well understood. Thus, testing of geometrically similar sub-scale models is not possible, until the scaling laws governing the phenomenon are understood. In particular, scaling laws are needed which account for the material behavior including elastic properties, failure initiation and ultimate strength, structural and topological details, as well as the loading characteristics.

5. Validation of Numerical Simulations

In addition to validating the numerical simulations by component and full-scale tests, a number of carefully selected benchmark tests are needed for assessing new computational strategies and numerical algorithms. These benchmark tests would provide a measure of confidence in new codes, or added functional capabilities to existing codes. They could also serve as a basis of code comparisons for efficiency and accuracy for modeling of impact problems involving large structural deformations in short time durations.

RELATED TASKS

In addition to the aforementioned technology needs, some related tasks need to be addressed before numerical crash simulations can have a significant impact on the design process. These are: 1) development of software for automated (or semiautomated) model (and mesh) generation; 2) pre- and post-processing software for efficient input and reduction of numerical simulation data; 3) use of advanced visualization technology; and 4) adaptation of AI tools (knowledge-based/expert systems and neural networks) to crash simulation systems.

Highlights of the Workshop

Ahmed K. Noor
Center for Computational Structures Technology
University of Virginia

Objectives and Format of Workshop

The numerical simulation of the nonlinear response of structures subjected to large impact loads has been the focus of intense efforts in recent years. Despite these efforts, major advances are needed in various areas of the technology before numerical simulations can be routinely used to satisfy crashworthiness design requirements of transportation vehicles. The objectives of the present workshop are (Fig. 1): to assess the state-of-technology of computational methods for crashworthiness; and to identify current and future needs for further development of the technology.

The workshop includes presentations and two panels. The presentations are included in the proceedings to illuminate some of the diverse issues, and to provide fresh ideas for future research and development.

Objectives

- To assess the state-of-technology in the numerical simulation of crash
- To identify future directions of research

Format

- Presentations
- Panels
 - Panel 1 - *Computational Needs for the Accurate Simulation of Crash*. Moderator: Ed Fasanella
 - Panel 2 - *Experimental Needs and the Coupling Between Experiments and Numerical Simulations*. Moderator: Huey Carden
- Proceedings

Figure 1

PRECEDING PAGE BLANK NOT FILMED

2

Assessment of the State-of-Technology

The first aspect of assessing the state-of-technology is to assess our understanding of the physical phenomena associated with crash. Some of the issues that affect these physical phenomena are listed in Fig. 2. These are: mechanics of large, dynamic deformations; material-level damage mechanisms, damage growth and subsequent structural failure; material strain-rate sensitivity; contact/impact conditions and friction modeling; energy absorbing characteristics of structures; and the influence of specimen size or scale factor on structural response.

Understanding of Physical Phenomena Associated with Crash

- Mechanics of large dynamic deformations
- Damage and failure mechanisms
- Effect of material strain-rate sensitivity
- Effect of inertia forces
- Contact/impact conditions
- Friction modeling
- Energy absorbing characteristics of structures
- Scaling laws

Figure 2

Assessment of the State-of-Technology (Cont'd.)

Current Capabilities

The second aspect of assessment of technology is that of current capabilities for numerical simulation of crash (Fig. 3). These capabilities include computational material models and damage mechanisms, modeling of structural details such as joints, seats, fasteners and occupant; efficiency of currently-used computational strategies for handling spatial discretization and temporal integration, frictional contact/impact conditions, hierarchical, global-local and adaptive refinement facilities; and assessment of software systems currently used for impact analysis of structures.

- ***Computational Material Models***

Constitutive models and material data, friction models, damage mechanisms and failure models

- ***Level of Details***

Modeling of the structure, seat, fasteners and occupant

- ***Efficiency of Computational Strategies***

- Spatial discretization and temporal integration
- Hierarchical, global-local, multilevel and adaptive strategies - interfaces between models
- Contact/impact algorithms

- ***Current Software Systems***

KRASH, MSC/DYTRAN, SUPER WHAMS, WRECKER, DYCAST, DYNA, NIKE, PRONTO, PAM CRASH, McALOG/RADIOSS

Figure 3

Future Directions of Research

Three factors should be taken into account in identifying future directions for research (Fig. 4):

- 1) characteristics of future transportation vehicles and their implications on design requirements for crashworthiness;
- 2) future computing environment and computing paradigm; and
- 3) recent and future developments in other fields of computational technology, which can be adapted to numerical simulation of crash.

Two of the important research tasks are:

- 1) validation of numerical simulations and selection of benchmark tests for assessing new computational strategies and numerical algorithms. The standardized tests would provide a measure of confidence in added functional capabilities to existing codes, or in new codes; and
- 2) treatment of uncertainties in material properties, geometry, boundary conditions, and operational environment through probabilistic analysis, stochastic modeling and sensitivity analysis.

- *Characteristics of future vehicles* and their implications on design requirements for crashworthiness
- *Impact of emerging and future computing environment* (high-performance computers, multimedia workstations, advanced visualization technology)
- *Impact of developments in other fields* of computational technology (e.g., CFD, computational mathematics)
- *Validation of numerical simulations* and effective coupling with experiments (Benchmarks)
- *Treatment of uncertainties* in material properties, geometry, boundary conditions, spatial and temporal distribution of loading and operational environment (probabilistic analysis, stochastic modeling and sensitivity analysis)

Figure 4

57-39
187032
p-28

N 9 4 - 1 9 4 6 6

Adaptive Methods for Nonlinear Structural Dynamics and Crashworthiness Analysis

Ted Belytschko
Northwestern University

ADAPTIVE METHODS FOR NONLINEAR STRUCTURAL DYNAMICS AND CRASHWORTHINESS ANALYSIS

Ted Belytschko
Northwestern University
Evanston, Illinois

ABSTRACT

The objective of this talk is to describe three research thrusts in crashworthiness analysis:

- 1) adaptivity
- 2) mixed time integration, or subcycling, in which different timesteps are used for different parts of the mesh in explicit methods
- 3) methods for contact-impact which are highly vectorizable.

The techniques are being developed to improve the accuracy of calculations, ease-of-use of crashworthiness programs and the speed of calculations. The latter is still of importance because crashworthiness calculations are often made with models of 20,000 to 50,000 elements using explicit time integration and require on the order of 20 to 100 hours on current supercomputers.

The methodologies will be briefly reviewed and then some example calculations employing these methods will be described. The methods are also of value to other nonlinear transient computations.

PRECEDING PAGE BLANK NOT FILMED

OUTLINE

- Adaptive mesh procedures in nonlinear analysis: why, how, and what is the status
- Subcycling (mixed time integration)
- New highly vectorizable methods for contact impact which are well suited to adaptive methods

Figure 1

PREDICTION

The 1990's will be the decade of *adaptivity*.

adaptive mesh refinement

adaptive targeting

adaptive organization objectives

Figure 2

PREDICTION

There are three types of adaptivity, which are known by the letters r, h, and p. These letters are mnemonic letters and refer to how the refinement is achieved. In r methods the nodes are relocated. In h methods, refinement is achieved by reducing the element size h. In p methods, refinement is achieved by increasing the order p of the element interpolance.

TYPE OF MESH ADAPTIVITY

r — method

↙ relocate nodes

h — method

↙ adapt element size h

p — method

↙ adapt order p of element interpolants

Figure 3

ADAPTIVITY IN NONLINEAR FEM

Adaptive methods are particularly useful in nonlinear problems such as crashworthiness because nonlinear response is often characterized by localization. In the areas of localized response more refinement is needed. When standard method is used, the user of the program must refine the mesh where he anticipates this localized deformation. Therefore, different meshes must be developed for different loadings. For example, in car crash, different meshes must be developed for frontal and rear impact, side impact, and overturning. This can be quite expensive from the viewpoint of manpower.

Why are adaptive methods particularly important in nonlinear problems?

Modes of failure of structures

- i. buckling, particularly with formation of hingelines
- ii. localization
- iii. fracture

All of these involve local phenomena whose location cannot be determined at the outset of a simulation.

Figure 4

COMMENTS ON ADAPTIVITY FOR SHELL AND CRASHWORTHINESS PROBLEMS

In comparing the different types of adaptivity for nonlinear structural dynamics problems such as crashworthiness, the following advantages, which are marked by a plus sign (+), and disadvantages which are marked by a minus sign (-), can be attributed to the various types of methods. From this study we concluded that the h-method was the most suitable method for adaptivity in crashworthiness.

r — method

- large elements cannot represent shape of shell
- + most accuracy with given NDOF compared to h
- history diffusion
- elements become distorted - decreases accuracy
- + easiest data structure

p — method

- awkward in nonlinear dynamics; no good lumped mass
- + easy data structure

h — method

- + relatively effective
- + no distortion of elements
- moderately complex data structure

Figure 5

TYPES OF ERROR INDICATORS

Error indicators are an important ingredient in adaptive methods since they are to guide the refinement of the mesh. Error indicators are classified by Oden in the following classes: residual, interpolation, and post-processing. In the work we are doing, we are using projection error criteria, a post-processing type, because they are very easy to implement and are quite effective for low-order elements.

1. Residual: Compute residual in governing equations and use its norm or use it to drive an element or local enriched solution.
 - a) Explicit: Evaluate a norm of the residual.
 - b) Implicit: Use residual to drive a local or element error equation.
2. Interpolation Methods: Estimate magnitude of derivatives of higher-order than contained in finite element space.
3. Projection (postprocessing) Methods: Obtain a smoothed solution and compare to finite element solution; sometimes called L2 projection methods.

Figure 6

ADAPTIVE SCHEMES FOR TRANSIENT AND NONLINEAR PROBLEMS

based on constant resource approach

1. Advance the solution n time steps
2. Compute element error indicators θ_e
3. Sort θ_e
4. Fission elements with $\theta_e > \text{tol}^{\text{fission}}$
Fuse elements with $\theta_e < \text{tol}^{\text{fusion}}$
5. Repeat the last n time steps with new mesh (optional)
6. go to 1

Note: If n is too small or $\text{tol}^{\text{fission}}$ too close to $\text{tol}^{\text{fusion}}$, we encounter "churning" which degrades accuracy. Our recent experience shows 5 is quite important.

Figure 7

REMARKS ON H-ADAPTIVITY

Constraints (or slave nodes in explicit methods) must be introduced at nodes where a large element has two or more neighbors on one side to enforce compatibility; easy in vector methods, awkward in matrix methods.

Usually a group of contiguous elements should be fissioned simultaneously because fissioning a single element does not provide much enrichment; only one new free node.

In wave propagation problems, change in element size can cause spurious reflections.

Usually mesh gradation is limited to 1-irregular meshes: large element cannot have more than 2 small neighbors on any side; see Devloo, Oden and Strouboulis (1987).

Data structure with fission and fusion is complex, particularly for real engineering meshes; see Belytschko, Wong and Plaskacz, *Computers and Structures*, 33(4-5), 1989, pp. 1307-1323.

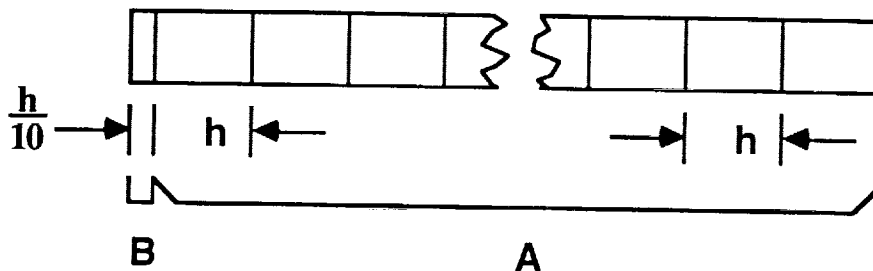
Figure 8

MIXED TIME INTEGRATION

In h-adaptive meshes, large variety of element sizes are found. When explicit methods are used of such meshes, the timestep is reduced dramatically by the presence of small elements. Therefore methods called mixed time integration (or subcycling) are being used.

Motivation : in explicit integration with same Δt over entire mesh, stiffest element sets Δt . also called subcycling, explicit-explicit partitions;

example



$$\Delta t_{\text{crit}} = \min \left(\frac{L}{c} \right) \quad c = \text{wave speed}$$

$$\text{for A} \quad \Delta t_{\text{crit}} = \frac{h}{c}$$

$$\text{for } A \cup B \quad \Delta t_{\text{crit}} = \frac{h}{10c}$$

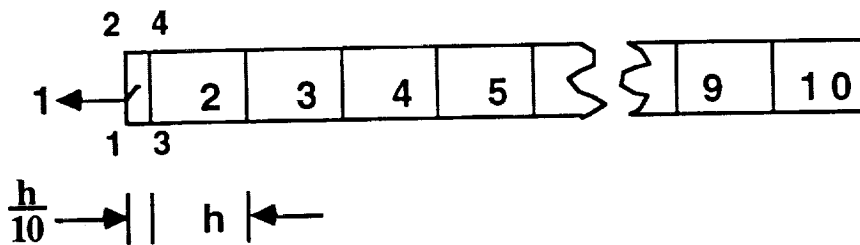
so $A \cup B$ is 10× as expensive as A

Figure 9

Mixed Time Integration

Integrate each element or subdomain with Δt_{crit} using an interface treatment that preserves stability + consistency.

In example



integrate element 1 and nodes 1 to 4 with

$$\Delta t = \frac{h}{10c}$$

elements 2 to 10 and remaining nodes with

$$\Delta t = \frac{h}{c}$$

cost savings: $\sim 90\%$

In adaptive methods, large range of stable time steps is unavoidable, so subcycling is crucial for efficiency.

Figure 10

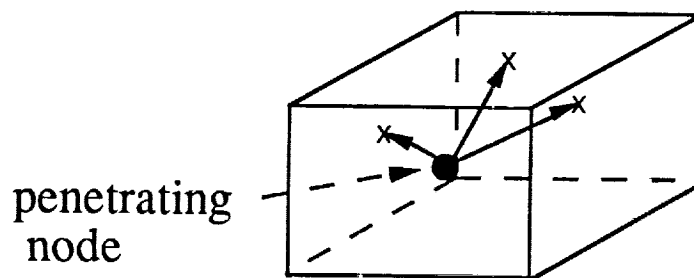
CONTACT-IMPACT

The modeling of contact-impact is very important in the simulation of crashworthiness. However, contact-impact algorithms often require more than fifty percent of the running time of a crashworthiness code because they are not easily vectorized. Therefore we have developed a pinball algorithm which is far more highly vectorizable.

Contact-impact is an important phenomenon in crash analysis, e.g.,

1. engine impact with body, fire wall
2. wheel impact with inner fender
3. contact of collapsing surfaces

Most contact-impact algorithms require many different branches.



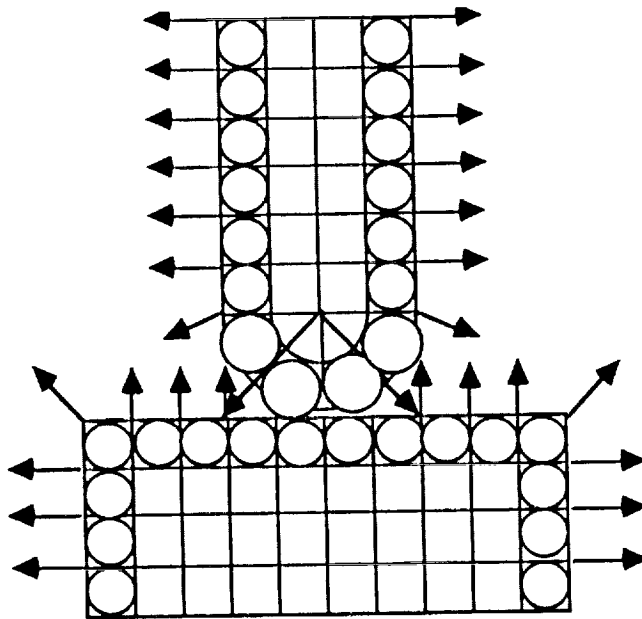
The branch of the algorithm which is activated depends on which surface is penetrated; there are special branches for edges, etc.

Figure 11

PINBALL PENALTY ALGORITHM

T. Belytschko and M. O. Neal, *International Journal for Numerical Methods in Engineering*, 31, 1991, pp. 547-572.

Interpenetration and interpenetration rate \dot{g} are computed on pinballs inserted in elements.



Enforces contact-impact conditions on spheres embedded in elements.

As $h \rightarrow 0$, impenetrability is enforced.

Algorithm is simple and highly vectorizable.

Figure 12

Salient Features of Algorithm

Radius of pinball is determined by equivoluminal expression

$$R^3 = \frac{3V_e}{4\pi}$$

Pinballs are classed by body; for single-surface slideline, smaller R needed.

Interpenetration has occurred when

$$d_{ij} < R_i + R_j$$

$$g = d_{ij}$$

Pinball forces are equally transferred to all nodes of associated element (a surface node option available).

The pinball method automatically places pinballs on outside elements by using assembled surface normal algorithm.

Figure 13

EXAMPLES OF NONLINEAR ADAPTIVE COMPUTATIONS

Nonlinear, transient computations with an explicit nonlinear finite element program WHAMS using h-adaptivity and pinball for contact impact; see Belytschko and Yeh (1992).

An L2 projection on the strain invariants was used to calculate an error estimate.

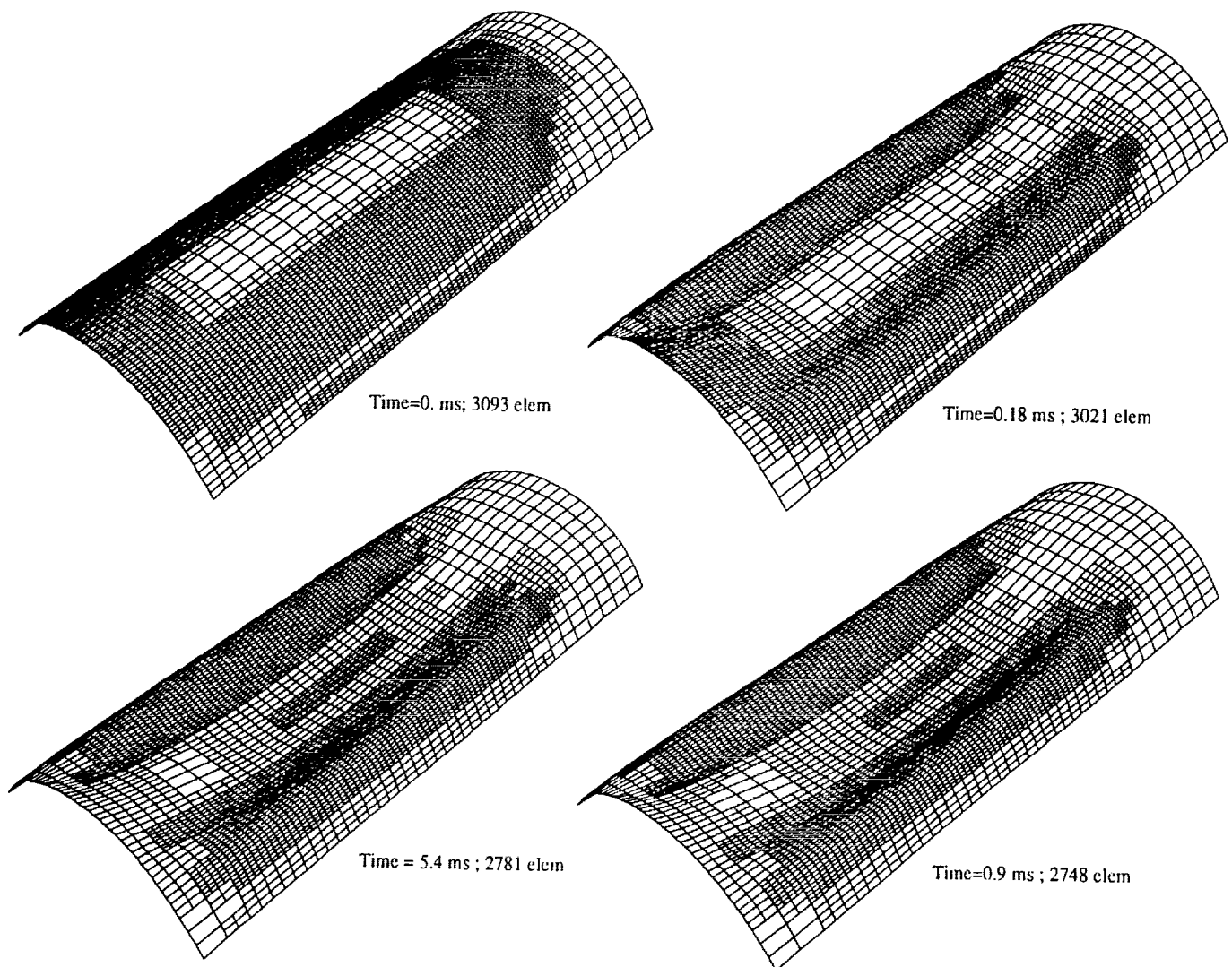
A commercial version of this program is available from:

KBS2, Inc.
455 Frontage Road
Burr Ridge, IL 60521
(708) 850-9444
Fax (708) 850-9455

Figure 14

TWO-LEVEL ADAPTIVE MESH OF CYLINDRICAL PANEL

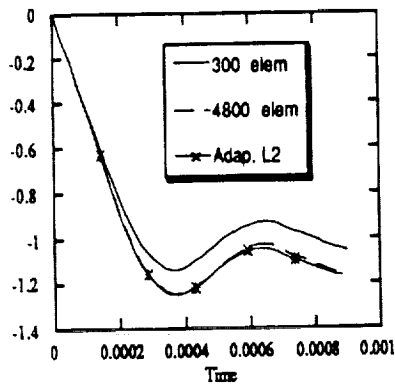
This shows an h-adaptive solution of a cylindrical panel which is impulsively loaded. Notice that the elements are refined along the side and at the support, where there is severe plastic bending deformation, and hinge lines consequently form.



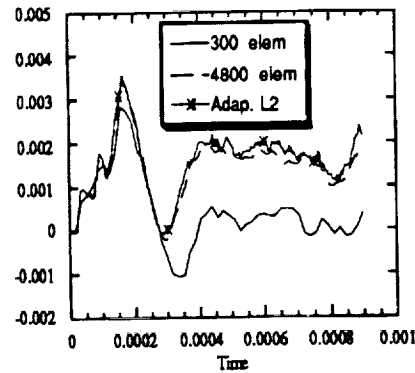
Two-level adaptive mesh of cylindrical panel.

Figure 15

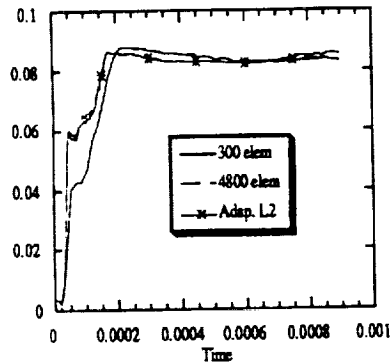
This figure shows a comparison between solutions obtained by h-adaptivity and those obtained using a very fine mesh and a coarse mesh. As can be seen, the adaptive solution compares well to the fine mesh solution. The differences in the displacements obtained by the coarse mesh and the fine mesh are not large, but for some of the stresses and strains, significant improvement is obtained by the use of adaptivity.



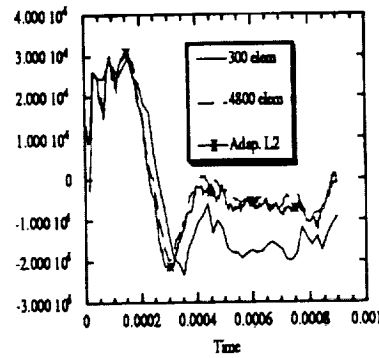
Displacement of point A
in cylindrical panel (MAXLEV=2)



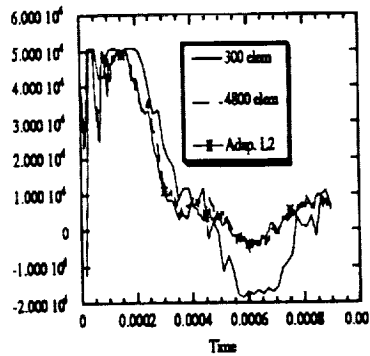
Strain Exx of element B
in cylindrical panel (MAXLEV=2)



Strain Eyy of element B
in cylindrical panel (MAXLEV=2).



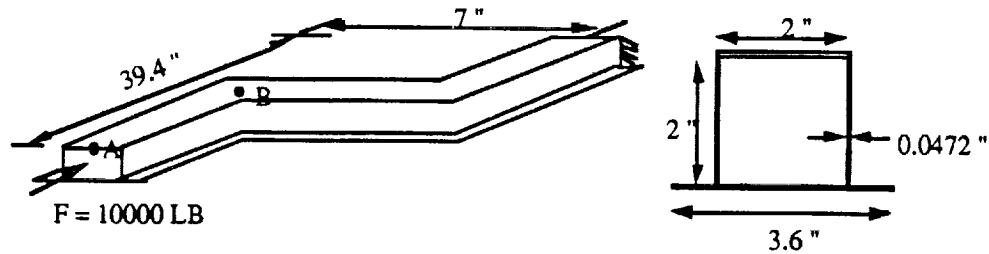
Stress Sxx of element B
in cylindrical panel (MAXLEV=2)



Stress Syy of element B in cylindrical panel (MAXLEV=2).

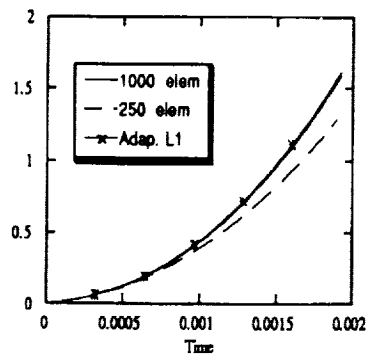
Figure 16

This shows results for an S-beam which is impulsively loaded. Again, significant differences occur in some of the strains for a coarse mesh solution as compared to an adaptive or fine mesh solution.

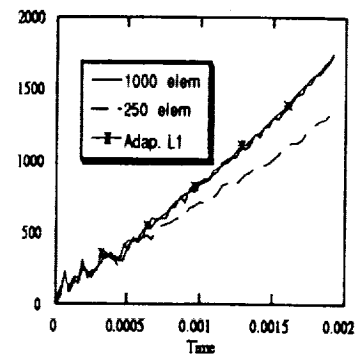


Material number 2 (Table 6)

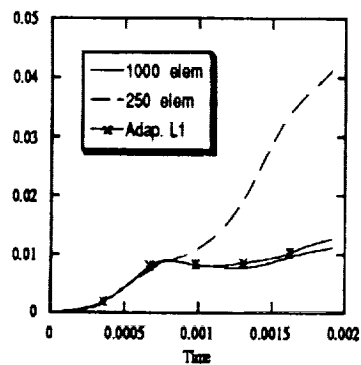
Geometry of T-shape cross section beam.



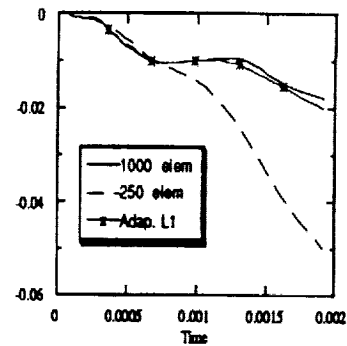
Axial displacement Dz of point A
in T-beam (MAXLEV=1).



Axial velocity Vz of point A
in T-beam (MAXLEV=1)



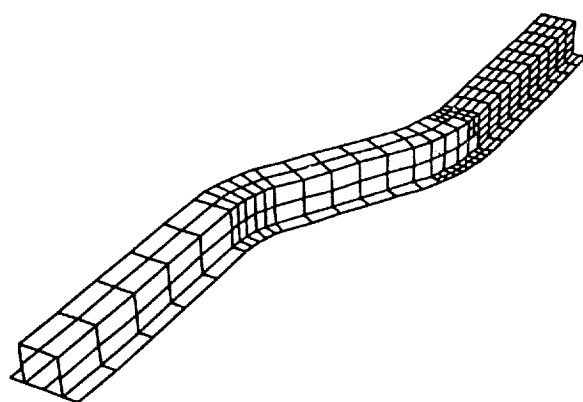
Strain Exx of element B
in T-beam (MAXLEV=1).



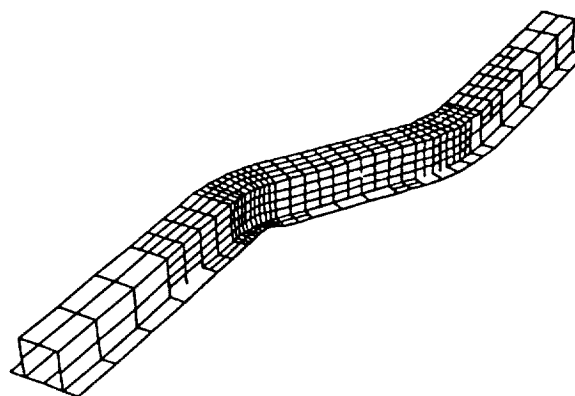
Strain Eyy of element
in T-beam (MAXLEV=1)

Figure 17

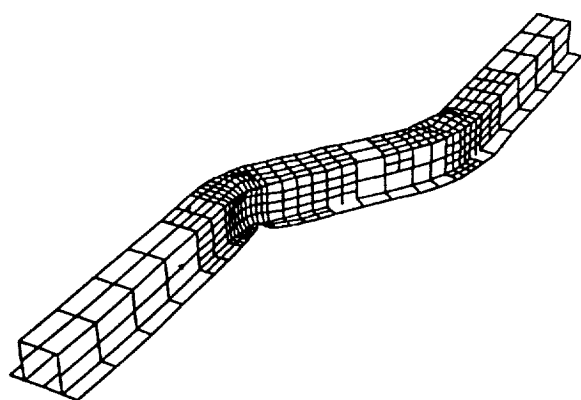
This shows the evolution of the mesh for the S-beam; note that the h-refinement occurs at a corner where local buckling takes place.



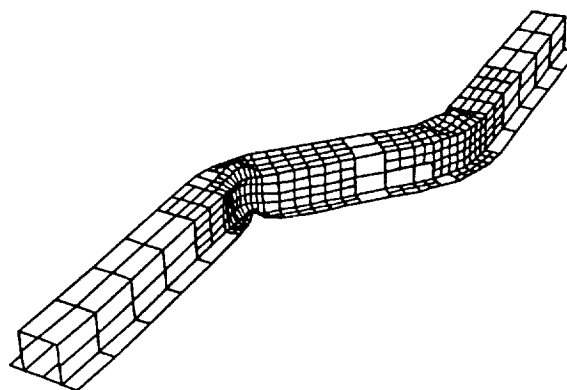
Time=0. ms; 442 elem



Time=0.64 ms ; 718 elem



Time = 1.28 ms ; 673 elem

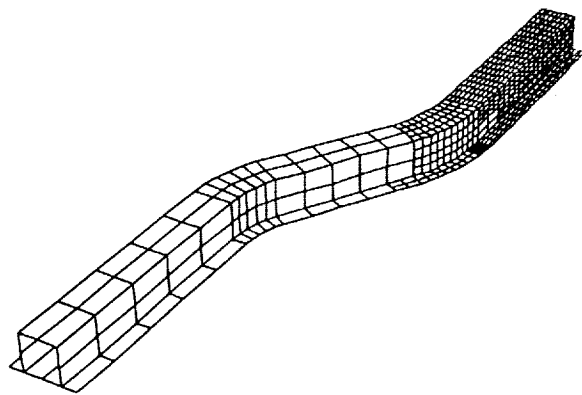


Time=1.92 ms ; 688 elem

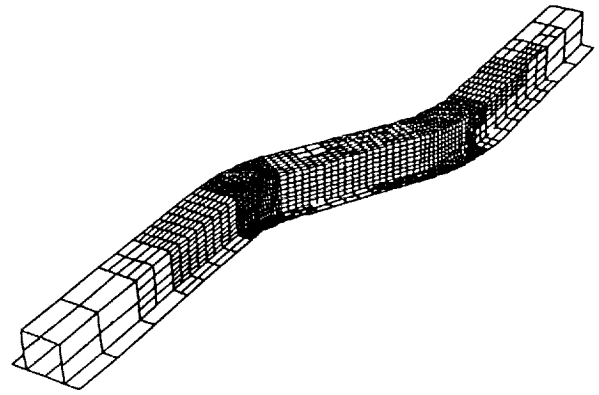
One-level adaptive mesh of T-beam.

Figure 18

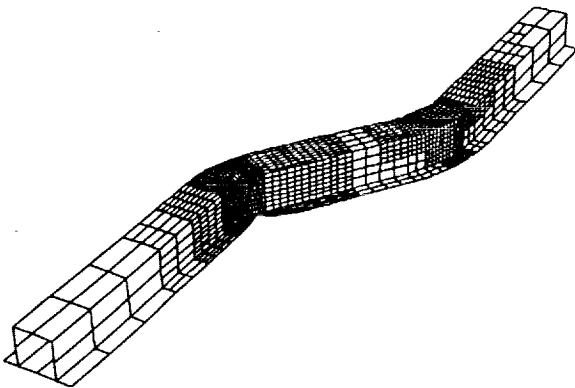
This is the same problem with a higher level of adaptivity. Far more elements are placed in the region of local buckling.



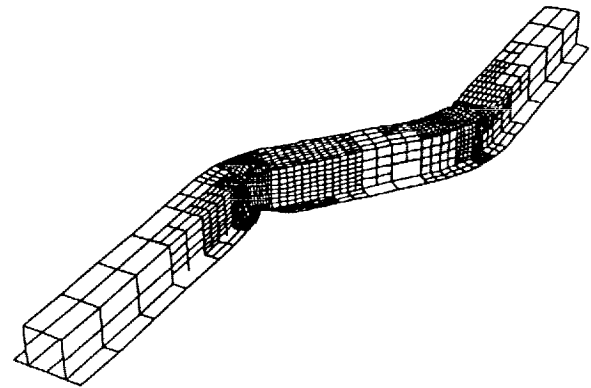
Time=0. ms; 1147 elem



Time=0.32 ms ; 2794 elem



Time = 0.96 ms ; 2581 elem

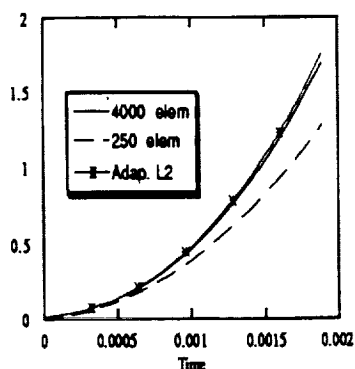


Time=1.6 ms ; 2212 elem

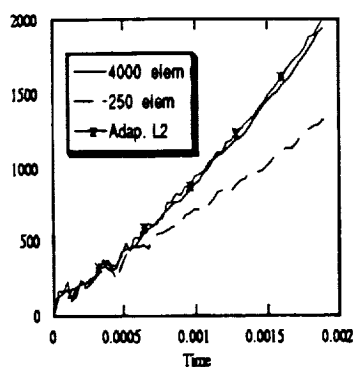
Two-level adaptive mesh of T-beam.

Figure 19

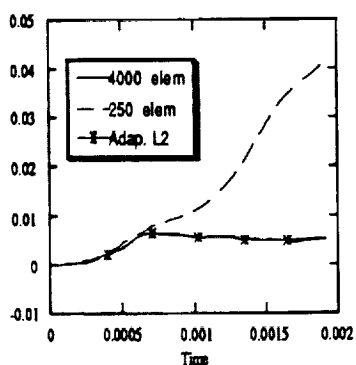
This again compares displacement in strains for coarse mesh, fine mesh, and adaptive solutions. Again the adaptive solutions agree very closely with the fine mesh solution.



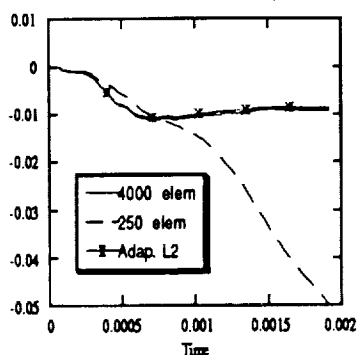
Axial displacement D_x of point A in T-beam (MAXLEV=2).



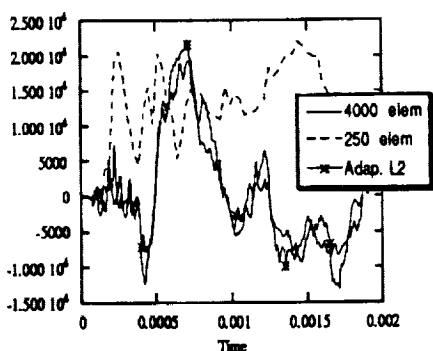
Axial velocity V_z of point A in T-beam (MAXLEV=2).



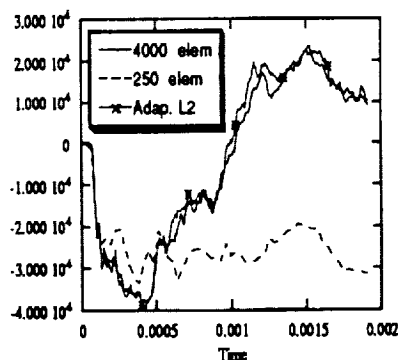
Strain E_{xx} of element B in T-beam (MAXLEV=2).



Strain E_{yy} of element B in T-beam (MAXLEV=2).



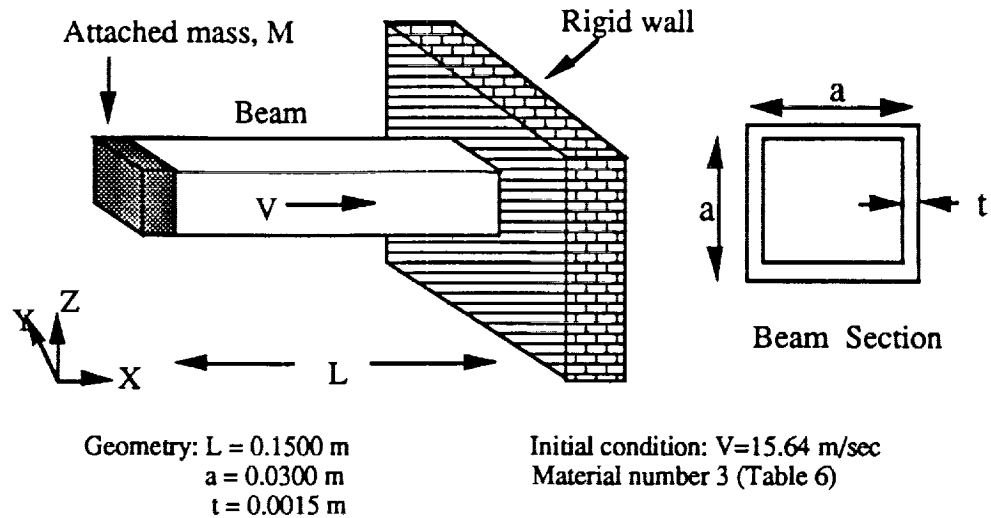
Stress S_{xx} of element B in T-beam (MAXLEV=2).



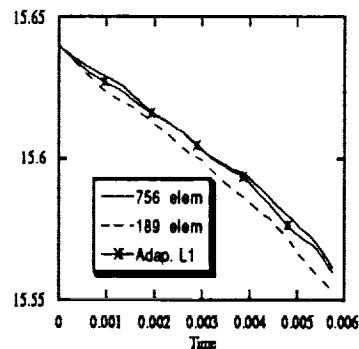
Stress S_{yx} of element B in T-beam (MAXLEV=2).

Figure 20

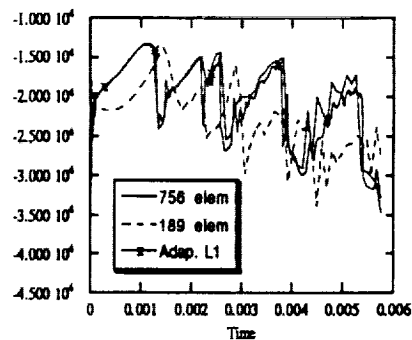
This is a solution of a box beam which has an initial velocity as shown with an attached mass at the back. This problem is often considered a model for crash analysis. The solutions for fine mesh, coarse mesh and adaptive meshes are shown; the adaptive solution agrees well with the fine mesh.



Box beam problem.



Velocity of point A in the box-beam (MAXLEV=1).



Reaction force of box-beam (MAXLEV=1).

Figure 21

This shows a timing for a full car model which is shown on the next page. It is solved with full contact-impact and subcycling. The important thing to notice is that subcycling gives a speedup of 1.7 and that the effective element cycle time on a CRAY-YMP here is 12 microseconds.

Timing

FULL-CAR MODEL

Elements:	17,297
-----------	--------

Mass (kg):	1,880
------------	-------

Time steps:	78,274
-------------	--------

80 msec simulation

CRAY-YMP

Without subcycling: 128 elements/block	7.63 hrs
---	----------

Element cycle time:	20 μ sec
---------------------	--------------

With subcycling: 64 elements/block	4.39 hrs
---------------------------------------	----------

Effective element cycle time:	12 μ sec
-------------------------------	--------------

Speedup:	1.7
----------	-----

Figure 22

win88 - von-mises shell material - subcycle
time = 0.000E+00

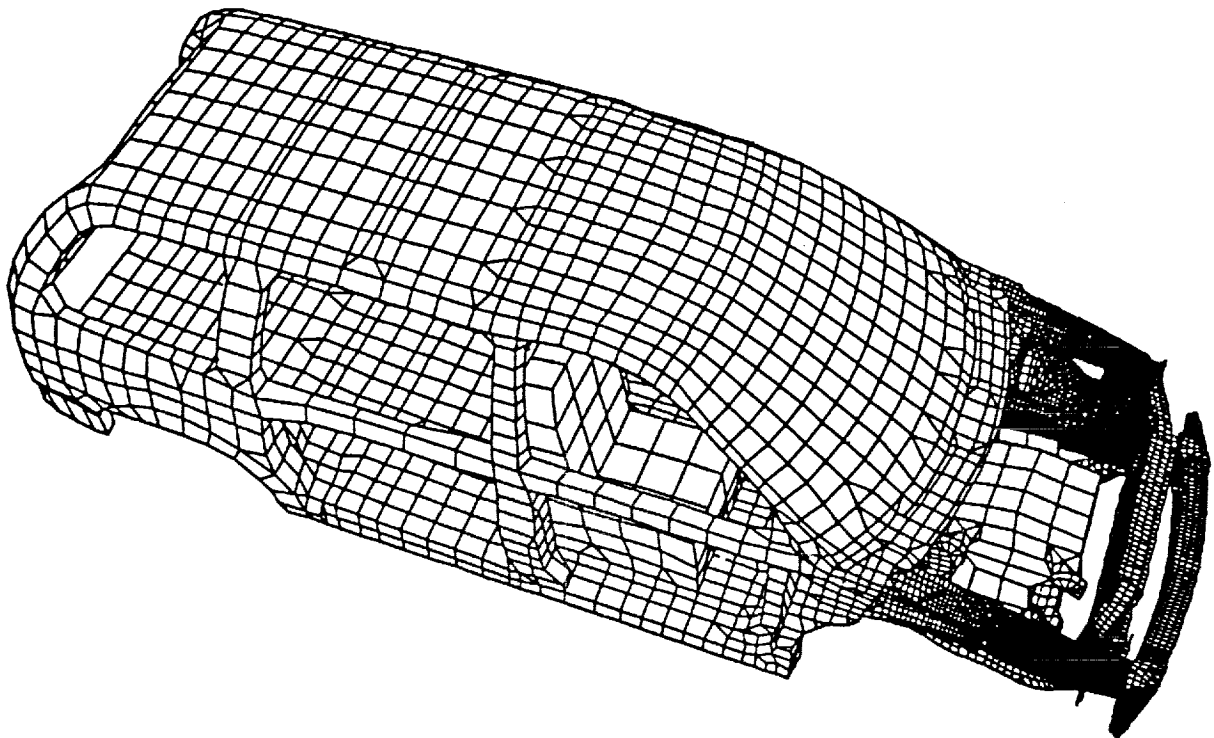


Figure 23

win88 - von-mises shell material - subcycle
time = 0.000E+00

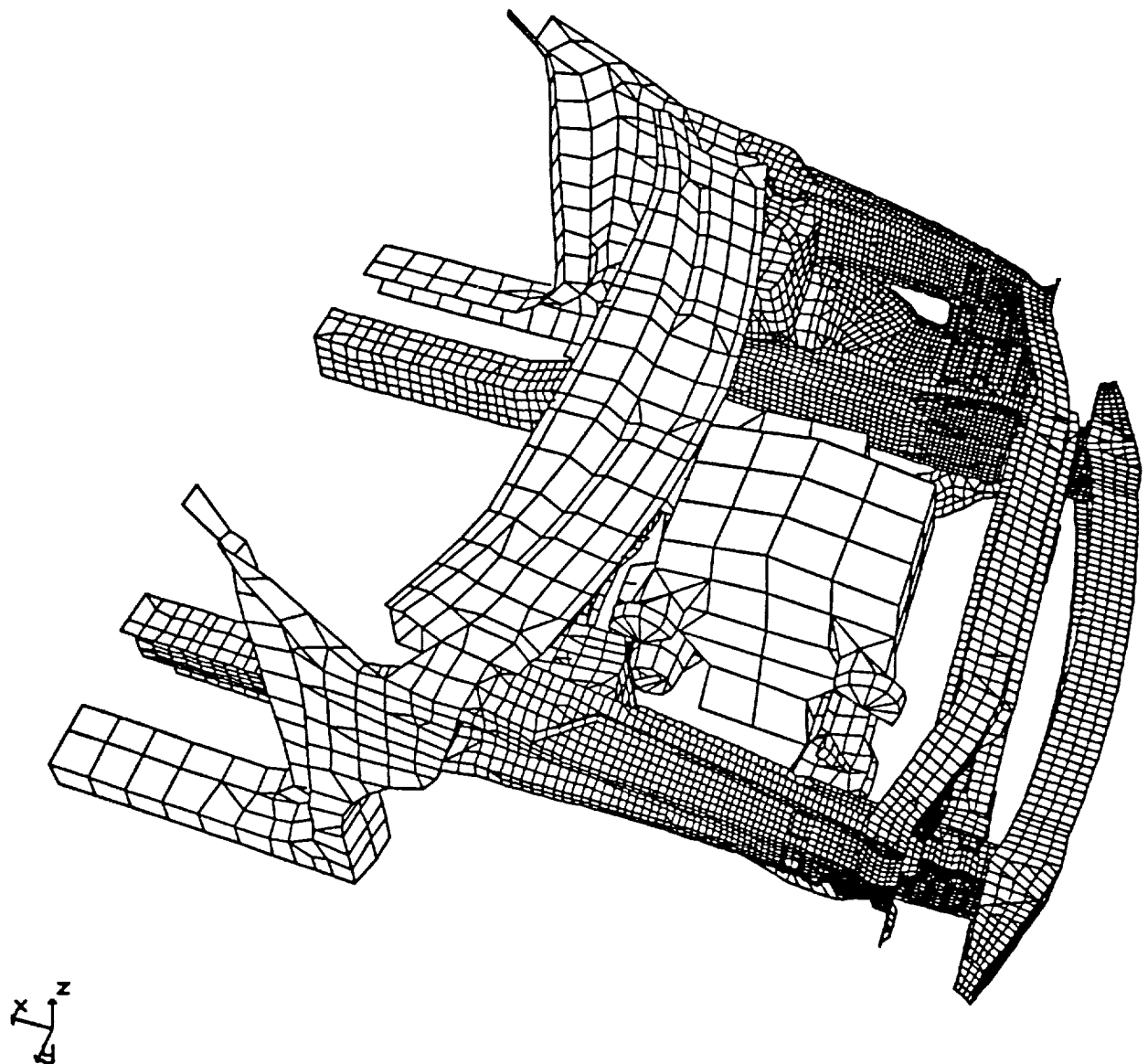


Figure 24

win88 - von-mises shell material - subcycle
time = 4.001E+01

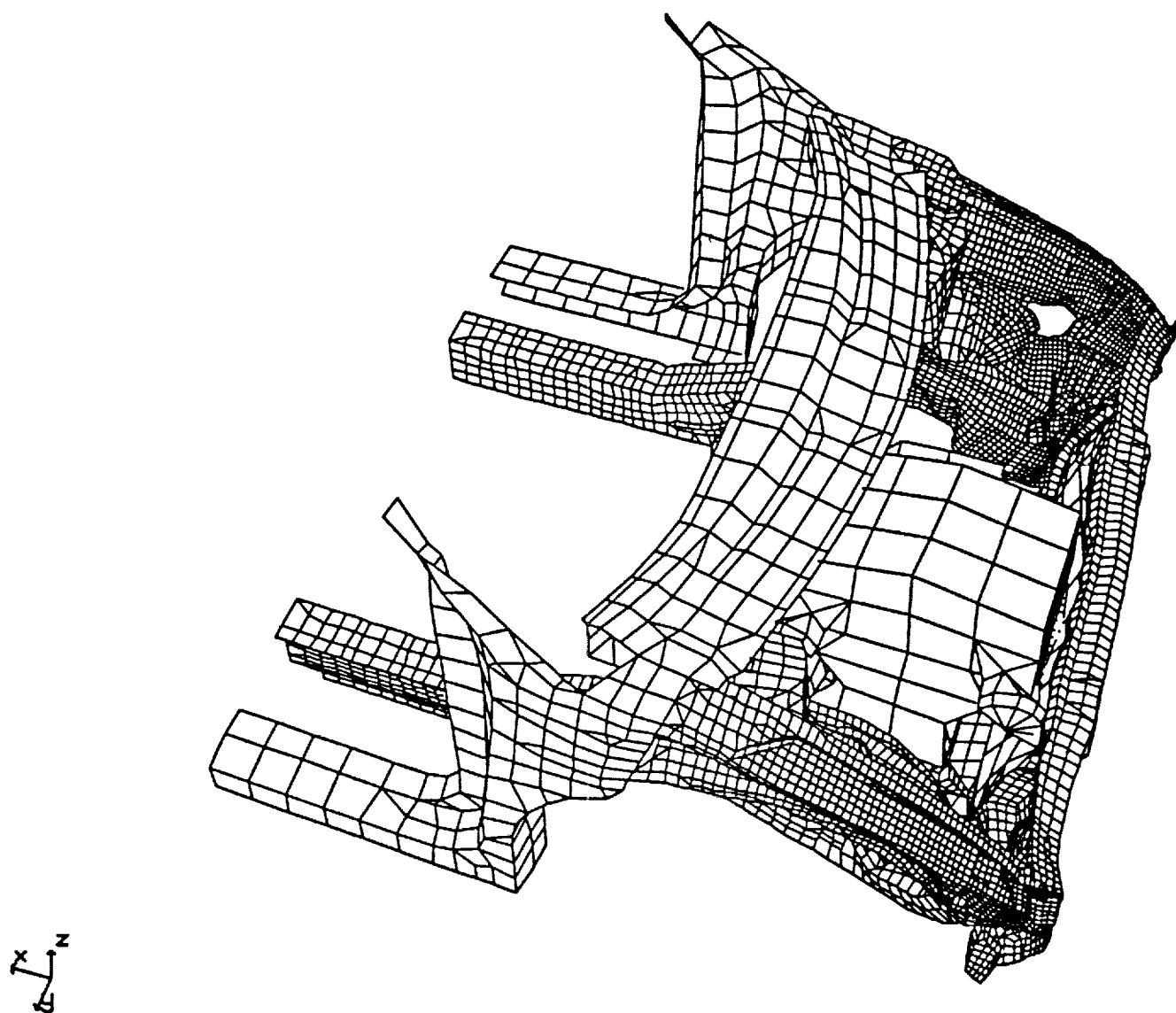


Figure 25

Implementation and Stability

Time steps are assigned to nodes and element blocks automatically.

Elements are sorted by Δt_e^{crit}

$$\Delta t_e^{\text{crit}} \leq \Delta t_2^{\text{crit}} \leq \dots \leq \Delta t_n^{\text{crit}}$$

Elements are arranged in blocks so that time steps of adjacent elements have integer ratios.*

Blocking of elements is necessary to take advantage of vectorization.

For analysis of stability, see Belytschko and Lu, ASME publication edited by G. Hulbert, et al, 1992.

*A new algorithm which does not require integer ratios has recently been developed (Belytschko and Neal, *Computer Methods in Applied Mechanics and Engineering*, 31, 1989, pp. 547-570).

Figure 26

REMARKS AND CONCLUSIONS

- H-adaptivity is a promising technique for simulating nonlinear structural response and structural failure.
- Improves accuracy.
- Simplifies model preparation.
- Subcycling and advanced contact-impact methods such as the pinball method can improve efficiency of explicit dynamic codes and is essential with h-adaptivity.
- Improved error criteria are needed for adaptive methods for nonlinear solid mechanics.

Figure 27

52-39
187833
N94-19467

Composite Impact Dynamics Research at NASA LaRC -- A Review

Huey D. Carden
NASA Langley Research Center
Hampton, VA

PRECEDING PAGE BLANK NOT FILMED

36 INTERNALLY BEAT

INTRODUCTION

The Landing and Impact Dynamics Branch of NASA Langley Research Center has been involved in impact dynamics research (Fig. 1) since the early 1970's. For the first ten years, the emphasis of the research was on metal aircraft structures in both the General Aviation Crash Dynamics Program (Refs. 1-13) and the Controlled Impact Demonstration (CID) Program, a transport aircraft program culminating in the controlled crash test of a Boeing 720 aircraft in 1984 (Refs. 14-16). Subsequent to the transport work, the emphasis has been on composite structures with efforts directed at understanding the behavior, responses, failure mechanisms, and general loads associated with the composite material systems under crash type loadings. Considerable work has been conducted to address the energy absorption characteristics (Refs. 17-20) and it indicates that composites can absorb as much if not considerably more energy than comparable aluminum structures. However, due to their brittle nature, attention must be given to proper geometry and designs to take advantage of the good energy absorbing properties while providing desired structural integrity. Achieving the desired new designs often requires an understanding of how more conventional designs behave under crash type loadings.

The purpose of this paper is to present a review of the composite impact dynamics research being conducted at NASA Langley Research Center. Examples are presented of experimental and analytical data to illustrate the activities in the four program elements of the composite research.

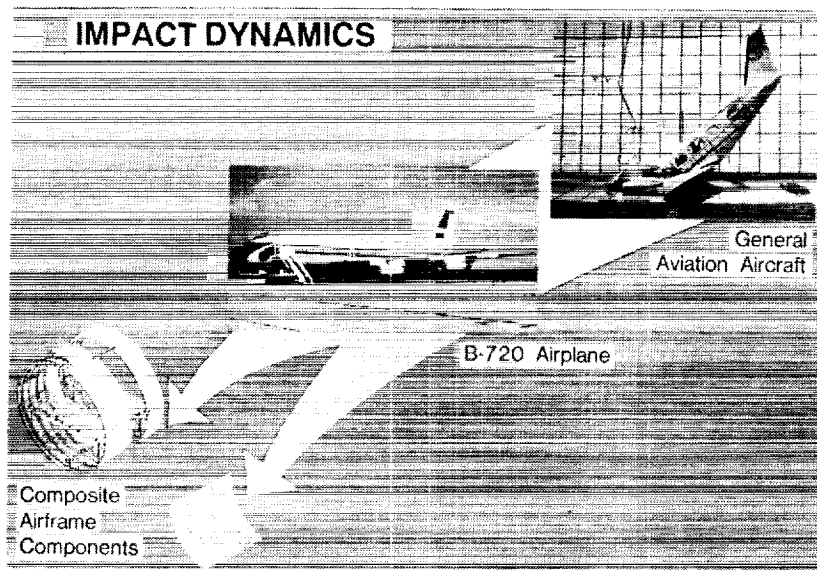


Figure 1

IMPACT DYNAMICS RESEARCH FACILITY

The research was conducted by personnel at the Langley Impact Dynamics Research Facility (Fig. 2) using test equipment located at the installation. The Impact Dynamics Research Facility (IDRF), originally the Lunar Landing Facility used by the astronauts during the Apollo Program for simulation of lunar landings, has been modified to allow crash tests of full-scale aircraft under controlled conditions. The aircraft are swung by cables from an A-frame structure which is approximately 400 ft long and 230 ft high. The impact runway can be modified to simulate other ground crash environments, such as packed dirt, to meet a specific test requirement.

Each aircraft is suspended by cables from two pivot points 217 ft above the ground and allowed to swing pendulum-style into the ground. The swing cables are separated from the aircraft by pyrotechnics just prior to impact. The length of the swing cables determines the aircraft impact angle (from 0 degrees (level) to approximately 60 degrees). Impact velocities can be obtained up to 65 mph (governed by the pullback height). Variations of aircraft pitch, roll, and yaw can be varied by changes in the aircraft suspension harness attached to the swing cables. Data from onboard instrumentation are transmitted through an umbilical cable hard wired to the control room at the base of the A-frame. Photographic data are obtained by onboard, ground-mounted, and A-frame mounted cameras. Maximum allowable weight of the aircraft is 30,000 lb. Reference 21 provides complete details of the facility and test techniques for full-scale aircraft testing.

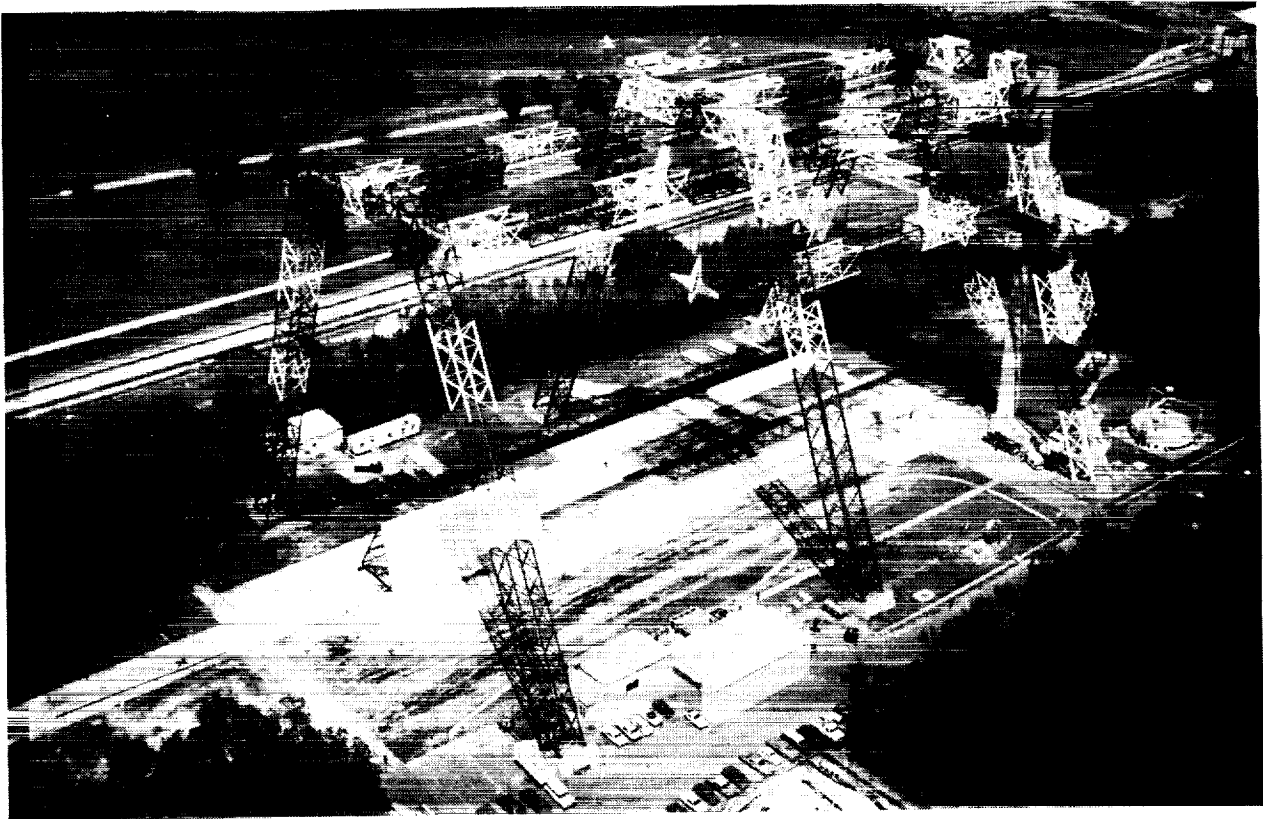


Figure 2

COMPOSITE IMPACT DYNAMICS RESEARCH PROGRAM ELEMENTS

The program elements of the Composite Impact Dynamics Research Program are illustrated in Fig. 3. Currently, efforts in crash dynamics research are in four areas: (1) development of a data base to understand the behavior, responses, failure mechanisms, and general loads associated with both conventional and innovative concepts using composite material systems under crash type loadings; (2) analytical studies/development relative to composite structures; (3) studies in scaling of composite structures under static and dynamic loads; and (4) full-scale tests of metal and composite structures to verify performance of structural concepts.

The overall goal of the research efforts is to gain a fundamental understanding of composite crash behavior and to formulate improved structural designs to meet performance, integrity, and energy absorption requirements. Examples of experimental testing relative to each program element will be highlighted in the paper. Analytical examples associated with the program elements will be presented at the appropriate time within the discussions of the experimental tests rather than in separate sections.

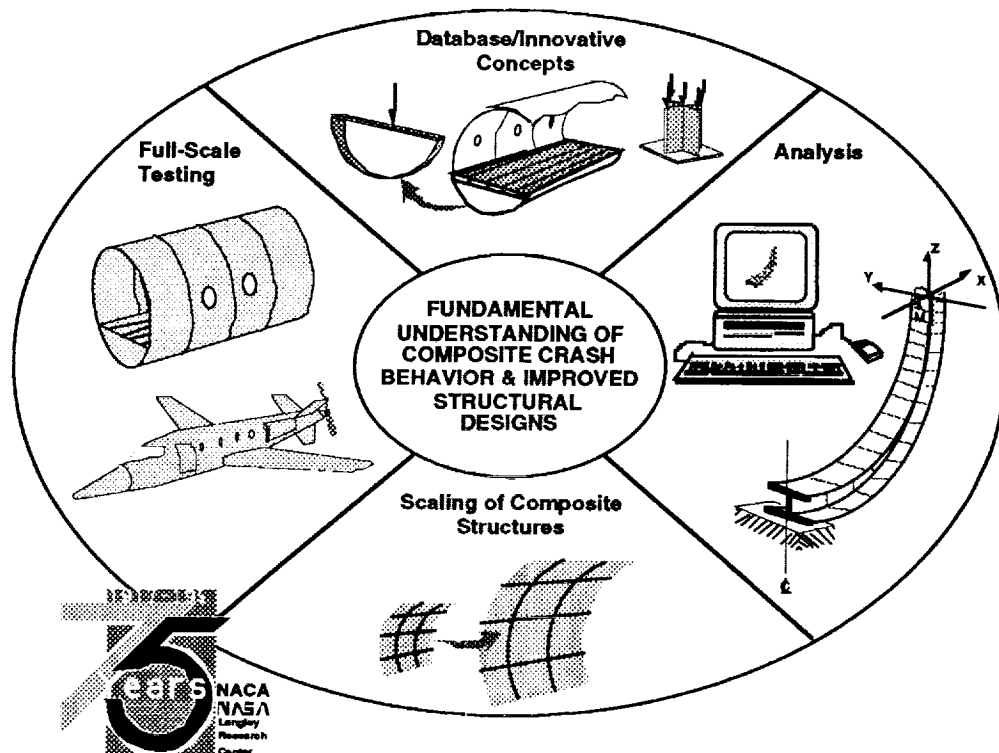


Figure 3

TYPICAL TRANSPORT FUSELAGE STRUCTURE

If one examines a typical transport fuselage structure as shown in Fig. 4, it becomes readily apparent that frames are one of the most important components used in the construction. As a consequence, the initial efforts in our studies were evaluation of individual frame components. The approach of studying simple structural elements and then moving to combinations of these elements in more complex substructures has been taken in the development of a data base on the dynamic response and behavior of composite aircraft structures. With this building block approach, more complex subfloor structures fabricated from the simpler components for both static and dynamic testing are discussed later in the paper.

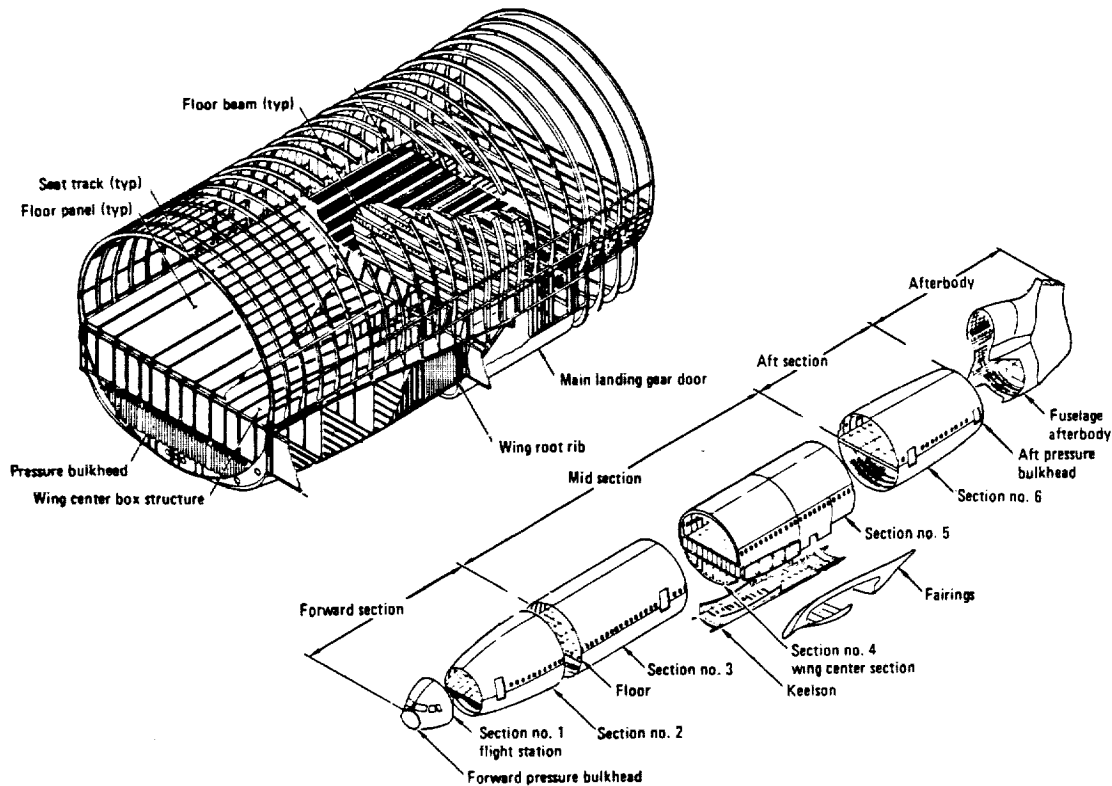


Figure 4

COMPOSITE FUSELAGE FRAME CONCEPTS

Various cross-sectional shapes for fuselage frames are used in metal aircraft and are often proposed for composite structures. Figure 5 presents sketches illustrating four of the more common geometries, I-, J-, C- and Z-cross sectional shapes. Several circular frames using these shapes were fabricated for testing. To add out-of-plane stability to the frames (with the exception of the Z-section frames), 3-1/2 inch wide skin material was added enhancing the ease of testing of both symmetrical and other nonsymmetrical sections. The skin, a $[\pm 45/0/90]_{2s}$ lay-up sixteen ply (.08 inches) thick, was cocured with the 6 foot diameter frames. The frames were constructed in two different heights, 1-1/2 inches and 3/4 inches, to investigate the effect of frame height on behavior and responses.

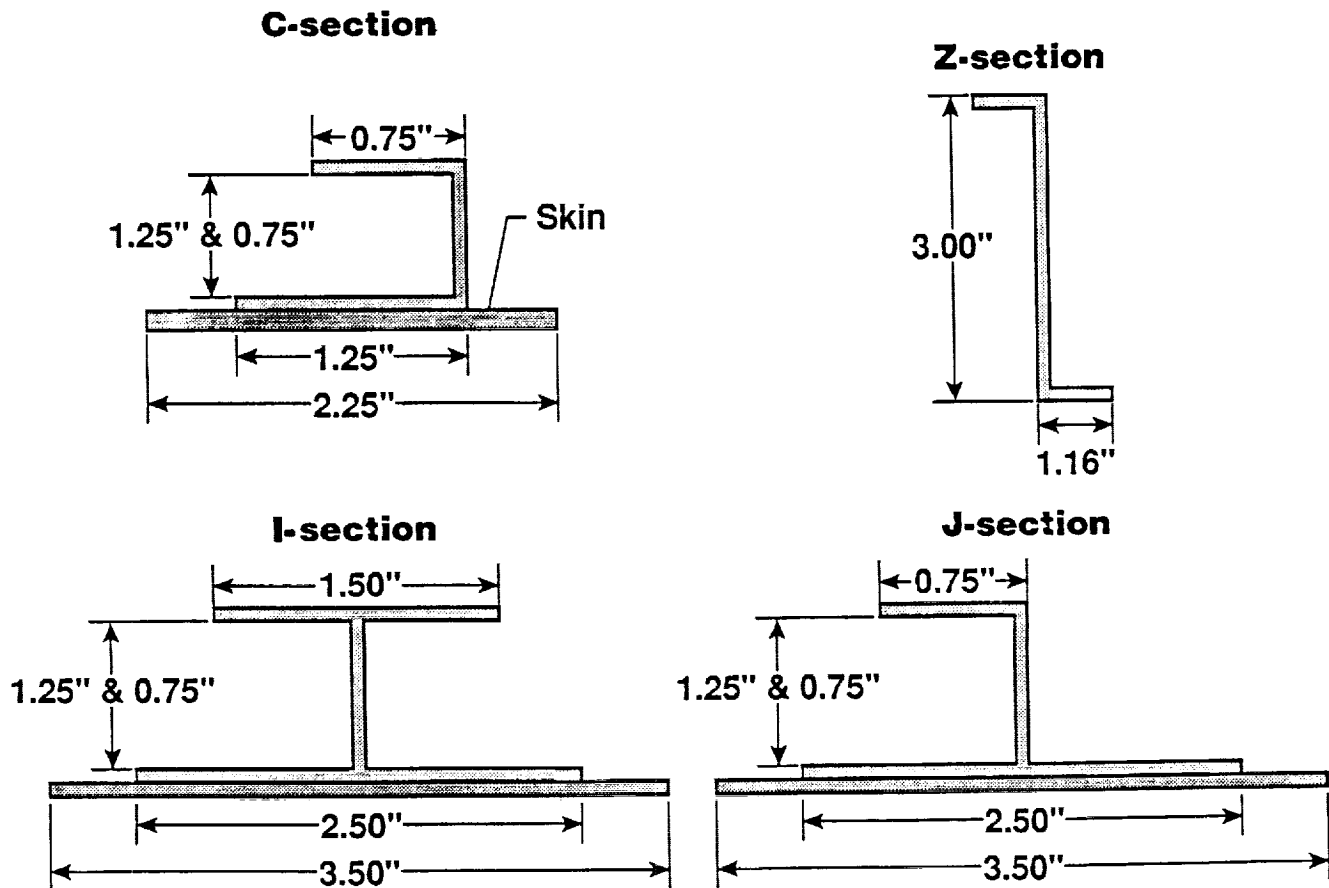


Figure 5

DYNAMIC LOADING BEHAVIOR OF COMPOSITE Z-FRAME

One of the first geometries to be studied under static and dynamic loadings was the Z-cross section. The six-foot diameter frames were constructed of 280-5HA/3502, a five harness satin weave graphite fabric. The height of the frame was 3 inches with a total width of 2.25 inches and about 0.08 inches thick. Lay-up of the frames was quasi- isotropic. Initial tests were with 360 degree frames made from four 90 degree segments joined with splice plates. Additional tests were conducted with half frames since the top half of the complete frames were undamaged in the tests.

Figure 6 presents results from the dynamic studies of the response of the Z-frames under approximately a 100 lbm floor loading at an impact velocity of 20 fps. As noted in the figure, the splice plates joining the segments of the frame are 45 degrees up the circumference from the point of impact. Also, complete failures (fractures) of the Z-section frames occurred at the bottom and approximately 60 degrees from the bottom. Potentially, it appears that the presence of the splice plates may have influenced the locations by moving the top failure points up a few degrees to about the 60 degree locations.

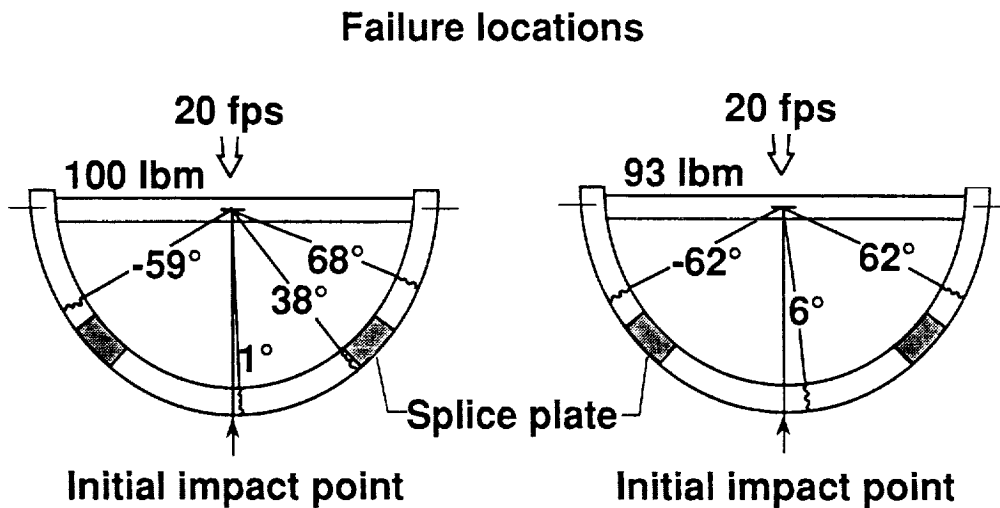


Figure 6

COMPOSITE FUSELAGE FRAME TEST

As a result of earlier tests with the Z cross-section circular frame, a 3.5 inch wide skin material was added to the I-, J-, and C- frame concepts to increase the torsional stiffness of the cross-sections and limit out-of-plane rotations and deformations. The skin, a $[\pm 45/0/90]_2$ sixteen ply (.08 inches) thick, was cured with the 6 foot diameter frames. Data in Fig. 7 are for a lay-up of the frame of $[\pm 45/45/90/0]_3$. Both the skin and the frame were fabricated with AS4/5208 graphite-epoxy material.

Figure 7 shows a typical set-up of a composite fuselage I-frame in a 120 000-lbf loading machine prior to a quasi-static test. The purpose of the study was to evaluate the effect of floor placement on the structural response and strength of the circular fuselage frames constructed of graphite-epoxy composite material. A steel I-beam was attached horizontally across the composite frame at the diameter position to simulate the floor. The horizontal floor positions were designated by the included angle measured between the ends of the floor attachments about the center of curvature of the frame. For example, the frame with the floor at the diameter is designated the 180° floor since the arc is 180° between the attachment points.

A vertical compressive load was applied to the composite fuselage frame through the simulated floor beam and the lower platen of the load machine. Special clamps (see lower right of Fig. 7) were used to bolt the I-beam to the composite frame and a 170° F melting point metal was poured into the small gap between the clamp and the frame to eliminate possible motion in the joint. As shown at the bottom left and top right of the figure, additional tests were conducted where the floor location was moved to produce 120° and 90° arcs. In each test the specimen was loaded at a rate of 500 lbf/minute up to a maximum of 1000 lbf.

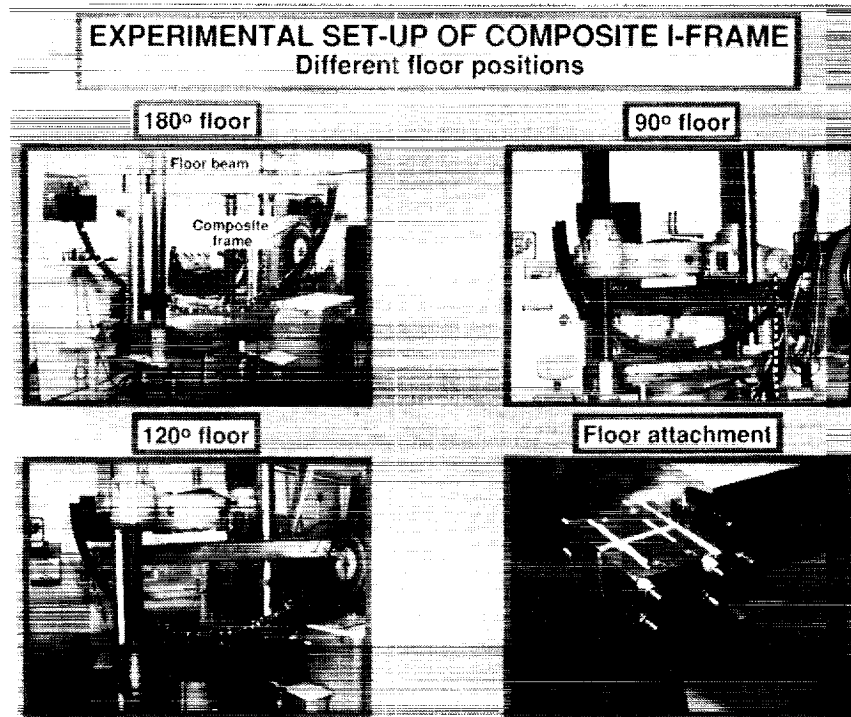


Figure 7

FINITE ELEMENT MODEL OF I-FRAME

To gain an understanding of the physics of behavior, the experimental research of structures under crash loadings is generally accompanied by analytical prediction or correlation studies whenever feasible. Various finite element codes with capabilities for handling dynamic, large displacement, non-linear response problems of metal and composite structures were used as tools in the research efforts. The analytical results presented in this paper were generated with a nonlinear finite element computer code called DYCAST (DYnamic Crash Analysis of STructures (Ref. 22) developed by Grumman Aerospace Corporation with principal support from NASA and the FAA.

Using the beam element from the DYCAST element library, the I-beam model illustrated in Fig. 8 was formulated. The combination of outer skin and I-frame were modeled with only I-beam elements. Since the skin lay-up provided less stiffness than the lay-up of the I-frame, the skin width was reduced by the ratio of the computed stiffnesses of the skin to the I-frame. As a result, the 3.5 inch skin width was reduced to approximately the same 2.5 inch width as the bottom flange of the I-frame itself. Thus, the resulting model consisted of straight ISEC elements with the bottom flange and skin combined to be 0.16 inches in thickness with only the material properties of the I-frame being used in the model. Symmetry was utilized and thirty-nine I-beam elements were used for the beam model. Both a force and a moment loading was applied to the top end of the frame. The static analytical load was increased linearly to a maximum load of 1000 lbf in 50 pound increments. The analytical results of the model are compared to the experimental data in the following section.

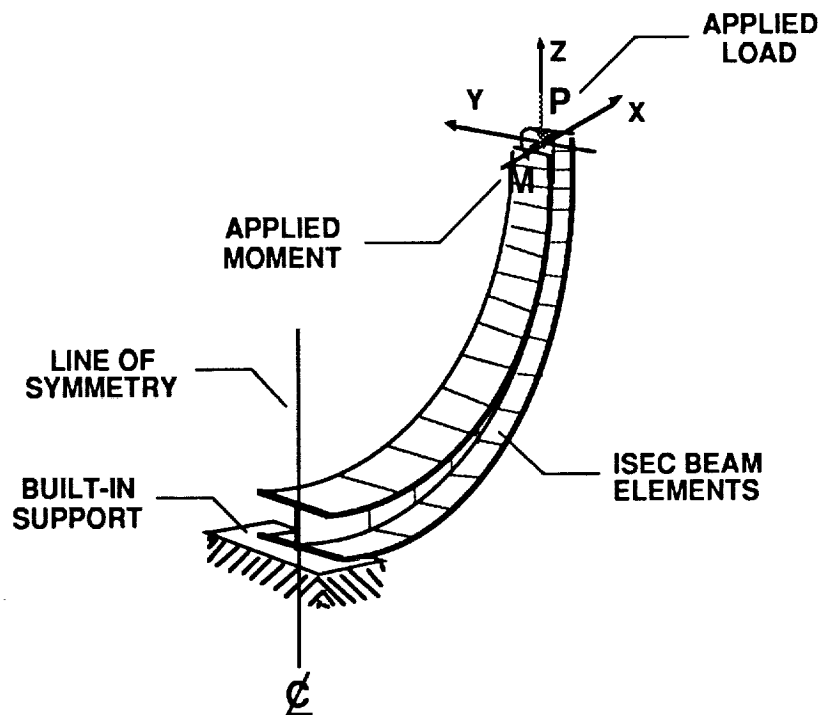


Figure 8

EXPERIMENTAL AND ANALYTICAL STRAIN COMPARISON FOR STATIC LOADING OF THE COMPOSITE I-FRAME

Comparisons of the experimental and analytical strain results on the I-frame were made. For example, Fig. 9 presents typical comparisons of the analytical distributions of strain with the experimental distributions for the 180°, the 120°, and the 90° floor positions, respectively, for both the skin and inner flange. Evaluation of the experimental and analytical strain distribution on the frame for the 0° or ground contact location with two secondary maximums occurring at symmetric locations between $\pm 55^\circ$ - 60° from the bottom contact area; (b) the predicted outer skin strain distribution exhibits the same "sea gull" shape as measured in the experiment; and (c) similar inverted circumferential strain distributions were noted for the inner flange of the frame as occurred in the experiment. The agreement in the magnitudes of the analytical and experimental strains and the shape of the distributions are considered excellent.

The effects on the response of the composite frame from changing the floor position in the composite frame were: (a) to alter the magnitude of the strain (moment) but not the common, general "sea gull" shape of the distribution under vertical loading; (b) to constrain the general "sea gull" shaped strain distribution to occur in the frame segment below the floor attachment locations; and (c) to increase the effective global structural stiffness of the frame as arc length of the frame was decreased.

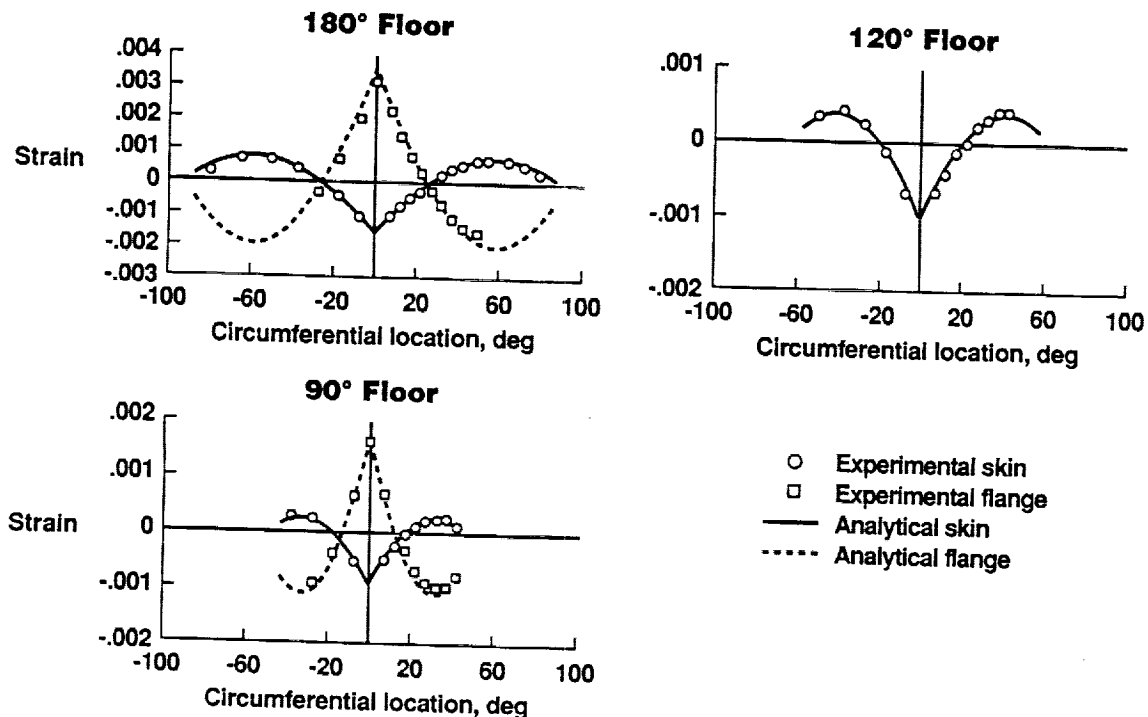


Figure 9

COMPOSITE SUBFLOORS WITH AND WITHOUT SKIN

As indicated previously, the approach of studying simple structural elements and then moving to combinations of these elements in more complex substructures has been taken in the development of a data base on the dynamic response and behavior of composite aircraft structures. The approach parallels the one used during the general aviation and transport aircraft programs. Consequently, three composite subfloor structures were fabricated following the initial investigation of the Z-frames discussed above.

Figure 10 is a photograph of the skeleton and skinned subfloor specimens constructed with three of the single Z-section frames similar to those that were studied earlier. Pultruded J-stringers attached the three frames through metal clips and secondary bonding methods. Aluminum floor beams tied the top diameter of the frames together to form the lower half of the subfloor. Notches in the frames allowed the stringers to pass through the frames. Two subfloors without skin (called skeleton subfloors) were fabricated. A third specimen (called skinned subfloor) had a ± 45 lay-up skin bonded and riveted to the frames to form the lower fuselage type structure. Both static and dynamic tests were conducted with the subfloors.

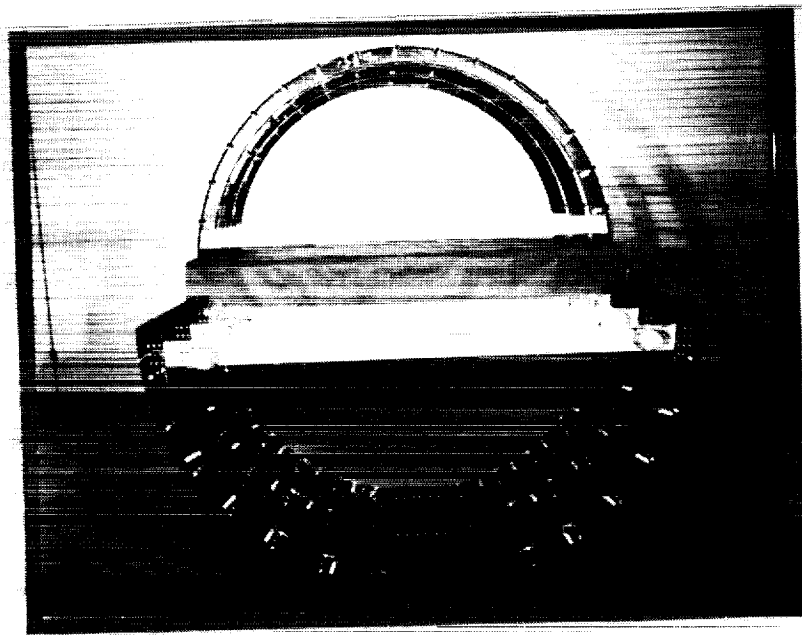


Figure 10

COMPOSITE SUBFLOOR BEHAVIOR--SPECIMEN WITHOUT SKIN

For the three composite subfloor specimens used for impact studies, two static and two dynamic tests were conducted on the subfloors. With the skeleton subfloor, a static and a dynamic test to destruction was conducted. With the skinned subfloor, a non-destructive static test followed by a dynamic test to failure was conducted.

Figure 11 shows the locations of fractures of the skeleton subfloor after an impact test onto a concrete surface at 20 feet per second. In the dynamic test of the skeleton subfloor, fractures were produced at notches in the frames. The locations, shown in Fig. 11, were also near the point of impact (about 11 degrees because of the splice plate) and at two other locations up the circumference of the frames (45 degrees and 78 degrees) and involved all three frames for a total of 15 fractures. The impact energy exceeded the energy absorbed by the local fractures and the floor bottomed out in the impact.

Skeleton subfloor

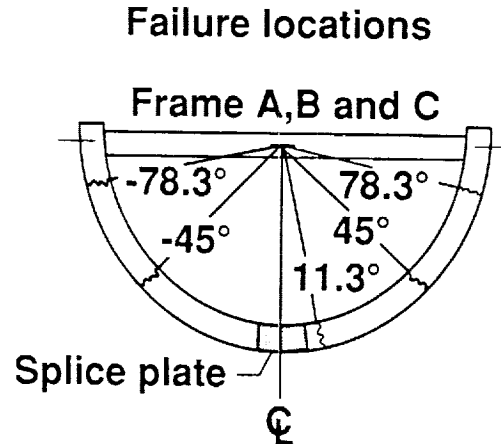


Figure 11

COMPOSITE SUBFLOOR BEHAVIOR--SPECIMEN WITH SKIN

Figure 12 presents impact results for the skinned subfloor after an impact of 20 feet per second. Points of failure of the frames in this specimen are indicated in the figure. Again the points of failure are at/near the impact point (within 12 degrees) and circumferentially at about 56 degrees up both sides of the frame on the middle and back frame and 45, 12 and 22.5 degrees on the front frame. It was observed that the subfloor impacted first on the front area which possibly explains the 12 and 22.5 degree fractures being different from the other locations. Again all three frames were involved in the failures. Some delamination of the frames from the skin was evident but the skin remained intact.

Skinned subfloor

Failure locations

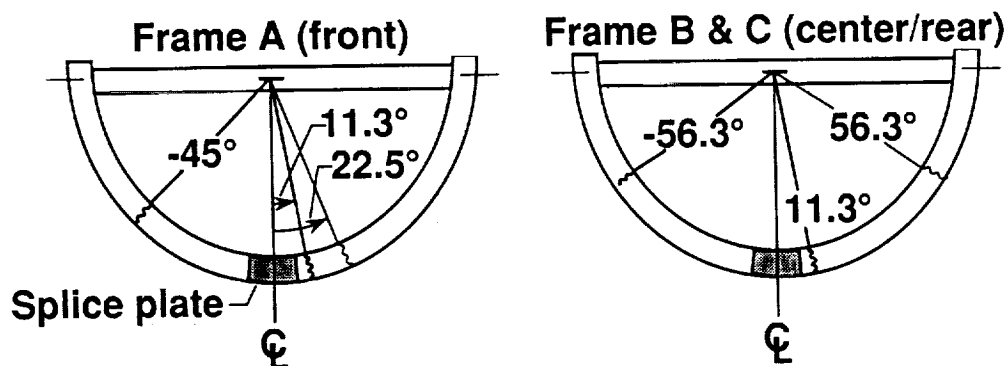


Figure 12

COMPARISON OF FRAME BEHAVIOR WITH SUBFLOORS

The determination of the effect of the floor location on the structural response of fuselage frames has aided in the understanding and prediction of full-scale subfloor or fuselage response to crash loading. For example, Fig. 13 shows a comparison of the normalized experimental dynamic strain distribution on the flange of the skeleton subfloor and the skin location corresponding to the flange position of the skinned composite subfloor specimens with the analytical I-frame strain. The results from the simple frame show a strong similarity to the response of the more complex subfloor structures. The structures share in common the generally circular or cylindrical shape, the vertical loading situations, and under vertical loads have strain (moment) distributions which have maximums at the point of loading and at approximately $\pm 45^\circ$ to $\pm 60^\circ$, depending on boundary conditions, around the circumference from the ground contact point. Analytical results show the same distribution with maximums corresponding to the experimental locations. Failures of the subfloor structures were noted between these same 45° to 60° circumferential locations in the dynamic tests (see Ref. 23).

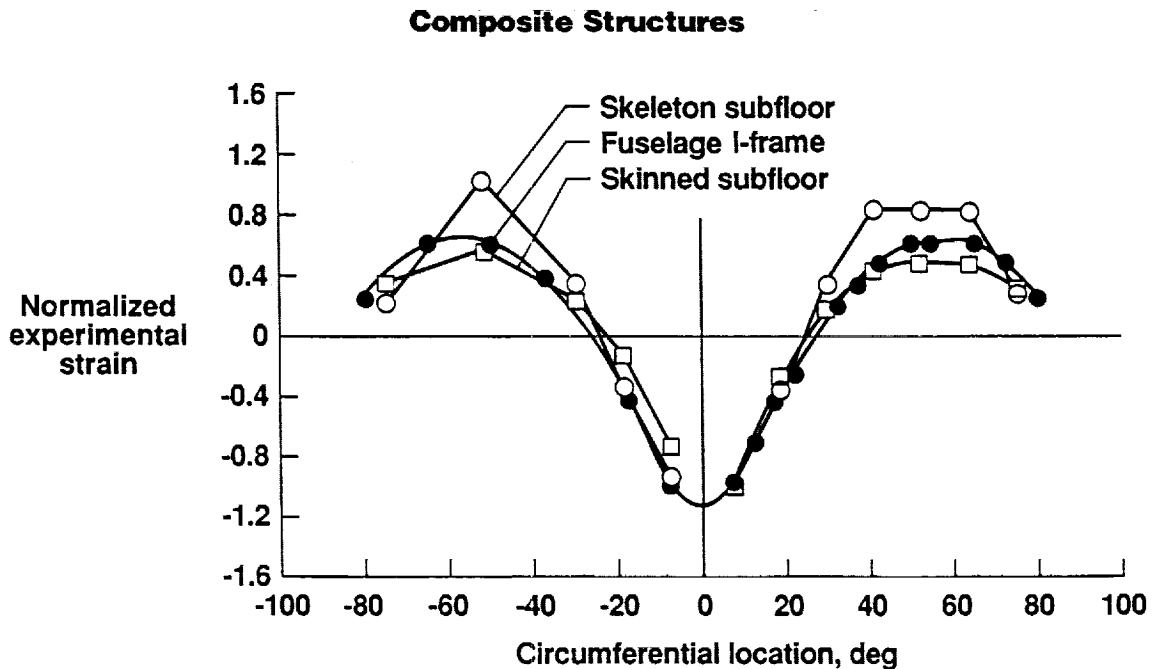


Figure 13

METAL TRANSPORT FUSELAGE FAILURE BEHAVIOR

To relate previous metal transport failure behavior to the current studies and observations with composite structures, data from tests of metal aircraft sections to support transport aircraft research efforts are included. NASA Langley Research Center conducted drop tests of two 12-foot long fuselage sections cut from an out-of-service Boeing 707 transport aircraft to measure structural, seat and occupant responses to vertical crash loads, and to provide data for nonlinear finite element modeling. One section was from a location forward of the aircraft wings and one was from aft of the wing location (Refs. 24 and 25). The sections were loaded with seats, anthropomorphic dummies, data acquisition system pallet, power pallet, and camera batteries to test not only structural, seat, and occupant responses but also to test equipment to be used in the full-scale transport crash conducted later.

Structural damage locations of the transport aircraft structures resulting from the 20 fps drop tests are shown in Fig. 14. The damage to the transport sections was confined to the lower fuselage below the floor level. Under the vertical impact of 20 fps, all of the frames ruptured near the bottom impact point. Plastic hinges formed in each frame along both sides of the fuselage at about 50 degrees up the circumference from the bottom contact point. The upward movement of the lower fuselage was approximately 22-23 inches at the forward end and 18-19 inches at the rear for the section taken from forward of the wing location, whereas in the section from aft of the wing location the crushing was about 14 inches forward and 18 inches in the rear. Although the aircraft structures are metal and the failures discussed above involve plastic deformations with some tearing of the metal rather than brittle fractures, the general observed failure pattern and locations for the transport fuselage sections are noted to be quite similar to the results of the composite frames and subfloors discussed herein.

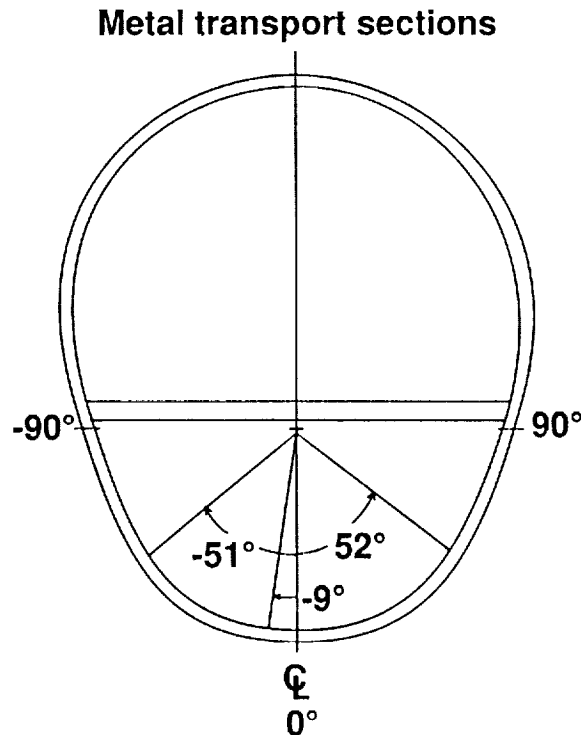


Figure 14

SUMMARY OF OBSERVED FAILURE BEHAVIOR

The response behavior determined during the studies of full-scale aircraft sections, fuselage frames, and subfloors are summarized in Fig. 15. The figure shows normalized moment distribution on a representative frame of the various specimens and the failure locations which were noted from static or dynamic tests. The visual impression is quite striking among the various specimens. It is suggested that from the results of simpler frames to the more complex subfloors and full-scale sections, a strong similarity is evident in the failure behavior of the structures. The structures share in common the generally circular or cylindrical shape, the normal loading situations, and what appears to be a similar pattern of failure behavior. Analytical models of frame structures under vertical loads have moment distributions which have maximums at the point of loading and at approximately 45 to 60 degrees (depending on boundary conditions) around the circumference from the ground contact point. Failures of the structures were noted at these same locations. Such observations can help dynamists gain a better understanding of what to expect from such structures in crash loading situations, can guide designers of new structures to better account for the vertical crash loads, and allow better energy absorption to be included in the new designs. Additionally, the observations can help analysts better model the aircraft structures for predicting the failure responses and behavior under crash situations.

Full-scale transport sections, single composite frames, composite subfloors (skinned and unskinned)

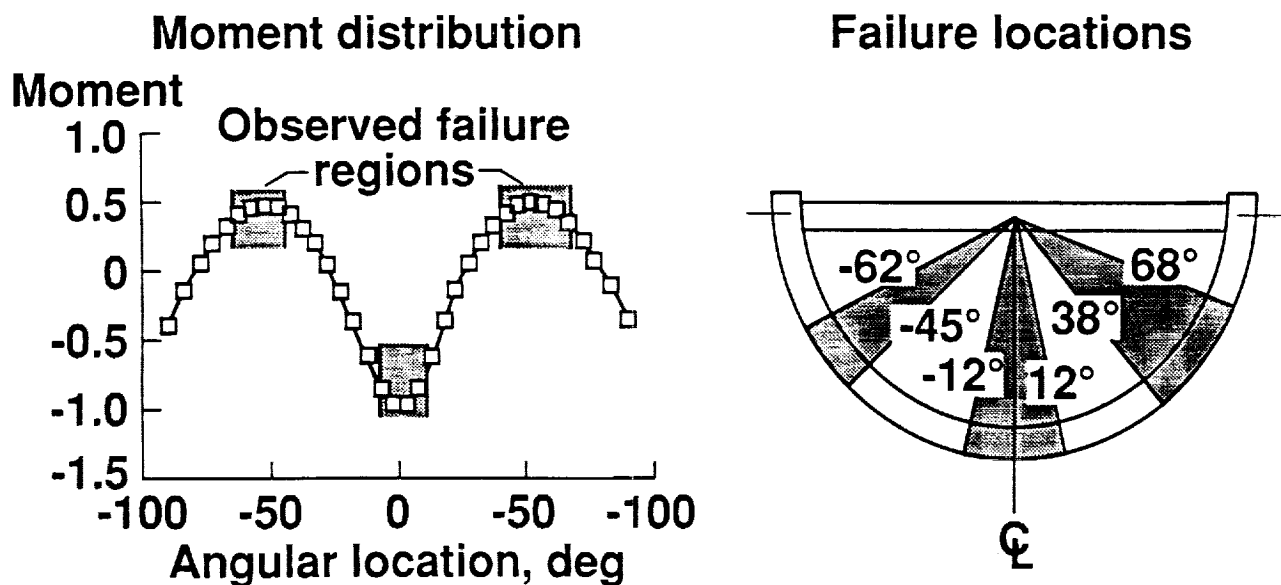


Figure 15

FULL-SCALE COMPOSITE AIRCRAFT CONCEPT

As was illustrated in Fig. 3, one of the four program elements of the Composite Impact Dynamics Research in the Landing and Impact Dynamics Branch of the Structural Dynamics Division at NASA Langley Research Center is full-scale testing of aircraft structures under crash loading conditions.

Two full-scale composite general aviation aircraft structures, two complete wing sets, and landing gears have been obtained for testing. As shown in Fig. 16, the full-scale test aircraft is an 8 place airplane with twin Pratt and Whitney engines (650 hp each) powering a pusher type propeller. The gross takeoff weight is approximately 7200 lbm with empty weight being approximately 4000 lbm. Overall length of the plane is 38 feet with a wing span of 39 feet. The structure of the test aircraft represents a composite skin/frame type fuselage construction concept with the exception of the interior floor structure which consists of aluminum beams on which the seat rails and seats are mounted. Design support testing is underway to replace the existing floor structure in one of the two aircraft with an energy absorbing concept constructed with composite materials. The retrofit approach is, of course, necessitated and as a consequence, special tests have been undertaken to develop the replacement floor concept to assure that structural behavior and failure loads and modes of failure are achieved in the concept prior to inclusion in the aircraft.



Figure 16

ENERGY ABSORBING BEAM DESIGN FOR COMPOSITE AIRCRAFT SUBFLOOR

A preliminary experimental program is being conducted to study the behavior of energy absorbing composite spars for aircraft subfloors. The study, which is a part of a wider full scale aircraft test program, examines the efficiency of replacement floor structures for an existing all composite fuselage aircraft shown in the lower right of Fig. 17. The efforts are a continuation of previous research (Refs. 7 and 13) dealing with crashworthy metal aircraft subfloor structures. A typical section of the composite fuselage with the original subfloor structure is shown in the center of the figure. As shown in the center figure, the four spars that support the seat rails are aluminum, whereas the rest of the subfloor structure is graphite composite. Static tests of such a subfloor section have shown that the existing structure is too stiff and too strong for cushioning loads resulting from crash speeds in the neighborhood of 30 fps, as recommended by the Part 23 of the Federal Aviation Regulations. Thus, the objective of this study is to design and test a retrofit subfloor structure that would provide the desired cushioning (less than 20 g of occupant load) at crush speeds of approximately 30 fps. In particular, the four aluminum spars are to be replaced by composite sine wave beams. The sine wave composite beam concept, shown at upper left, has been examined previously with encouraging results (Ref. 19).

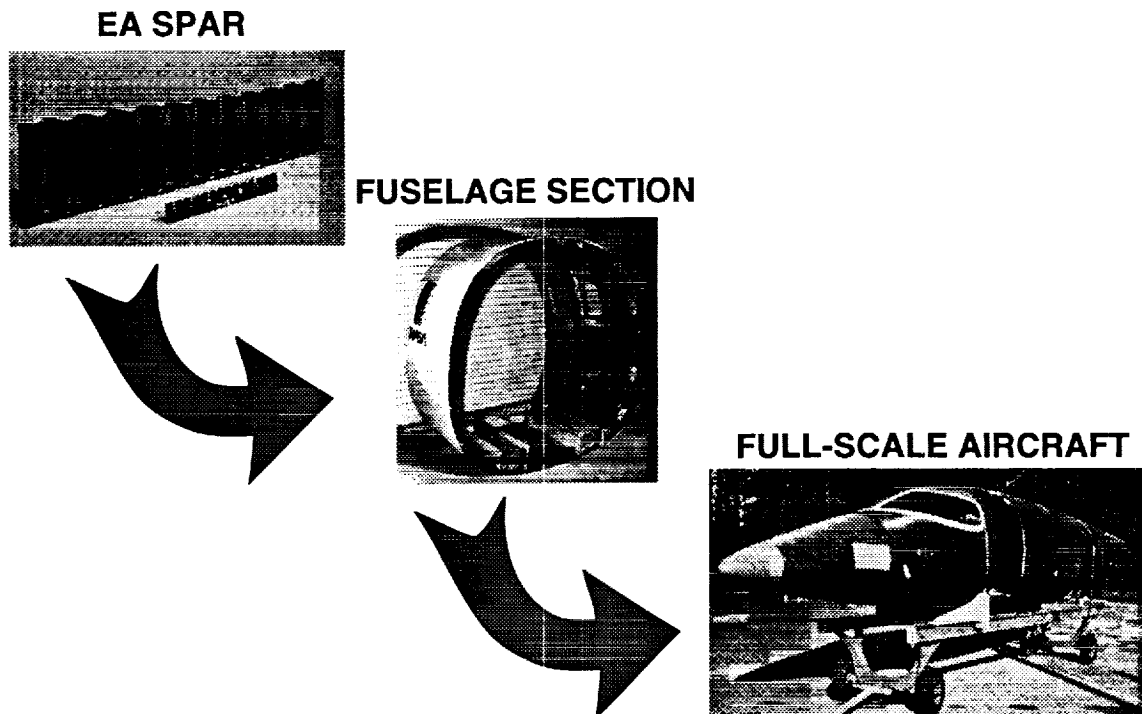


Figure 17

PROPOSED COMPOSITE SUBFLOOR STRUCTURE

A schematic of the proposed subfloor structure is shown in Fig. 18. An ideal beam design should contain two flanges for improved stiffness which, in addition, would offer two crush initiators, one in juncture between the web and the flange. However, because of the double curvature of the fuselage and the retrofit nature of the problem, the beams under construction are limited to a single flange on the top which contains the single crush initiator.

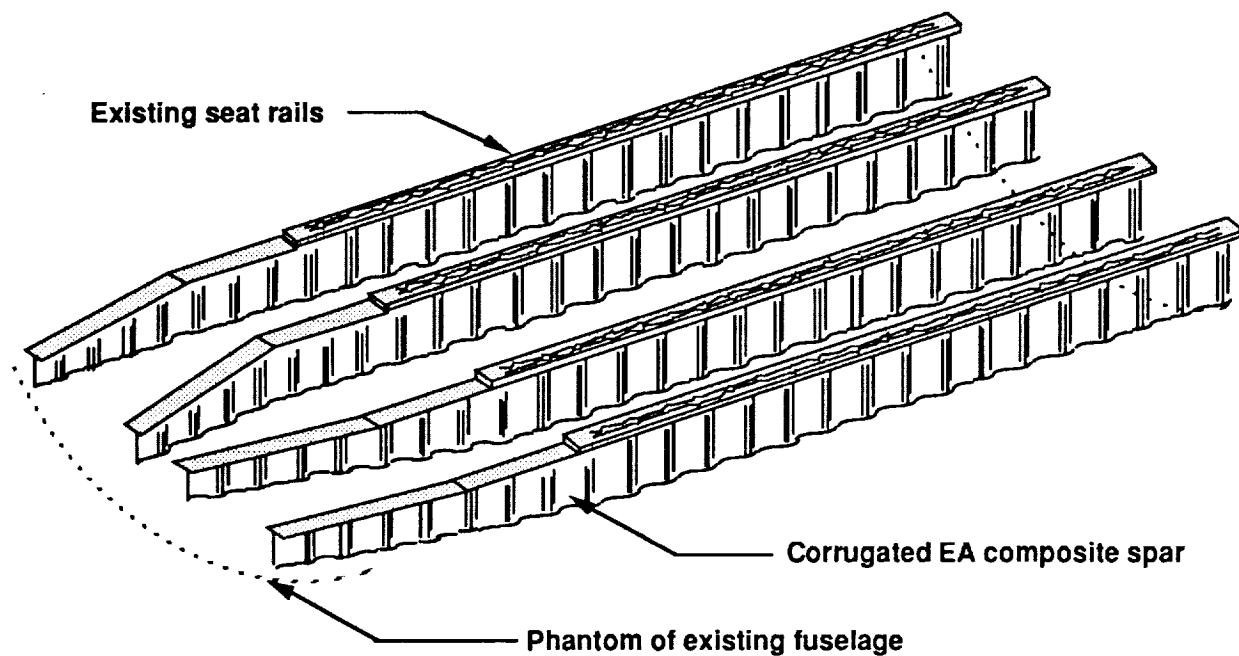
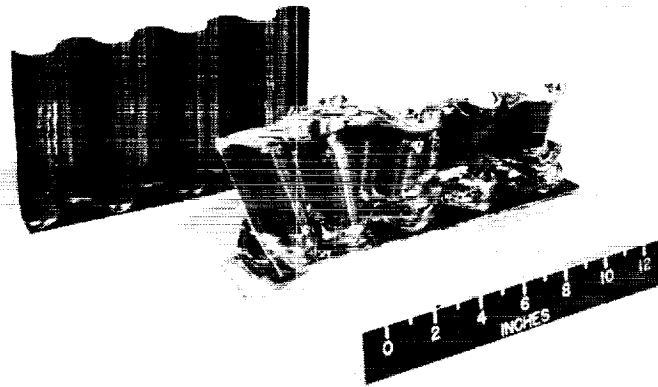


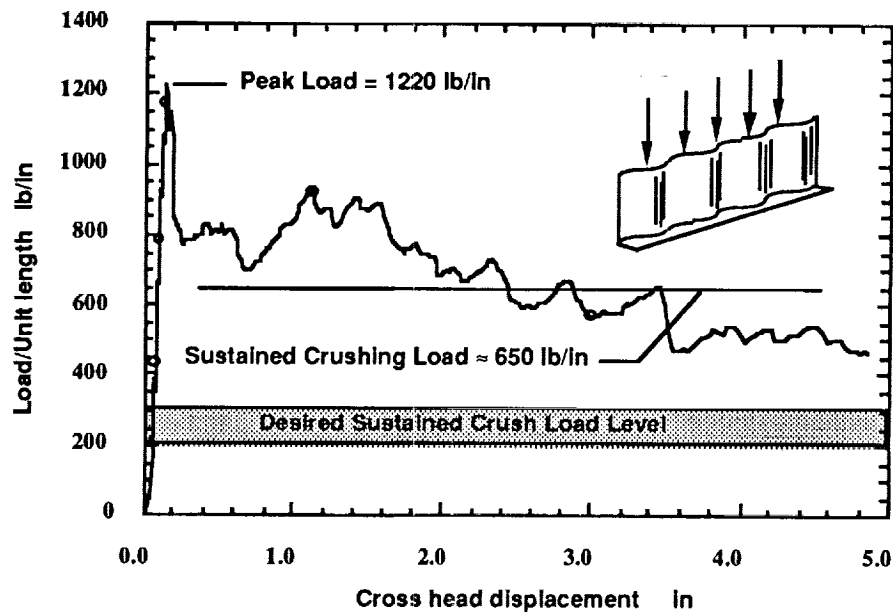
Figure 18

STATIC RESPONSE OF INITIAL COMPOSITE SPAR DESIGN

A preliminary spar beam with an inverted "L" cross section has been fabricated according to the suggested geometric details in Ref. 19. The stacking sequence and composite systems were selected such that the stiffness of the beam transverse to the longitudinal axis was half that of the aluminum spars. Both graphite and aramid reinforced epoxy have been used in the stacking sequence; ($\pm 30^\circ \text{gr.}/\pm 45^\circ \text{kevlar fabric}/0^\circ \text{gr.}$)_s. A series of static and dynamic tests have been conducted to evaluate the overall performance of the spar design. A typical virgin and crushed spar section is shown in Fig. 19 (a) and a load/displacement plot of a quasi-statically loaded composite spar is shown in Fig. 19 (b). Note that, while the section crushed progressively, thus absorbing a large amount of energy, the ultimate load and the sustained crushing loads of approximately 1200 and 650 lb/in respectively are far too high as opposed to 200 - 300 lb/in of desired load.



(a)

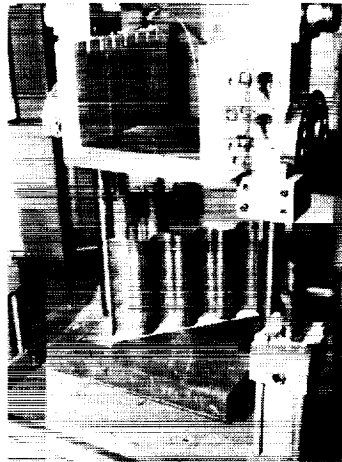


(b)

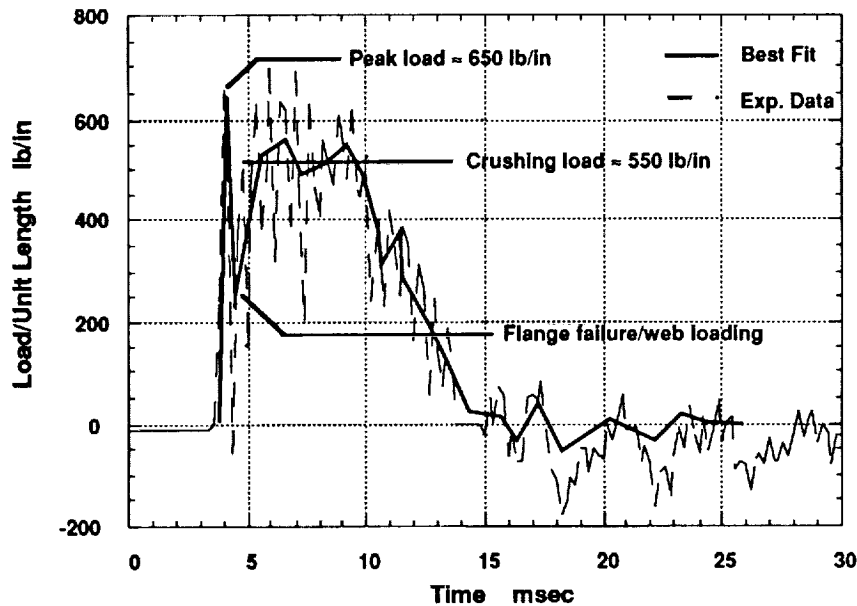
Figure 19

DYNAMIC RESPONSE OF INITIAL COMPOSITE SPAR DESIGN

A series of dynamic tests were carried out on a 14 ft drop tower shown in Fig. 20 (a) to simulate a 30 fps mass drop equal to the corresponding weight of the seat and the occupant which would load the spar section. The mass for a 12" long spar section was 184 lbm. A typical load/time plot from a dynamic test is shown in Fig. 20 (b). Note that, while the value of the sustained crushing load was comparable to the one obtained in the corresponding static tests, the ultimate load was much lower. The dynamic results, shown in Fig. 20 (b), indicate that there was no dynamic rate effect up to the 30 fps impact velocity of the test as compared to the static data and that the loads from the dynamic test of the preliminary beam design is also much too high for a human occupant.



(a)



(b)

Figure 20

CONSIDERATIONS FOR NEW COMPOSITE SPAR DESIGN

The previous results together with the experience gained in the fabrication of the first spars influenced the design of a new set of spars and tests. Some of the factors and constraints that controlled the design of the new spars included:

- (1) simplification of the fabrication process - eliminate unidirectional prepreg, complex angles, and hybridization
- (2) elimination, if possible, of the graphite reinforced material to improve ductility under dynamic loads- to ensure survivability of the flange under normal landing loads
- (3) improvement of the web bending stiffness to ensure adequate longitudinal spar bending stiffness following the loss of the flange
- (4) reduction of the ultimate and the sustained crushing loads to less than 300 lb/in (and greater than 200 lb/in) - to improve cushioning
- (5) symmetric loading - apply load symmetrically from the flange to the web to improve global stability of the spar-web and improve stroke efficiency

It was found that more design goals could be met with a sandwich construction and that some of the additional complications associated with the fabrication of the sandwich spars could also be offset with the simplification of the skin lay-up. Thus, a "T" section illustrated at the bottom of Fig. 21 was chosen instead of the original "L" section. A number of sandwich spar sections are being fabricated with fabric kevlar webs and hybrid flanges. A full test matrix is shown above the sketch of the "T" section. Static and dynamic testing of these sections will commence after specimens have been instrumented.

Flange Cover Stacking Sequence	Web Stacking Sequence	Flange Core* Thickness Density	Web Core* Thickness Density	Flange Width in	Specimen Length in	Specimen Height in	No. of Specimens	Type of Test
$\pm 45f/0/\pm 45f^{\square}$ Carbon	$\pm 45f$ Kevlar	1/4 in 3lb/ft ³	1/4 in 3lb/ft ³	3	12	8	2	Static Dynamic
$\pm 45f/0/\pm 45f^*$ Carbon	$\pm 45f$ Kevlar	/	1/4 in 3lb/ft ³	3	12	8	2	Static Dynamic
$\pm 45f/0/\pm 45f^*$ Carbon	($\pm 45f$)s Kevlar	1/4 in 3lb/ft ³	1/4 in 3lb/ft ³	3	12	8	2	Static Dynamic
$\pm 45f/0/\pm 45f^*$ Carbon	($\pm 45f$)s Kevlar	/	1/4 in 3lb/ft ³	3	12	8	2	Static Dynamic
$\pm 45f/0/\pm 45f^*$ Carbon	$\pm 45f$ Kevlar	/	1/2 in 3lb/ft ³	3	12	8	2	Static Dynamic
$\pm 45f/0/\pm 45f^*$ Carbon	($\pm 45f$)s Kevlar	/	1/2 in 3lb/ft ³	3	12	8	2	Static Dynamic

* - LAST-A-FOAM
 \square - Fabric

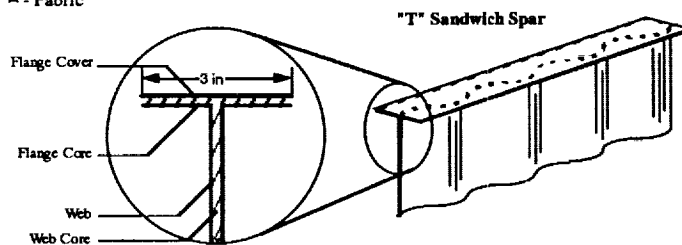


Figure 21

FINITE ELEMENT MODELING OF THE COMPOSITE AIRCRAFT

As part of the overall program, along with the full-scale testing of the composite aircraft concept, finite element predictions of the behavior and loads of the aircraft under crash conditions will be conducted. The computer program KRASH (Ref. 26), which is a three-dimensional, hybrid, finite element modeling technique, will be used to predict response and loads of the test aircraft under selected impact parameters using the KRASH finite element aircraft model (or variation thereof) shown in Fig. 22. As depicted in the figure, KRASH represents the structure of the aircraft as a combination of masses, beams, rigid connections, and external springs.

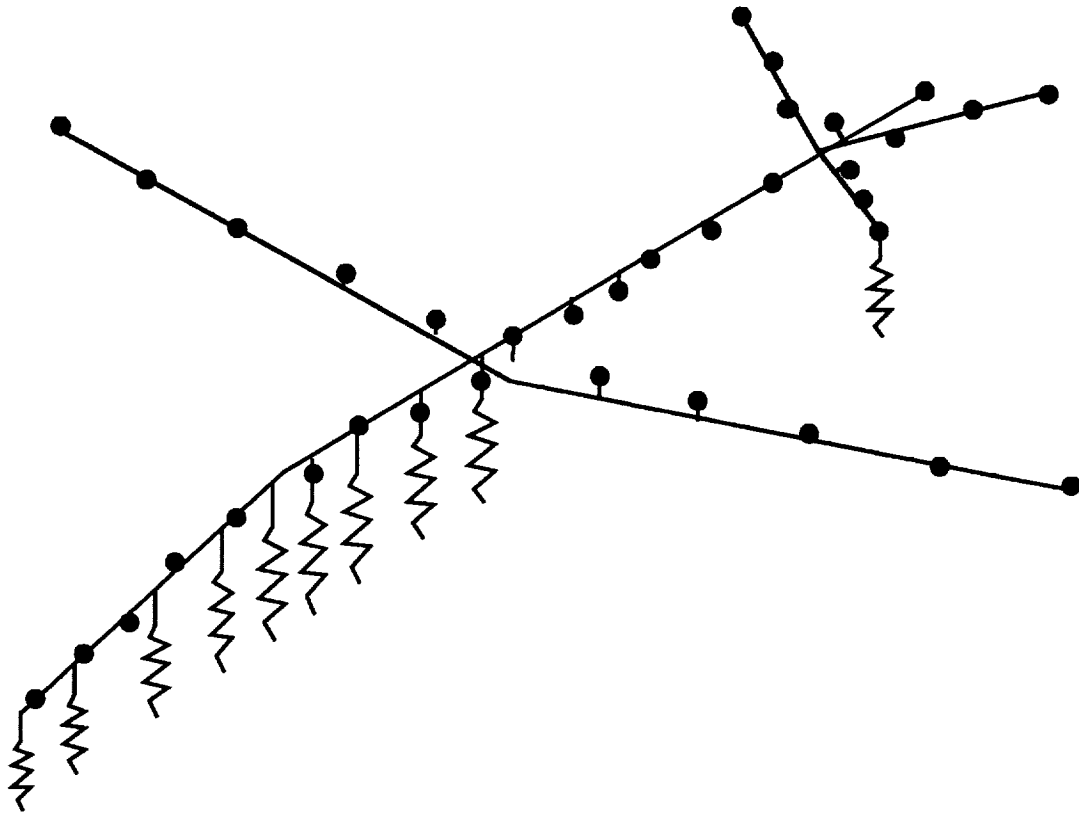


Figure 22

SCALING OF COMPOSITE STRUCTURES

The final research area in Composite Impact Dynamics Research is the scaling of composite structures. One activity is discussed herein, but Refs. 27 to 31 deal with other studies.

Figure 23 shows some typical results of a study to isolate the factors responsible for scale effects in the tensile strength of angle ply graphite/epoxy composite laminates. Two generic $\pm 45^\circ$ lay-ups were studied, one with blocked plies and one with distributed plies with stacking sequences containing between 8 and 32 plies. The 8-ply laminate consisted of off-axis plies arranged in a $(+45^\circ/-45^\circ)_2s$ sequence, and was denoted the baseline or model stacking sequence. A high modulus, high strength brittle graphite-epoxy system (AS4/3502) was used to fabricate six "scaled-up" laminates with the following stacking sequences: $(+45^\circ_n/-45^\circ_n)_2s$ (blocked plies), and $(+45^\circ/-45^\circ)_{2n}s$ (distributed plies), where $n = 2, 3$, and 4 . Tensile coupon specimens having four scaled sizes were constructed including full scale size, $3/4$, $2/4$, and $1/4$, corresponding to n equal $4, 3, 2$, and 1 , respectively. Angle ply laminates are commonly used for damage tolerance in the surface of composite laminates where the load bearing plies are shielded against impact and fatigue loads. It is therefore important to understand the effect of specimen thickness and stacking sequence on the stress-strain response, the ultimate strength, and the mode of failure for this class of laminates.

Results in Fig. 23 indicate that for increasing specimen size: (1) strength decreased for blocked ply laminates; (2) strength increased for distributed ply laminates; and (3) strength of distributed laminates is greater than blocked laminates for a given specimen size. The significance of these findings, beyond the scaling of structures issues, is that ASTM standard tests for determination of the in-plane shear stiffness and strength are based on $\pm 45^\circ$ angle ply testing, although exact specifications for the laminate stacking sequence are not stated. Results of this research show that the values of strength can vary tremendously depending on whether the laminate stacking sequence contains blocked or distributed plies. Also, the size of the laminate, especially the number of plies, is important. Recommendations to improve the standard testing practices have been made to the ASTM so that a meaningful shear strength value, independent of specimen size, can be determined from tensile tests on $\pm 45^\circ$ laminates.

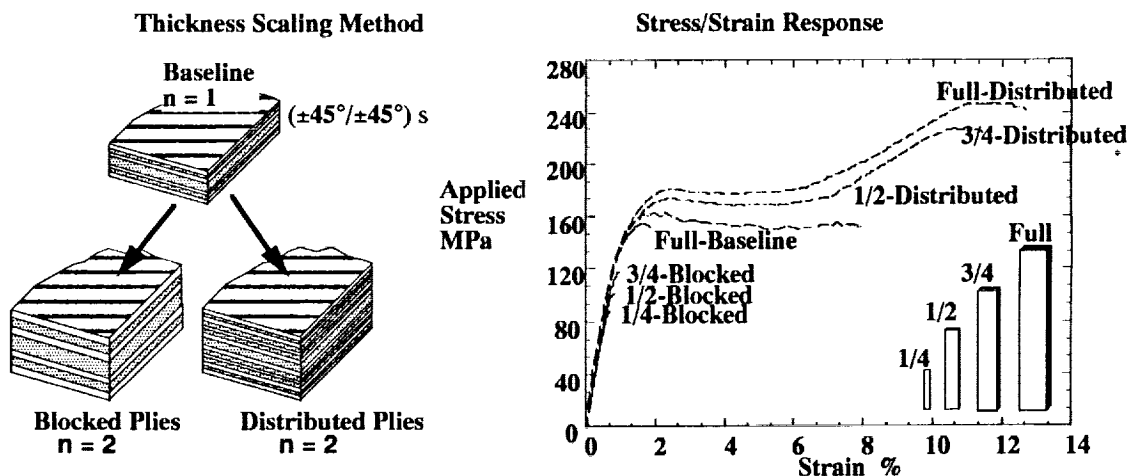


Figure 23

CONCLUDING REMARKS

The Composite Impact Dynamics Research Program at NASA LaRC focuses on generating a database for understanding composite structural behavior under crash loads, examines conventional and innovative metal and composite structures for meeting performance, integrity, and energy absorption requirements, analyzes/enhances analysis tools for composite applications, studies scaling effects in composite structures under static and dynamics loads, and conducts full-scale structures to verify performance of structural concepts.

Typical examples of research in each of the program elements were presented to illustrate the research effort. Experimental and analytical results were presented which showed the effect of floor placement on the structural response of circular fuselage frames constructed of graphite-epoxy composite material. The results from the simple frame showed a strong similarity to the response of more complex subfloor structures. The structures share in common the generally circular or cylindrical shape, the vertical loading situations, and under vertical loads have strain (moment) distributions which have maximums at the point of loading and at approximately $\pm 45^\circ$ to $\pm 60^\circ$, depending on boundary conditions, around the circumference from the ground contact point. Analytical results show the same distribution with maximums corresponding to the experimental locations. Failures of the subfloor structures were noted between these same 45° to 60° circumferential locations in the dynamic tests.

A design support test program to develop a composite energy absorbing floor structure to replace metal floor in a composite aircraft concept was outlined and preliminary results presented. A preliminary spar beam with an inverted "L" cross-section has been fabricated. A series of static and dynamic tests have been conducted to evaluate the overall performance of the spar design. A typical spar section crushed progressively absorbing a large amount of energy, but the ultimate load and the sustained crushing loads were far too high for human survivability. In the dynamic tests, the value of the sustained crushing load was found to be comparable to the one obtained in the corresponding static tests; however, the loads from dynamic tests of the preliminary beam design were also much too high for a human occupant. New design goals were established which should be met with sandwich type spar construction.

Scaling results were presented which have had wide-spread influence on standard test practices for material properties. ASTM standard tests for determination of the in-plane shear stiffness and strength are based on $\pm 45^\circ$ angle ply testing, although exact specifications for the laminate stacking sequence are not stated. Results of this research have shown that the values of strength can vary tremendously depending on whether the laminate stacking sequence contains blocked or distributed plies. In addition, size of the laminate, especially the number of plies, is important. Recommendations to improve the standard testing practices have been made to the ASTM so that a meaningful shear strength value, independent of specimen size, can be determined from tensile tests on $\pm 45^\circ$ laminates.

The Composite Impact Dynamics Research Program will contribute to the technology necessary for the development of improved composite structural aircraft concepts for energy absorption and enhanced passenger protection under crash loads.

REFERENCES

1. Alfaro-Bou, Emilio; and Vaughan, Victor L., Jr.: Light Airplane Crash Tests at Impact Velocities of 13 and 27 m/sec. NASA TP 1042, November 1977.
2. Castle, Claude B.; and Alfaro-Bou, Emilio: Light Airplane Crash Tests at Three Flight-Path Angles. NASA TP 1210, June 1978.
3. Hayduk, Robert J.: Comparative Analysis of PA-31-350 Chieftain (N44LV) Accident and NASA Crash Test Data. NASA TM 80102, October 1979.
4. Castle, Claude B.; and Alfaro-Bou, Emilio: Light Airplane Crash Tests at Three Roll Angles. NASA TP 1477, October 1979.
5. Vaughan, Victor L., Jr.; and Alfaro-Bou, Emilio: Light Airplane Crash Tests at Three Pitch Angles. NASA TP 1481, November 1979.
6. Vaughan, Victor L., Jr.; and Hayduk, Robert J.: Crash Tests of Four Identical High-Wing Single-Engine Airplanes. NASA TP 1699, August 1980.
7. Carden, Huey D.; and Hayduk, Robert J.: Aircraft Subfloor Response to Crash Loadings. SAE Paper 810614, April 1981.
8. Williams, M. Susan; and Fasanella, Edwin L.: Crash Tests of Four Low-Wing Twin-Engine Airplanes with Truss-Reinforced Fuselage Structure. NASA TP 2070, September 1982.
9. Carden, Huey D.: Correlation and Assessment of Structural Airplane Crash Data with Flight Parameters at Impact. NASA TP 2083, November 1982.
10. Carden, Huey D.: Impulse Analysis of Airplane Crash Data with Consideration Given to Human Tolerance. SAE Paper 830748, April 1983.
11. Castle, Claude B.; and Alfaro-Bou, Emilio: Crash Tests of Three Identical Low-Wing Single-Engine Airplanes. NASA TP 2190, September 1983.
12. Thomson, Robert G.; Carden, Huey D.; and Hayduk, Robert J.: Survey of NASA Research on Crash Dynamics. NASA TP 2298, April 1984.
13. Carden, Huey D.: Full-Scale Crash Test Evaluation of Two Load-Limiting Subfloors for General Aviation Airframes. NASA TP 2380, December 1984.
14. Hayduk, Robert J. (Editor): Full-Scale Transport Controlled Impact Demonstration. NASA CP 2395, April 1985.
15. Fasanella, Edwin L.; Widmayer, E.; and Robinson, M. P.: Structural Analysis of the Controlled Impact Demonstration of a Jet Transport Airplane. AIAA Paper 86-0939-CP, May 1986.
16. Fasanella, Edwin L.; Alfaro-Bou, Emilio; and Hayduk, Robert J.: Impact Data From a Transport Aircraft During a Controlled Impact Demonstration. NASA TP 2589, September 1986.

17. Farley, Gary L.: Energy Absorption of Composite Materials. NASA TM 84638, AVRADCOM TR-83-B-2, 1983.
18. Bannerman, D.C.; and Kindervater, C.M.: Crashworthiness Investigation of Composite Aircraft Subfloor Beam Sections. IB 435-84/3(1984), Deutsche Forschungs-und Versuchsanstalt fur Luft-und Raumfahrt, February 1984.
19. Cronkhite, J.D.; Chung, Y.T.; and Bark, L.W.: Crashworthy Composite Structures. ASAAVSCOM TR-87-D10, U.S. Army, December 1987. (Available from DTIC as AD B121 522.)
20. Jones, Lisa E.; and Carden, Huey D.: Evaluation of Energy Absorption of New Concepts of Aircraft Composite Subfloor Intersections. NASA TP 2951, November 1989.
21. Vaughan, Victor L.; and Alfaro-Bou, Emilio: Impact Dynamics Research Facility for Full-Scale Aircraft Crash Testing. NASA TN D-8179, April 1976.
22. Pifko, A.B.; Winter, R.; and Ogilvie, P.L.: DYCAST - A Finite Element Program for the Crash Analysis of Structures. NASA CR 4040, January 1987.
23. Carden, Huey D.; and Robinson, Martha P.: Failure Behavior of Generic Metallic and Composite Aircraft Structural Components Under Crash Loads. NASA RP 1239, November 1990.
24. Williams, M. Susan; and Hayduk, Robert J. : Vertical Drop Test of a Transport Fuselage Section Located Forward of the Wing. NASA TM-85679, 1983.
25. Fasanella, Edwin L.; and Alfaro-Bou, Emilio: Vertical Drop Test of a Transport Fuselage Section Located Aft of the Wing. NASA TM-89025, 1986.
26. Gamon, M.A.; Wittlin, G.; and LaBarge, W.L.: KRASH85 User's Guide--Input/Output Format, Lockheed-California Company, Report N0. DOT/FAA/CT/-85-10, Federal Aviation Administration, Washington, D.C., May 1985.
27. Kellas, Sortiris; and Morton, John : Strength Scaling in Fiber Composites. NASA CR 4335, November 1990.
28. Jackson, Karen E.; and Morton, John: Evaluation of Some Scale Effects in the Response and Failure of Composite Beams. Proceedings of the First Annual NASA Advanced Composites Technology (ACT) Conference, Oct 29-Nov 1, 1990.
29. Jackson, Karen E.: Analytical and Experimental Evaluation of the Strength Scale Effect in the Flexural Response of Graphite-Epoxy Composite Beams. AIAA-91-1025, AIAA 32nd Structures, Structural Dynamics, and Materials Conference, Baltimore, MD, April 8-10, 1991.
30. Kellas, Sotiris; Morton, John; and Jackson, Karen E.: An Evaluation of the ± 45 Degree Uniaxial Test for the Determination of the In-Plane Shear Strength. Proceedings of ICCM Conference 8, Vol. 4, pp 36/M/1-12, July 1991.
31. Kellas, Sotiris; and Morton, John: Scaling Effects in Angle-Ply Laminates. NASA CR 4423, February 1992.

53-39
187834
p. 99

N 9 4 - 1 9 4 6 8

Impact Analysis of Composite Aircraft Structures

Allan B. Pifko
Grumman Corporate Research Center
Bethpage, NY

Alan S. Kushner
State University of New York at Stony Brook
Stony Brook, NY

OUTLINE

- Background remarks on aircraft crashworthiness
- Comments on modeling strategies for crashworthiness simulation - past
- Initial study of simulation of progressive failure of an aircraft component constructed of composite material
- Research direction in composite characterization for impact analysis

PRECEDING PAGE BLANK NOT FILMED

66

STRUCTURAL CRASHWORTHINESS

The key point of this definition is protection of the occupant during a crash event. The structure must be designed to absorb kinetic energy while controlling dynamic forces to within acceptable human tolerances and the maintenance of livable space around the occupant.

- Definition:

The ability of a vehicle to reduce dynamic forces experienced by occupants to acceptable levels while maintaining a survivable envelope around them during a specified crash event.

STRUCTURAL CRASHWORTHINESS (Continued)

There are three key points shown here. The first is that structural crashworthiness, made mandatory by government regulations, is now a design criteria for automobiles and helicopters. Because of this it is essential to assess vehicle crashworthiness during the design cycle. This involves simulation of nonlinear behavior of complex structures during impact which is computationally and theoretically intensive, involving state-of-the-art developments in computational mechanics. These developments are on-going.

- Structural crashworthiness has become a design criteria for occupant carrying vehicles - especially for automobiles and helicopters.
- A requirement exists to assess vehicle crashworthiness during the design cycle.
- Numerical simulation of the dynamic response of vehicles subjected to impact loading is computationally intensive and has/will involve state-of-the-art developments in computational mechanics.

ESSENTIAL REQUIREMENTS OF STRUCTURAL CRASHWORTHINESS

The mechanics of structural deformation during a crash involves geometric nonlinearities due to large shape changes, material nonlinearity due to elastic-plastic behavior and nonlinearities due to variable contact/rebound of structural parts.

Characterization of elastic-plastic behavior of metallic structures is reasonably well understood. Efficient computational algorithms have been developed and implemented into finite element programs. It should be emphasized that these algorithms are sensitive to actual material properties so that there is continuing need for experimental data. Impact of composite materials is a newer and challenging problem as the phenomena of failure differs from metals. Progressive failure and damage laws must be developed that describe fiber failure, matrix cracking, ply debonding and sublaminar buckling. These phenomena then must be implemented into simulation codes for crashworthiness of composite structures. Obviously, an extensive suite of tests must be performed ranging from coupon tests to subcomponents to full-scale section tests.

Simulating variable contact between an impacting structure and external or internal surfaces is computationally intensive. Nevertheless, algorithms have been developed and implemented into a number of simulation codes. Contact friction between surfaces is usually treated using simple Coulomb friction.

- Large elastic-plastic deformation with failure
 - accurate characterization of the constitutive material behavior
 - failure prediction for composite laminate construction
- Variable contact/rebound
 - contact with external surfaces
 - contact between internal parts
 - friction between contacted parts

ESSENTIAL REQUIREMENTS OF STRUCTURAL CRASH SIMULATION (Continued)

Developments in computational algorithms are ongoing. Two areas come to mind that will increase the viability of crash simulation. These are temporal and mesh adaptivity, error estimates and parallel computations. The first area is necessary in order to assure that the discrete model is efficiently and accurately predicting structural impact behavior. The second is to provide the computing power to perform crash simulation on a routine and timely basis within the design cycle as well as to accommodate more detailed models that may be dictated by introducing adaptivity.

In any occupant-carrying vehicle, there are parts designed specifically to absorb energy during a crash. In an automobile these can be rails that are designed to progressively crush. Very detailed models are required to simulate the accordion folds and internal contact of these parts although current full vehicle models include the rails in the entire model. The situation for aircraft and helicopters is equally complex. Energy absorbing subfloor concepts have been developed that appear to be extremely difficult to model. The open question still remains. Is it possible to model these highly nonlinear regions in an accurate and cost-effective manner? Currently, crush data is developed from component testing and then implemented into a model as nonlinear springs. What about structures constructed of composite materials?

- Accurate and efficient computational techniques
 - ? parallel computation
 - ? adaptive methods
- Modeling capability for a variety of structural types
 - including special energy absorbing structural concepts
 - either metallic or composite
 - hybrid materials

MODELING STRATEGIES - PAST EXPERIENCE

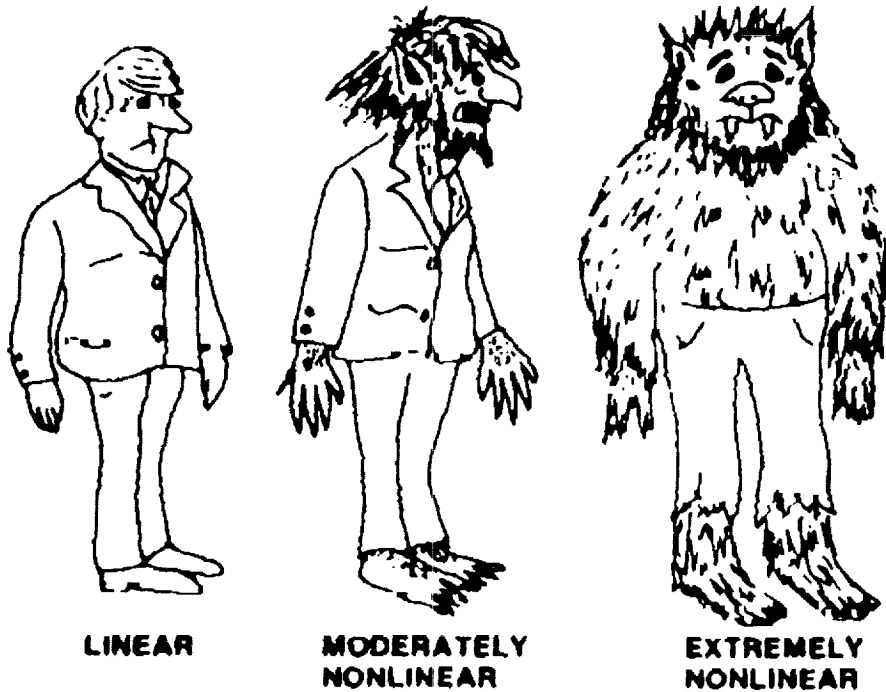
There are three distinct behavioral regions that must be considered when performing a crash simulation.

- A model for crash simulation can be separated into three distinct modeling regions
 - linear
 - moderately nonlinear
 - extremely nonlinear
- Pictorially this is shown on the next visual.

BEHAVIOR ZONE CHARACTERISTICS

Yes, modeling the extremely nonlinear crushing regions is still a monster!

BEHAVIOR ENCOUNTERED IN CRASH SIMULATION



BEHAVIOR ZONE CHARACTERISTICS - LINEAR

Modeling the linear zone is obvious. Use as little computational resources as necessary.

- **Linear zone**
 - elastic
 - small deflection
- **Modeled with**
 - rigid bodies with lumped mass
 - relatively few elastic finite elements
 - substructure; most dof's omitted

BEHAVIOR ZONE CHARACTERISTICS - MODERATELY NONLINEAR

These areas begin to be computationally expensive. Current technology in nonlinear structural mechanics is in place to adequately treat these regions. Allow for any possible global collapse modes.

- Moderately nonlinear
 - elasto-plastic
 - large displacements on the global scale
- Modeled with
 - nonlinear finite elements
 - allowance for possible global collapse modes

BEHAVIOR ZONE CHARACTERISTICS - EXTREMELY NONLINEAR

These are the very difficult and computationally intensive areas to model. These areas often involve special energy absorbing components that exhibit large deformation on a local scale. The bottom line is that these parts require very detailed FEM models.

- Extremely nonlinear
 - large deflection on a local scale, i.e., accordion folding of metallic structural components, crushing of subfloor structure in aircraft, local deformation and failure of composites
 - specially designed energy absorbing structure
 - crushable nonstructural parts
 - requires fine model (thousands of dof's)

BEHAVIOR ZONE CHARACTERISTICS - EXTREMELY NONLINEAR (Continued)

In the past these areas were exclusively modeled with nonlinear spring elements. The explicit codes currently used make use of a detailed representation of highly nonlinear regions in automobile structural components. However, there still may be areas of a built-up structure that are currently not amenable to detailed modeling. This is particularly true for aircraft structures that involve complex energy absorbing floor concepts. Composites offer new challenges in detailed modeling of crushable components. More research is required in this area before viable crash simulation is feasible.

- Modeled with:

- Nonlinear spring elements

- Spring properties from test or other analysis require intimate understanding of the structural and material behavior

- Detailed discrete representation??

- Trade-off between "hybrid" model and detailed nonlinear finite element model

MODELING CRASHWORTHINESS OF COMPOSITE STRUCTURES

In modeling the behavior of a composite airframe under impact conditions, the levels to which material failure must be included are far more detailed than for metallic airframes. In a traditional airframe, material failure modes which influence the structural failure process are primarily ductile crack growth and tearing and ductile rupture. Each of these is a distinct failure which renders a region of the structure incapable of transmitting any load. Just as important, because of the ductile nature of the material, significant impact energy can be absorbed by the material prior to failure. In laminates composed of graphite-epoxy lamina, failure at the material level is primarily brittle with very little prefailure energy absorption. For composite laminates, impact induced material damage modes such as matrix cracking and delamination lead to a structural material which still can transmit load, albeit at a reduced ultimate level and with a reduced stiffness and cross-sectional modulus. Thus, local material failures can have significant impact on the mode of structural failure.

Because sublaminates material failure in composite laminates can propagate over large regions without leading to total laminate failure, the overall structural failure mode can be significantly altered. Buckling and collapse modes are highly dependent on the modulus and bending stiffness of the structural cross section. Zones of highly degraded material stiffness caused by fiber breaking/buckling, delamination, and matrix microcracking can thus cause structural failure modes significantly different than those seen in an undamaged structure of the same laminate construction.

- Composite aircraft structures pose new computational and modeling challenges for crashworthiness design and analysis
 - brittle failure
 - diverse failure mechanisms
 - adhesive joints
 - three-dimensional effects in thick laminates
- Failure modes in composite structures
 - buckling/collapse
 - fiber breakage (local)
 - delamination (structural)
 - microcracking (local and structural)
- Material failure can change the buckling/collapse behavior

MODELING CRASHWORTHINESS OF COMPOSITE STRUCTURES CURRENT RESEARCH DIRECTIONS

As a first step in modeling the crashworthiness of composite structures, a progressive failure algorithm was implemented into the DYCAST code. This entailed introducing capability to describe classical laminate behavior, i.e., building a laminate from individual ply properties and orientation. This leads to the usual integrated material stiffness matrices; $[A]$, the in-plane stiffness matrix, $[D]$, the bending stiffness matrix, and $[B]$, the matrix that couples the in-plane and bending behavior of the laminate for unsymmetric lay-ups.

Initially three maximum strain failure criteria were implemented. These are described in the next figure. Currently, a strain based criterion based on the theory proposed by Christensen is being implemented and tested (see subsequent figures).

Nonlinear material behavior was also investigated by implementing the Sandhu method for nonlinear composite materials. This method uses four uni-axial curves to define material behavior; two direct stress versus strain, shear stress versus shear strain and the variation of Poisson's ratio versus strain. Further investigation must be made of the effect of matrix material nonlinearities.

- In response to the program directions set by the Impact and Dynamics Branch at NASA LRC, the following enhancements are being incorporated into DYCAST:
 - Ply-by-ply progressive failure laws
 - maximum strain
 - Christensen strain-based quasi three-dimensional
 - Tsai-Wu
 - Nonlinear material behavior
 - Sandhu method for nonlinear composite materials
 - nonlinear elastic shear response
 - ? matrix plasticity

MAXIMUM STRAIN FAILURE CRITERIA

The table below describes the three maximum strain failure criteria initially implemented into the DYCAST code. The first two are for uni-directional composites and the third is for a fabric composite. The failure criterion chosen is checked at each finite element stress integration point in each ply of the built-up laminate. As indicated in the figure below, when fiber failure is detected, the moduli E_{11} and Poisson's ratio, ν_{12} as well as the stress, σ_{11} , are set to zero. Similar procedures are followed for matrix and shear failure. Options 2 and 3 are similar to option 1 but add an induced coupling based on heuristic arguments that, for example, fiber failure induces shear ineffectiveness. Based on these considerations, the [A], [D], [B] matrices are reformulated and reflect the progressive softening of the damaged structure.

	Option 1 (Unidirectional Composite)		Option 2 (Unidirectional Composite)		Option 3 (Fabric Composite)	
Primary Failure Direction *	Induced Additional Failure	Zeroed Out Quantities	Induced Additional Failure	Zeroed Out Quantities	Induced Additional Failure	Zeroed Out Quantities
Fiber Failure, $\epsilon_{11} = \epsilon_{11}$ FAIL	None	E_{11}, ν_{12} σ_{11}	Shear	E_{11}, G_{12}, ν_{12} σ_{11}, τ_{12}	Shear	E_{11}, G_{12}, ν_{12} σ_{11}, τ_{12}
Matrix or Fiber Failure**, $\epsilon_{22} = \epsilon_{22}$ FAIL	None	E_{22}, ν_{12} σ_{22}	Shear	E_{22}, G_{12}, ν_{12} σ_{22}, τ_{12}	Shear	E_{22}, G_{12}, ν_{12} σ_{22}, τ_{12}
Shear Failure**, $\gamma_{12} = \gamma_{12}$ FAIL	None	G_{12} τ_{12}	Matrix	G_{12}, E_{22}, ν_{12} τ_{12}, σ_{22}	Fiber	$G_{12}, E_{11}, E_{22},$ $\nu_{12}, \tau_{12}, \sigma_{11}$ σ_{22}

* The subscript FAIL on ϵ_s denotes prescribed failure strain. Here, primary means the failure that induces the additional failures.

** Note that with Option 2, primary matrix and shear failures lead to the same overall failure mode.

Fiber failure pertains only to Option 3

CHRISTENSEN STRAIN-BASED FAILURE CRITERION

New strain-based failure laws are being explored. Criteria used to decide on the failure law to be implemented were based on considerations for modeling progressive failure of modern composites under impact loading. With the application of thicker section laminate constructions and more ductile fiber-matrix systems, it is felt that strain-based theories which clearly delineate between fiber failure and fiber-matrix interaction failure are essential for accurate modeling of progressive lamina failures. In addition, the failure law should be capable of including three-dimensional strain and stress states typical of thick section laminate constructions.

- New strain-based failure criterion:
 - applicable to more ductile lamina
 - based on Christensen's quasi-three-dimensional laminate theory
 - coupled theory, interactions of strain (stress) components
 - clearly delineates between fiber failure and fiber/matrix interaction failure

CHRISTENSEN STRAIN-BASED FAILURE CRITERION (Continued)

The failure criterion shown below is a modification of one first proposed by Christensen. In this law, e_{ij} is the dilatation (first invariant strain) and ϵ_{KK} is the deviatoric strain. We have added the term $\beta \epsilon_{KK}^2$, the quadratic deviatoric component which was not included in Christensen's work. This allows us to have different transverse failure strains in tension and compression, a necessary feature to reproduce failure in most lamina constructions.

- CHRISTENSEN FAILURE CRITERION:

- Fiber failure

$$\epsilon_f \geq \epsilon_{11} \geq \epsilon_f^*$$

- Fiber/Matrix Interaction Failure

$$\alpha \epsilon_{KK} + \beta \epsilon_{KK}^2 + e_{ii} e_{jj} = \kappa^2$$

α , β , κ are determined by simultaneously fitting to three failure states usually shear in the 1-2 plane, and positive and negative stress transverse to the fiber direction.

INITIAL STUDIES OF PROGRESSIVE FAILURE OF COMPOSITE AIRCRAFT COMPONENTS

The figure below summarizes the initial capabilities developed to simulate the impact behavior of a composite aircraft structural component.

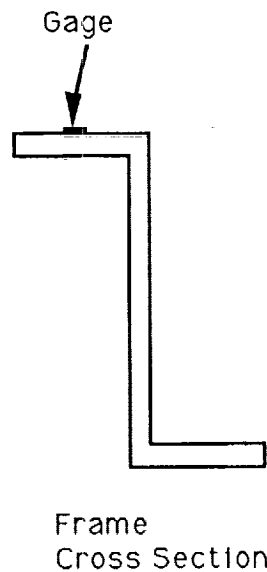
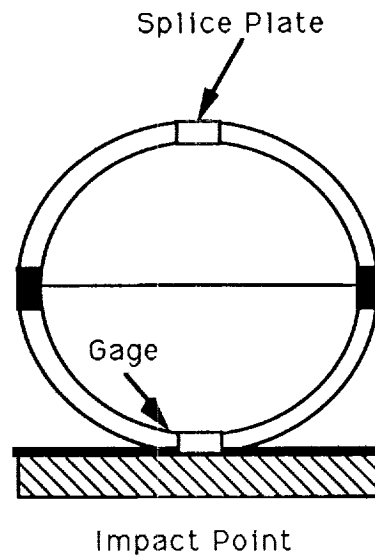
- Classical Composite Laminate Theory
 - composite laminate can be built up layer-by-layer by specifying materials moduli, angle of orientation and stacking sequence of each ply
 - each layer can be linear elastic or elasto-plastic
 - maximum strain failure criteria for continuous filament reinforced composite material
- Implemented into a three-node DKT triangular element in DYCAST code
- Used to simulate NASA drop test of Z-section graphite epoxy frame

NASA DROP TEST OF A Z-SECTION GRAPHITE-EPOXY CIRCULAR FRAME

This test program is described in "Drop Test and Analysis of Six-Foot Diameter Graphite-Epoxy Frames," by Richard L. Boitnott and Huey D. Carden, presented at the AHS National Specialists' Meeting on Crashworthy Design of Rotorcraft, April 7-9, 1986. The key features of the test are summarized below. The Z-section frame was constructed from four 90-degree sections that were attached by splice plates. The laminated composite material was constructed of graphite-epoxy fabric. Another feature which added to the computational difficulties was a rear steel restraining plate and forward plexiglass plate. The purpose of the plates was to restrain lateral motion. Consequently, contact conditions had to be described between these plates and the forward and rear face of the Z-section flanges.

- Five graphite-epoxy frames were dropped onto a concrete floor
- Tests were performed at NASA LRC Impact and Dynamics Branch under the supervision of Huey Carden and Richard Boitnott
- Complete frames were fabricated from four 90-degree sections and joined with splice plates
- Z-section cross-sections typical of fuselage structure of advanced composite transport aircraft
- Lateral motions were restrained by a plexiglass and a steel plate
- Impact was at a splice plate
- Impact speed was 27.5 FPS
- Twenty pounds of added weight at the floor beam

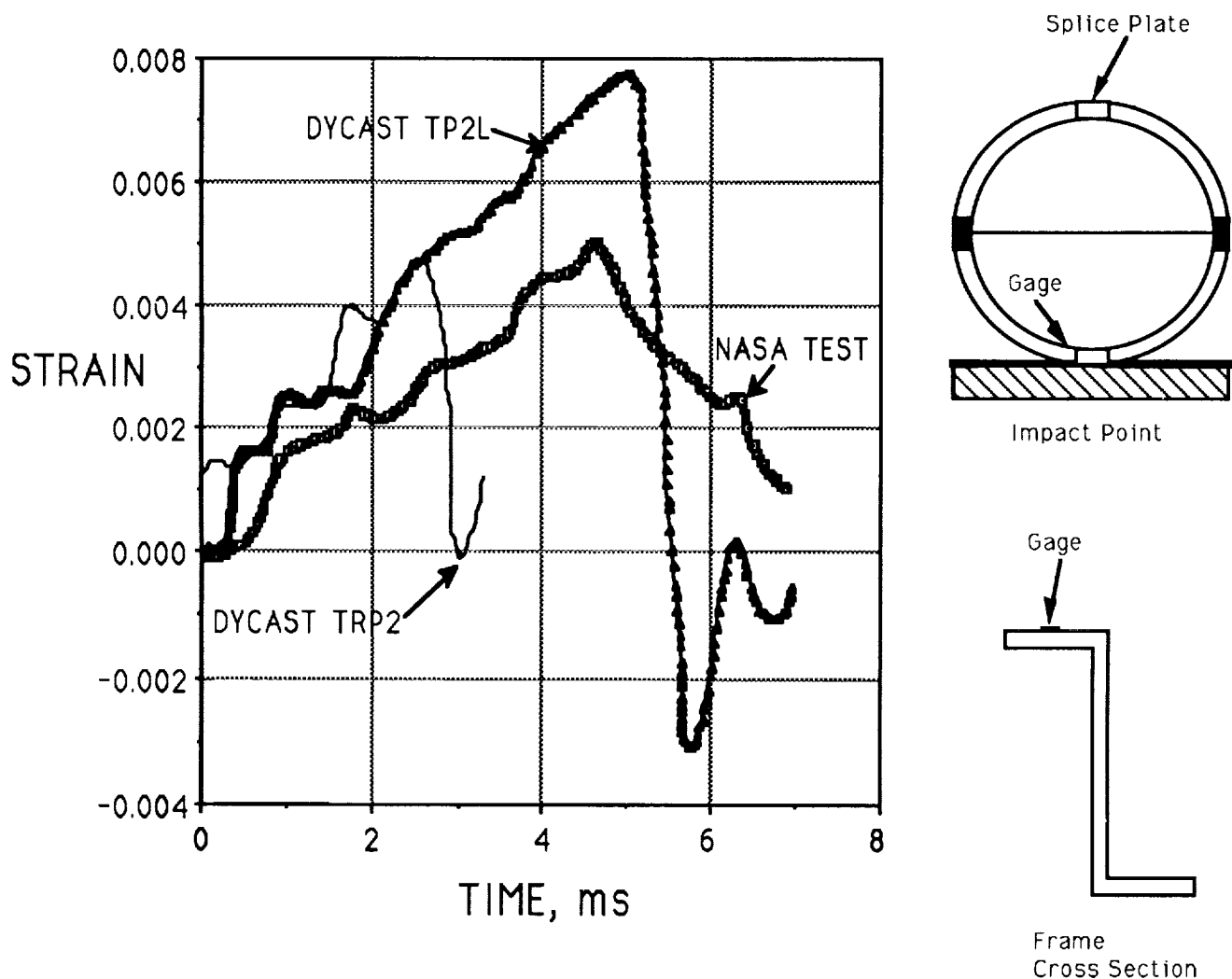
This figure shows the general configuration of the frame. The frame was modeled with DKT triangular finite elements with the material characteristics described above. A number of models were investigated. The final model used eight elements through the web at the point of contact. The model progressively was made coarser away from the contact point. Beam elements were used in the upper quadrant. The final model of one-half of the frame had 867 nodes, 2108 elements, and 5133 degrees of freedom.



PROGRESSIVE FAILURE OF LAMINATED COMPOSITES

This figure shows a strain trace at the impact point at the inner flange. The location of the strain gage is shown on the previous figure. The comparison indicates that the essential features of the response were predicted. The time and location and progression of failure also approximated the simulation of a composite aircraft structure. However, it should be pointed out that the test involved a number of features that increased the difficulty of the analysis so that the primary behavior was not composite failure alone. These are: contact between the frame and the face plates, unknown friction coefficient, stiffness of the splice plates. Consequently, further analysis and tests on simpler components must be performed in order to investigate the use of composite failure criteria in a crash simulation.

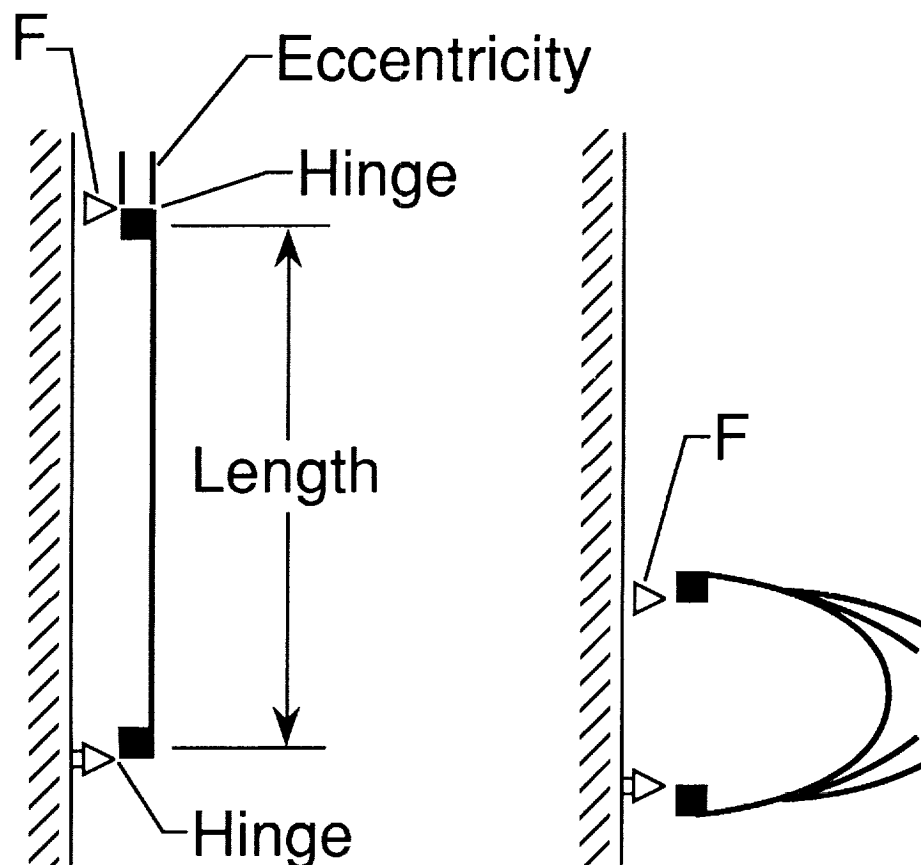
Graphite-Epoxy Fuselage Frame Drop Test



STRUCTURAL IMPACT OF A/C COMPOSITES

This figure outlines areas of continued research.

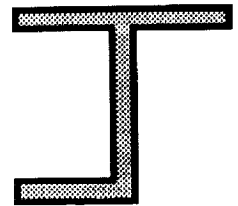
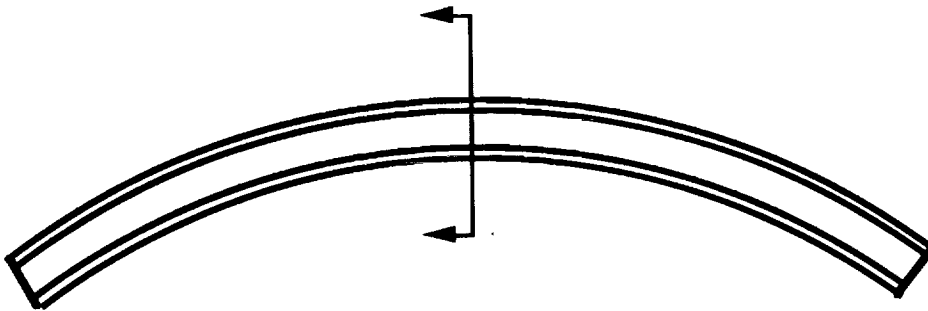
- Improved composite failure criteria
 - New, fully interactive strain-based Christensen lamina failure criterion to be tested in DYCAST
 - Distinction between fiber and matrix failure modes maintained
 - Evaluate by simulating NASA experiments



NONLINEAR COMPOSITE BEAM ELEMENT

A curved open-section composite beam element has been developed. Each flange and web can be described as a distinct laminate construction.

- Nonlinear, composite finite element developed for DYCAST Code
 - Applicable to curved, thin-walled beam/columns with open cross-section typical of aircraft frames and stiffeners
- Each individual flange and web can be a distinct laminate composite construction



NONLINEAR COMPOSITE BEAM ELEMENT

Future work will involve applying failure criterion to each ply of the laminate web or flanges. Ultimately, a more detailed global/local representation must be developed to account for local three-dimensional effects at the point of impact.

- Material behavior
 - Laminate composite
- Failure criteria can be applied to each ply of flange/web defining progressive failure during crash loading



STUDY OF THE EFFECT OF SHEAR STRESS/STRAIN NONLINEARITY ON IMPACT BEHAVIOR

The next four figures illustrate the influence of material nonlinear behavior and failure mode on the dynamic buckling and collapse behavior of composite shells. To examine this, we consider a cylindrical shell with diaphragm ends constructed of typical graphite epoxy lamina with a $[0,90,45,-45]_s$ construction. The shell is subjected to a hydrostatic step wave pressure loading. Under crash conditions, one would like to have the energy absorption mechanisms for the structure contained in localized "failure" zones with the remainder of the structure experiencing little catastrophic damage. To examine the role of nonlinear material behavior, we compared the effects of composite failure and shear stress-strain nonlinearity. The composite failure law used is the modified Christensen law described previously and material nonlinearity was treated by the simple cubic shear stress-strain law due to Tsai and Hahn shown below.

- Nonlinear shear stress strain behavior can significantly alter the dynamic buckling behavior of composites structures
- Example:
 - cylindrical shell with diaphragm ends
 - subjected to a step hydrostatic pressure loading
- Used Tsai-Hahn stress strain relation

$$\gamma_{12} = [G_{12}^{-1} + 3S_{66}\tau_{12}^2] \tau_{12}$$

$$G_{12} = 0.71 \times 10^6$$

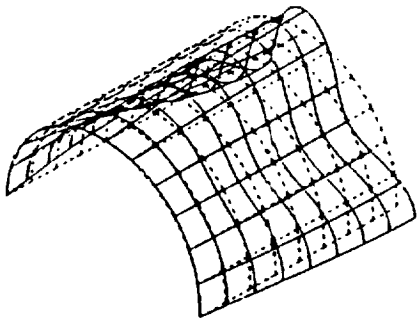
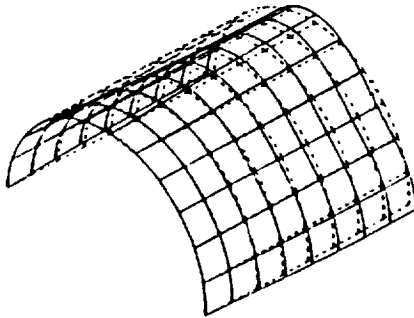
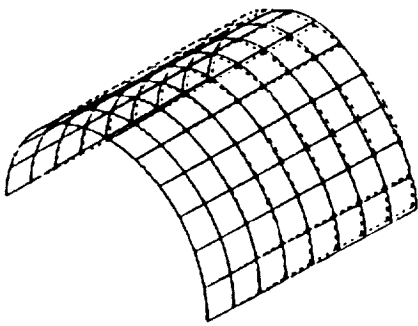
STUDY OF THE EFFECT OF SHEAR STRESS/STRAIN NONLINEARITY ON IMPACT BEHAVIOR (Continued)

The effect of shear stress nonlinearity is summarized below and shown on the next visual.

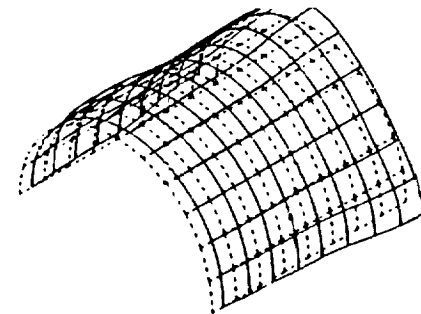
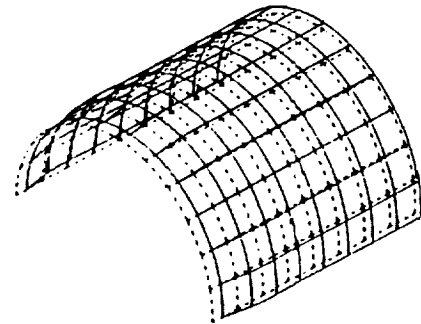
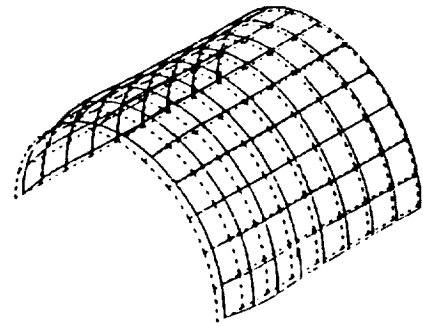
- Under hydrostatic, step wave loading, the dynamic collapse occurs in a mode dominated by the first bifurcation buckling mode of the linearly elastic structure if the degree of shear nonlinearity is small
- For large shear nonlinearities, the collapse resembles a plastic instability mode rather than a bifurcation buckling mode
- Energy absorption and force transmittal characteristics for these two modes are quite different and may lead to different crash behavior

STUDY OF THE EFFECT OF SHEAR STRESS/STRAIN NONLINEARITY ON IMPACT BEHAVIOR (Continued)

Two sets of results are shown below. On the left are results for essentially linearly elastic response with the parameter S_{66} in the Tsai-Hahn relation set equal to 0.5×10^{-13} . The set on the right increases the level of nonlinearity by setting S_{66} to 0.5×10^{-10} . As can be observed, a transition occurs with the increase in shear nonlinearity from a traditional buckling mode as shown on the left to a mode that is more characteristic of a general collapse as shown on the right. The general collapse mode in which there is a larger observed region of high "failure" strains around the circumference of the shell is far more damaging to the shell. These initial considerations indicate that material characterization and an understanding of the material behavior during impact conditions is an important consideration in predicting structural response to a crash loading situation.



$$S_{66} = 0.5 \times 10^{-13}$$

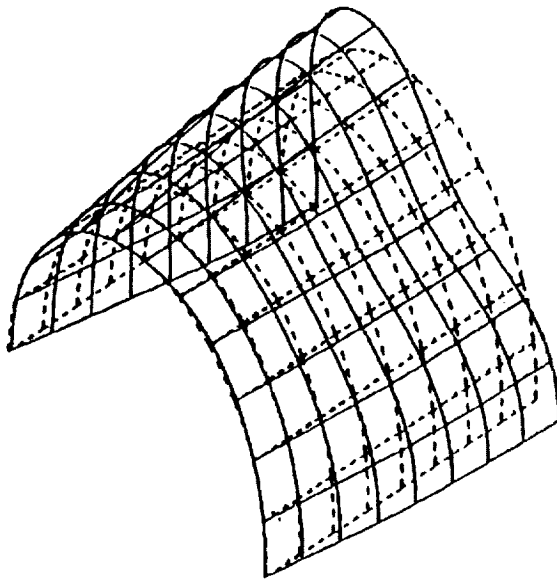


$$S_{66} = 0.5 \times 10^{-10}$$

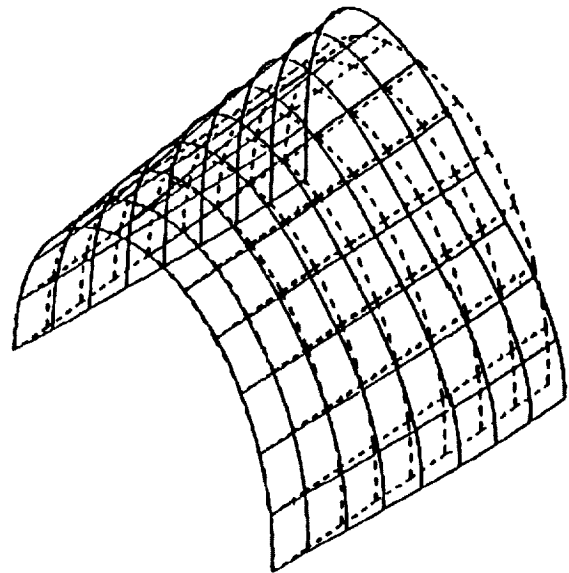
EFFECT OF FAILURE STRAIN ON MODE OF DEFORMATION

This figure shows the effect that the mode of failure has on the structural response. The figure on the right shows the response of the shell when published values of fiber failure are used in the analysis. Once again the modified Christensen failure law is used. In this case, initial matrix failure occurs which quickly spreads through the cross-section near the center of the shell. The observed failure (shown on the right) is similar to a collapse mode shown previously. If the fiber failure strain is reduced so that fiber failure occurs first, then the failure mode is more predominately like a buckling mode as seen in the figure on the left.

In the designing of aircraft structures for impact, it is crucial that the dynamic collapse behavior of the primary structural components be in modes not highly prone to distributing material failure. As has been shown, this requires a thorough understanding of the material behavior when subjected to impact loadings.



FIBER FAILURE



MATRIX FAILURE

SUMMARY

There are four points made below. Before we can simulate the behavior of composite structures due to impact loading in order to evaluate crashworthiness, the material and laminate phenomena must be identified and understood. Carefully controlled test programs must be designed in order to achieve these goals. Because of the complexity of phenomena and the current status of computational techniques, there still is a "trade-off" between detailed finite element modeling and "hybrid" modeling of energy absorbing structures constructed of composite materials. This may also be true for metallic aircraft structures.

- It is essential to characterize the progressive failure behavior of laminated composite materials subjected to impact loadings and to implement this capability into finite element simulation codes
- Carefully controlled tests of composite components must be performed to better understand modes of failure, energy absorbing capabilities and to provide data for correlation with crash simulation codes
- There still may be a "trade-off" between detailed finite element and hybrid modeling of laminated composite material in some sections of the structure
- It is essential that crashworthiness be incorporated into the structural design for composite materials

54-39
187835
N94-19469

**Development and Use of Computational Techniques in
Army Aviation R&D Programs for Crash Resistant
Helicopter Technology**

LeRoy T. Burrows
Aviation Applied Technology Directorate
U.S. Army Aviation Systems Command
Fort Eustis, VA

INTRODUCTION

During the 1960's over 30 full-scale aircraft crash tests were conducted by the Flight Safety Foundation under contract to the Aviation Applied Technology Directorate (AATD) of the U.S. Army Aviation Systems Command (AVSCOM). The purpose of these tests were to conduct crash injury investigations that would provide a basis for the formulation of sound crash resistance design criteria for light fixed-wing and rotary wing aircraft. This resulted in the Crash Survival Design Criteria Designer's Guide which was first published in 1967 and has been revised numerous times, the last being in 1989 (Ref. 1). Full-scale aircraft crash testing is an expensive way to investigate structural deformations of occupied spaces and to determine the decelerative loadings experienced by occupants in a crash. This gave initial impetus to the U.S. Army to develop analytical methods to predict the dynamic response of aircraft structures in a crash. It was believed that such analytical tools could be very useful in the preliminary design stage of a new helicopter system which is required to demonstrate a level of crash resistance and had to be more cost effective than full-scale crash tests or numerous component design support tests. From an economic point of view, it is more efficient to optimize for the incorporation of crash resistance features early in the design stage. However, during preliminary design it is doubtful if sufficient design details, which influence the exact plastic deformation shape of structural elements, will be available. The availability of simple procedures to predict energy absorption and load-deformation characteristics will allow the designer to initiate valuable cost, weight and geometry tradeoff studies. The development of these procedures will require some testing of typical specimens. This testing should, as a minimum, verify the validity of proposed procedures for providing pertinent nonlinear load-deformation data. It was hoped that through the use of these analytical models, the designer could optimize aircraft design for crash resistance from both a weight and cost increment standpoint, thus enhancing the acceptance of the design criteria for crash resistance.

PRECEDING PAGE BLANK NOT FILMED

96

INTENTIONALLY BLANK

SYSTEMS APPROACH TO CRASH RESISTANCE

For maximum effectiveness, design for crash resistance dictates that a total systems approach be used and that the designer consider survivability issues in the same light as other key design considerations such as weight, load factor, and fatigue life during the initial design phase of the helicopter. Figure 1 depicts the system's approach required relative to management of the crash energy for occupant survival for the vertical crash design condition. The crash G loads must be brought to within human tolerance limits in a controlled manner to prevent injury to the occupants. This can be accomplished by using the landing gear, floor structure, and seat to progressively absorb most of the crash energy during the crash sequence. Thus, the occupant is slowed down in a controlled manner by stroking/failing the landing gear, crushing the floor structure, and stroking the seat at a predetermined load before being subjected to the crash pulse which by then has been reduced to within human tolerance limits. In addition, the large mass items such as the overhead gearbox are arrested by stroking/failing of the landing gear or fuselage structure, and in some cases, by stroking of the gearbox within its mounts. In this example, assuming that the landing gear has been designed to meet the minimum requirements of MIL-STD-1290A, i.e., 20 ft/sec, the fuselage would be decelerated to approximately 37 ft/sec at the time of contact with the surface. The Army's most recent helicopters, the UH-60 Black Hawk and AH-64 Apache, are both designed generally in accordance with the requirements of MIL-STD-1290A.

- LANDING GEAR
- SEATS
- FUSELAGE STRUCTURE
- OTHER

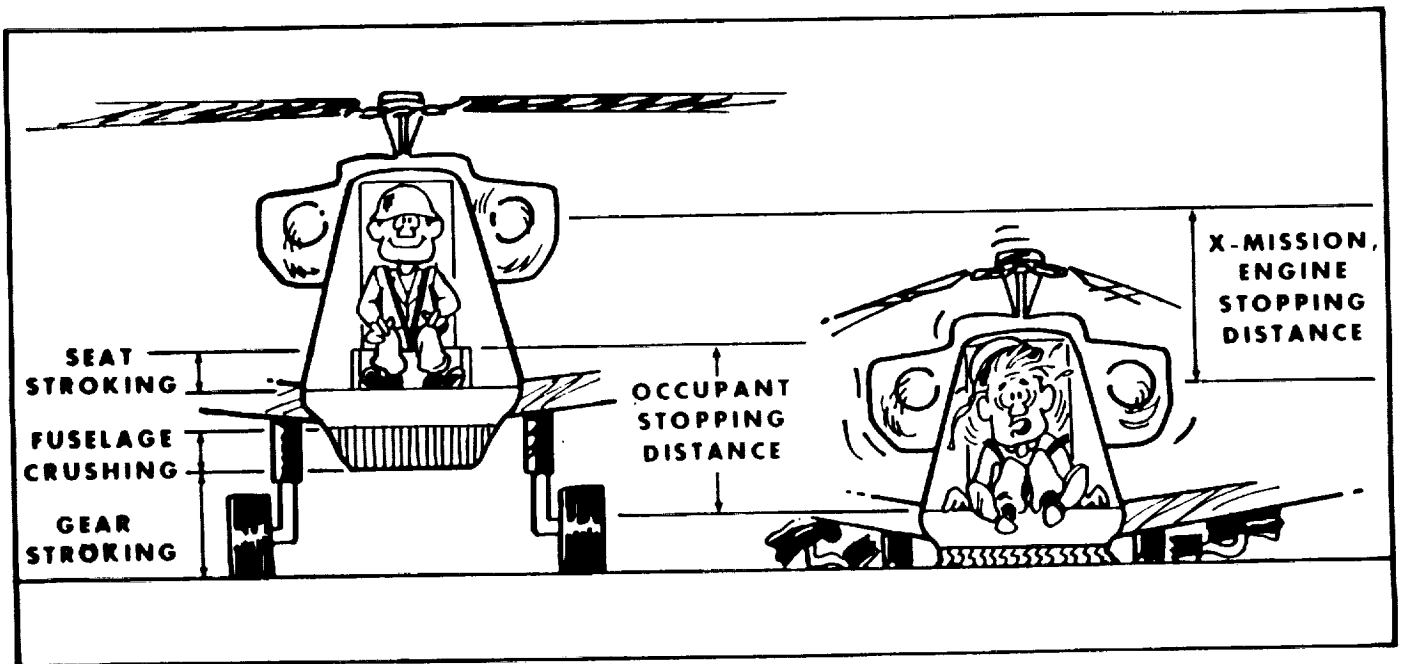


Figure 1 - Energy Management System

MODEL KRASH DEVELOPMENT

Figure 2 depicts the chronology of the development of model KRASH which is the most commonly used computer analysis of the dynamic response of aircraft structure during a crash impact. Model KRASH represents the structure with beam elements, crushable springs and lumped masses. It is intended to provide designers with simplified techniques with which to perform crashworthiness studies during the aircraft preliminary design phase.

In any crash resistant aircraft design a total systems approach must be employed to determine the most effective mix of energy attenuation from the landing gear, airframe structure and stroking seat. This is where program KRASH can allow you to quickly assess the relative effects of different energy attenuating component mixes, thus pointing the way to an optimized system design for crash resistance.

• DYNAMIC SCIENCE/US ARMY	1969-1971
• LOCKHEED/US ARMY	1972-1974
• LOCKHEED/FAA	1975-1990
• DRI/FAA/NAVY	1990-1991
• US ARMY R&D PROGRAMS	1975-1992
• IR&D EFFORTS	1980-1992

Figure 2 - Model KRASH Development

KRASH MODEL CORRELATION

As part of the development of KRASH, full-scale UH-1 cabin floor sections were crash tested to determine the load-deflection characteristics of the subfloor springs. In addition, a full-scale UH-1 was crash tested to help develop and validate the KRASH model (Fig. 3). Later, each time an aircraft was to be crash tested by the U.S. Army, whatever the reason, the aircraft would be modeled for the planned impact conditions using KRASH before the test and then the results would be compared to the test data and post test structure deformation. Using the actual impact conditions, if different, along with test results, the KRASH program would be exercised to fit the actual test and result. This empirical approach to improving the model or to just better understand influences of various structural concepts was used in full-scale testing of both the Bell and Sikorsky Advanced Composite Aircraft Program (ACAP) helicopters. The latter two tests were unique in that they provided the utility of model KRASH for composite structures.

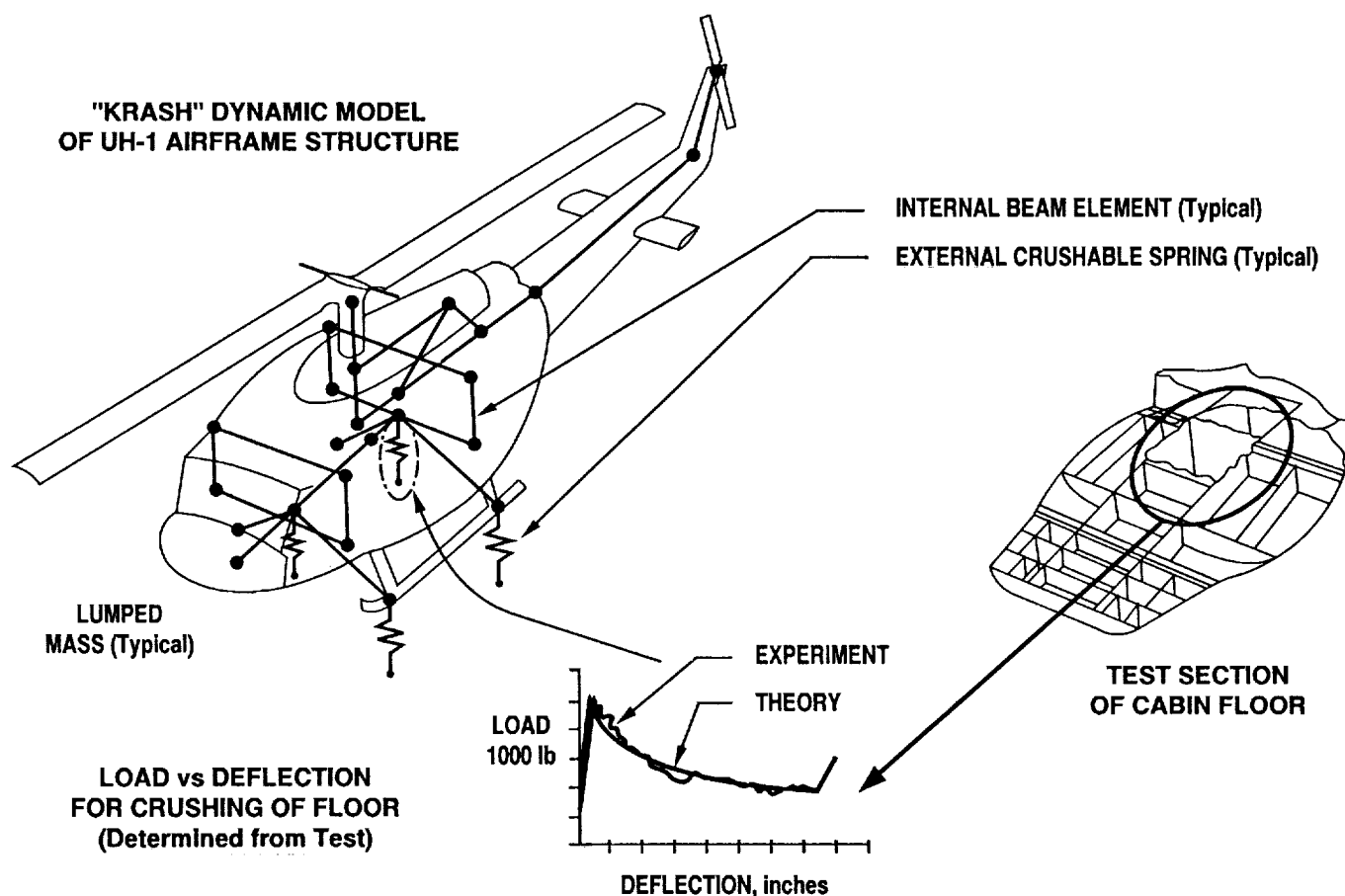


Figure 3 - KRASH Model Correlation

DESIGN SUPPORT TESTING TO SUPPORT ANALYSIS

KRASH is being used worldwide and has proven to be a useful tool in the preliminary design process for crash resistance in new rotorcraft. However, in preliminary design, energy absorbing subfloor spring constants are assumed based upon elemental structural test data, sometimes not much more than coupon specimen data. All too often, once the preliminary design advances into detail design and some elemental design support testing is conducted, it is found that the structural concept does not perform correctly and that the spring constants used initially are very difficult if not impossible to obtain within the structure weight allocated. This leads the designer into a trial and error design support test effort (see Fig. 4) with associated high costs, to obtain the elusive good crash initiators, good energy attenuation and a nice rectangular load-deflection relationship. Since this seems to be the case almost all the time, especially with composite structures, it seems that if we could develop a database from all this trial and error testing and make it available to all designers, we could significantly reduce the duplication of test effort that is currently going on with all kinds of test specimens. Furthermore, the analyst could use these test data as an empirical base to develop finite element models of the structural elements, thus reducing design support testing, though ultimately the final design would still have to be tested under realistic impact conditions. The sharing of data and increased use of analytical models will permit crash resistance component design formulation in less time at far less cost.

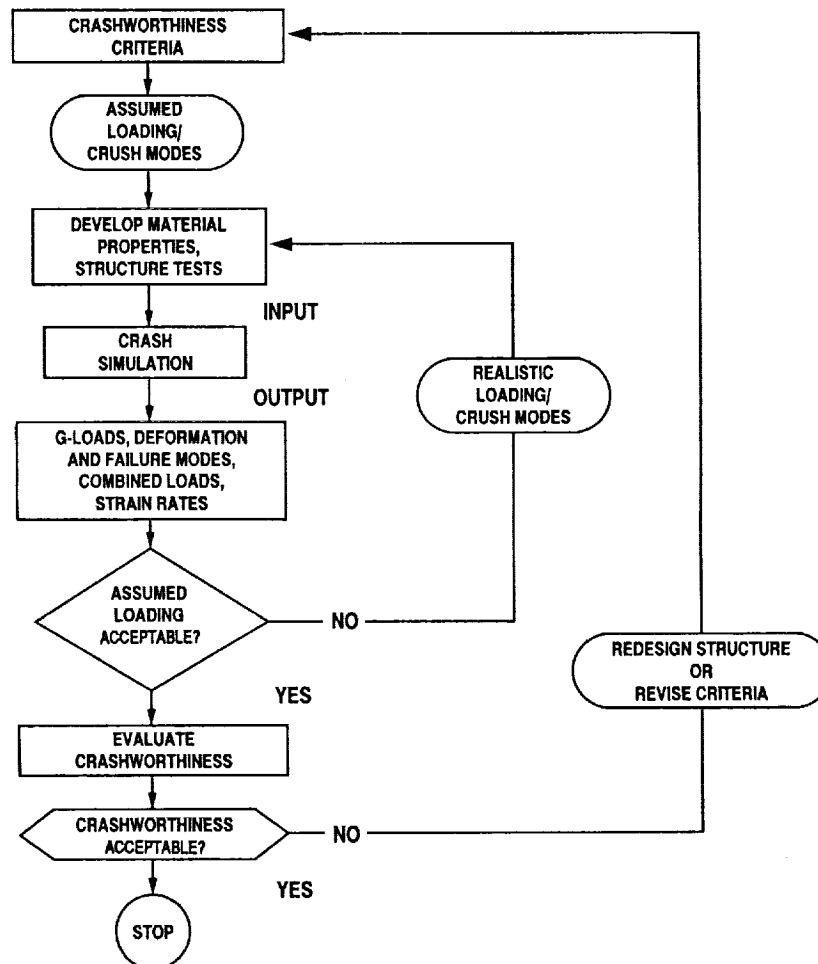


Figure 4 - Analysis/Test Logic Path

SOM-LA

Program SOM-LA (Seat/Occupant Model-Light Aircraft) has been developed for use in evaluating the crashworthiness of aircraft seats and restraint systems. It combines a three-dimensional dynamic model of the human body with a finite element model of the seat structure. It is intended to provide the design engineer a tool with which he can analyze the structural elements of the seat as well as evaluate the dynamic response of the occupant during a crash.

The occupant model consists of 12 masses that represent the upper and lower torso, neck, head, and two segments for each of the arms and legs. An optional model of the human body includes beam elements in the spine and neck, but is restricted to two-dimensional motion.

External forces are applied to the occupant by the cushions, floor and restraint system. Interface between the occupant and seat is provided by the seat bottom cushion, back cushion, and an optional headrest. The restraint system can consist of a lap belt alone or combined with a single shoulder belt, over either shoulder, or a double-strap shoulder harness. A lap belt tiedown strap, or negative G strap, can also be included. Each component of the restraint system can be attached to either the seat or the aircraft structure. SOM-LA is summarized in Fig. 5.

- **FINITE ELEMENT MODEL OF SEAT**
- **DYNAMIC MODEL OF 50TH PERCENTILE HUMAN MODEL AND ANTHROPOMORPHIC DUMMY**
- **GIVES STRUCTURAL BEHAVIOR OF SEATING AND RESTRAINT SYSTEMS UNDER TRANSIENT DYNAMIC LOADING CONDITIONS**
- **CAPABLE OF PREDICTING SEAT STROKE, OCCUPANT MOTIONS, OCCUPANT-FLOOR, OCCUPANT-CUSHION, AND OCCUPANT-RESTRAINT FORCES**
- **CAN ACCEPT ANTHROPOMETRY INPUT**
- **CANNOT ACCEPT FORCES OF OCCUPANT CONTACT WITH SURROUNDING STRUCTURE**

Figure 5 - Seat Occupant Model/Light Aircraft (SOM-LA)

ARTICULATED TOTAL BODY MODEL

The Articulated Total Body (ATB) Model is primarily designed to evaluate the three-dimensional dynamic response of a system of rigid bodies when subjected to a dynamic environment consisting of applied forces and interactive contact forces. Although the ATB Model was originally developed to model the dynamic response of crash dummies and, with later modifications, the response of the human, the ATB Model is quite general in nature and can be used to simulate a wide range of physical problems that can be approximated as a system of connected or free rigid bodies.

The approach used in the ATB Model to model the human or manikin body (the "body" in the ATB Model simulation) is to consider the body as being segmented into individual rigid bodies (the "segments" in the ATB Model) each having the mass of the body between body joints or, in the case of single-jointed segments, such as the foot, distal to the joint. An example would be the left upper arm segment, which represents the mass of the body between the shoulder joint and elbow joint. Segments are assigned mass and moments-of-inertia and joined at locations representing the physical joints of the human body, such as the shoulder joint or the knee joint. For the ATB Model the Generator of Body Data (GEBOD) is a source of anthropomorphic data for the zero to 100th percentile male, female, infant, child and dummy. These data include body masses, moment-of-inertia, and c.g.'s.

A personal computer version of ATB is named DYNAMAN which along with the ATB model has been useful in R&D programs to delethalize the helicopter cockpit. The ATB model is summarized in Fig. 6.

- **PREDICTS GROSS HUMAN BODY RESPONSE TO VARIOUS DYNAMIC ENVIRONMENTS**
- **CAN ACCEPT INPUT OF STROKING SEATS AND RESTRAINTS**
- **GEOMETRIC BODY MODELER (GEBOD) IS A SOURCE OF A WIDE RANGE OF ANTHROPOMORPHIC DATA INPUT**
- **CAN PREDICT CONTACT FORCES ON OCCUPANT**

Figure 6 - Articulated Total Body Model

REFERENCES

1. Desjardins, S., et al, Aircraft Crash Survival Design Guide, USAAVSCOM TR-89-D-22A through E, 5 volumes, Dec. 1989.
2. Gatlin, C., et al, Analysis of Helicopter Structural Crashworthiness, Vol. I - Mathematical Simulation and Experimentation Verification for Helicopter Crashworthiness, and Vol. II - User Manual for "Crash," A Computer Program for the Response of a Spring-Mass System Subjected to One-Dimensional Impact Loading (UH-1D/H Helicopter Application), USAAVLABS TR-70-71A and 71B, Jan. 1971.
3. Wittlin, G. and Gamon, M., Experimental Program for the Development of Improved Helicopter Structural Crashworthiness Analytical and Design Techniques, Vol. I - Computerized Unsymmetrical Mathematical Simulation and Experimental Verification for Helicopter Crashworthiness in which Multidirectional Impact Forces are Present, and Vol. II - Test Data and Description of an Unsymmetrical Crash Analysis Computer Program, Including a User's Guide and Sample Case, USAAMRDL TR-72-72A and 72B, May 1973.
4. Wittlin, G. and Park, K., Development and Experimental Verification of Procedures to Determine Nonlinear Load-Deflection Characteristics of Helicopter Substructures Subjected to Crash Forces, Vol. I - Development of Simplified Analytical Techniques to Predict Typical Helicopter Airframe Crushing Characteristics and the Formulation of Design Procedures, Vol. II - Test Data and Description of Refined Program "KRASH" Including a User's Guide and a Sample Case, USAAMRDL TR-74-12A and 12B, May 1974.
5. Badrinath, Y., Simulation, Correlation and Analysis of the Structural Response of a CH-47A to Crash Impact, USARTL-TR-78-24, Aug. 1978.
6. Berry, V. and Cronkhite, J., YAH-63 Helicopter Crashworthiness Simulation and Analysis, USAAVRADCOM-TR-82-D-34, Feb. 1983.
7. Cronkhite, J., et al, Investigation of the Crash Impact Characteristics of Advanced Airframe Structures, USARTL-TR-79-11, Sept. 1979.
8. Cronkhite, J. and Berry, V., Investigation of the Crash Impact Characteristics of Helicopter Composite Structures, USAAVRADCOM-TR-82-D-14, Feb. 1983.
9. Cronkhite, J., et al, Crashworthy Composite Structures, USAAVSCOM-TR-87-D-10, Dec. 1987.
10. Sen, J., Advanced Technology Landing Gear, USAAVSCOM-TR-89-D-13A and 13B, Aug. 1990.
11. Laananen, D., et al, Computer Simulation of an Aircraft Seat and Occupant in a Crash Environment, Vol. I - Technical Report, and Vol. II - Program SOM-LA Users Manual, DOT/FAA/CT-82/33-1 and 33-11, March 1983.
12. Bark, L. and Lou, K., Comparison of SOM-LA and ATB Programs for Prediction of Occupant Motions in Energy Absorbing Seating Systems, TR-91020, American Helicopter Society, May 1991.

55-39

187836

P-18

N97-19470

Explicit Solution Techniques for Impact with Contact Constraints

Robert E. McCarty
Wright Laboratory
Wright-Patterson Air Force Base, OH

1

INTRODUCTION

Modern military aircraft transparency systems, windshields and canopies, are complex systems which must meet a large and rapidly growing number of requirements. As illustrated in Fig. 1, many of these transparency system requirements are conflicting, presenting difficult balances which must be achieved. One example of a challenging requirements balance or trade is shaping for stealth versus aircrew vision.

The large number of requirements involved may be grouped in a variety of areas including man-machine interface; structural integration with the airframe; combat hazards; environmental exposures; and supportability. Some individual requirements by themselves pose very difficult, severely nonlinear analysis problems. One such complex problem is that associated with the dynamic structural response resulting from high energy bird impact.

OBJECTIVE:

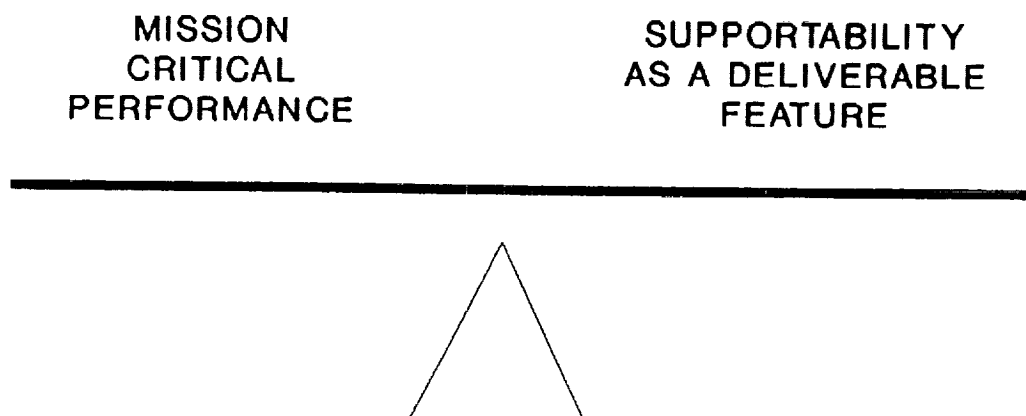


Figure 1 - Balance between performance and supportability requirements for an aircraft transparency system.

¹ Brockman, R. A.; and Held, T. W.: *Explicit Finite Element Method for Transparency Impact Analysis*, WL-TR-91-3006, 1991.

NONLINEAR FINITE ELEMENT ANALYSIS OF AIRCRAFT TRANSPARENCY BIRD IMPACT

Impact phenomena encompass a broad range of structural behavior and response times, which depend upon the stiffness, strength, mass, geometry, velocities, and failure characteristics of the bodies involved. Soft body impacts, such as transparency bird impacts, are unusual: while the response is often highly nonlinear, critical features of the response may occur either at early times or long (milliseconds) after the impact is finished as illustrated in Fig. 2. For over ten years, implicit solution techniques with isoparametric solid finite element technology (Ref. 1) have been used successfully to analyze aircraft transparency bird impact response (Refs. 2-5). An impact solution may be dominated by complicated contact conditions which preclude the use of large time steps, so that the advantages of an implicit solution are lost. Practical transparency analysis remains a time-consuming and laborious process, and in some circumstances the present inventory of analysis tools may not be optimal.

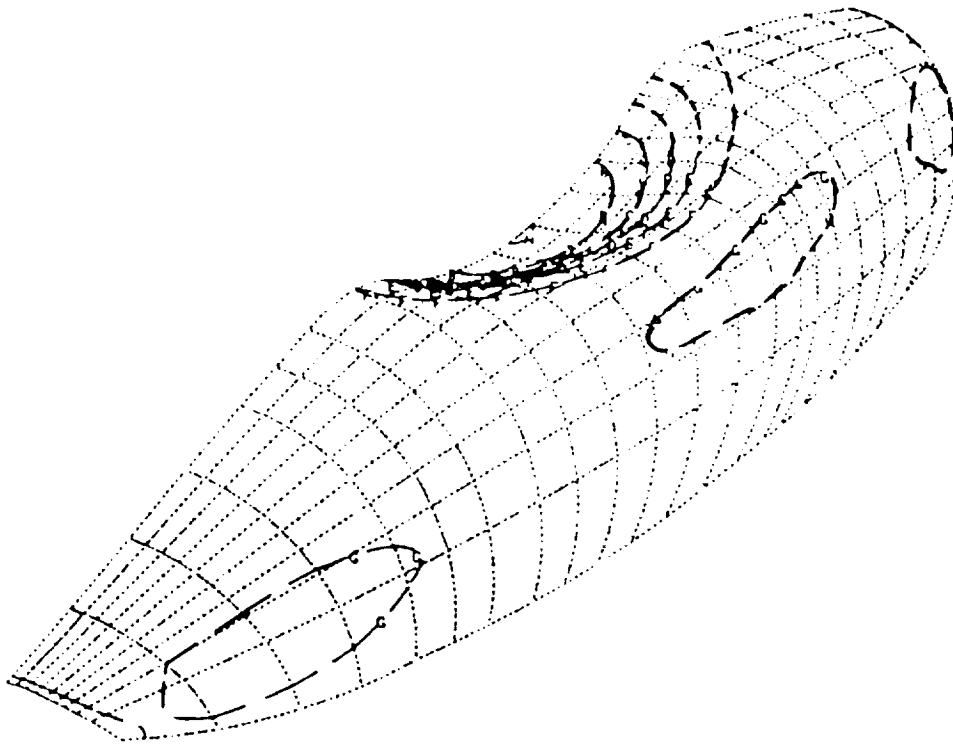


Figure 2 - Dynamic bird impact response of F-16 fighter aircraft
prototype canopy design at 20 msec.

EXPLICIT FINITE ELEMENT METHOD FOR AIRCRAFT TRANSPARENCY BIRD IMPACT

This paper outlines the development of new computational techniques for analyzing structural response to high-speed impact. The key improvements in the new technique are listed in Fig. 3. The analytical technique discussed is an explicit finite element method of the type used widely for the numerical solution of shock and wave propagation problems. The explicit family of time integration algorithms is attractive because it is readily adapted to high performance on the current generation of supercomputers, which combine parallel or pipeline processors, moderate amounts of high-speed memory, and relatively slow disk performance. An added benefit is the ability to implement more detailed material and failure models. The particular implementation discussed here is a computer code called X3D. X3D is an explicit, three-dimensional finite element program intended for use in solving impact, wave propagation, and other short-duration problems in structural dynamics.

- *Soft-body impact loads:* the bird appears explicitly in the finite element model, so that ad hoc estimates of the impact loading distribution are unnecessary
- *Material modeling:* the material models include strain rate sensitivity and failure
- *Layered shells:* multilayered constructions, including those with soft interlayers, can be modeled using a single layer of surface elements

Figure 3 - Key improvements offered by explicit finite element methods for nonlinear dynamic aircraft transparency bird impact.

X3D EXPLICIT THREE-DIMENSIONAL FINITE ELEMENT PROGRAM FOR SHORT-DURATION STRUCTURAL DYNAMIC PROBLEMS

X3D contains two types of finite elements: solids and plates. The solid elements are an eight-node hexahedron, based on a mean-stress approximation with anti-hourglass stabilization (Ref. 6); and a four-node tetrahedron. The eight-node solid hexahedron element is illustrated in Fig. 4. The solid hexahedral finite element uses a displacement and velocity approximation based upon trilinear polynomials; that is, the element's displacement and velocity components each vary linearly along each edge of the element. In addition, the stress components are computed from a mean stress approximation using only the mean velocity gradient for the element (Ref. 6). This measure is desirable to maintain good element performance, and also reduces the effort required for element computations. However, the resulting element is a constant stress element, and therefore a generous number may be necessary for accurate modeling. In particular, a single layer of these solids is incapable of developing a bending moment. The material model used for solids consists of a polynomial equation of state coupled with a von Mises plasticity model, a simple power-law correction for strain rate sensitivity, and a failure criterion based upon the ultimate stress.

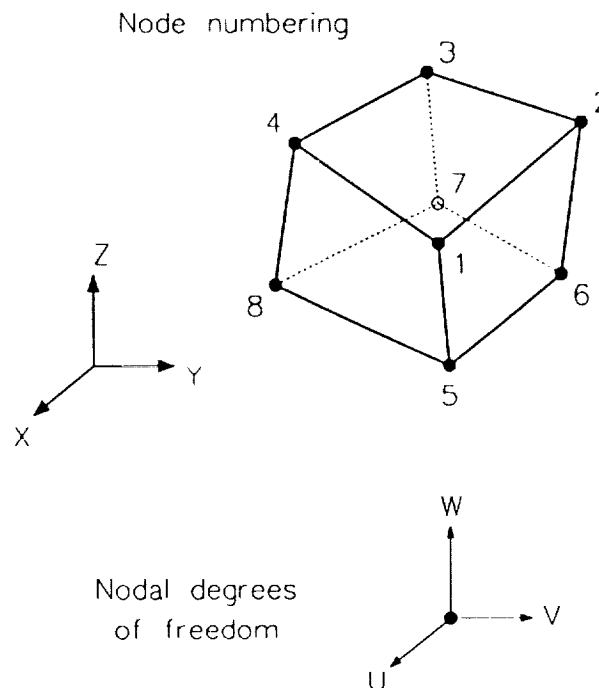


Figure 4 - Eight-node solid hexahedron X3D element.

X3D SOLID HEXAHEDRAL AND TETRAHEDRAL ELEMENTS

Because of the mean stress approximation, certain modes of deformation exist for the hexahedron which are stress-free but do not represent rigid body motions. These hourglassing deformation modes correspond to linearly varying stress patterns which are not detected by the mean stress approximation as shown in Fig. 5. To stabilize these potentially unstable motions, an anti-hourglass viscosity is employed to resist the hourglass motions through internal damping forces (Ref. 7). The tetrahedral solid is a constant-strain, constant-stress element based upon fully linear displacement and velocity field approximations. The element is quite similar to the hexahedron, but does not use an anti-hourglass viscosity. The twelve degrees of freedom for the element capture the six rigid-body motions and the six uniform strain/stress modes, so that no unstable deformation patterns exist for individual elements. The tetrahedron is included in X3D for its utility in soft-body impact modeling. Since the element has no unstable modes, it can be used to follow very large distortions without causing numerical problems. The tetrahedron is used to model the bird in bird impact simulations, using an equation of state typical of water, a very low strength deviatoric model, and an ultimate failure strain of about 5 (500%). The tetrahedron is implemented as a five-node element, the fifth node coinciding with the first. This artifice serves to distinguish the four-node tetrahedron from the four-node quadrilateral plate element during input.

HOURGLASS DEFORMATION PATTERNS FOR 8-NODE SOLID
DISPLACEMENT DIRECTION ← →

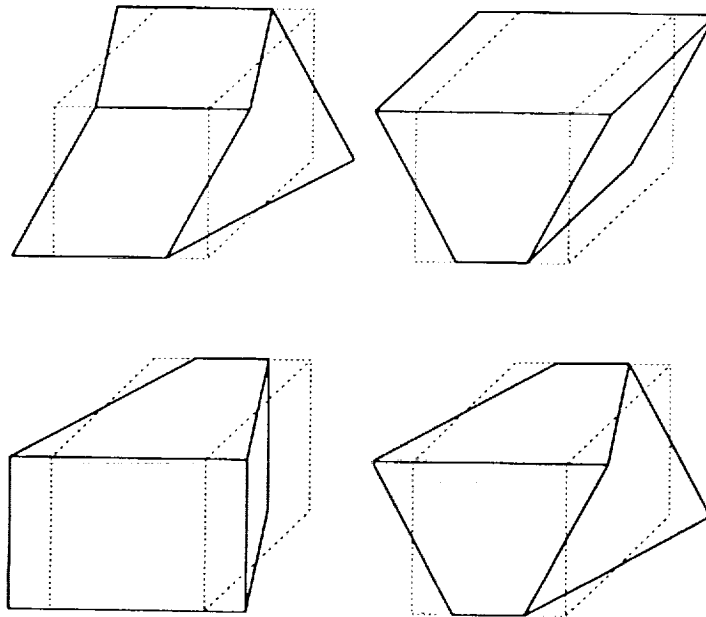


Figure 5 - Hourglass deformation patterns for solid element.

MATERIAL MODELS

The material constitutive relationships used for both the solid and plate finite elements consist of a deviatoric (shear) relation and a bulk (pressure-volume) model. The stress tensor is composed of a hydrostatic, or pressure, stress, and a deviatoric stress tensor which is independent of the pressure. These two contributions to the stress tensor are determined independently in the material model by a deviatoric stress model and a mechanical equation of state. The deviatoric material model used for solids is a rate-dependent, isotropic, hypoelastic theory appropriate for moderate to large deformations. The parameters which define the material's deviatoric behavior are shown in Fig. 8. An experimental feature provides an isotropic Newtonian fluid model for the three-dimensional solid elements for potential use in hydrodynamic impact modeling. The bulk behavior is described in polynomial form as for a solid, while the deviatoric stress is related linearly to the rate of deformation. In the plate element, the elastic-plastic material model is slightly more complicated than for three-dimensional solids because of the zero normal stress constraint. During the plasticity calculation, it is necessary to determine a final state of stress which not only lies on the yield surface, but which satisfies the condition for the normal stress to be zero. The deviatoric model and the bulk model (equation of state) are not entirely independent, and must be solved simultaneously with the normal stress constraint.

- Linear shear modulus
- Quasi-static yield stress
- Rate sensitivity scale factor
- Rate sensitivity exponent
- Hardening modulus
- Ultimate stress

Figure 8 - Parameters for material deviatoric behavior.

X3D SOLID HEXAHEDRAL AND TETRAHEDRAL ELEMENTS

Because of the mean stress approximation, certain modes of deformation exist for the hexahedron which are stress-free but do not represent rigid body motions. These hourglassing deformation modes correspond to linearly varying stress patterns which are not detected by the mean stress approximation as shown in Fig. 5. To stabilize these potentially unstable motions, an anti-hourglass viscosity is employed to resist the hourglass motions through internal damping forces (Ref. 7). The tetrahedral solid is a constant-strain, constant-stress element based upon fully linear displacement and velocity field approximations. The element is quite similar to the hexahedron, but does not use an anti-hourglass viscosity. The twelve degrees of freedom for the element capture the six rigid-body motions and the six uniform strain/stress modes, so that no unstable deformation patterns exist for individual elements. The tetrahedron is included in X3D for its utility in soft-body impact modeling. Since the element has no unstable modes, it can be used to follow very large distortions without causing numerical problems. The tetrahedron is used to model the bird in bird impact simulations, using an equation of state typical of water, a very low strength deviatoric model, and an ultimate failure strain of about 5 (500%). The tetrahedron is implemented as a five-node element, the fifth node coinciding with the first. This artifice serves to distinguish the four-node tetrahedron from the four-node quadrilateral plate element during input.

HOURGLASS DEFORMATION PATTERNS FOR 8-NODE SOLID
DISPLACEMENT DIRECTION $\leftarrow \rightarrow$

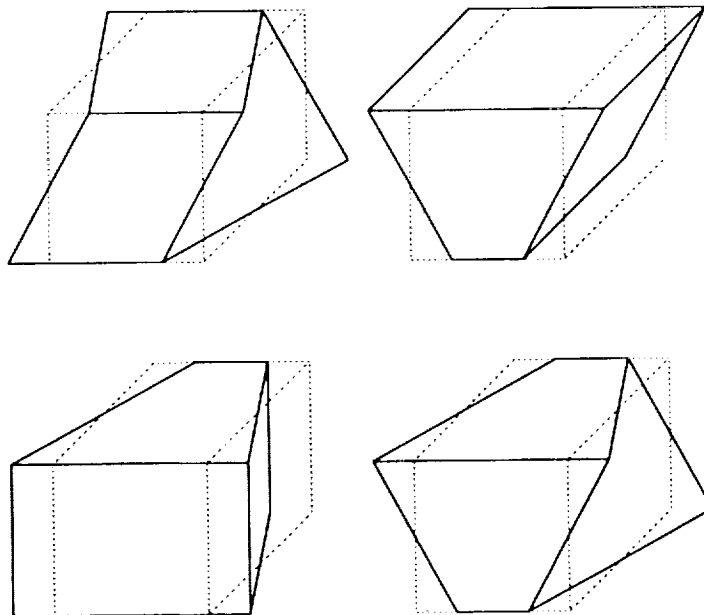


Figure 5 - Hourglass deformation patterns for solid element.

X3D PLATE AND SHELL ELEMENT

The plate and shell element in X3D is a four-node quadrilateral based upon a Mindlin-Reissner type thick-plate theory. A corotational axis system, which rotates with the element but does not deform, is used to simplify the element kinematics. The plate and shell element uses a reduced (one-point) Gaussian quadrature, in conjunction with anti-hourglass stabilization techniques. An approximate model for layered media is implemented for the element, so that plates and shells having layers with large differences in stiffness can be represented effectively using a single element in the thickness direction. For each layer of the X3D plate and shell element, the material is elastic, perfectly plastic, and obeys plane stress assumptions. Transverse shear stresses in the element are uncoupled from the tangential stresses, and follow an elastic constitutive relation. The plate and shell element has six degrees of freedom per node as shown in Fig. 6. The displacement and rotation components each are interpolated separately, using bilinear polynomials. The resulting element is quite similar to that described by Belytschko (Ref. 8).

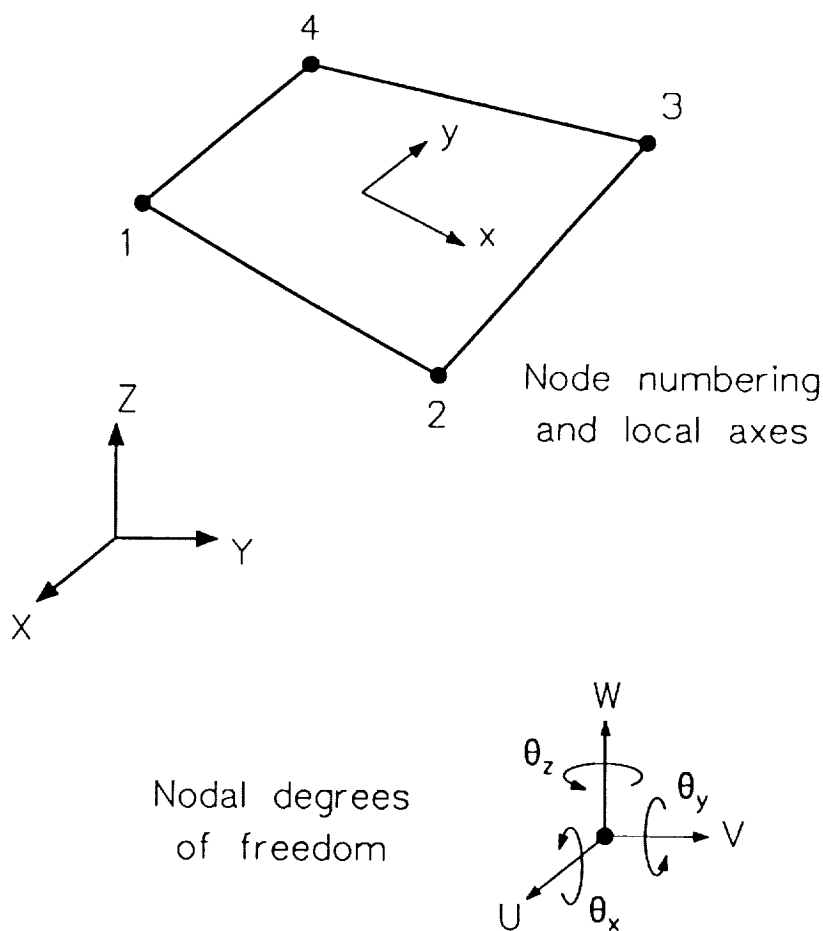


Figure 6 - Four-node quadrilateral plate element.

X3D PLATE AND SHELL ELEMENT

Unlike the solid elements, the plate element must be formulated in a local axis system because of the differing treatment of the plate thickness from that of the planform directions. A corotational coordinate system which rotates with the element is employed, and therefore is constructed anew at each time step of the solution based upon the current element geometry. The plate element shape functions are formulated entirely in local coordinates. The element calculations are performed with respect to the "mean plane" of the element, and corrected as necessary to account for out of plane warping of the reference surface. The plate uses a mean-stress approximation for its inplane directions, similar to the solid hexahedron. At any thickness station, the velocity gradient is evaluated at the centroid of the element, and assumed to be constant throughout the element (except through the thickness). To resist unstable motions resulting from the assumption of a uniform velocity gradient, the plate element uses a stiffness hourglass control scheme (Ref. 6). Other aspects of element design are listed in Fig. 7.

- Simpson's Rule integration through the thickness
- Each layer may be a different material and even use a different material model
- Layered constructions with dramatic stiffness characteristics variation from layer to layer require special treatment
- Formulation of lumped mass coefficients relieves stringent time step restriction without upsetting convergence (Ref. 9)
- No inertia is assigned to the "drilling" rotation in the local coordinate system

Figure 7 - X3D plate and shell element features.

MATERIAL MODELS

The material constitutive relationships used for both the solid and plate finite elements consist of a deviatoric (shear) relation and a bulk (pressure-volume) model. The stress tensor is composed of a hydrostatic, or pressure, stress, and a deviatoric stress tensor which is independent of the pressure. These two contributions to the stress tensor are determined independently in the material model by a deviatoric stress model and a mechanical equation of state. The deviatoric material model used for solids is a rate-dependent, isotropic, hypoelastic theory appropriate for moderate to large deformations. The parameters which define the material's deviatoric behavior are shown in Fig. 8. An experimental feature provides an isotropic Newtonian fluid model for the three-dimensional solid elements for potential use in hydrodynamic impact modeling. The bulk behavior is described in polynomial form as for a solid, while the deviatoric stress is related linearly to the rate of deformation. In the plate element, the elastic-plastic material model is slightly more complicated than for three-dimensional solids because of the zero normal stress constraint. During the plasticity calculation, it is necessary to determine a final state of stress which not only lies on the yield surface, but which satisfies the condition for the normal stress to be zero. The deviatoric model and the bulk model (equation of state) are not entirely independent, and must be solved simultaneously with the normal stress constraint.

- Linear shear modulus
- Quasi-static yield stress
- Rate sensitivity scale factor
- Rate sensitivity exponent
- Hardening modulus
- Ultimate stress

Figure 8 - Parameters for material deviatoric behavior.

LAYERED PLATE AND SHELL MODEL

X3D provides a method of approximation for plates and shells having large stiffness variations from layer to layer, such as those for a laminated aircraft transparency system shown in Fig. 9. Layered structures of this type often require detailed and expensive models, since conventional plate and shell finite elements do not reproduce the correct transverse shear strain distributions through the wall thickness. The X3D method requires only a single layer of elements having six engineering degrees of freedom per node, regardless of the number of layers in the structure. The approximation uses closed-form elasticity solutions to develop transverse shear flexibility corrections, which bring this contribution to the energy into line with that caused by pure bending, twisting, and extension. For large displacement problems, the technique is applied in corotational coordinates. Changes in stiffness caused by plasticity can be accounted for by recomputing the flexibility corrections based upon instantaneous moduli. Applied forces in X3D may consist of body forces and surface pressure. Kinematic boundary conditions may include prescribed nodal displacements, rigid-wall constraints, and contact between specified surfaces within the mesh. Initial conditions may be specified for the translational velocity components for all or part of the finite element model.

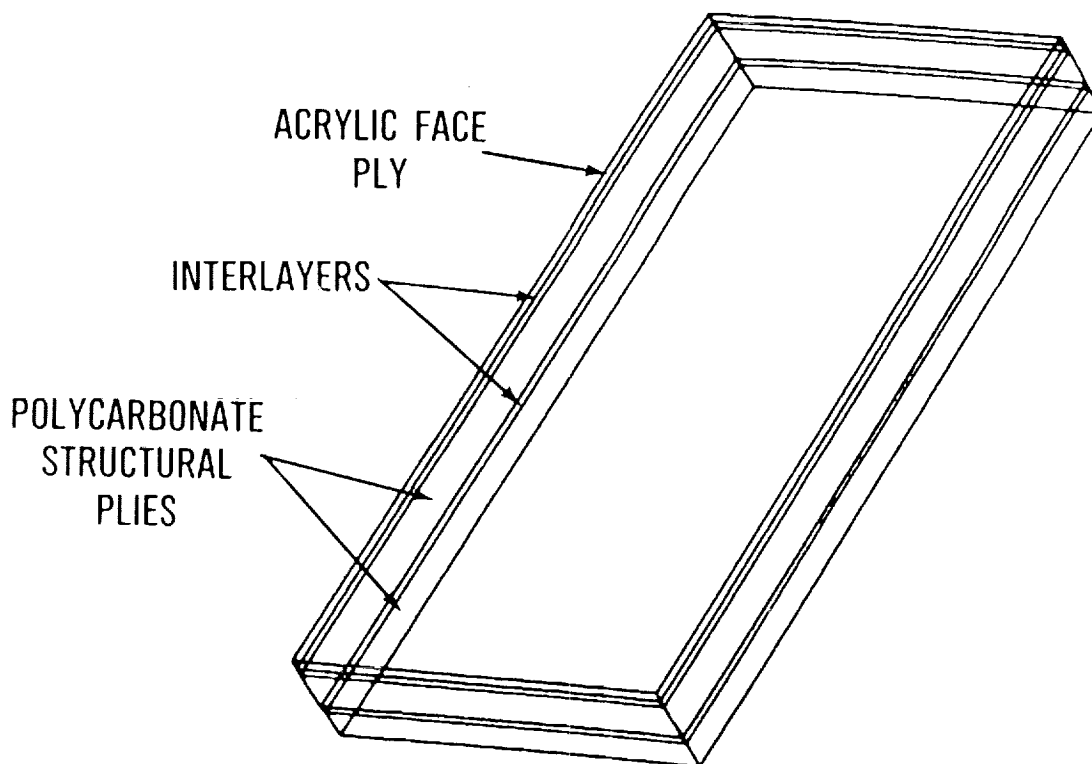


Figure 9 - Laminated windshield design for the T-46A aircraft.

TAYLOR CYLINDER SAMPLE ANALYSIS

The Taylor cylinder experiment, which is used to estimate the mechanical properties of metals at high strain rates, involves the normal impact of a cylinder onto a rigid surface. It is a common benchmark problem with a well-known solution. An X3D model was prepared for one quarter of the cylinder using 1350 8-node solid elements. Material constants typical of copper were used. Purely isotropic strain hardening was assumed, and no ultimate stress was specified (i.e., elements could not fail during the solution). Virtually all of the kinetic energy of the cylinder is dissipated through plastic deformation within about 80 microseconds. Figure 10 shows a deformed mesh plot of the cylinder in its final state.

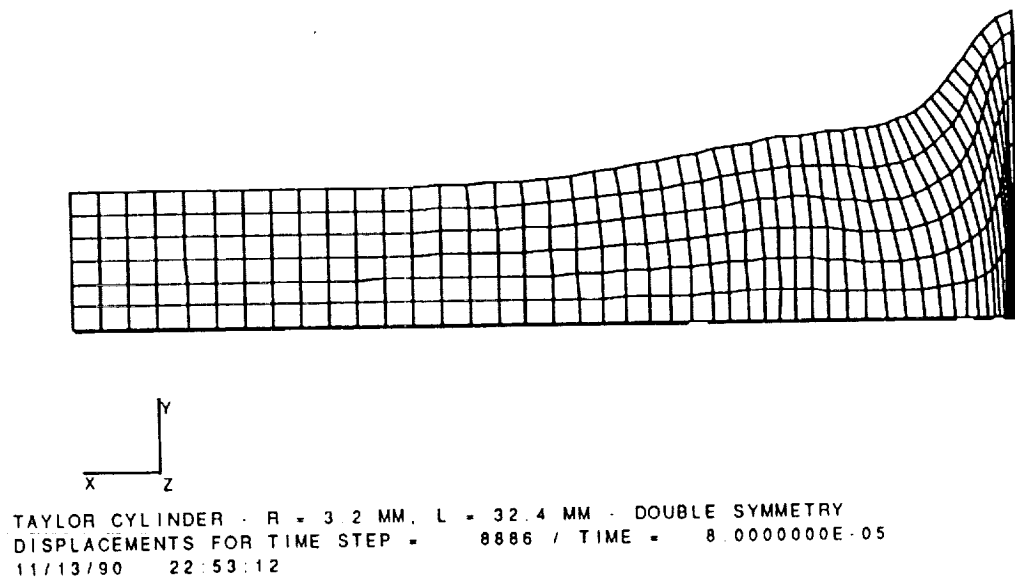


Figure 10 - Deformed geometry of Taylor Cylinder.

TAYLOR CYLINDER SAMPLE ANALYSIS

Figure 11 shows a time history of the cylinder's length. The analysis was performed in 8886 time steps, and required 6 hours, 36 minutes on a VAX 8650 computer (about 0.00198 CPU seconds per element time step). The same analysis runs in about 40 minutes on a CRAY X-MP (.0002 seconds per element time step). Results from the X3D solution compare very well with analyses using the DYNA and NIKE codes, as shown below.

QUANTITY	X3D	DYNA2D	DYNA3D	NIKE2D
Final length, mm	21.47	21.47	21.47	21.47
Maximum radius, mm	7.081	7.127	7.034	7.068
Maximum strain at center	2.95	3.05	2.95	2.97

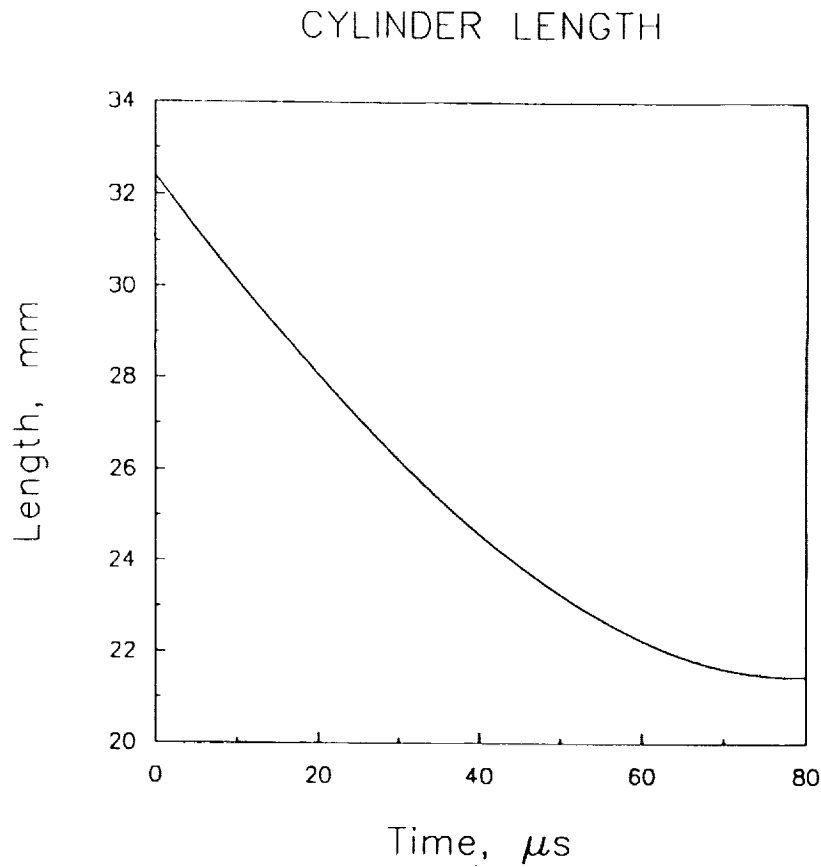


Figure 11 - Cylinder length versus time.

EXPLOSIVELY LOADED CYLINDRICAL SHELL SAMPLE ANALYSIS

Marchertas and Belytschko present both computational and experimental results for this problem (Ref. 10). A 120 degree cylindrical panel is loaded by igniting a charge spread over most of the surface. In the numerical solution, we represent this impulsive loading by a uniform initial velocity along the radius of the shell. A three point integration through the thickness of the shell was used with X3D. This is the minimum thickness integration order, and may give a solution which is slightly too flexible. Figure 12 shows the geometry of the explosively loaded cylindrical shell. The geometric and material parameters for the shell were:

Radius	2.9375 in.	Tensile modulus	10,500,000 psi
Thickness	0.125 in.	Density	0.0965 lb/cu.in.
Length	12.56 in.	Yield stress	44,000 psi
Velocity	5,650 in./sec (initial)		

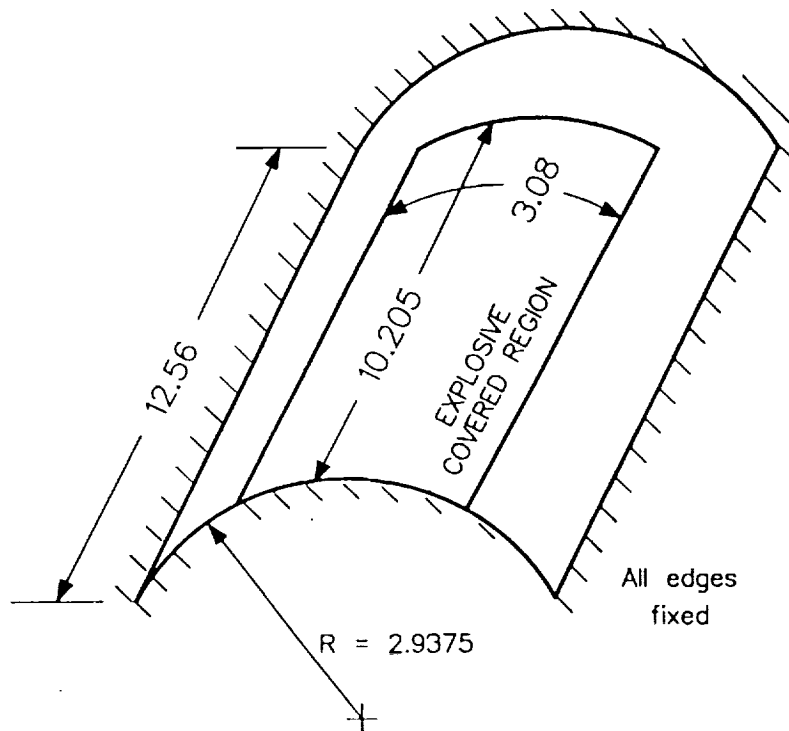


Figure 12 - Geometry of explosively loaded cylindrical shell.

EXPLOSIVELY LOADED CYLINDRICAL SHELL SAMPLE ANALYSIS

Results of the X3D solution, which was performed in 886 time steps, are shown in Fig. 13. The response mainly involves a flattening of the inner portion of the shell, consisting mostly of permanent deformation. The displacements peak at around 0.4 ms, with the largest inward displacements approaching half the radius. After this point, there is some elastic recovery (lasting about another 0.1-0.2 ms), but only very small vibration, since most of the energy has been dissipated through plastic flow. Displacement histories at selected points agree quite well with experimental results. Note that the initial velocity components are directed radially inward, and that points on the edges of the loaded region were assigned half the nominal initial velocity to provide the correct impulse to the shell.

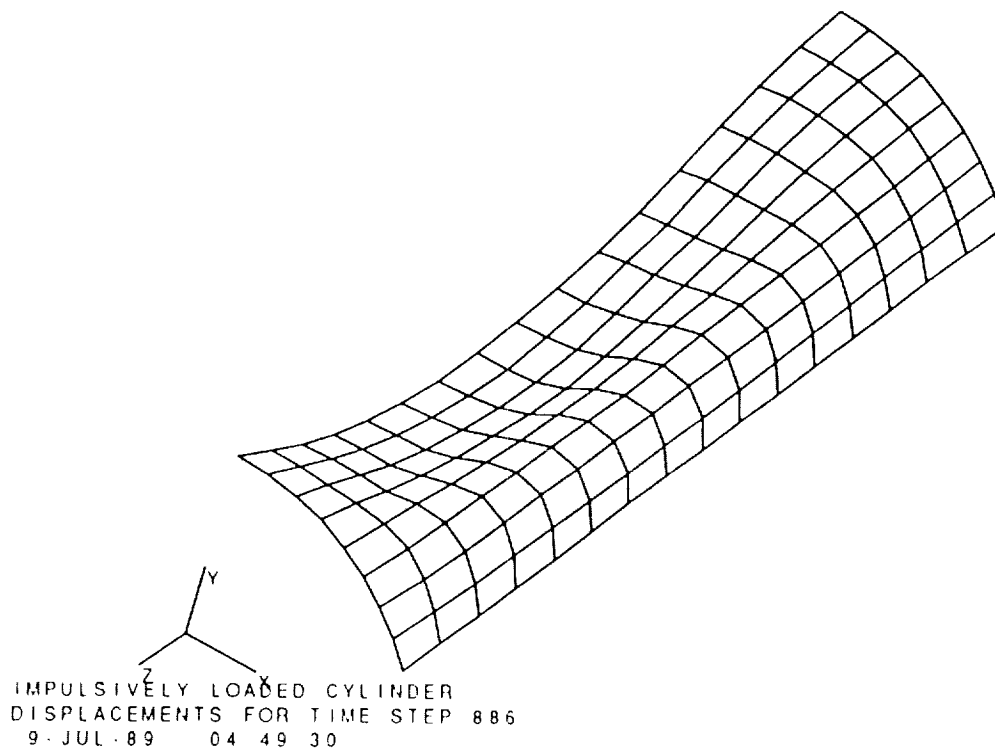


Figure 13 - Final deformed shape of cylindrical shell.

F-16 AIRCRAFT CANOPY BIRD IMPACT SAMPLE ANALYSIS

The F-16 bubble canopy provides a useful example for validation since the impact response involves very large motions, and the coupling between the load distribution and the deformation is strong. As a first step in validating the X3D code for bird impact simulation, several analyses of centerline impacts were carried out for the original production canopy, a 0.5 in. thick monolithic polycarbonate design. This design is capable of defeating 4 lb bird impact at airspeeds up to about 350 knots. Figure 14 shows the geometry of the transparency and of the projectile, a 4 lb bird idealized as a right circular cylinder. The patch outlined around the crown of the canopy and the entire bird are covered with contact elements. The canopy model consists of 928 quadrilateral plate elements. The bird is represented by 960 tetrahedral solids with equation-of-state coefficients typical of water, and very small shear stiffness and strength. The *low-strength* bird model, used in about half of the simulations, produces a pressure-volume response similar to water, and a "brittle" shear behavior. The ultimate and yield stresses coincide, so that element failure occurs at relatively small strains.

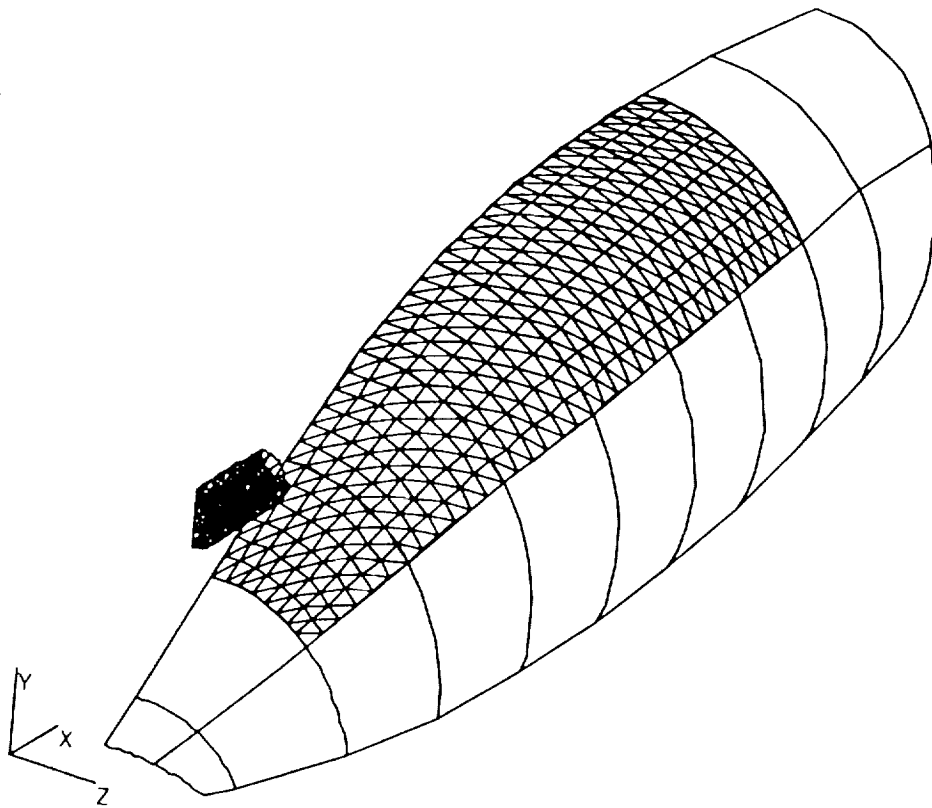


Figure 14 - Contact element grid for bird impact problem.

F-16 AIRCRAFT CANOPY BIRD IMPACT SAMPLE ANALYSIS

A *high-strength* bird model was used as well, which permits roughly 500% plastic (deviatoric) strain before the material is declared failed. The question of which bird model is more realistic has not been resolved because so many details are unknown with regard to material properties, precise support conditions, and center of impact location. Note that when elements of the bird model fail due to large shear distortion, their mass is retained in the problem, and the corresponding nodes continue to be used in contact calculations. Therefore, portions of the impacting body which have "failed" continue to transfer momentum to the target, but do not contribute to the summation of internal forces. In the deformed plot shown in Fig. 15, nodes attached to failed elements in the bird model are shown as small circles representing the center of mass positions. For the cases considered, the center of impact is at fuselage station 112 (measured in inches), which is about two feet aft of the forward edge of the canopy. The initial velocity of the bird is horizontal and equal to 350 knots (7,094) in./sec) at all nodes. The solution illustrated in Fig. 15 employs the low-strength bird. The displacement results are similar to experimentally observed values, although the computed deformed shape exhibits larger displacements in the forward region.

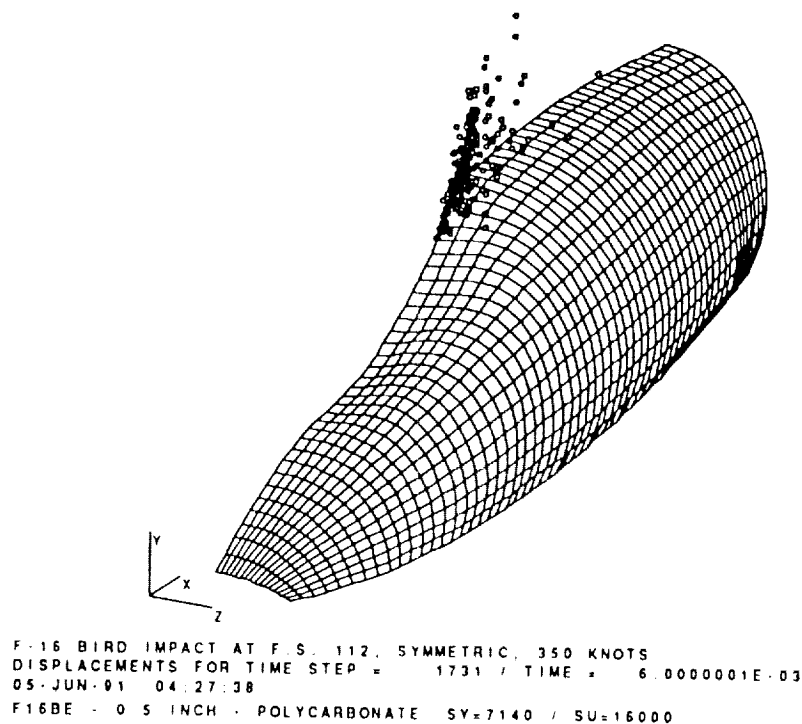


Figure 15 - Deformed geometry of F-16 canopy for low-strength bird 350 knot impact.

SUMMARY AND CONCLUSIONS

An improved analytical capability for soft-body impact simulation has been developed. Advances have been made in modeling impact loads, nonlinear materials, and layered wall constructions. The explicit approach adopted exploits the strengths of the current generation of supercomputer hardware, so that analysis cost and turnaround times are reduced significantly over the previous generation of bird impact analysis software. Experience in performing applications indicates that the solution methodology is very reliable, requiring minimal user intervention to avoid or correct problems with the solution. Implicit methods used in earlier work on these problems demand a great deal of user attention for stable, accurate, and convergent results, while the explicit technique is relatively trouble-free. The work reported here is a significant step toward a reliable capability for design screening and parametric investigation. Figure 16 lists the two primary research needs required to complete such a capability. With a modest effort in these areas of research need, the techniques and software described can become a truly useful and reliable tool for design and evaluation of a new generation of bird-impact resistant aircraft transparency systems.

- *Model Validation.* Additional comparisons of analytical predictions with full-scale impact test data are needed to develop confidence in the accuracy of the analysis and knowledge of its limitations.
- *Materials Characterization.* The transparency materials in wide use are high-polymer compounds with very complex characteristics. Much more experimental and analytical work is needed to understand these materials adequately and model their behavior faithfully.

Figure 16 - Research needs for aircraft transparency bird impact, explicit finite element analysis methods.

REFERENCES

1. Brockman, R. A., *MAGNA (Materially And Geometrically Nonlinear Analysis), Part I - Finite Element Analysis Manual*. AFWAL-TR-82-3098, Part I, 1982.
2. McCarty, R. E., *MAGNA Computer Simulation of Bird Impact on the TF-15 Aircraft Canopy*. AFWAL-TR-83-4154, 1983.
3. McCarty, R. E., *Analytic Assessment of Bird Impact Resistant T-46A Aircraft Windshield System Designs using MAGNA*. WRDC-TR-89-4044, 1989.
4. McCarty, R. E., *MAGNA Analysis of Space Shuttle Orbiter Windshield System Bird Impact Protection*. WRDC-TR-89-4044, 1989.
5. Bouchard, M. P., *Finite Element Analysis of the B-1B Windshield System*. WRDC-TR-89-4044, 1989.
6. Flanagan, D. P. and Belytschko, T., "A Uniform Strain Hexahedron and Quadrilateral with Orthogonal Hourglass Control," *International Journal for Numerical Methods in Engineering*, Vol. 17, 1981, pp. 679-706.
7. Brockman, R. A., *Finite Element Analysis of Soft-Body Impact*. AFWAL-TR-84-3035, 1984.
8. Belytschko, T., Lin, J. I. and Tsay, C. S., "Explicit Algorithms for the Nonlinear Dynamics of Shells," *Computational Methods in Applied Mechanics and Engineering*, Vol. 42, 1984, pp. 225-251.
9. Hughes, T. J. R., Cohen, M. and Haroun, M., "Reduced and Selective Integration Techniques in the Finite Element Analysis of Shells," *Nuclear Engineering Des.*, Vol. 46, 1978, pp. 203-222.
10. Marchertas, A. H. and Belytschko, T., *Nonlinear Finite Element Formulation for Transient Analysis of Three-Dimensional Thin Structures*. ANL-8104, 1974.

56-39

187837

p. 14

N 94-19471

Numerical Simulation of Vehicle Crashworthiness and Occupant Protection

Nripen K. Saha
Ford Motor Company
Dearborn, MI

PRECEDING PAGE BLANK NOT FILMED

124 INTENTIONALLY BLANK

VEHICLE CRASHWORTHINESS DESIGN

Objectives

To design the vehicle structure for optimum impact energy absorption, and to design the restraint system (seatbelts, airbags, bolsters, etc.) for optimum occupant protection.

Approach

A major part of the impact energy is to be absorbed by the vehicle structure. The restraint components will provide protection against the remaining crash energy.

Certain vehicle components are designed to deform under specific types and speeds of impact in a desired mode for sound energy management.

Structural components such as front side rails, rear rails, door structure and pillars undergo large amounts of deformation.

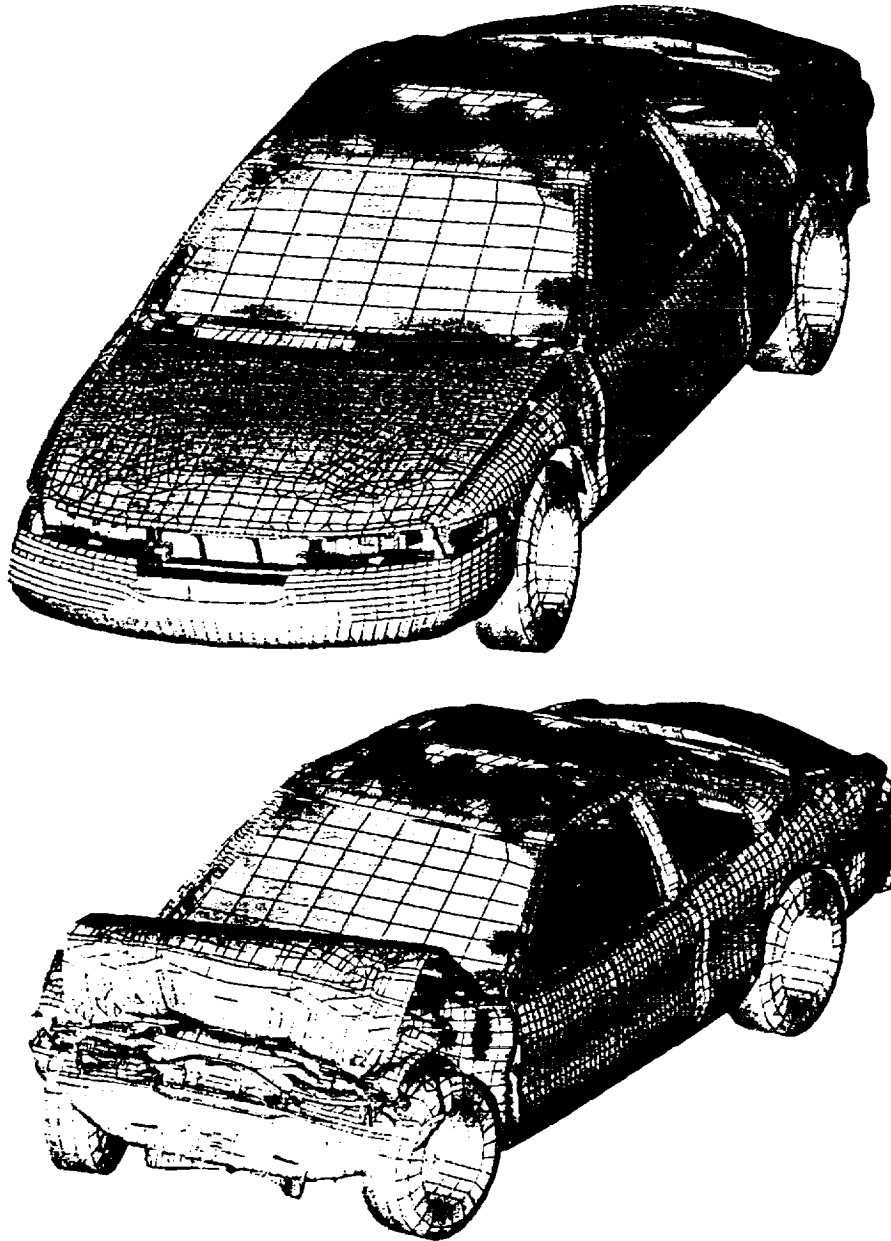
With properly designed geometry and material these components assist in mitigating the effects of impact.

* RECEDING PAGE BLANK NOT FILMED

176

Frontal Crash FEA Model

The original and deformed geometry of a frontal barrier impact model is shown below. Typically, model size is approximately 25000 elastic plastic shell and solid elements. Computer runtime for 100 milliseconds of crush is about 20 hours on CRAY YMP. The analysis is performed with a commercially available code, RADIOSS, from Mecalog, France.



Role of CAE

CAE is playing a vital role in crashworthiness design of automobiles.

Instead of being dependent on numerous prototypes, the design process is rapidly becoming CAE guided.

This new approach allows engineers to examine many alternatives in a shorter time period.

Also, CAE models are complimenting prototype tests.

Models are used to predict crash performance of:

Components
Subassembly, and
Full-vehicle systems.

CAE Tools for Crashworthiness Analysis

Four types of CAE models are generally used in the industry. These are:

- Concept models (lumped masses and springs)
- Occupant simulation models (rigid body type)
- Hybrid models (concept and FEA combined with test data)
- Detailed finite element models.

Use of these models depends on the stage of vehicle development and accuracy of results desired.

CPU usage and modeling turnaround time is also a key factor.

Finite Element Models

Currently at Ford Motor Company nonlinear finite element models are used to simulate:

Front Crash

- Frontal perpendicular barrier impact
- Frontal angular barrier impact
- Frontal pole impact

Side Impact

- Side impact simulation

Rear Impact

- Vehicle rear-end impact with moving rigid barrier
- Car-to-car rear offset impact

Roof Crush

- Quasi-static roof crush of vehicle structure

Frontal Crash Models

Applications:

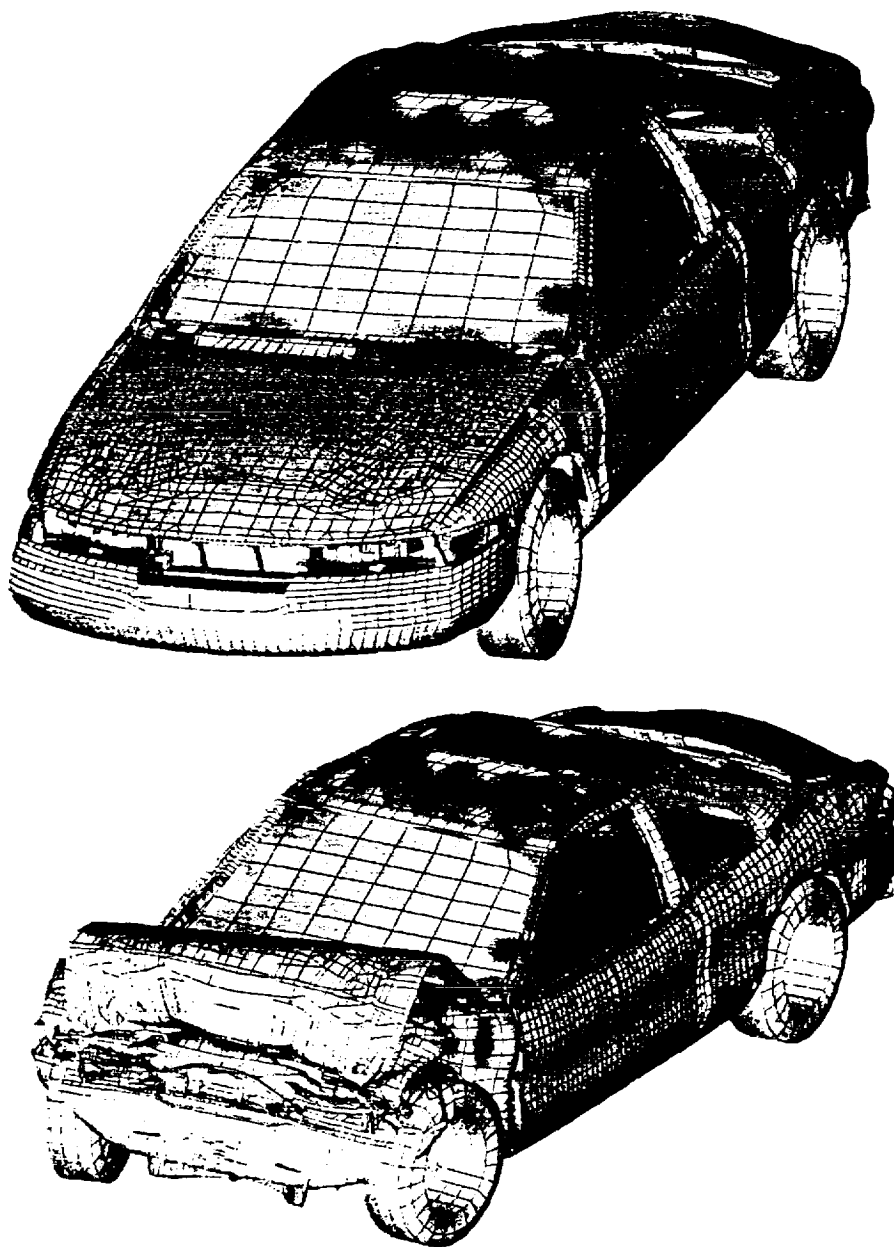
- Front-end structural design of the vehicle
- Provide design directions for airbag sensor development
- Provide input for occupant simulation models

FEA Model Output:

- Total vehicle and component collapse pattern
- Engine compartment energy absorption
- Front bumper and side rail load-displacement
- Engine block movement and dash wall intrusion
- Deceleration pulse in passenger compartment
- Displacement and velocity histories at critical locations

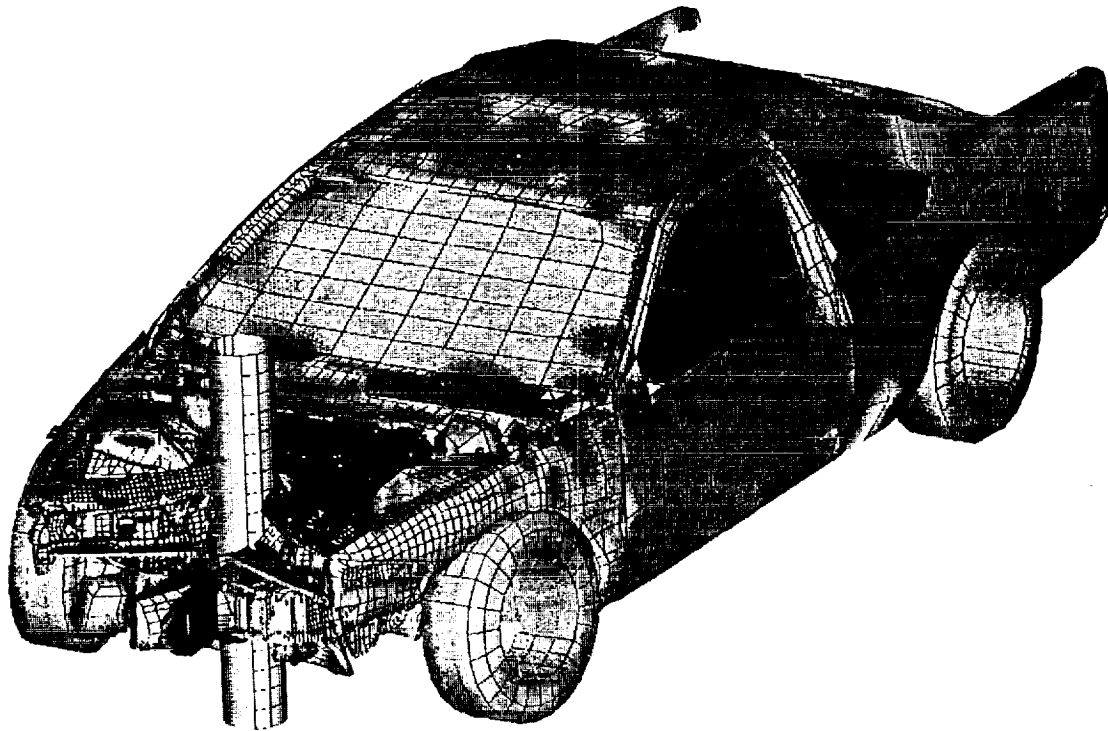
Frontal Crash FEA Model

The original and deformed geometry of a frontal barrier impact model is shown below. Typically, model size is approximately 25000 elastic plastic shell and solid elements. Computer runtime for 100 milliseconds of crush is about 20 hours on CRAY YMP. The analysis is performed with a commercially available code, RADIOSS, from Mecalog, France.

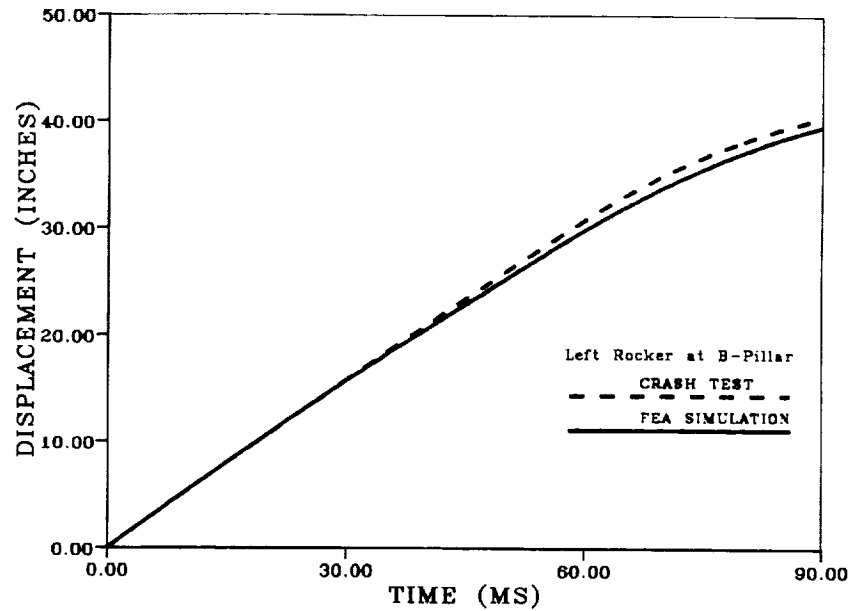


Frontal Pole Impact Model

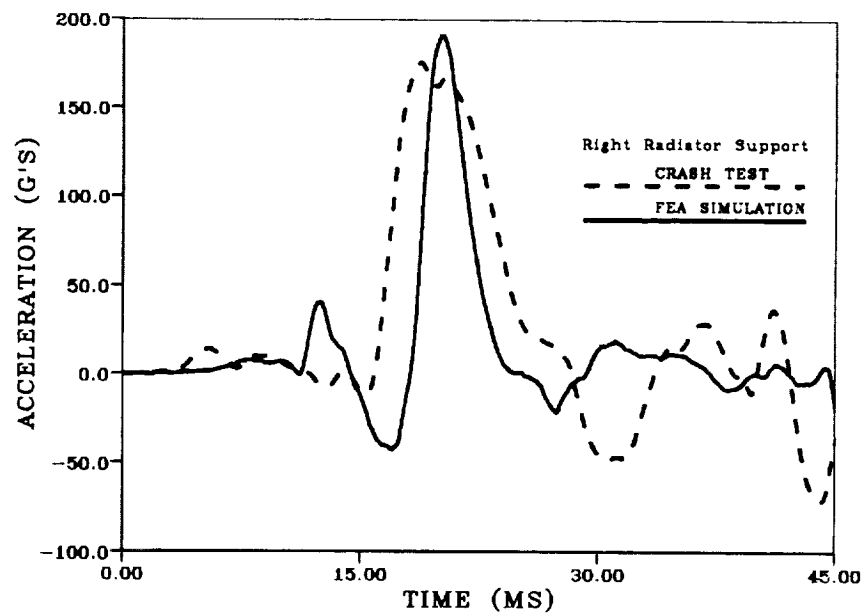
Finite element model of a vehicle impacting a rigid pole at 31 mph is shown below. The model has approximately 28000 elements. The deformed geometry shows that the pole is wrapped around by the front bumper beam and the engine block is pushed rearward.



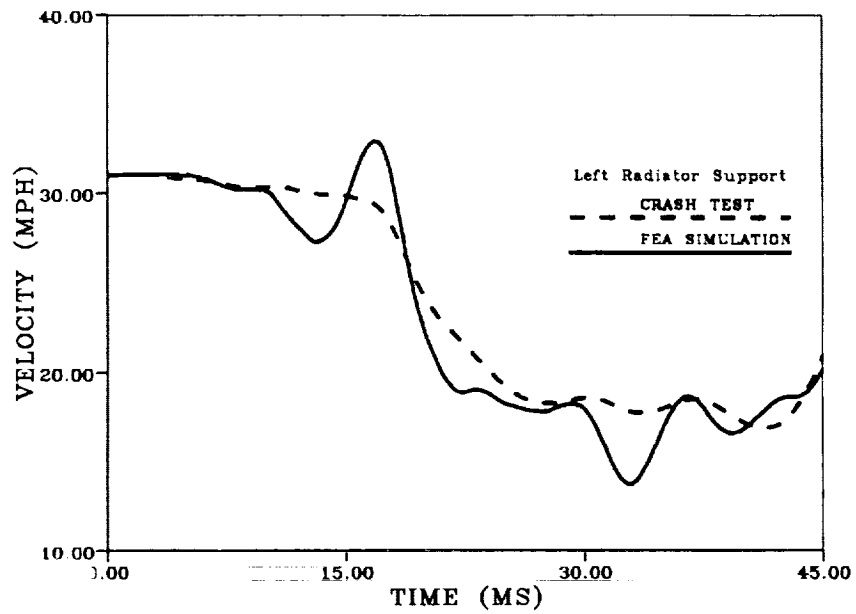
Comparison of B-Pillar/Rocker Joint Longitudinal Displacement with Test Data



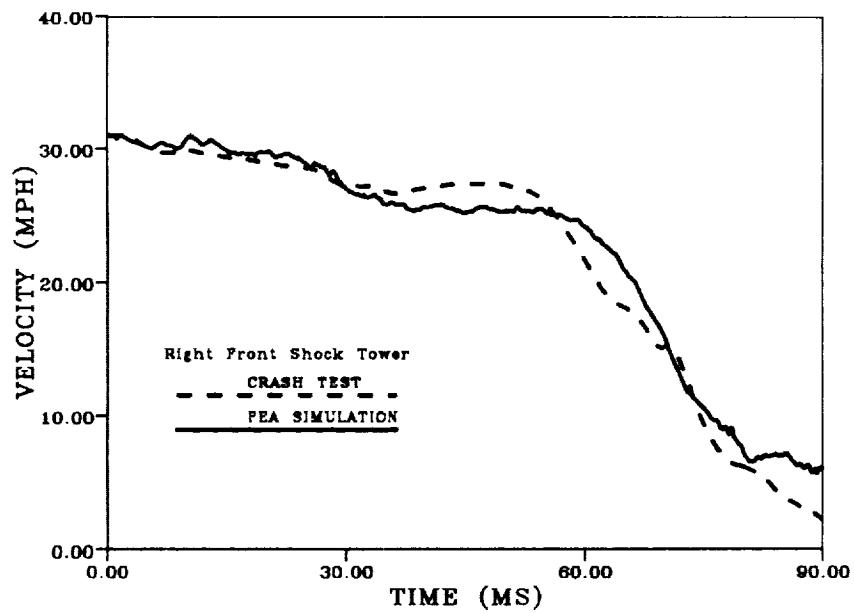
Accelerations at Right Side Radiator Support From Model and Test



Comparison of Predicted Velocity at Left Side Radiator Support with Test Data

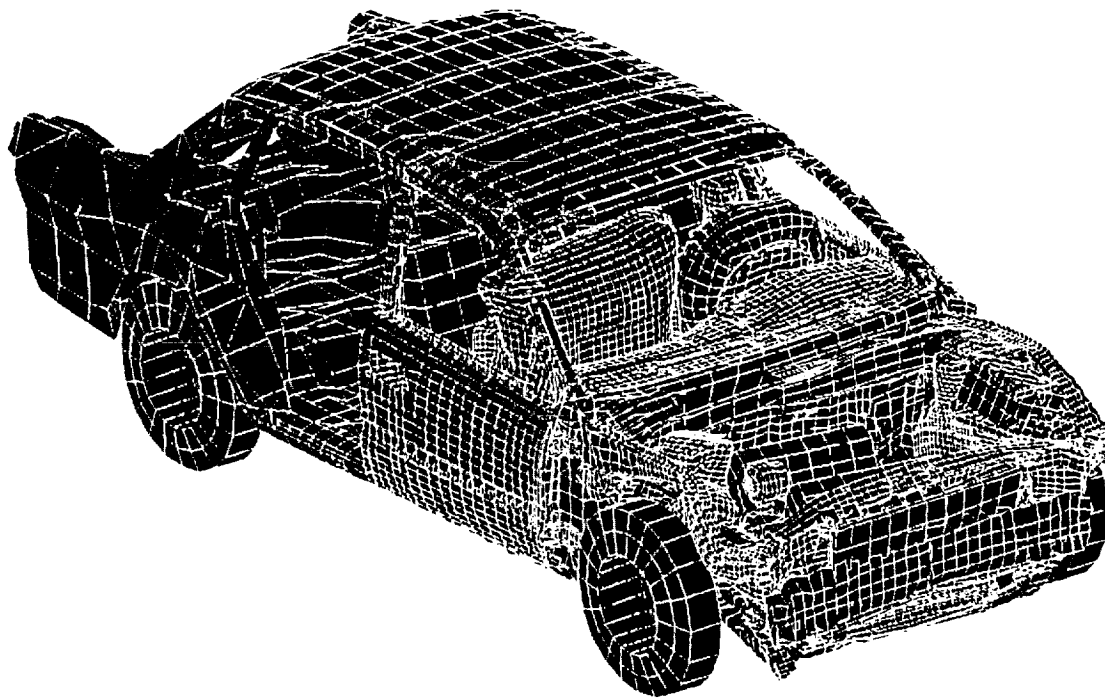


Comparison of Predicted Velocity at Right Shock Tower with Test Data



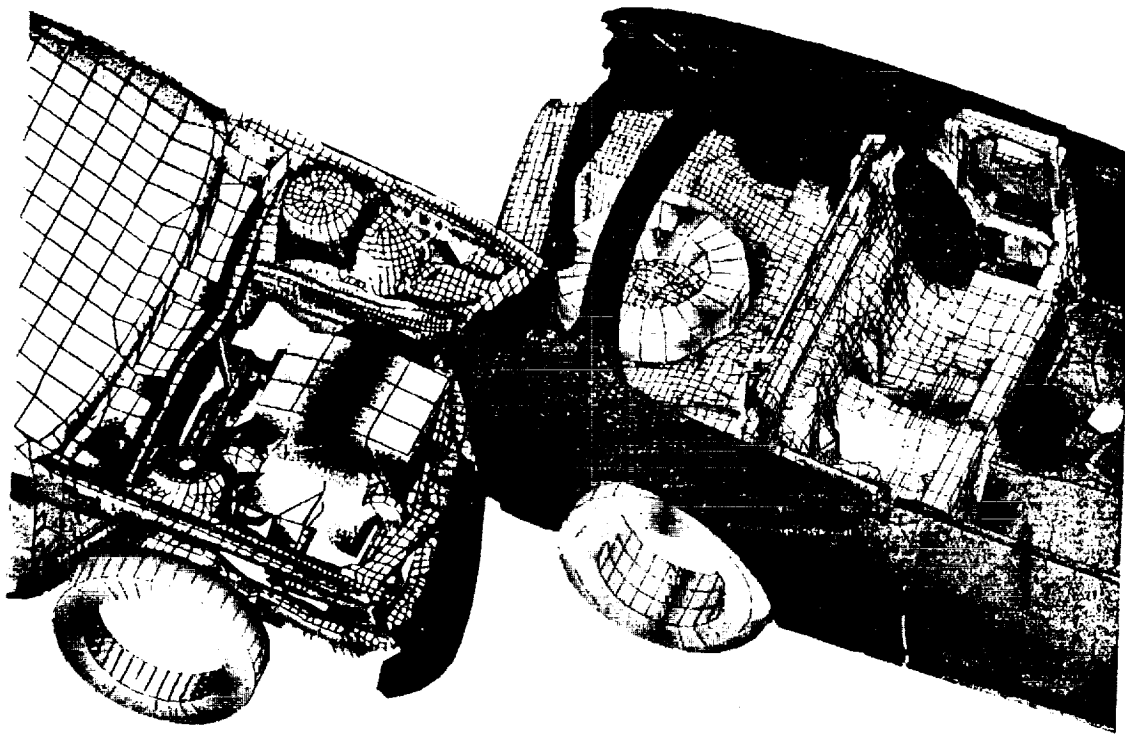
Front Crash System Model

Integrated system model consisting of vehicle, occupant, airbag, steering column systems, and other interior environment to predict both structural and dummy responses from the same run.



Vehicle Rear Impact Simulation

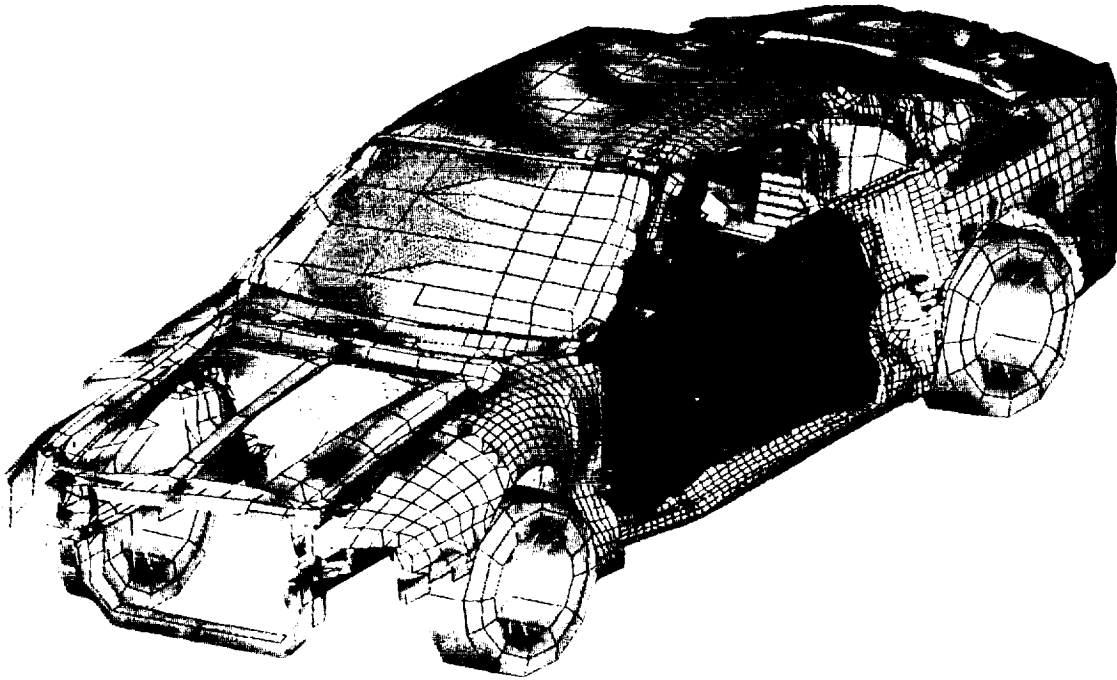
The car-to-car offset impact model is developed to predict strength and energy absorption of vehicle rear-end (rear rails, rear bumper system, lower back, quarter panel and rear floor). The main tasks are to minimize fuel tank deformation under severe impact, predict relative motion of bullet and target vehicles and displacement, velocity and deceleration histories all over the vehicles.



FEA Dummy-Structure Side Impact System Model

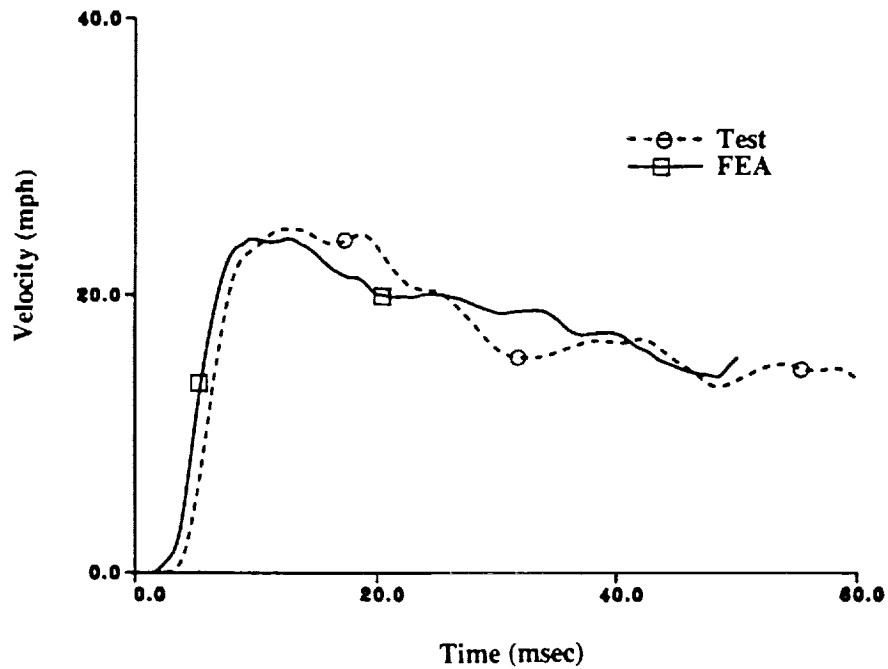
The side impact system model consists of a moving deformable honeycomb barrier, side impact dummy model and the vehicle structure. Approximate model size is 16000 elements and CPU needed on CRAY YMP is about 15 hours.

The detailed FEA model predicts strength and energy absorption by side structure (door, pillars, quarter panels) and energy absorption by trim and bolster as well as front and rear seat dummy responses (pelvic, spine and rib accelerations).

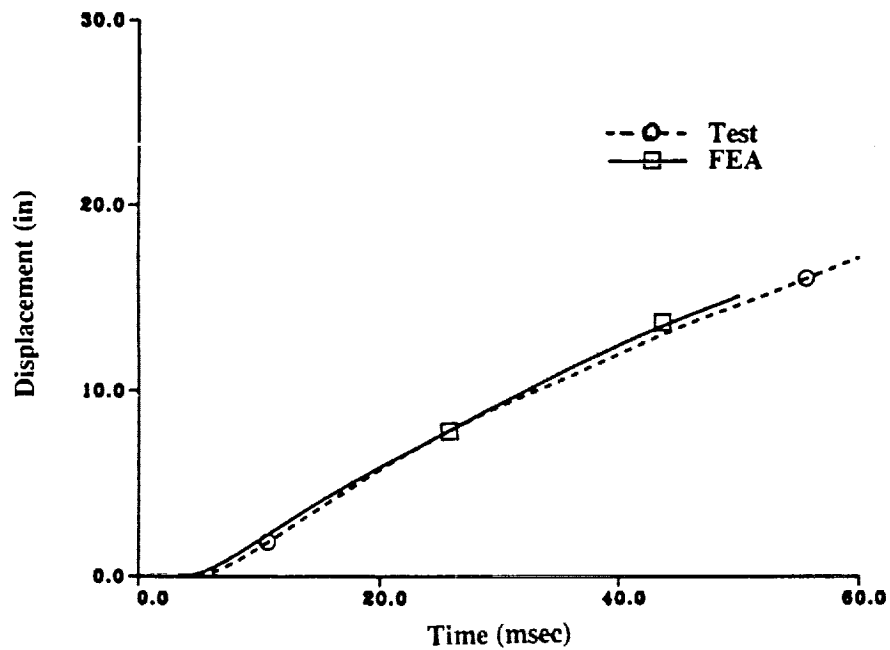


Vehicle Structure Response From Side Impact Model

Comparisons of model predictions of B-pillar lateral velocity and displacement histories with corresponding test data.



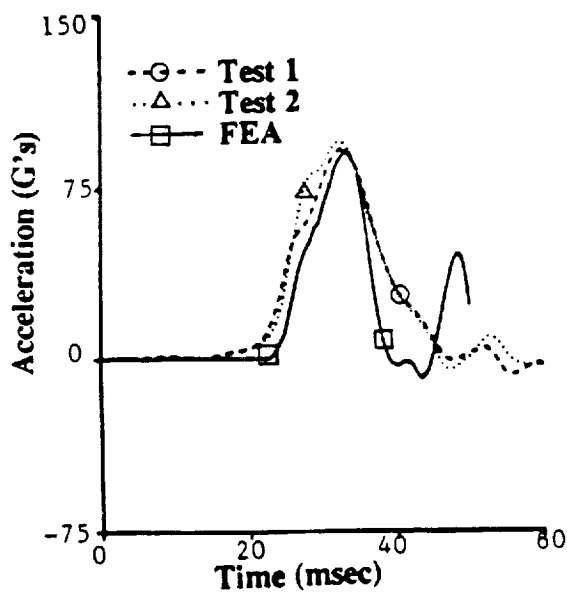
(a) B-pillar Velocity



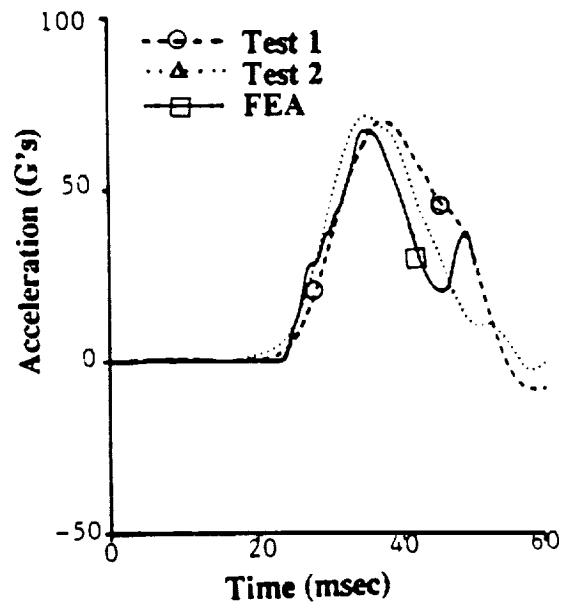
(b) B-pillar Lateral Displacement

Occupant Responses From Side Impact System Model

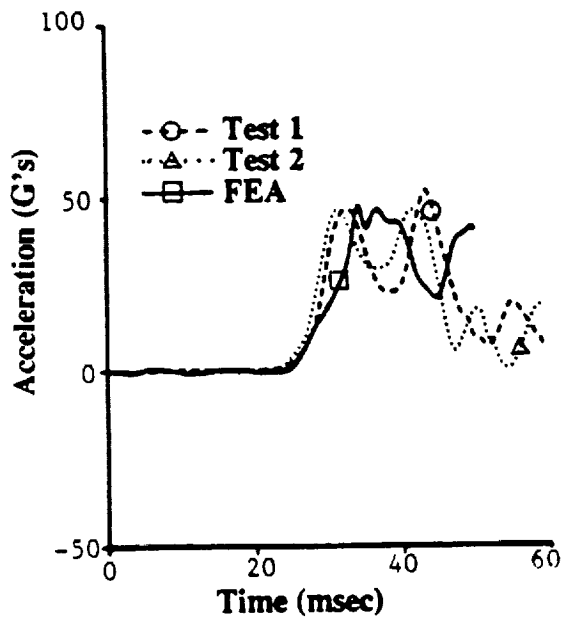
Comparisons of front dummy pelvis acceleration, T12 acceleration and upper and lower rib accelerations from model and tests.



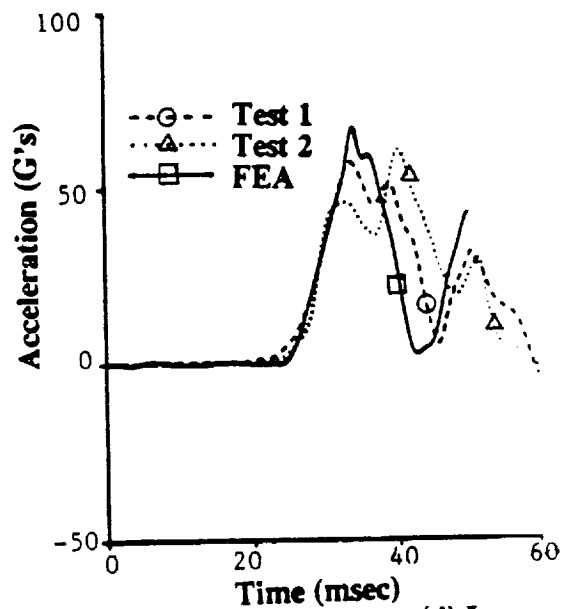
(a) Pelvic



(b) T12



(c) Upper Rib



(d) Lower Rib

PUBLICATIONS ON CRASHWORTHINESS

1. Saha, N. K., Wang, H. C. and Achkar, R. E., "Frontal Offset Pole Impact Simulation of Automotive Vehicles," ASME Int. Computers in Engineering Conference, San Francisco, CA, Aug. 2-6, 1992.
2. Saha, N. K., Mahadevan, S. K., Midoun, D. E. and Yang, J. S., "Finite Element Structure-Dummy System Model for Side Impact Simulation," ASME Winter Annual Meeting, Atlanta, GA, Dec. 1-6, 1991.
3. Saha, N. K., "Design of Automotive Components for Crash Energy Management Using Nonlinear Finite Element Techniques," Proceedings of the 21st Midwestern Mechanics Conference, Houghton, MI, Aug. 13-16, 1989.
4. Devries, R. I., Saha, N. K., et al., "Structural Optimization of Beam Sections for Minimum Weight Subject to Inertial and Crash Strength Constraints," Proceedings of the Sixth SAE Int. Conference on Vehicle Mechanics, Detroit, MI, April 22-24, 1986.
5. Mahmood, H. F., Saha, N. K. and Paluszny, A., "Stiffness and Crash Strength Characteristics of Thin-Walled Plate Components," Proceedings of the ASME Int. Computers in Engineering Conference, Boston, MA, Aug. 1985.

57-39

187838

p-13

N 9 4 - 1 9 4 7 2

Directions for Computational Mechanics in Automotive Crashworthiness

James A. Bennett and T. B. Khalil
General Motors
Warren, MI

PRECEDING PAGE BLANK NOT FILMED

141

140 INTENTIONALLY BLANK

INTRODUCTION

The automotive industry has used computational methods for crashworthiness since the early 1970's. These methods have ranged from simple lumped parameter models to full finite element models. The emergence of the full finite element models in the mid 1980's has significantly altered the research direction. However, there remains a need for both simple, rapid modeling methods and complex detailed methods. This paper will discuss some directions for continuing research.

OCCUPANT MODELS

Although most of the published work has focused on the structural models, some work is starting to appear on interior components and the occupant. Typically, the occupant modeled is the mechanical surrogate used in tests rather than the actual human. In these cases the accuracy of the finite element model is compared to the performance of the mechanical surrogate, called the anthropomorphic test dummy (ATD) rather than to the human response. The performance requirements for the ATD are specified based on bio-mechanical modeling of the human. Federal mandated standards are based on mechanical quantities (acceleration, force) that are measured on the ATD. Thus, in the figure below the human cadaver results were used to establish a corridor of behavior in which the Hybrid III ATD chest should perform.

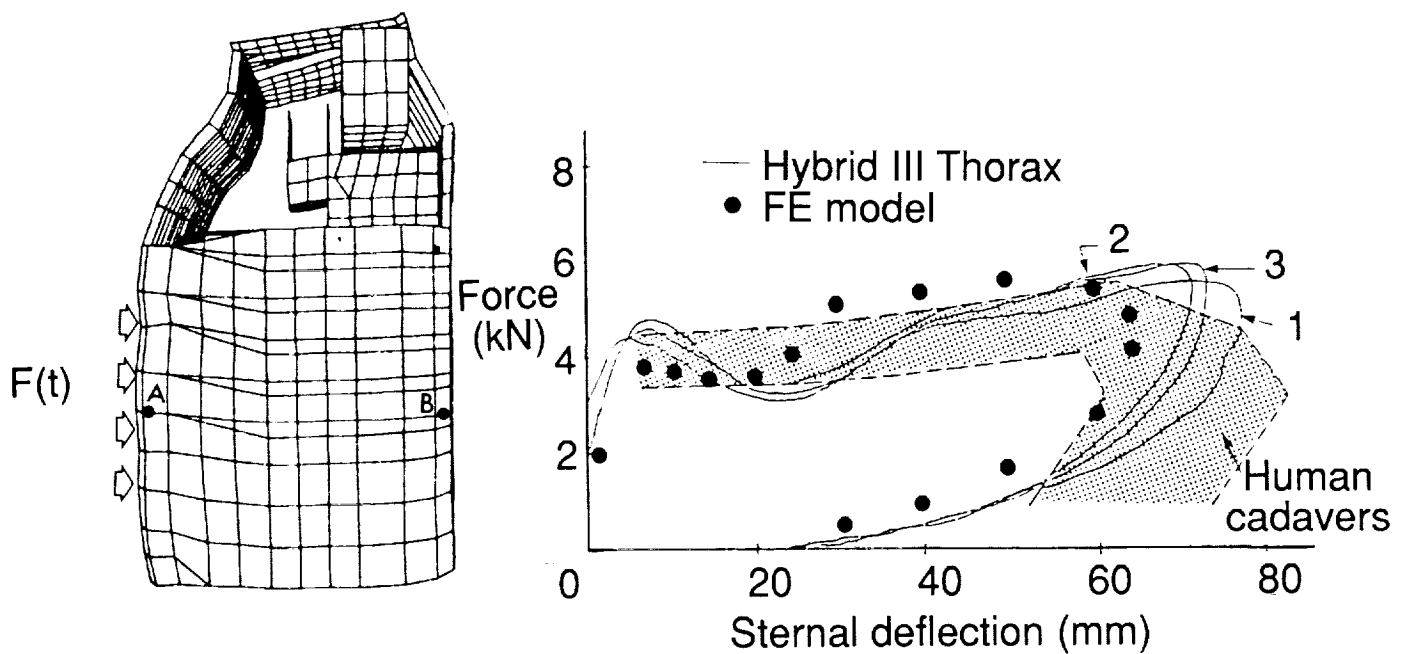


Figure 3. ATD thoracic response for pendulum impact (Ref. 2).

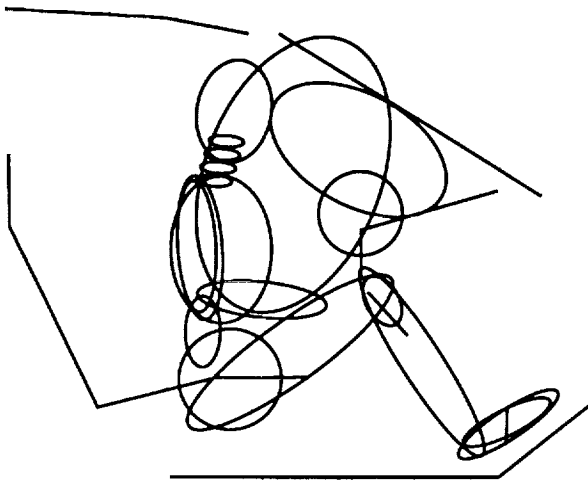
INTRODUCTION

The automotive industry has used computational methods for crashworthiness since the early 1970's. These methods have ranged from simple lumped parameter models to full finite element models. The emergence of the full finite element models in the mid 1980's has significantly altered the research direction. However, there remains a need for both simple, rapid modeling methods and complex detailed methods. This paper will discuss some directions for continuing research.

148

COMPUTATIONAL METHODS FOR CRASHWORTHINESS

Although the design problem in automotive safety is coupled, traditionally automotive crashworthiness analysis has been separated into methods that address the structural performance and methods that address the occupant performance. The coupling is usually handled by using the results of the structural analysis, typically passenger compartment accelerations and some panel motions, as input into the occupant analysis. In addition, a wide range of modeling methods are used ranging from simple lumped parameter models to full nonlinear finite element models and including virtually all possible intermediate hybridizations. The simple models have the advantages of ease of generation and interpretation with some sacrifice of accuracy, whereas the finite element methods have the potential to express our best knowledge of mechanics but at the expense of model creation and computational time.



Lumped parameter occupant model with air cushion

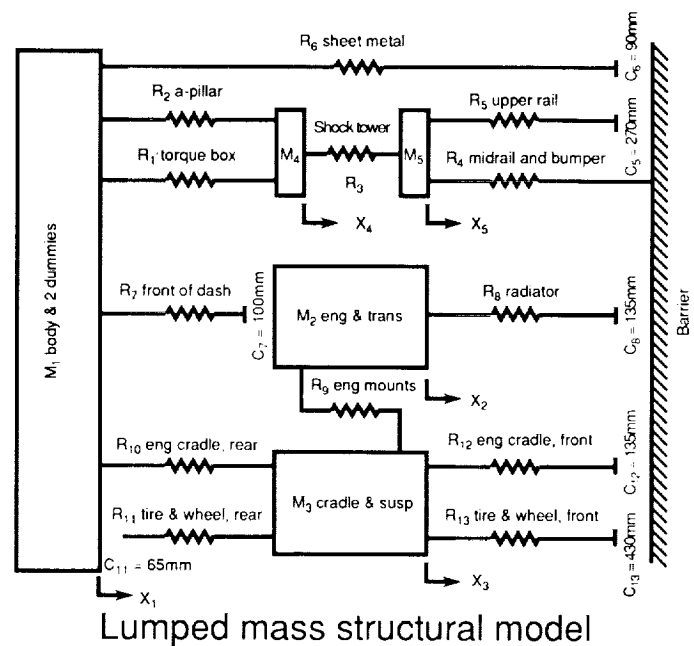
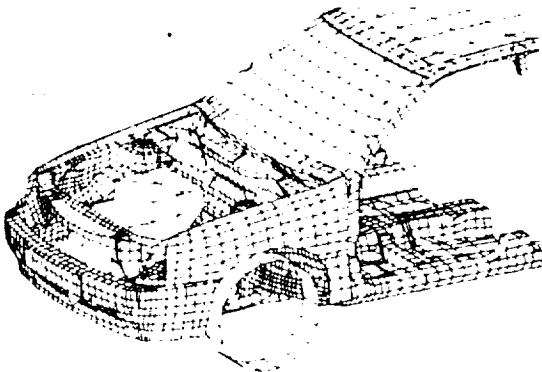
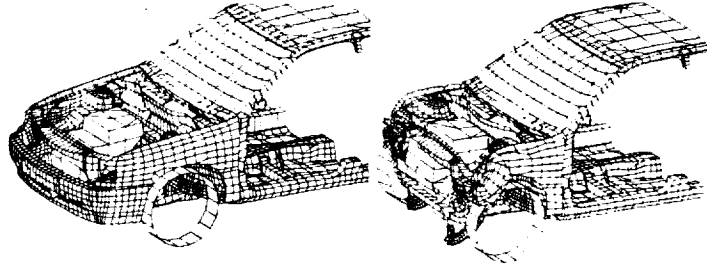


Figure 1. Typical computational models.

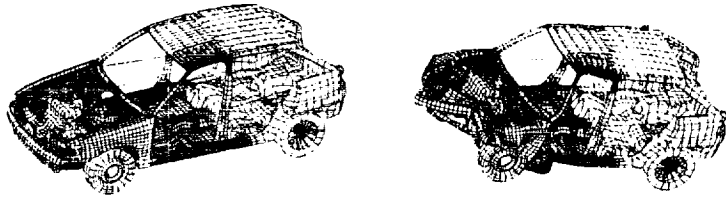
USE OF NONLINEAR FINITE ELEMENT METHODS

Since the thrust of this workshop is to focus on new directions in computational methods, this presentation will concentrate on the finite element methods. By now virtually every automotive company has published simulations using one of the many commercially available nonlinear finite element programs. These simulations are reaching significant complexity, showing front, side, rear, car-to-car and angled impacts. The typical results that are shown are a deformed mesh plot and some overall measure of accuracy, typically a passenger compartment deceleration.

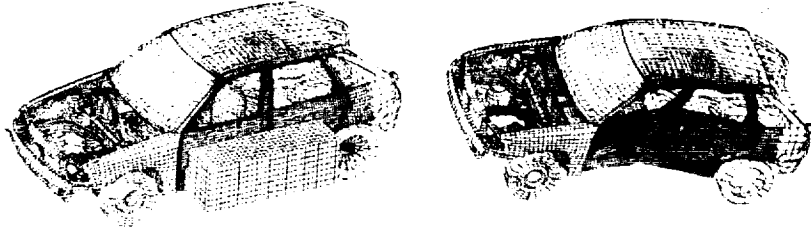
Front impact



Oblique impact



Side impact



Rear impact
(car-to-car)

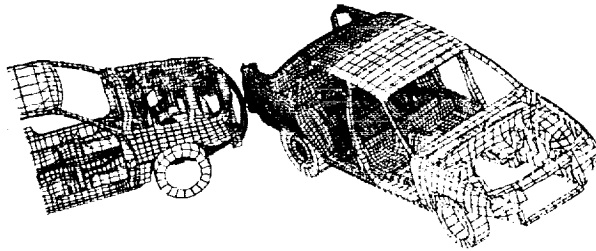


Figure 2. Typical nonlinear finite element results (Ref. 1).

OCCUPANT MODELS

Although most of the published work has focused on the structural models, some work is starting to appear on interior components and the occupant. Typically, the occupant modeled is the mechanical surrogate used in tests rather than the actual human. In these cases the accuracy of the finite element model is compared to the performance of the mechanical surrogate, called the anthropomorphic test dummy (ATD) rather than to the human response. The performance requirements for the ATD are specified based on bio-mechanical modeling of the human. Federal mandated standards are based on mechanical quantities (acceleration, force) that are measured on the ATD. Thus, in the figure below the human cadaver results were used to establish a corridor of behavior in which the Hybrid III ATD chest should perform.

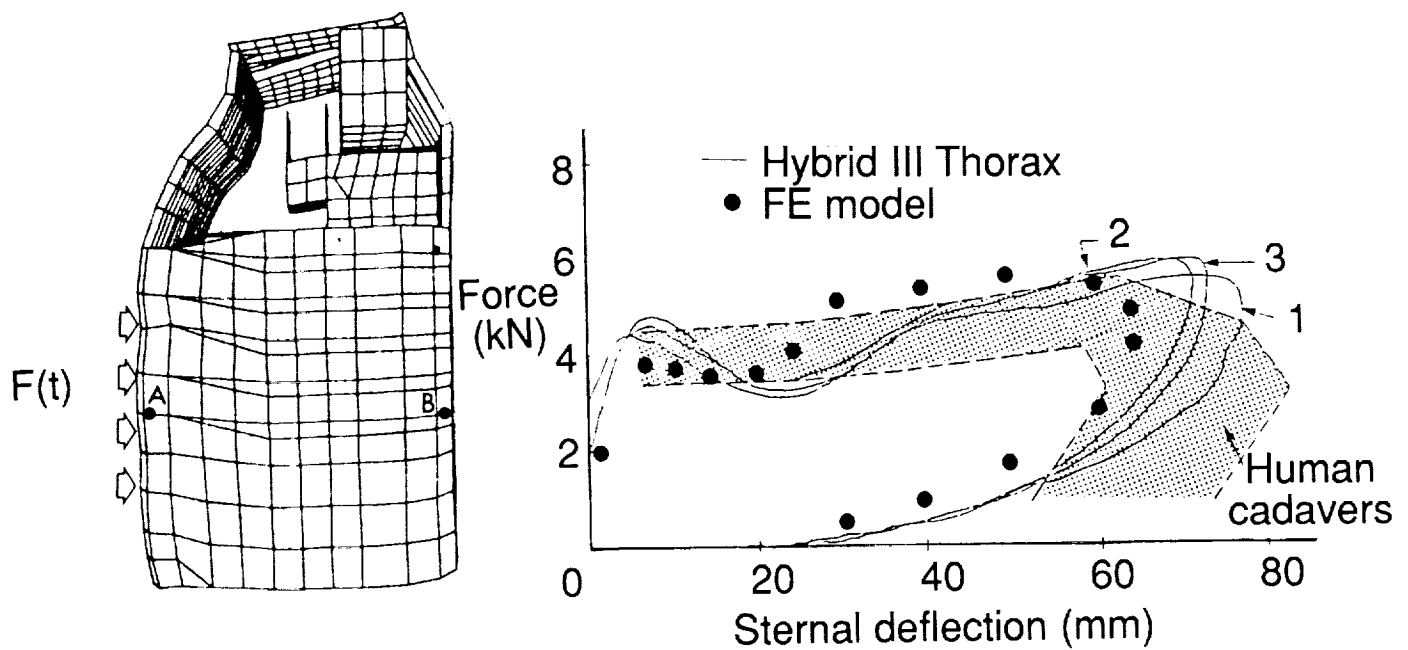


Figure 3. ATD thoracic response for pendulum impact (Ref. 2).

SO WHAT ARE THE PROBLEMS?

Reading the literature, one would conclude that nonlinear finite element methods are a well used and understood technology and that there is relatively little research work that needs to be pursued. We believe that there are four areas that need to be examined. First, the published work tends to mask a real difficulty in capturing local details of response that can be significant in crash performance. There is a dearth of appropriate failure models of any except the traditional isotropic materials. The issue of implementation for these techniques on the next generation of parallel computers is important. Finally, how these models are integrated in a rapidly shrinking design cycle must be addressed.

- 1. ACCURACY OF LOCAL DETAILS**
- 2. MODELS FOR NON-TRADITIONAL MATERIALS**
- 3. MASSIVELY PARALLEL IMPLEMENTATIONS**
- 4. DESIGN**

Figure 4. Issues to be addressed.

FIDELITY OF LOCAL MODELS

The literature rarely contains the efforts that are expended to produce high quality local results that ultimately lead to high quality global results. In this figure two models of an engine cradle are shown. The engine cradle is used to attach the engine to the front rails in a front wheel drive vehicle. The difference in these two models is the inclusion of the small lightening holes which are approximately 1 cm. diameter. The subsequent difference in geometric failure modes defines how the engine will move in the crash and may lead to a significant difference in occupant behavior.

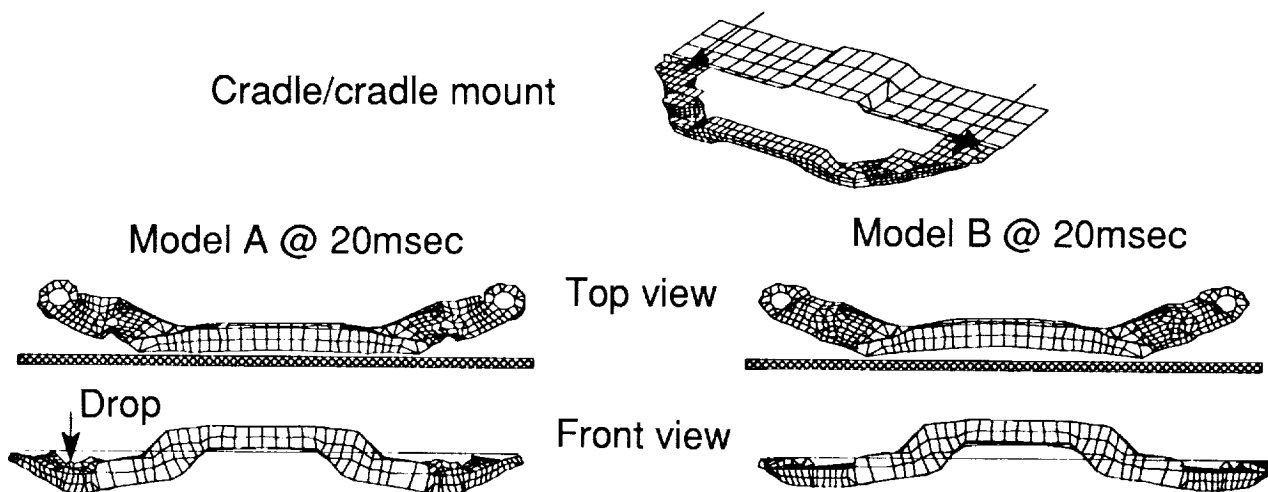


Figure 5. Two detailed models of an engine cradle (Ref. 3).

FIDELITY OF LOCAL MODELS

A second example is the rail shown below. The difference in the two models is the level of mesh density. Clearly the failure modes are different. While it is easy to dismiss these two examples as trivial examples of modeling techniques, virtually every project that we are aware of has encountered similar difficulties that could not be resolved without careful examination of test results and repeated remodeling. To become an effective design tool we need to be able to better understand the complexity of modeling required to make design decisions.

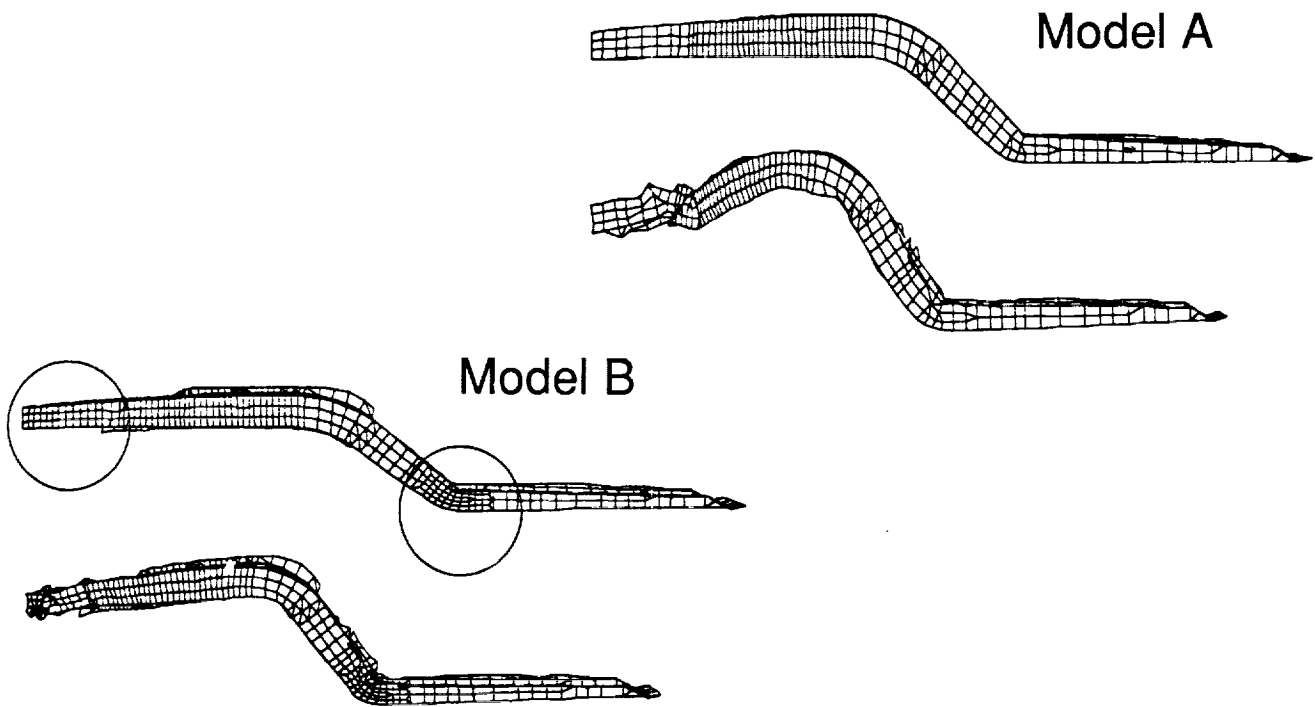


Figure 6. Influence of mesh density on front rail response (Ref. 3).

MATERIAL MODELS

As indicated earlier the current suite of effective material models available in the nonlinear finite element programs is somewhat limited to isotropic materials. Although there are current efforts to model non-traditional materials, our success rate for modeling nonlinear and failure behavior of non-traditional materials for design is not strong. In particular, we see a need to model fabric (airbag), composites (chopped and continuous), honeycombs, and foams.

NONTRADITIONAL MATERIALS

AIRBAGS

CHOPPED AND CONTINUOUS FIBER COMPOSITES

HONEYCOMB

FOAMS

Figure 7. Non-traditional materials.

COMPUTATIONAL EFFICIENCY

There is a widespread belief that the next big leap in computational efficiency will come from the massively parallel computer architecture. There is also a belief that this will require fundamental changes to the current group of codes that are being developed. As the figure shows, for example, significant speedups can be obtained if contact algorithms are properly implemented. If the changes needed to implement these massively parallel versions of existing codes are as great as presently thought, it is possibly a project for which a cooperative approach would be appropriate.

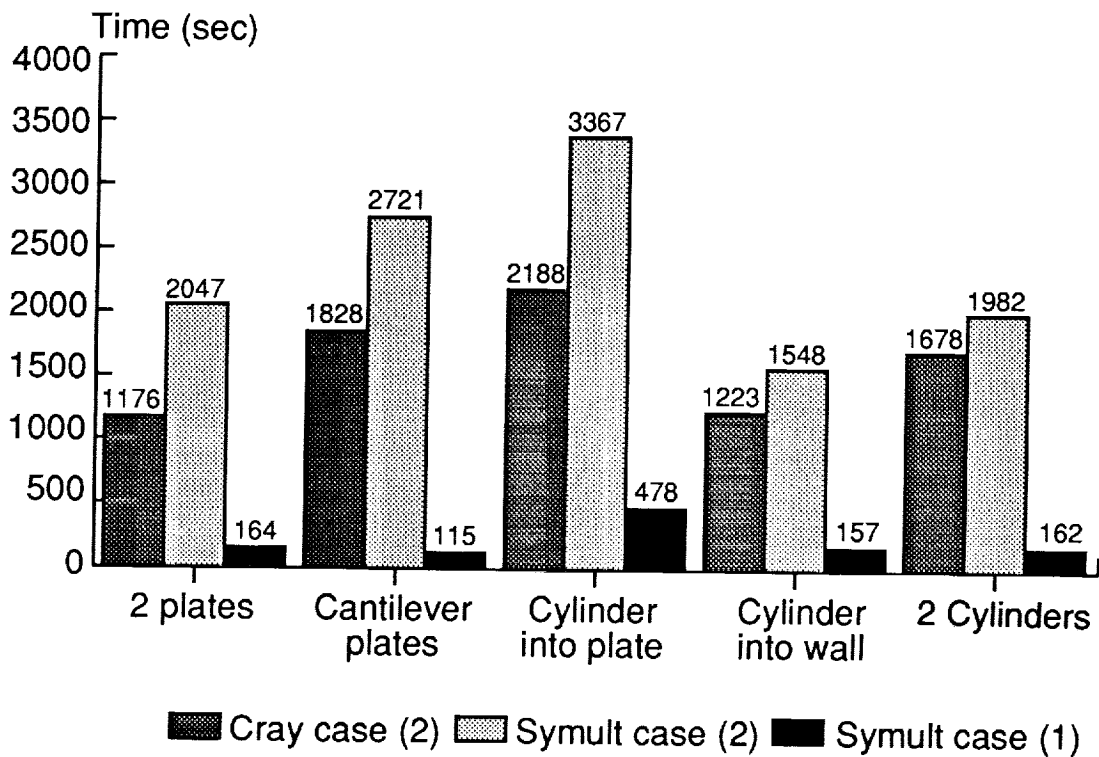


Figure 8. Comparison of execution times for case(1) (improved parallel contact) and case (2) (no parallel contact) (Ref. 4).

REFERENCES

1. Kaiser, A., "Some Examples of Numerical Simulation in Vehicle Safety Development," Proceedings of the Eighth International Conference on Vehicle Structural Mechanics, Society of Automotive Engineers, 1992, pp. 107-117.
2. Khalil, T. B. and Lin, K. H., "Hybrid III Thoracic Impact on Self-Aligning Steering Wheel by Finite Element Analysis and Mini-Sled Experiments," Proceedings of the 35th Stapp Car Crash Conference, Society of Automotive Engineers, 1991, pp. 73-84.
3. Sheh, M. Y. and Reid, J. D., "Vehicle Crashworthiness Analysis Using Numerical Methods and Experiments," Proceedings of the Eighth International Conference on Vehicle Structural Mechanics, Society of Automotive Engineers, 1992, pp. 119-128.
4. Malone, J. G. and Johnson, N. L., "A Parallel Contact Algorithm for Finite Element Analysis of Shell Structures," Proceedings of the Eighth International Conference on Vehicle Structural Mechanics, Society of Automotive Engineers, 1992, pp. 165-170.
5. Lust, R., "Structural Optimization with Crashworthiness Constraints," General Motors Research Laboratories Publication, GMR-7154, Sept. 1990.

COMPUTATIONAL EFFICIENCY

There is a widespread belief that the next big leap in computational efficiency will come from the massively parallel computer architecture. There is also a belief that this will require fundamental changes to the current group of codes that are being developed. As the figure shows, for example, significant speedups can be obtained if contact algorithms are properly implemented. If the changes needed to implement these massively parallel versions of existing codes are as great as presently thought, it is possibly a project for which a cooperative approach would be appropriate.

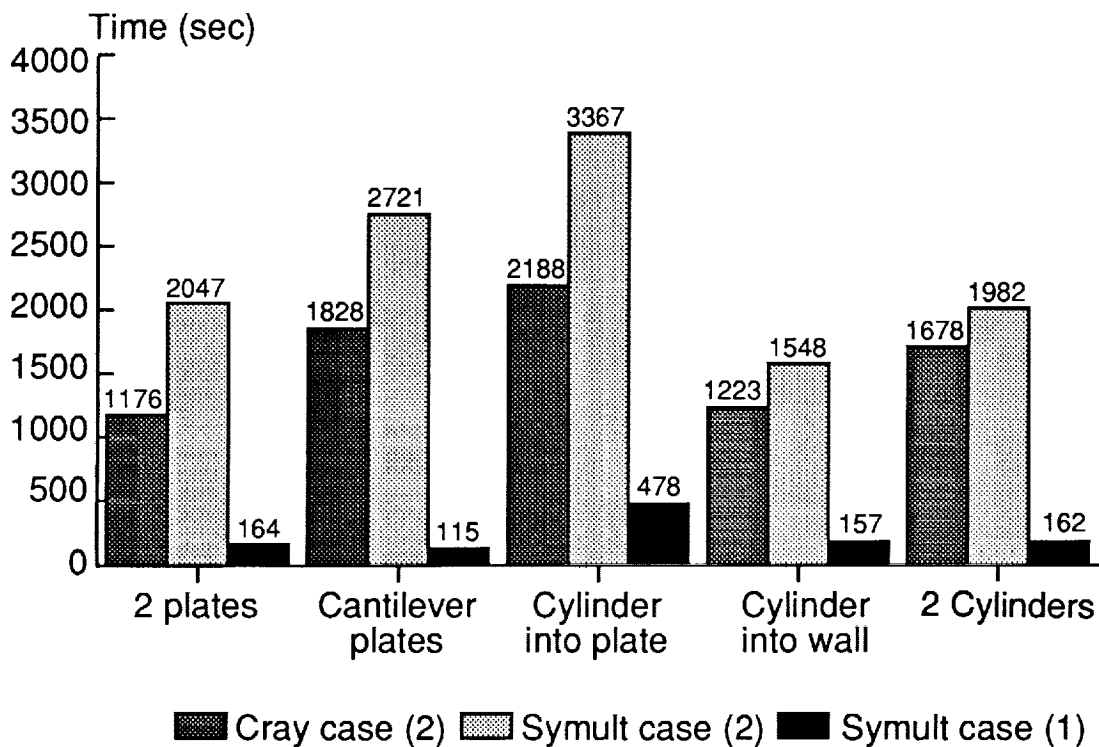


Figure 8. Comparison of execution times for case(1) (improved parallel contact) and case (2) (no parallel contact) (Ref. 4).

DESIGN ISSUES

Currently it takes from three to six months to develop a validated full vehicle finite element model that can be effectively used for design direction. With the current push to reduce the automotive vehicle design cycle into the 24-month time range, this model building cycle is clearly unacceptable. Thus, even if we cut the execution time for the codes to minutes rather than hours, we still may not have significantly affected the design process. Although fully automatic mesh generators for two-dimensional fields have been around for almost ten years (for both triangles and quads), they have not been effectively used for assembled structures. This suggests that more work needs to be focused on this critical problem.

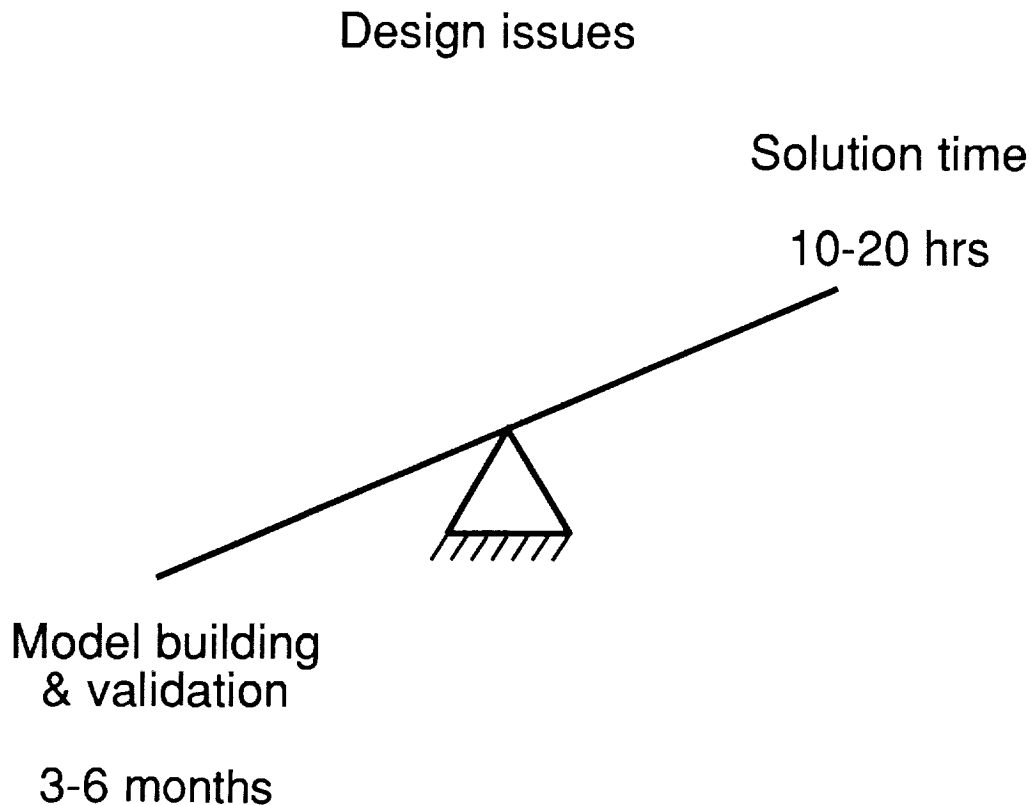


Figure 9. Significance of improved modeling methods.

DESIGN ISSUES

Finally, although linear elastic structural optimization is one of the most developed fields of engineering design research, there have been a mere handful of papers in the area of crashworthiness optimization. Based on work in linear elastic structural optimization, there are two potentially fruitful areas of research. First, there is the question of efficient calculation of sensitivity information. This is made doubly difficult because of the presence of nonlinearities introduced by contact. Second is the idea of constructing inexpensive, robust local design space approximations. In the example shown below, a lumped mass model was used as the local approximation and the finite element model was used only at a few number of points in the design space.

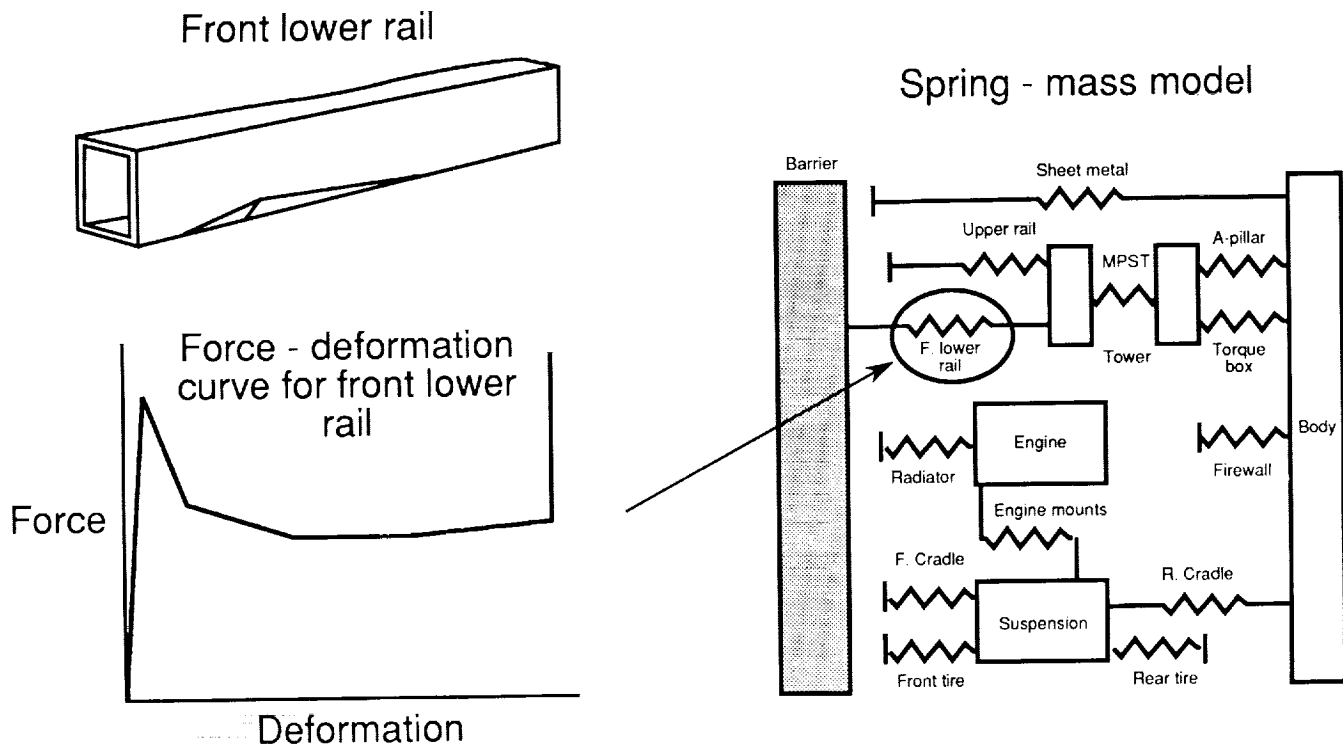


Figure 10. Optimum design with crashworthiness constraints (Ref. 5).

REFERENCES

1. Kaiser, A., "Some Examples of Numerical Simulation in Vehicle Safety Development," Proceedings of the Eighth International Conference on Vehicle Structural Mechanics, Society of Automotive Engineers, 1992, pp. 107-117.
2. Khalil, T. B. and Lin, K. H., "Hybrid III Thoracic Impact on Self-Aligning Steering Wheel by Finite Element Analysis and Mini-Sled Experiments," Proceedings of the 35th Stapp Car Crash Conference, Society of Automotive Engineers, 1991, pp. 73-84.
3. Sheh, M. Y. and Reid, J. D., "Vehicle Crashworthiness Analysis Using Numerical Methods and Experiments," Proceedings of the Eighth International Conference on Vehicle Structural Mechanics, Society of Automotive Engineers, 1992, pp. 119-128.
4. Malone, J. G. and Johnson, N. L., "A Parallel Contact Algorithm for Finite Element Analysis of Shell Structures," Proceedings of the Eighth International Conference on Vehicle Structural Mechanics, Society of Automotive Engineers, 1992, pp. 165-170.
5. Lust, R., "Structural Optimization with Crashworthiness Constraints," General Motors Research Laboratories Publication, GMR-7154, Sept. 1990.

58-54

187839

0.8

N94-19473

Efficiency and Biofidelity of Occupant Simulations

Walter D. Pilkey
University of Virginia
Charlottesville, VA

R AND G PARAMETERS: ATB SIMULATOR UNLOADING BEHAVIOR

This figure demonstrates how unloading is handled in the ATB occupant simulator for contact planes and seatbelts. Two parameters, R and G, are specified. R is the ratio of rebound energy to initial energy and G is the ratio of permanent deformation to maximum deformation. The program unloads along a quadratic curve which intersects the x-axis at D1, the point defined by G. The quadratic function is chosen to match the requested value of R as closely as possible while satisfying the G condition exactly. This puts an upper limit on R, which for linear loading and unloading is seen to be 1.0 G. Excessive rebound energy from the seatbelts prompted an investigation of the program's sensitivity to these parameters.

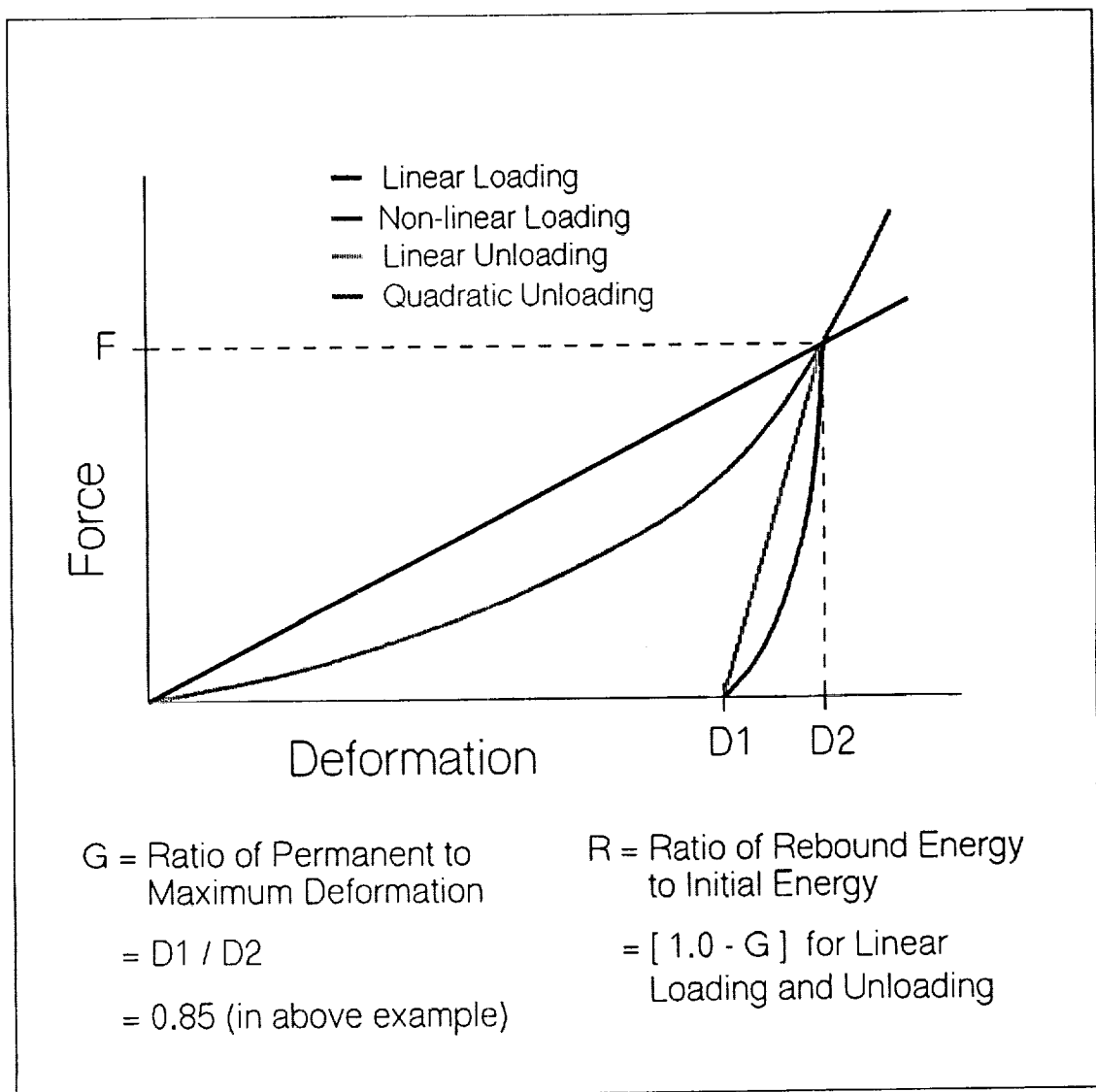


Figure 1

MOTION OF SPHERE RELATIVE TO VEHICLE AFTER VEHICLE DECELERATES

The sketch at the top of this figure shows an ATB model developed by the consulting firm, David James, Ltd. It is simply a sphere, restrained by a single belt, and sliding on a frictionless, decelerating plane (or vehicle). From their study they concluded that the ATB R and G parameters were essentially nonfunctional for the seatbelt. They passed their results on to UVA where initial simulations seemed to confirm their conclusions. However, changing the integration step-size caused a significant change in the results, particularly in the rebound energy of the sphere. A systematic study of step-size sensitivity was undertaken. The sketch at the bottom shows an equivalent restraint situation with the belt replaced by a contact plane. This model was used for comparison to the belt model.

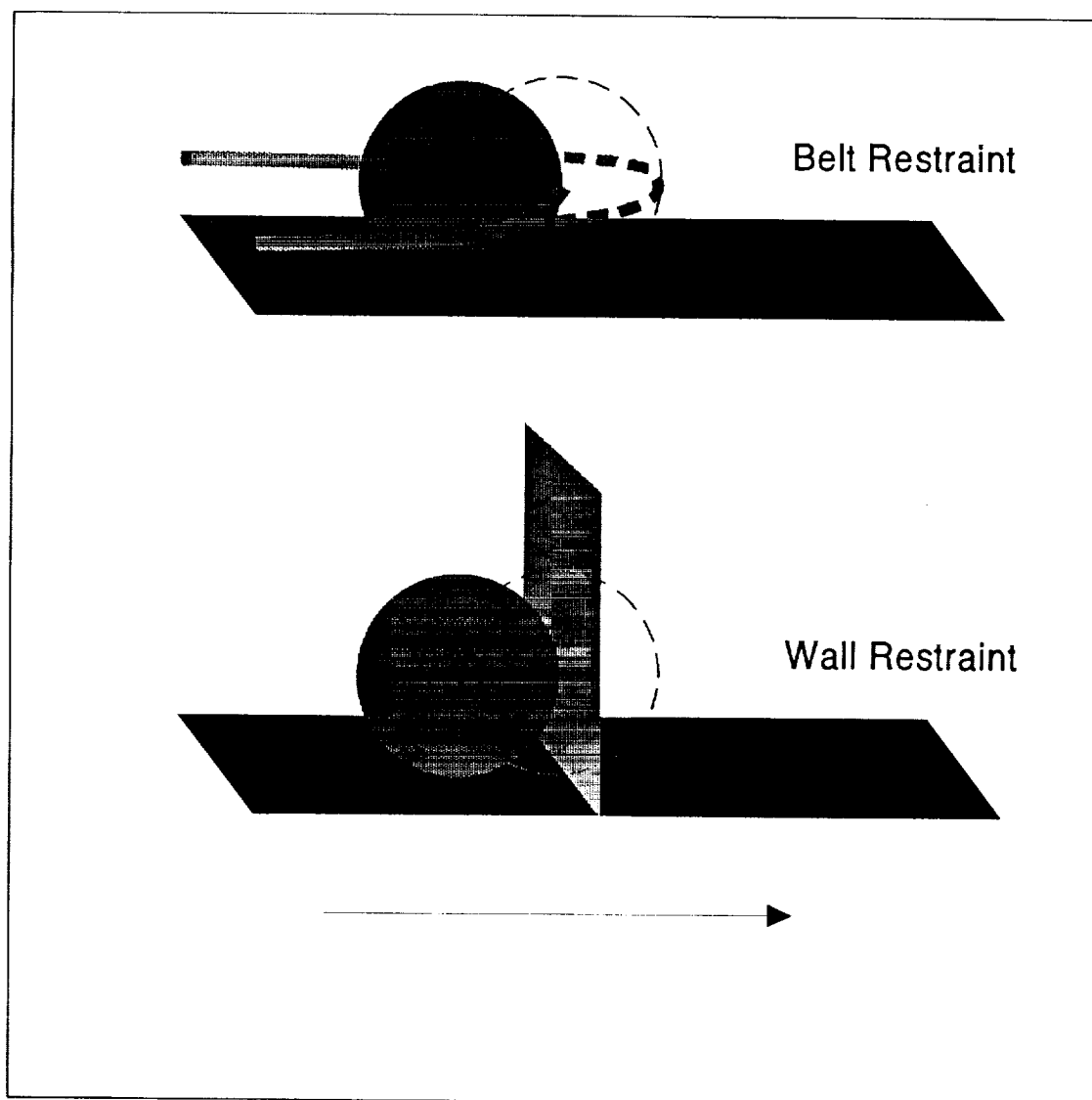


Figure 2

SPHERE DATA FOR BELT RESTRAINT

This figure displays the family of curves that were generated by lowering the integration step-size from 1.0 msec (the value used in the initial R and G investigation) to 0.01 msec. The G value was 0.85. As the 1.0 msec curve shows, the final rebound velocity is indeed greater than the maximum forward velocity. The energy return for the smallest step-size, however, is approximately 0.16, which is near the maximum for linear loading and unloading. Furthermore, the curves do appear to be converging. Unfortunately, the step-size required for convergence is extremely small, much smaller than is normally necessary for motion of an unbelted occupant. The conclusion of this study is that the belt algorithm does work, including the R and G parameters, but very small step-sizes are needed to get reasonable results.

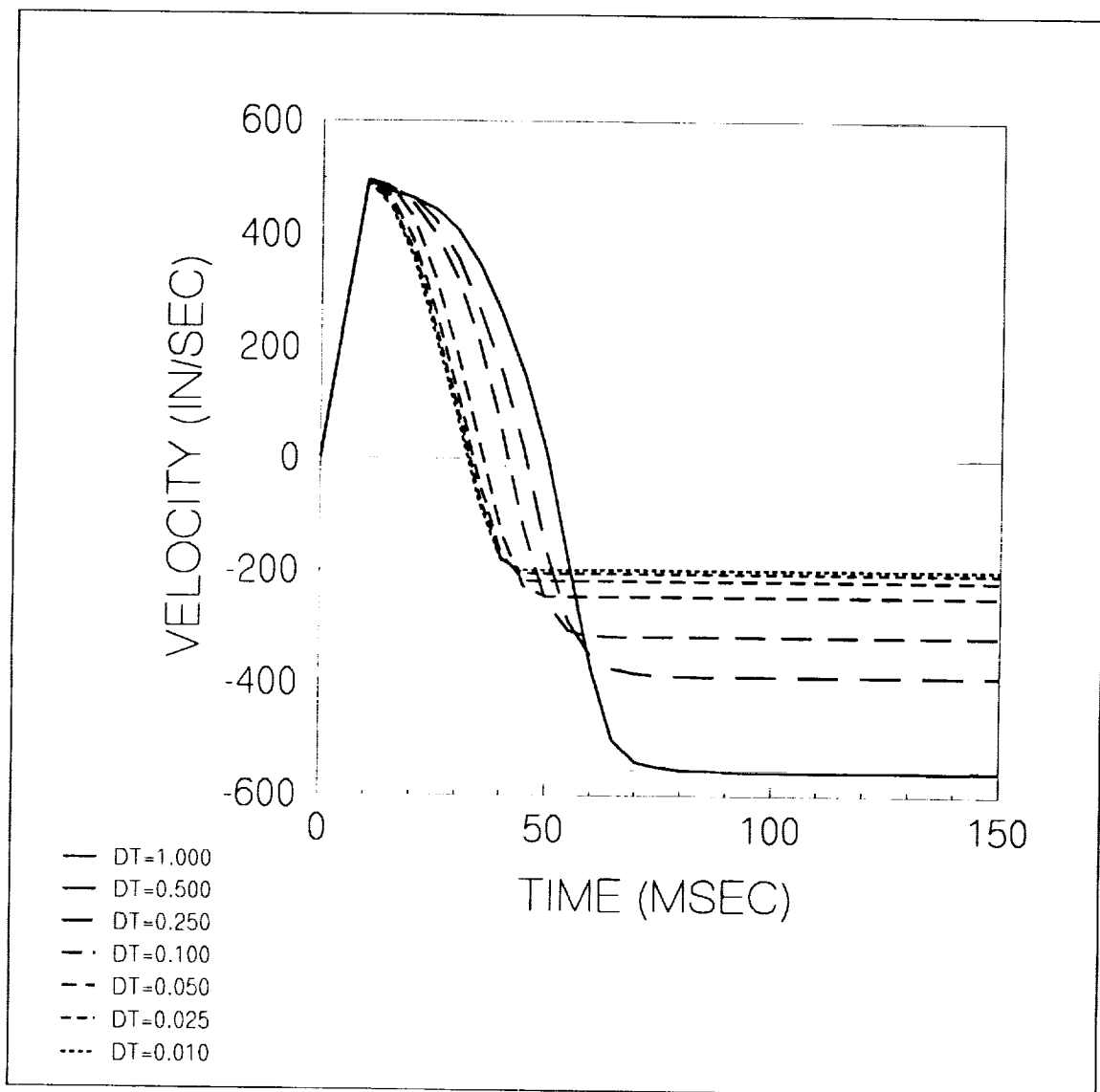


Figure 3

SPHERE DATA FOR BELT RESTRAINT

This figure displays the family of curves that were generated by lowering the integration step-size from 1.0 msec (the value used in the initial R and G investigation) to 0.01 msec. The G value was 0.85. As the 1.0 msec curve shows, the final rebound velocity is indeed greater than the maximum forward velocity. The energy return for the smallest step-size, however, is approximately 0.16, which is near the maximum for linear loading and unloading. Furthermore, the curves do appear to be converging. Unfortunately, the step-size required for convergence is extremely small, much smaller than is normally necessary for motion of an unbelted occupant. The conclusion of this study is that the belt algorithm does work, including the R and G parameters, but very small step-sizes are needed to get reasonable results.

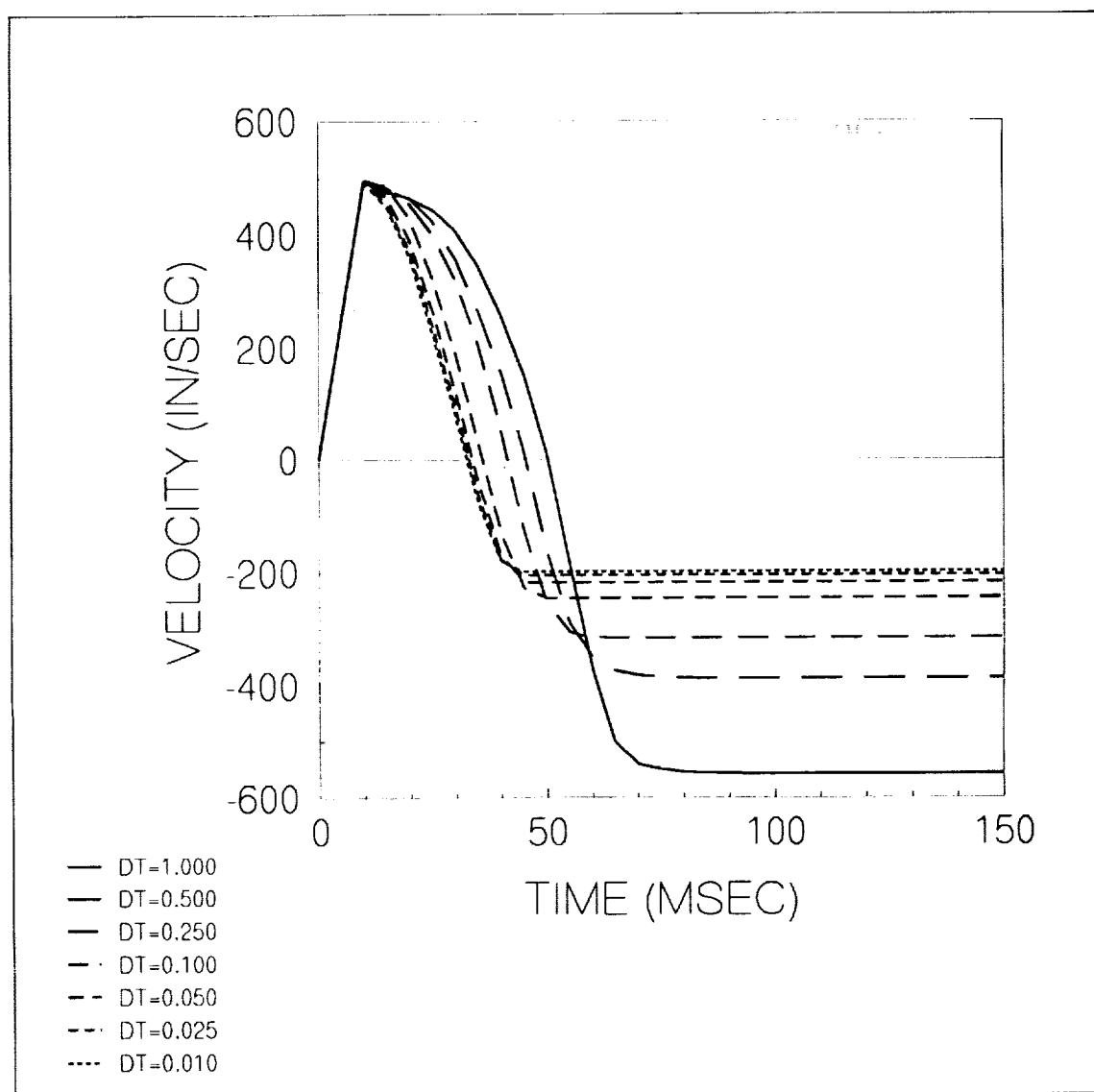


Figure 3

SPHERE DATA FOR WALL IMPACT

To check that the integration problems were limited to the seatbelt, an equivalent model was set up, as described in Fig. 2, with the belt replaced by a contact plane (or wall). This figure shows that the wall impact results are nearly identical to the best belt results and that there is no discernable difference between the wall results for 1.0 msec and for 0.01 msec. In fact, the two cases exhibited four-digit agreement. Thus, the basic integration method is apparently sound and problems are limited to the belt algorithm.

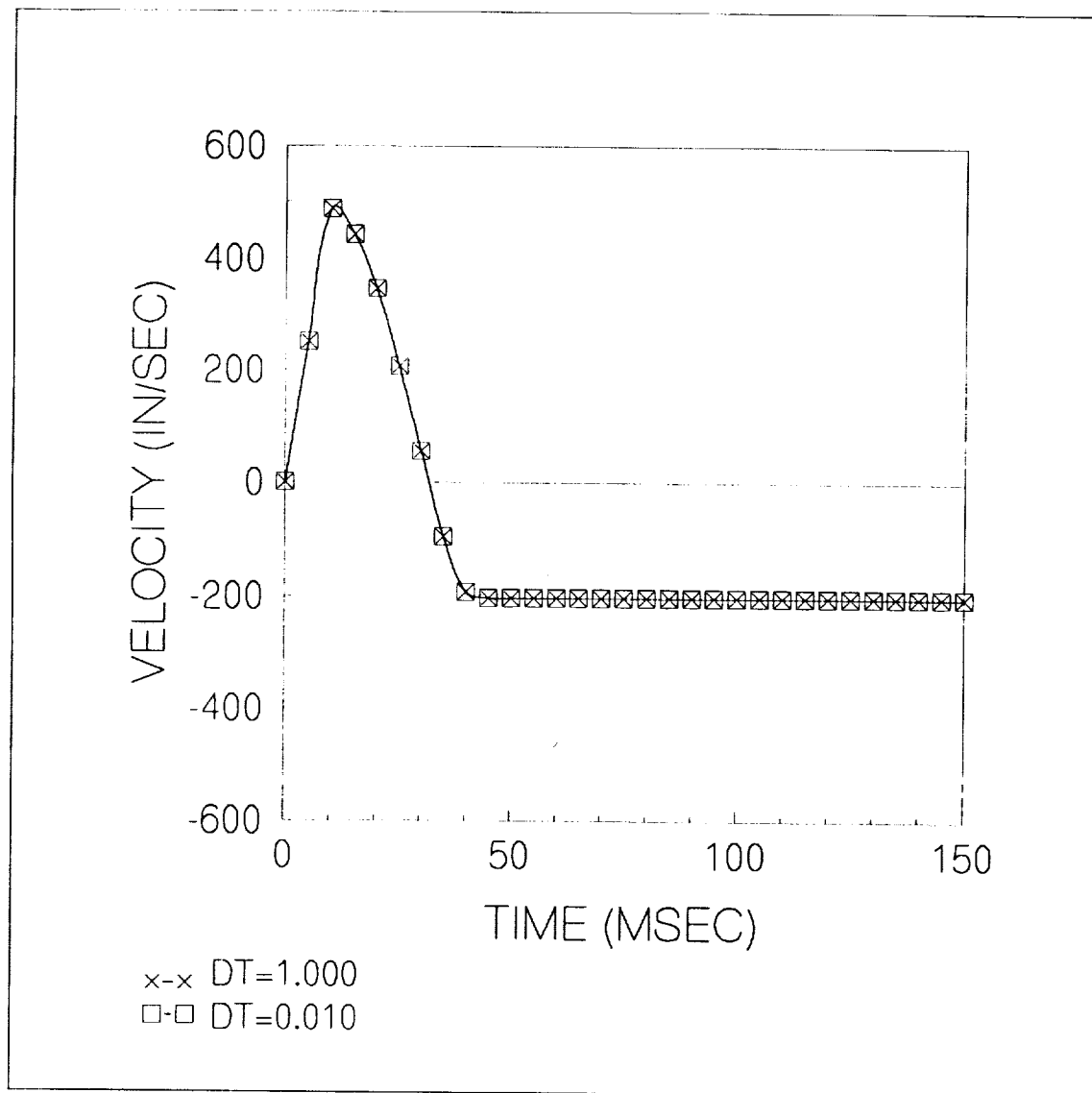


Figure 4

HEAD ACCELERATION VS. BELT SLACK X-DIRECTION (MEASURED)

This figure shows head acceleration curves from two UVA impact sled tests which used the same parameters except for the amount of slack in the shoulder belt. Of particular interest is the secondary peak that occurs near 85 msec for the curve generated by the run with 3 inches of slack. This peak had been noticed before in sled tests and in simulations, but had been considered not to have any significance since its magnitude was always much lower than that of the primary peak. It appears, however, that the secondary peak may be associated with experimental parameters such as belt slack. Thus, while they are not of great importance from the standpoint of injury prediction, this and other secondary features have the potential to be of useful diagnostic value if their appearance in the pulse can consistently be associated with known parameters.

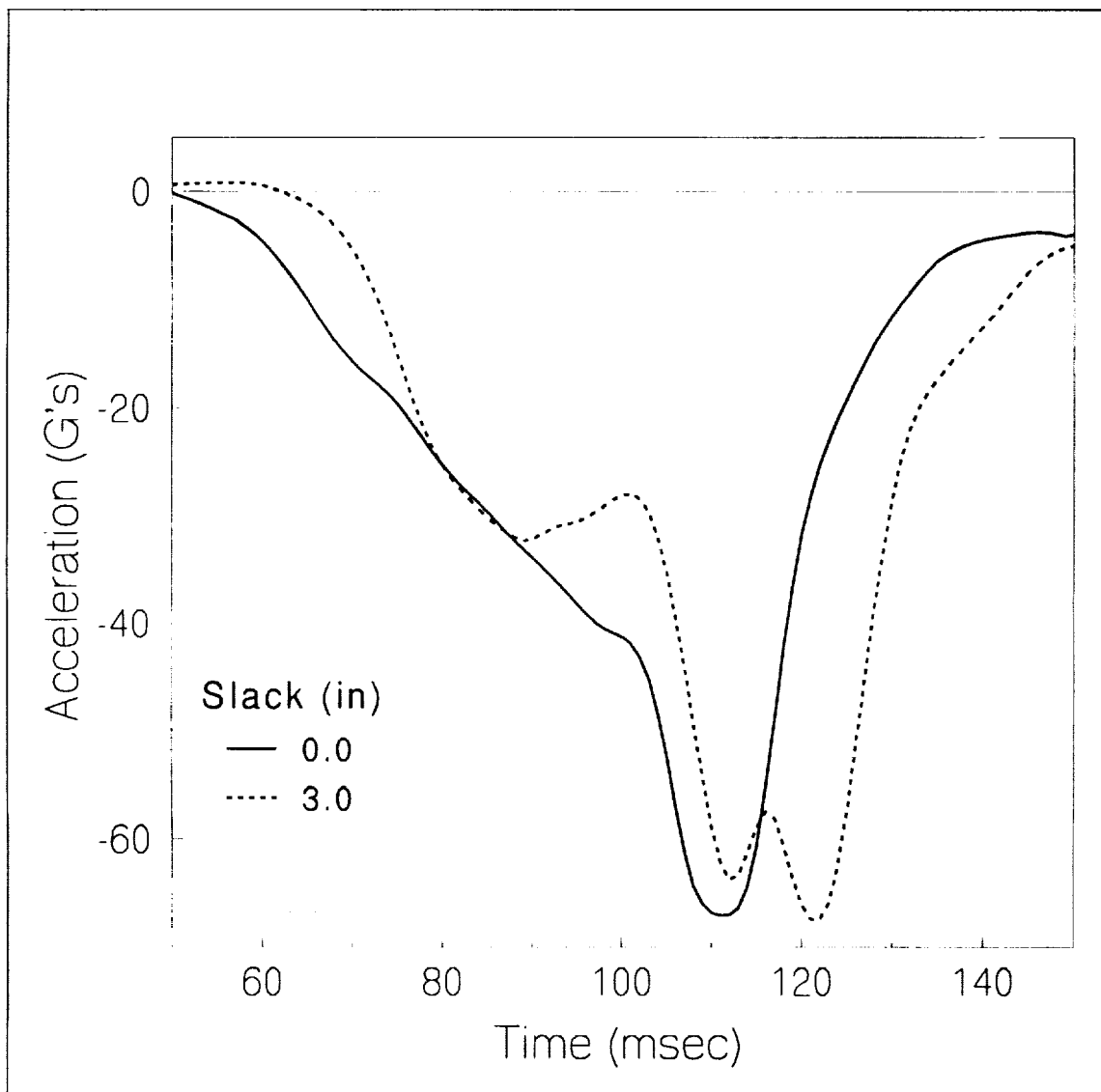


Figure 5

HEAD ACCELERATION VS. BELT SLACK X-DIRECTION (SIMULATED)

This figure shows ATB simulator results which are similar to the sled measurements. The shape and timing of the pulses need some improvement before they are compared directly to the sled results, but the appearance of a secondary peak resulting from the introduction of belt slack is clearly demonstrated.

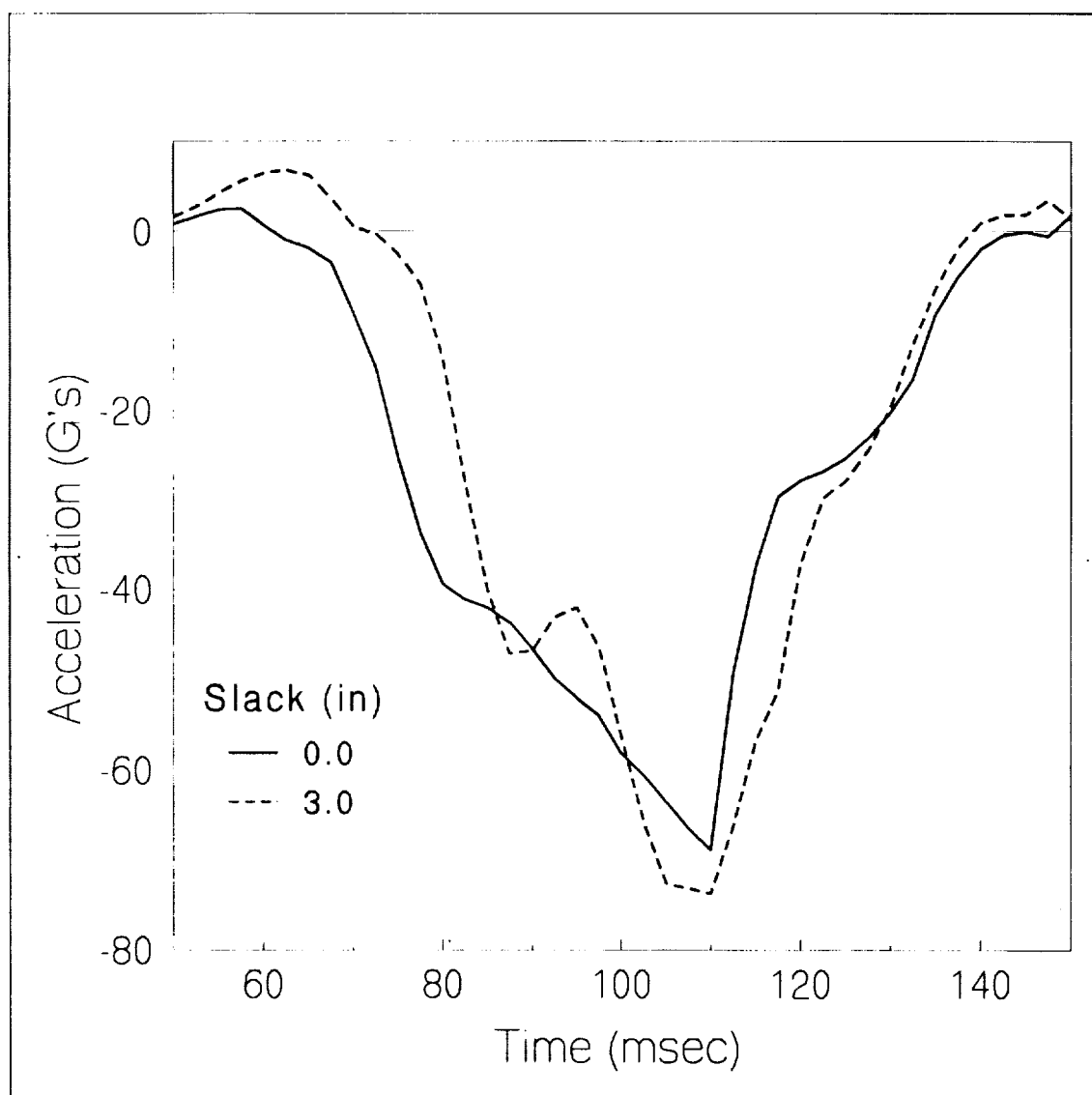


Figure 6

HEAD ACCELERATION VS. BELT SLACK X-DIRECTION (SIMULATED)

This figure shows that the secondary peak is not an anomaly associated with a particular value of belt slack. It appears for higher and lower values as well, and demonstrates a predictable sensitivity to the amount of slack. Note that it shows greater sensitivity to the slack parameter than does the primary peak, particularly in terms of timing and the depth from the peak to the following trough. This increased sensitivity may be exploitable when diagnosing test results.

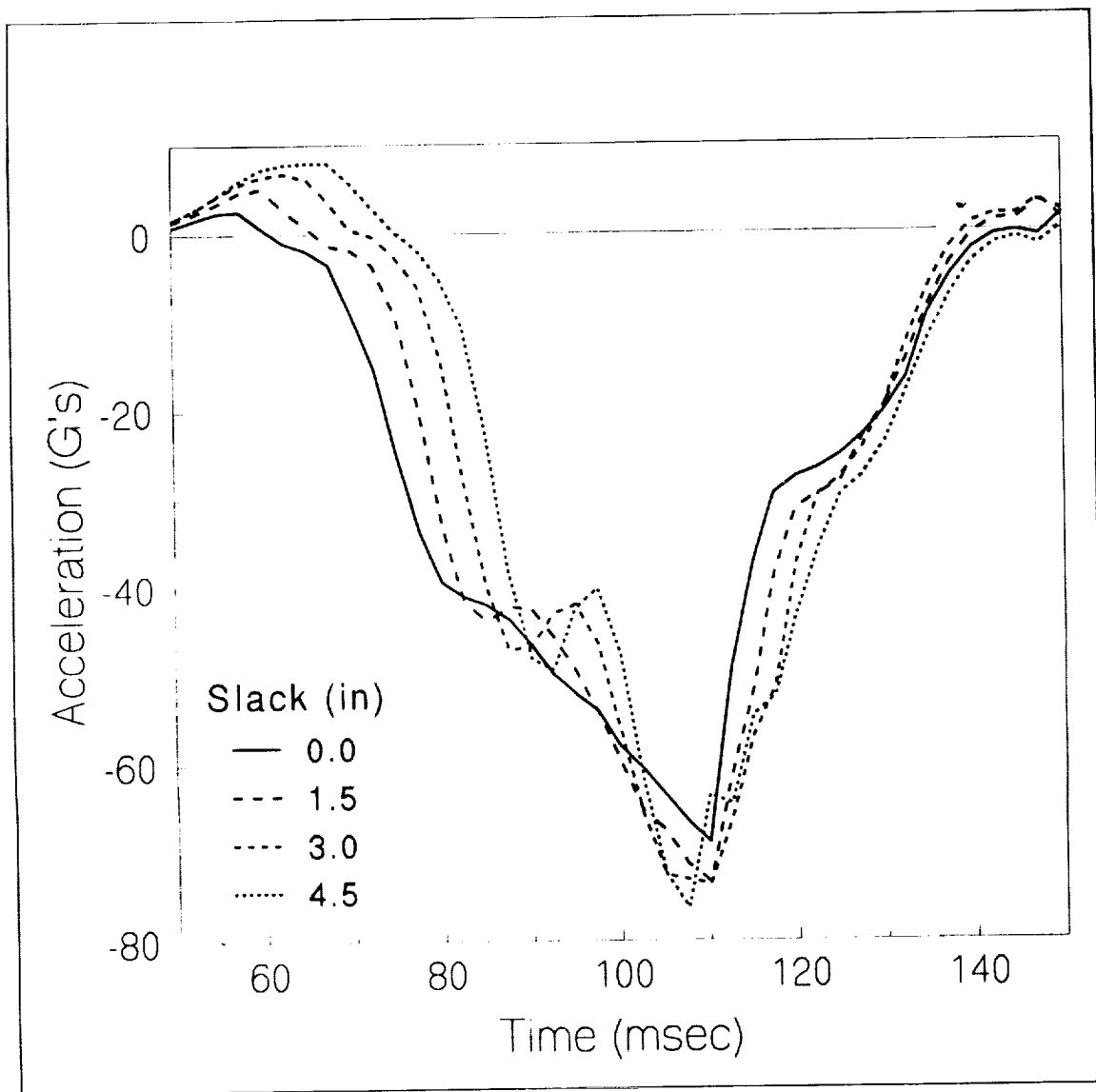


Figure 7

59-39

187840

p. 19

N 9 4 - 1 9 4 7 4

**Current Capabilities for Simulating the Extreme
Distortion of Thin Structures Subjected
to Severe Impacts**

Samuel W. Key
KEY Associates
Albuquerque, NM

PRECEDING PAGE BLANK NOT FILMED

164

165

SUMMARY

The explicit transient dynamics technology in use today for simulating the impact and subsequent transient dynamic response of a structure has its origins in the "hydrocodes" dating back to the late 1940's. The growth in capability in explicit transient dynamics technology parallels the growth in speed and size of digital computers. Computer software for simulating the explicit transient dynamic response of a structure is characterized by algorithms that use a large number of small steps.

In explicit transient dynamics software there is a significant emphasis on speed and simplicity. The finite element technology used to generate the spatial discretization of a structure is based on a compromise between completeness of the representation for the physical processes modelled and speed in execution. That is, since it is expected in every calculation that the deformation will be finite and the material will be strained beyond the elastic range, the geometry and the associated gradient operators must be reconstructed, as well as complex stress-strain models evaluated at every time step. As a result, finite elements derived for explicit transient dynamics software use the simplest and barest constructions possible for computational efficiency while retaining an essential representation of the physical behavior. The best example of this technology is the four-node bending quadrilateral derived by Belytschko, Lin and Tsay (1984).

Today, the speed, memory capacity and availability of computer hardware allows a number of the previously used algorithms to be "improved." That is, it is possible with today's computing hardware to modify many of the standard algorithms to improve their representation of the physical process at the expense of added complexity and computational effort.

The purpose of this presentation is to review a number of these algorithms and identify the improvements possible. In many instances, both the older, faster version of algorithm and the improved and somewhat slower version of the algorithm are found implemented together in software. Specifically, the following seven algorithmic items are examined:

- 1) The invariant time derivatives of stress used in material models expressed in rate form.
- 2) Incremental objectivity and strain used in the numerical integration of the material models.
- 3) The use of 1-point element integration versus mean quadrature.
- 4) Shell elements used to represent the behavior of thin structural components.
- 5) Beam elements based on stress-resultant plasticity versus cross-section integration.
- 6) The fidelity of elastic-plastic material models in their representation of ductile metals.
- 7) The use of Courant subcycling to reduce computational effort.

INVARIANT TIME DERIVATIVE OF STRESS

To account for the fact that bodies subjected to large displacements undergo significant rigid body rotations, material models in rate form rely on an *invariant* time derivative of the stress. For example, a linear elastic material expressed in terms of rates has the form:

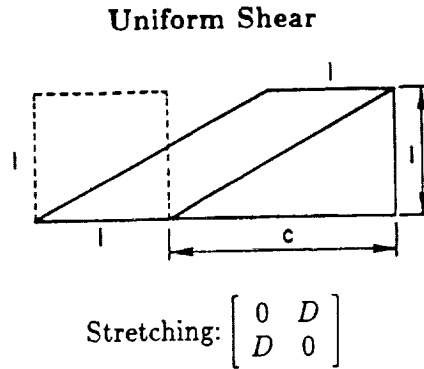
$$\begin{aligned}\dot{t}^{rs} &= \dot{t}^{rs} - \delta^{rk} \omega_{km} t^{ms} - \delta^{sk} \omega_{km} t^{mr} \\ &= C^{rsmn} d_{mn},\end{aligned}\tag{1}$$

where ω_{km} is a rotation rate, d_{mn} is the stretching and C^{rsmn} , the material's elastic modulus. To date the majority of simulations have used the Jaumann invariant derivative which uses the spin for the rotation rate, $\omega_{km} = (v_{k,m} - v_{m,k})/2$.

This formulation is very sensitive to shear strains that are greater than 20% in the presence of rotations (Dienes, 1979).

A more accurate invariant time derivative is the Green-McInnis derivative which is based on the rotation from the polar decomposition of the deformation gradient, $\omega_{km} = \dot{R}_{kn}^T R_m^n$, where $F_\alpha^m = R^{mn} U_{n\alpha}$ (Dienes, 1979).

Computing the uniform shearing of a 1×1 coupon demonstrates the difference in predicted behavior using kinematic hardening plasticity for these two invariant time derivatives (Fig. 1).



$$\begin{aligned}VOL &= 1 \\ \omega &\neq 0 \\ \dot{t}_{12} &= 2\mu d_{12} + \omega_{12}(t_{22} - t_{11}) \\ \dot{t}_{11} &= +2\omega_{12}t_{12} \\ \dot{t}_{22} &= -2\omega_{12}t_{12}\end{aligned}$$

Non-Radial Loading in Plasticity

(Note: $\ln(\ell/\ell_0) = 5 \Rightarrow C = 10$)

Figure 1 - Uniform shearing of a 1×1 coupon

INVARIANT TIME DERIVATIVE OF STRESS (Cont'd.)

An examination of the shear stress as a function of shear strain produces very interesting results (Fig. 2). The results based on using the Green-McInnis derivative in Fig. 2 are denoted by "Dienes." As can be seen, extreme distortions using the Jaumann derivative lead to physically unrealistic stress variations that change sign. The monotone increasing curve denoted by "Dienes" exhibits a physically realistic stress-strain representation. This anomalous behavior exhibited by the Jaumann derivative must be avoided in a simulation if practical results are to be obtained.

For the sake of reliability, today's software will offer the Green-McInnis form of the invariant time derivative of stress along side of the Jaumann derivative for material models based on rate formulations.

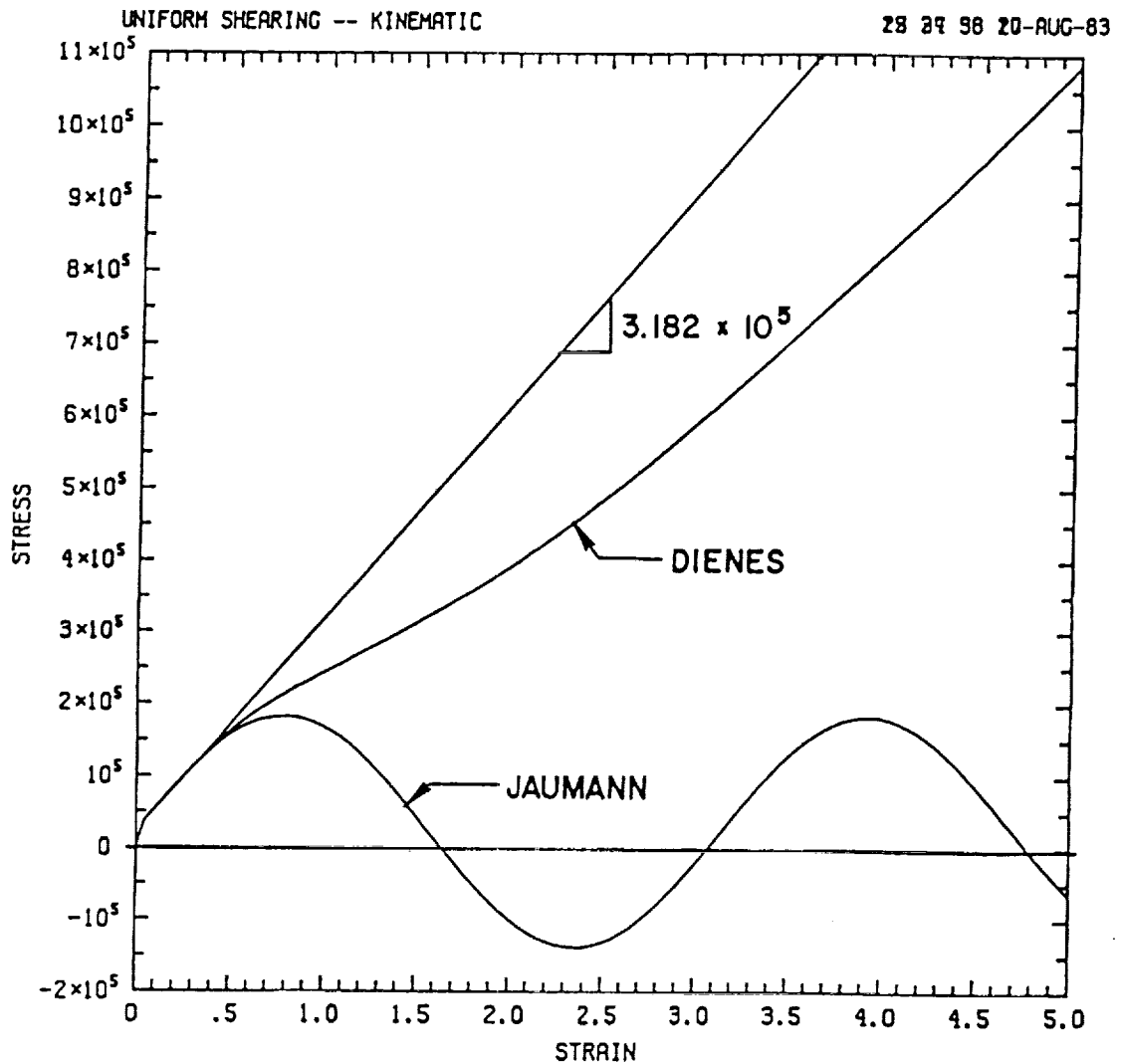


Figure 2 - Kinematic hardening plasticity predictions of shear

INCREMENTAL OBJECTIVITY FOR STRAIN

In numerical simulations differential expressions are replaced with incremental expressions. Incremental expressions for such things as rotation and strain increments can produce errors even for small steps if the properties of the differential expression are lost. For example, when the time derivative of an *orthogonal rotation* is approximated, it is very easy to lose the orthogonal properties associated with the differential form.

The same thing can happen when integrals of strain rates are replaced by sums of strain increments, particularly when finite strains are involved. Traditionally, a strain increment is obtained from the stretching with $\Delta E_{mn} = \Delta t \, d_{mn}$, $d_{mn} = (v_{m,n} + v_{n,m})/2$.

This approach to generating strain increments can be sensitive to cyclic strain histories in the presence of rotations.

A more accurate, but computationally more costly approach, is to base the strain increment on the symmetric stretch tensor U obtained from the polar decomposition of the deformation gradient,

$F_{\alpha}^m = R^{mn} U_{n\alpha}$. This latter approach has been termed *strong objectivity* by M. Rashid (1992), who refers to the traditional approach as *weak objectivity*.

Computing the hoop vibration of a rotating ring provides a good example of the contrasting results that can come from the use of the faster, classical formulations that are weakly objective and the more accurate and costly formulations that are strongly objective. Figure 3 shows an elastic ring given an initial angular velocity of 4,000 radians per second.

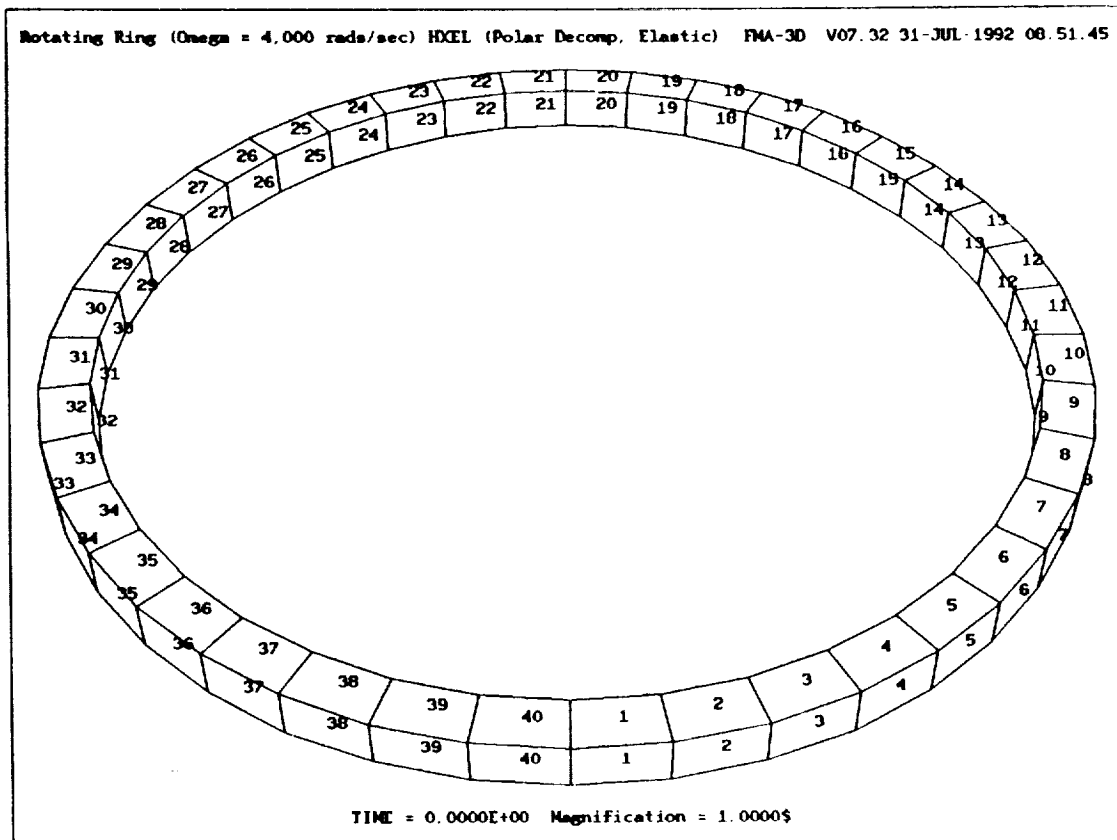


Figure 3 - An elastic ring with an initial 4,000 rad/s angular velocity

INCREMENTAL OBJECTIVITY FOR STRAIN (Cont'd.)

The ring rotates approximately 360 degrees in 1.5 milliseconds. During that time the ring oscillates radially five times (Fig. 4). Of particular interest is the increase in kinetic energy with time (Fig. 4). This is a closed system to which no additional energy is being added. The increase in kinetic energy reflects the accumulation of errors from the strain increments in the classical formulation that is weakly objective in spite of the very small steps in the algorithm.

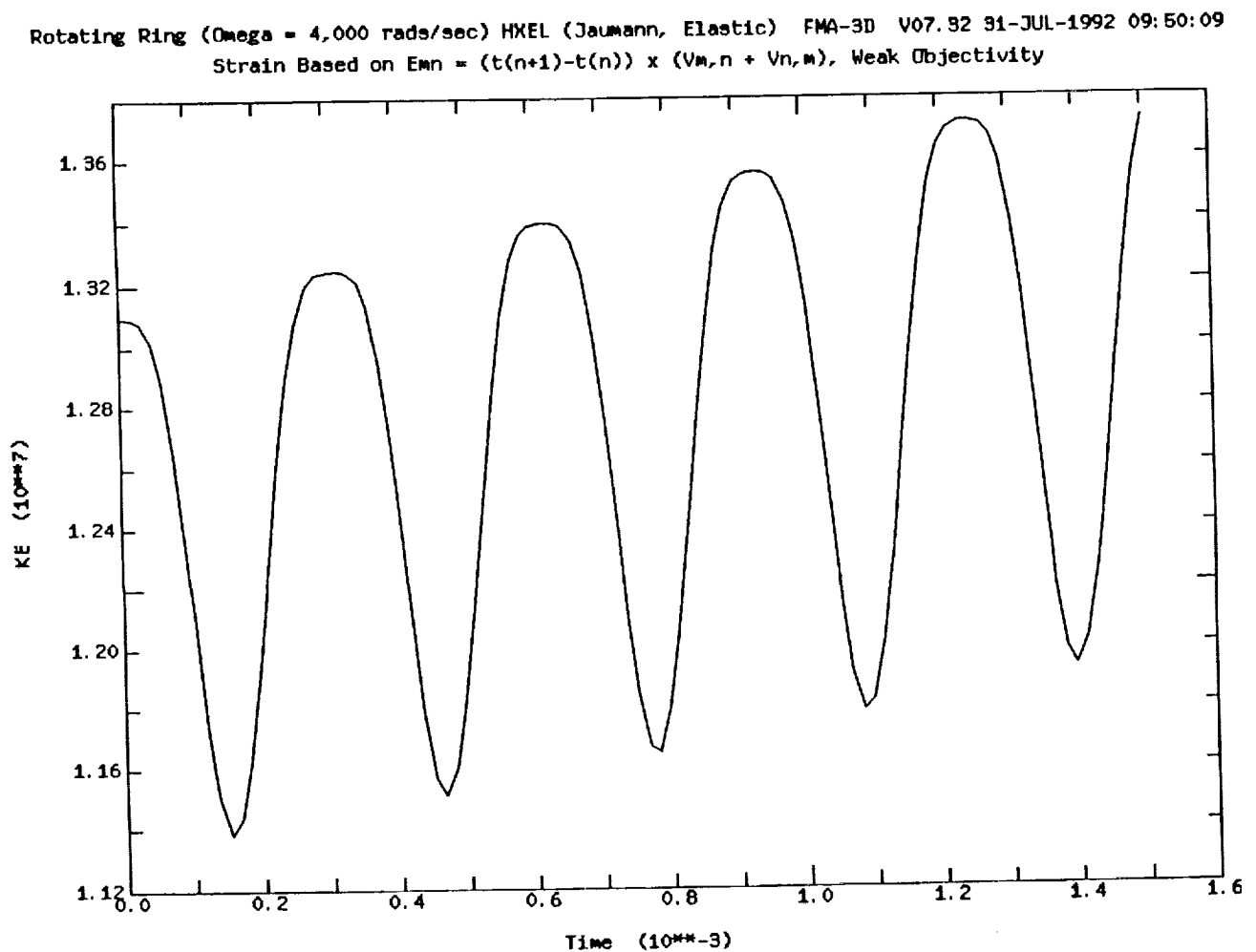


Figure 4 - Kinetic energy response with only weak objectivity

INCREMENTAL OBJECTIVITY FOR STRAIN (Cont'd.)

The same computation using a formulation that is strongly objective in the sense of Rashid shows the expected response (Fig. 5); namely, a kinetic energy that oscillates between two limits that are constant in time. This latter calculation shows an exemplary energy exchange between kinetic energy and internal strain energy as the ring rotates and oscillates radially.

In spite of the increased expense, today's software should offer as the default a strain increment formulation meeting the requirements for strong objectivity.

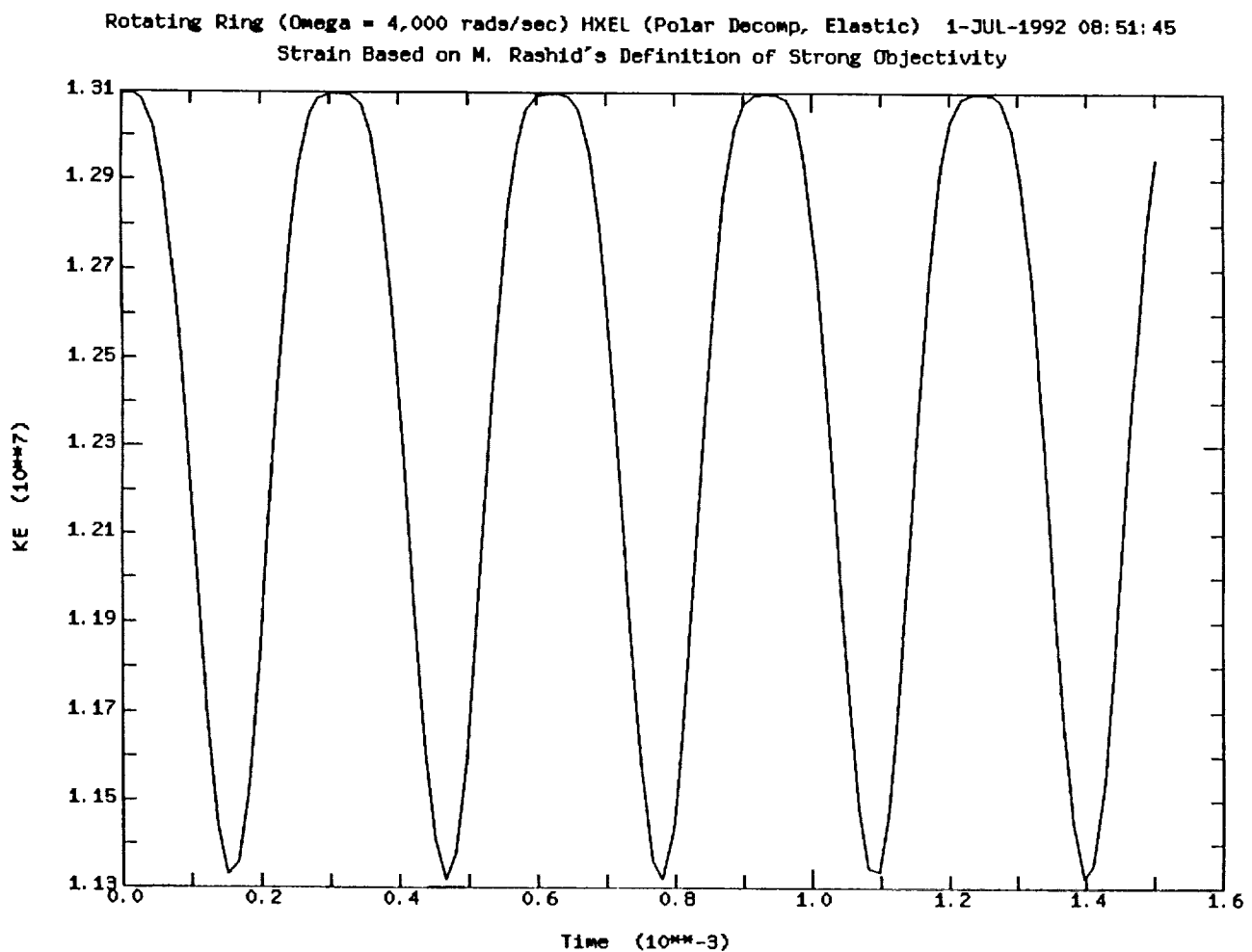


Figure 5 - Kinetic energy response with strong objectivity

ELEMENT INTEGRATION

In the interest of speed, explicit transient dynamic computer programs routinely use "constant stress" elements. In effect, only the uniform strain states of the element are used to represent the structures behavior. Strain states and, consequently, stress states that vary over the element are ignored. Such approximations result in complex, short wavelength, stress-free deformation patterns that are called *hourglass modes*.

The quickest way to obtain a constant stress element is to evaluate the integrals over the area or volume of the element defining the gradient and divergence operators with a single integration point; hence, the terminology *1-point integrated* elements. Unfortunately, such elements can fail the Iron's patch test. That is, a collection of irregularly-shaped elements subjected to a linear motion on the boundary will not produce a constant state of strain in the interior and, therefore, the collection of irregularly-shaped elements will not produce a constant state of stress.

A more accurate approach is to evaluate the integrals over the area or volume of the element defining the gradient and divergence operators exactly for a constant state of stress, effectively a projection calculation. The result is a much more reliable and well-behaved simulation, albeit requiring the execution of a greater number of algebra expressions. The *mean quadrature* elements while still constant strain elements, pass the Iron's patch test.

The greatly reduced excitation of the hourglass modes and the greatly improved hourglass control offered by the mean quadrature integration over the 1-point integration virtually renders obsolete the older 1-point integration technology. (In the special case of two-dimensional continuum elements, both approaches yield the same results.)

Current users of explicit transient dynamic software should only expect to use 1-point integrated elements in place of elements based on mean quadrature to obtain "quick and dirty" results.

QUADRILATERAL SHELL ELEMENTS

In explicit transient dynamics software there is a significant emphasis on speed and simplicity. That is, since it is expected in every calculation that the deformation will be finite and the material will be strained beyond the elastic range, the geometry and the associated gradient operators must be reconstructed, as well as, complex stress-strain models evaluated at every time step. As a result, finite elements derived for explicit transient dynamics software use the simplest and barest constructions possible for computational efficiency while retaining an essential representation of the physical behavior. The best example of this technology is the four-node bending quadrilateral derived by Belytschko, Lin and Tsay (1984).

The BLT element is based on a constant stress assumption coupled to a flat plate geometric approximation of what is usually a warped geometry (the element's geometry is warped when the four nodal points do not define a flat surface). In certain situations the BLT element exhibits shortcomings in representing the response of a structure. Two examples are the bending of a twisted beam (Example 1), and the response of a hemisphere loaded by opposing forces across the hemisphere's diameter (Example 2).

A four-node bending quadrilateral has been developed that exhibits the expected behavior in these two examples. The element has two properties that provide the expected response:

- 1) a warping deformation that possesses proper structural stiffness as opposed to being an hourglass mode, and
- 2) a derivation that is based on the actual geometry of the element as opposed to treating the geometry as flat.

Example 1. The tip-loaded, twisted cantilever beam is an example of a structure with a nonplanar geometry that can be nontrivial to reproduce with the finite element technology available today in explicit transient dynamic software (Fig. 6).

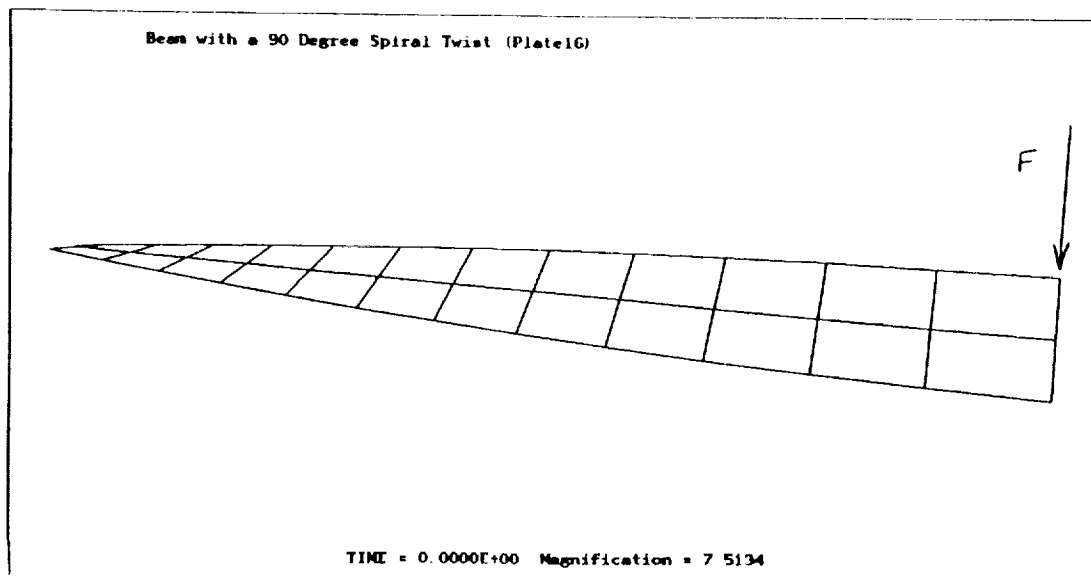


Figure 6 - Twisted beam with a constant tip load

QUADRILATERAL SHELL ELEMENTS (Cont'd.)

The tip load is applied suddenly at time equal to zero and held constant in magnitude and orientation. Based on a length of 12.0 in., a width of 1.1 in., a thickness of 0.32 in. and the selected properties (a Young's modulus of 2.9×10^7 psi, a Poisson's ratio of 0.22, and a density of 2.5×10^{-4} lbf-sec²/in⁴), the static deflection equals 0.005424 in. (MacNeal and Harder, 1985). The fundamental period equals 8.0 milliseconds.

As can be seen from Fig. 7, the BLT element with zero hourglass stiffness predicts an unacceptably large deflection amplitude and response period; see also the results reported by Belytschko, Wong and Chiang (1989).

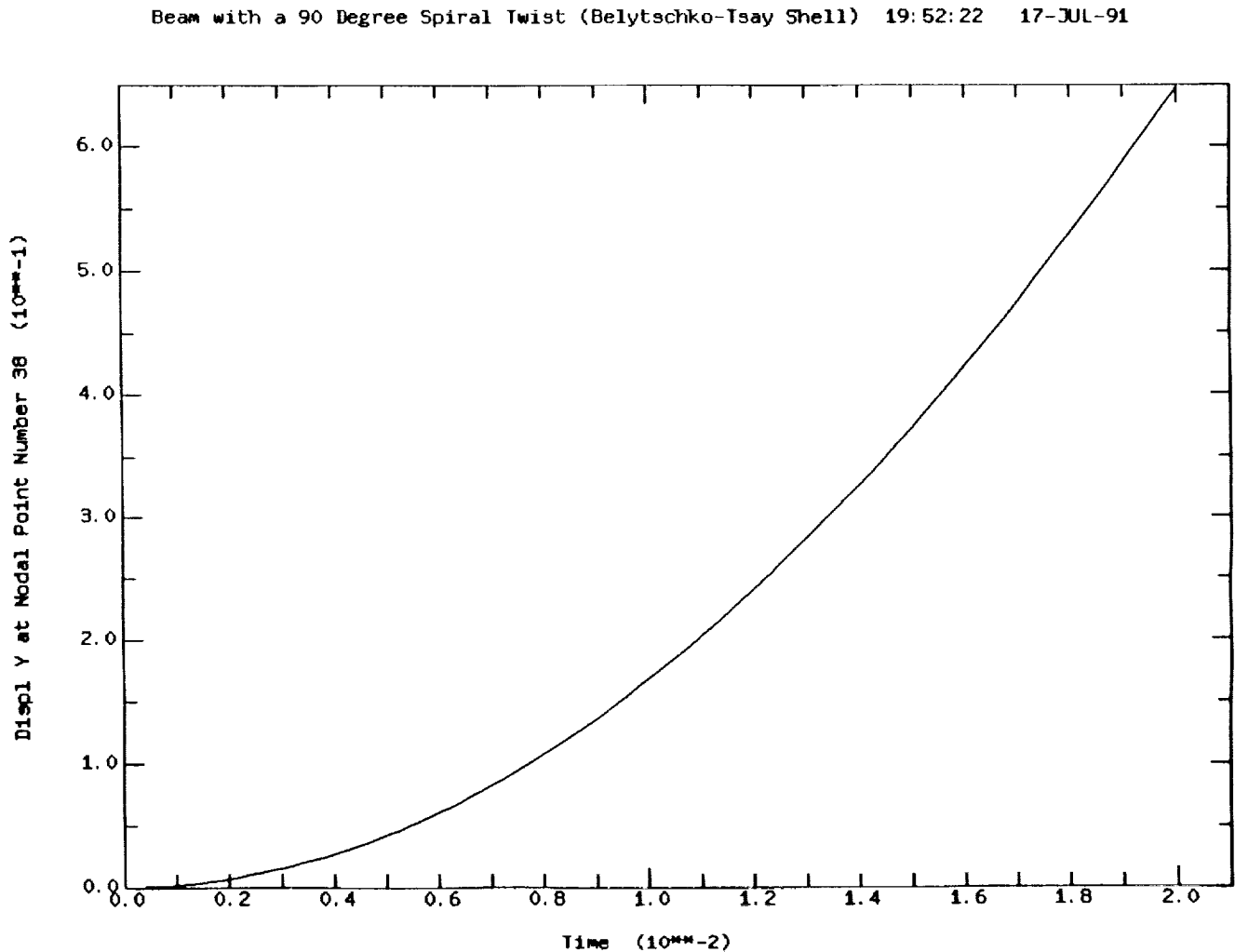


Figure 7 - Beam tip motion prediction using Belytschko-Tsay shell

QUADRILATERAL SHELL ELEMENTS (Cont'd.)

The technology developed by KEY Associates predicts very nearly the exact amplitude and period (Fig. 8).

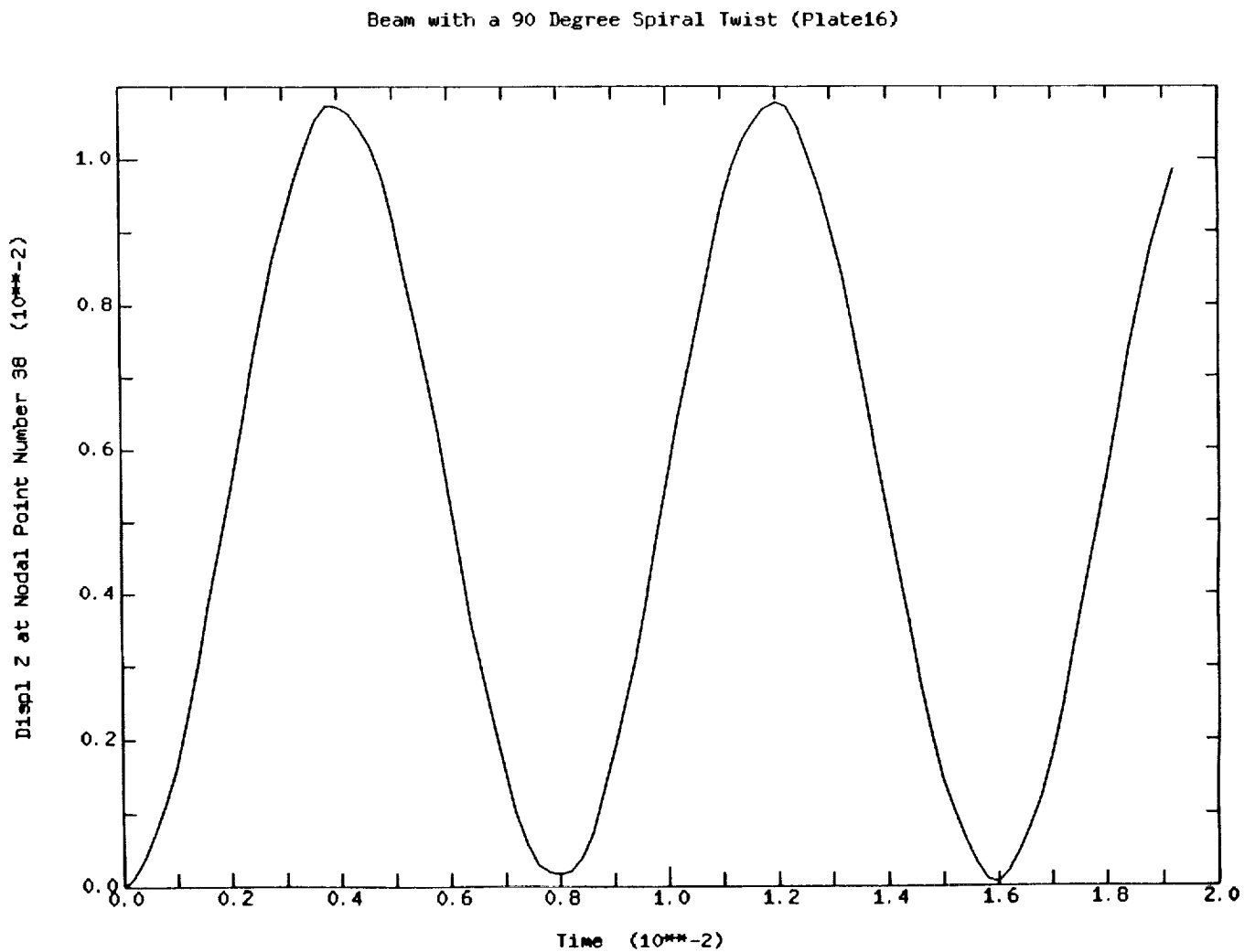


Figure 8 - Beam tip motion prediction using improved four-node shell

QUADRILATERAL SHELL ELEMENTS (Cont'd.)

Example 2. A hemisphere loaded by two sets of diametrically opposed forces in the plane of the equator, separated by 90 degrees and alternating in sign, is a problem in which both bending and membrane deformation occur. The loads enter the structure by generating moments including warping or twisting moments in the elements adjacent to the loads.

The loads are applied suddenly at time equal to zero and held constant in magnitude and orientation (Fig. 9).

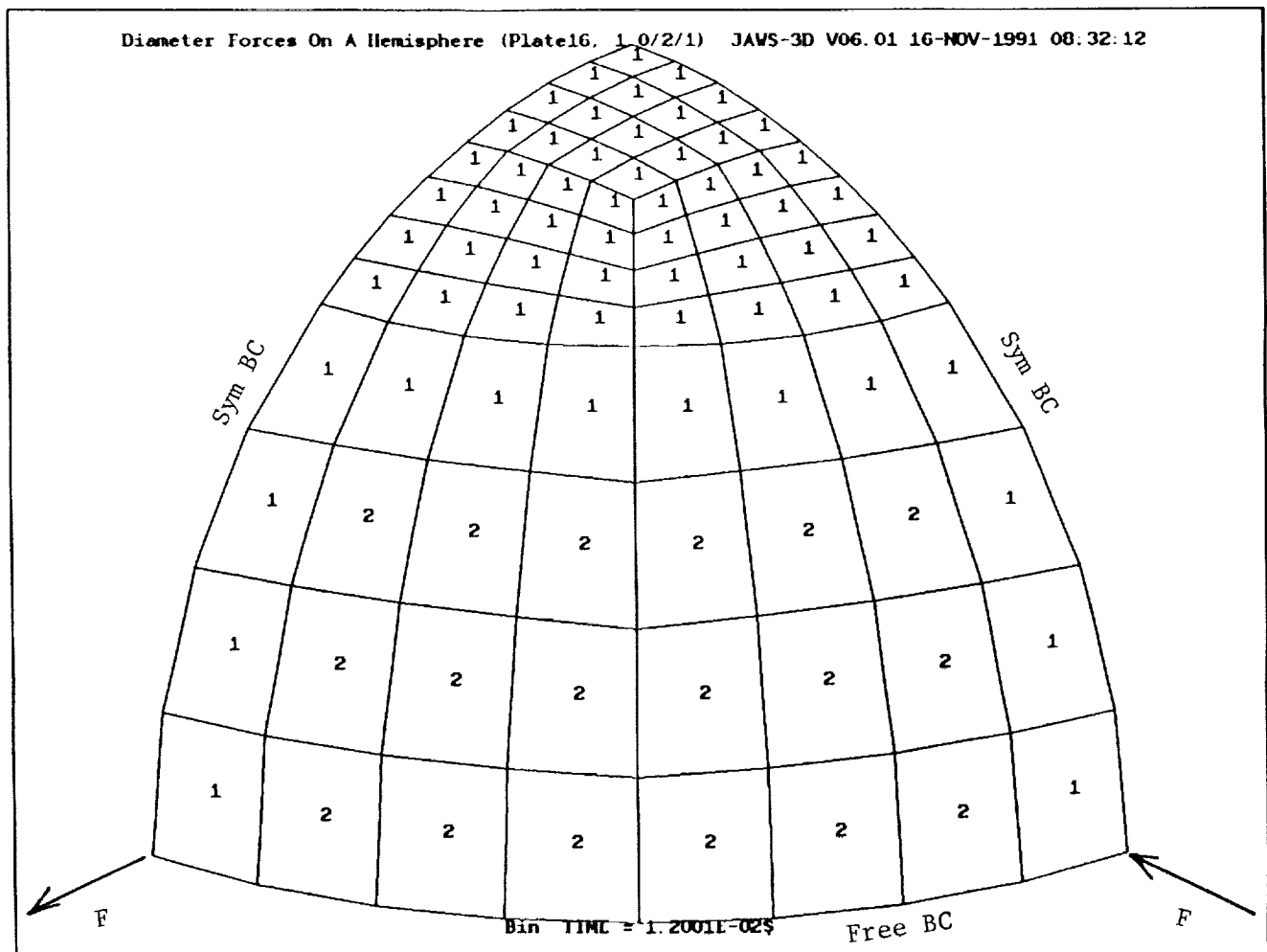


Figure 9 - Quadrant of a hemisphere loaded across two diameters

QUADRILATERAL SHELL ELEMENTS (Cont'd.)

Based on the hemisphere's radius of 10.0 in., a thickness of 0.04 in. and the selected properties (a Young's modulus of 6.825×10^7 psi, a Poisson's ratio of 0.3, and a density of 2.5×10^{-4} lbf-sec²/in⁴), the static deflection equals 0.094 inches (MacNeal and Harder, 1985).

As can be seen from Fig. 10, the BLT element with zero hourglass stiffness predicts an unacceptable cyclic accumulation of displacement; see also the results reported by Belytschko, Wong and Chiang (1989).

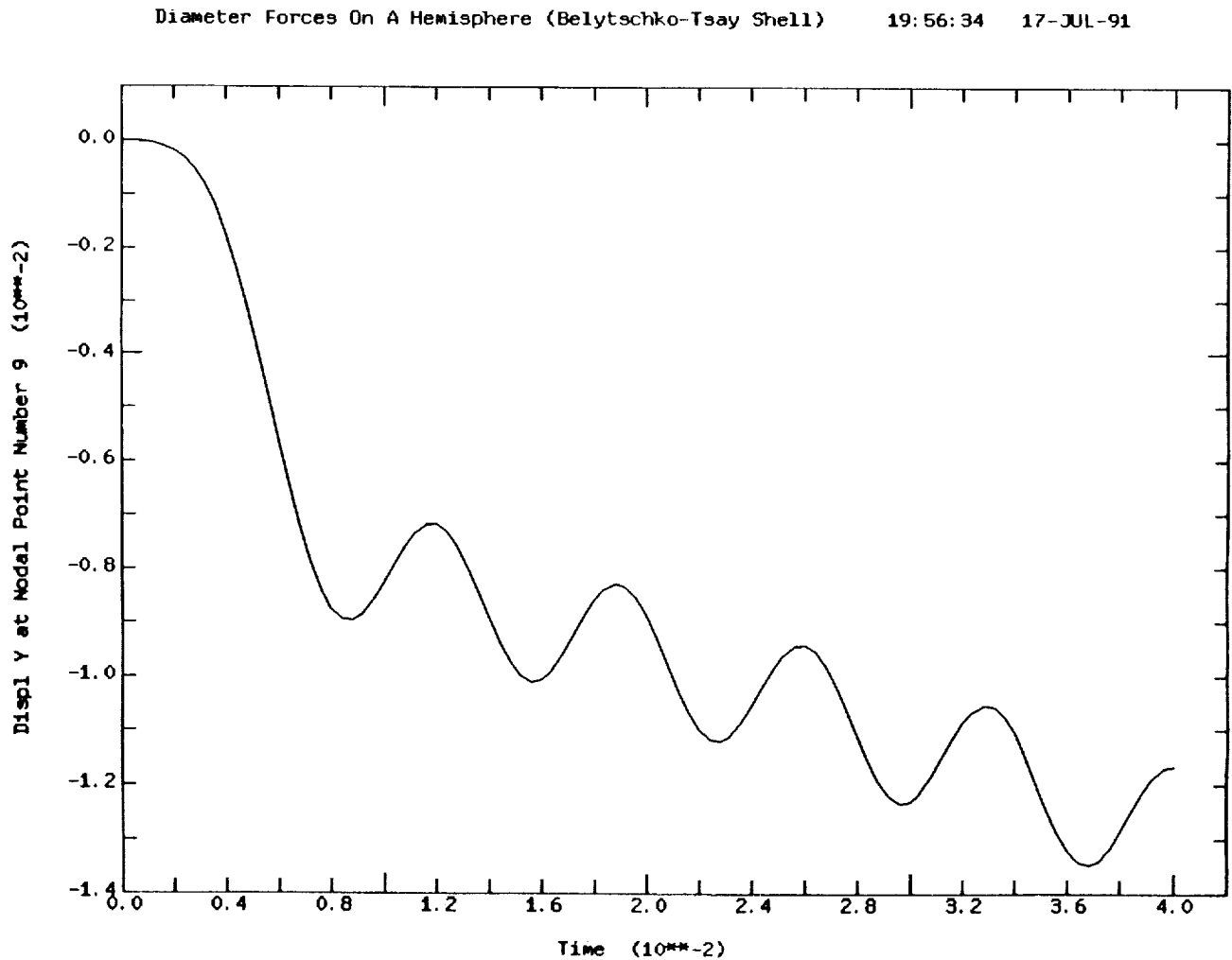


Figure 10 - Radial motion prediction using Belytschko-Tsay shell

QUADRILATERAL SHELL ELEMENTS (Cont'd.)

The technology developed by KEY Associates predicts a steady periodic (constant amplitude) result that is within 0.2% ($\text{Maximum_Internal_Energy} / 4.0$) of the expected deflection (0.094 inches) (Fig. 11).

Remarks. This element is suitable for both large in-plane and bending strains. These particular calculations were carried out without any hourglass control suggesting this element will not be overly sensitive to the development of hourglass distortions. In addition, this technology is based on six (6) degrees of freedom per nodal point meaning that no further numerical constraints or adaptations are needed to eliminate the "drilling" rotation to obtain satisfactory results. Modeling such additional physical features as edge beams, or modeling folded plate structures does not present any particular difficulty.

The low level of loading in both of these examples results effectively in infinitesimal strains. The material response is linear elastic. However, both of these examples require a proper computation of the gradient and divergence operators to obtain the correct results. The examples are sensitive indicators of the correctness of the representation for the element geometry and the element twisting stiffness.

While the BLT four-node bending quadrilateral remains a computationally efficient element, there are numerous applications for which an accurate representation of the warped geometry and the twisting stiffness is essential to obtaining a satisfactory result. Without a doubt, up-to-date software should contain an efficient four-node bending quadrilateral with the capabilities discussed here.

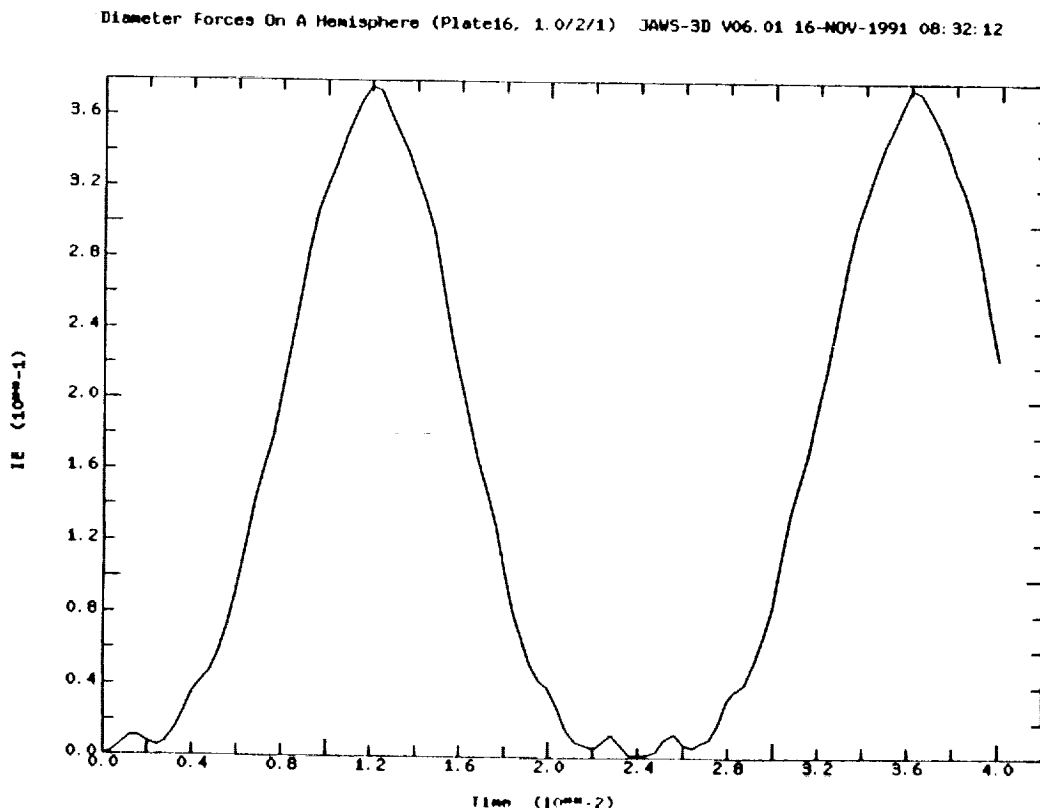


Figure 11 - Radial motion prediction ($= IE/4$) using improved four-node shell

REFERENCES

1. Belytschko, T., Lin, J. I. and Tsay, C. S., "Explicit Algorithms for the Nonlinear Dynamics of Shells," *Computational Methods in Applied Mechanics and Engineering*, Vol. 42, 1984, pp. 225-251.
2. Belytschko, T., Wong, B. L. and Chiang, H. Y., "Improvements in Low-Order Shell Elements for Explicit Transient Analysis," in *Analytical and Computational Models for Shells*, A. K. Noor, T. Belytschko and J. C. Simo (eds.), ASME Winter Annual Meeting, San Francisco, CA, Dec. 1989, ASME, NY, CED Vol. 3, 1989, pp. 383-398.
3. Dienes, J. K., "On the Analysis of Rotation and Stress Rate in Deforming Bodies," *Acta Mechanica*, Vol. 32, 1979, pp. 217-232.
4. MacNeal, R. H. and Harder, R. L., "A Proposed Standard Set of Problems to Test Finite Element Accuracy," *Finite Elements in Analysis and Design*, Vol. 1, 1985, pp. 3-20.
5. Rashid, M. M., "Incremental Kinematics for Finite Element Applications," Sandia National Laboratories, Albuquerque, NM (to appear).

QUADRILATERAL SHELL ELEMENTS (Cont'd.)

The technology developed by KEY Associates predicts a steady periodic (constant amplitude) result that is within 0.2% (Maximum_Internal_Energy / 4.0) of the expected deflection (0.094 inches) (Fig. 11).

Remarks. This element is suitable for both large in-plane and bending strains. These particular calculations were carried out without any hourglass control suggesting this element will not be overly sensitive to the development of hourglass distortions. In addition, this technology is based on six (6) degrees of freedom per nodal point meaning that no further numerical constraints or adaptations are needed to eliminate the "drilling" rotation to obtain satisfactory results. Modeling such additional physical features as edge beams, or modeling folded plate structures does not present any particular difficulty.

The low level of loading in both of these examples results effectively in infinitesimal strains. The material response is linear elastic. However, both of these examples require a proper computation of the gradient and divergence operators to obtain the correct results. The examples are sensitive indicators of the correctness of the representation for the element geometry and the element twisting stiffness.

While the BLT four-node bending quadrilateral remains a computationally efficient element, there are numerous applications for which an accurate representation of the warped geometry and the twisting stiffness is essential to obtaining a satisfactory result. Without a doubt, up-to-date software should contain an efficient four-node bending quadrilateral with the capabilities discussed here.

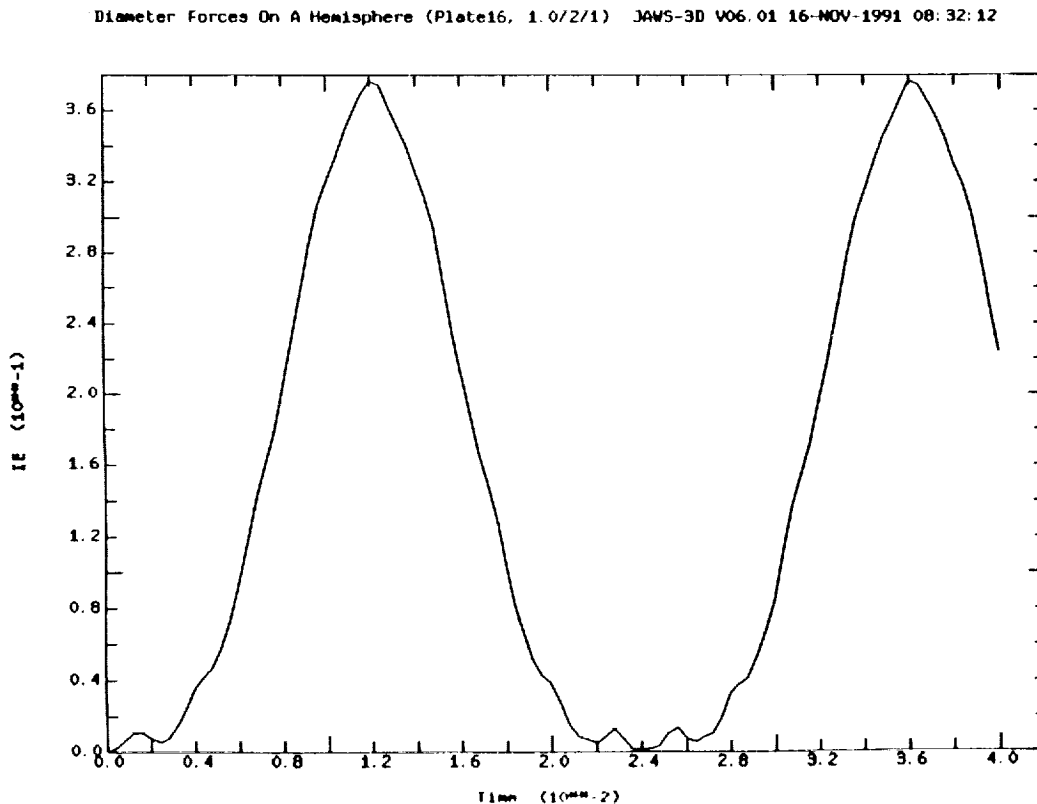


Figure 11 - Radial motion prediction ($= I E / 4$) using improved four-node shell

BEAM ELEMENTS

Beam elements, while on the surface appearing to be very elementary structural components, can be very intense from a computational standpoint when finite strains and inelastic material behavior are modeled. A portion of the computational complexity comes from the need to evaluate the stress-strain behavior at many points over the cross section (16 integration stations is a typical number). Membrane, bending and torsional stress resultants are produced from weighted sums over these points.

A very fast and direct method of obtaining stress resultants for elastic-plastic material behavior is to introduce stress-resultant plasticity. In effect, the beam cross-section is either completely elastic or completely plastic. For simulations in which the beam is deformed well into the plastic range, considerable computational effort can be eliminated with stress-resultant plasticity (the evaluation of elastic-plastic stress-strain models at numerous individual points over the cross section is not required).

If only a portion of the beam cross section yields plastically, stress-resultants plasticity will not capture any of the detail.

Quality software seeking to provide options for both rapid results and accurate results will offer both beam formulations.

COURANT SUBCYCLING

The central difference time integrator is only *conditionally* stable. That is, the integration procedure must be used with a time step that is less than the *critical time step*. The critical time step is very nearly equal to the minimum transient time for a disturbance to cross between any two nodal points in the mesh. The algorithm is very effective for an excitation that uses the maximum resolution the mesh can provide; for example, a shock wave.

There are two very common circumstances when an explicit time integration algorithm becomes less efficient: first, when there are significant differences in the spacing between nodal points over the mesh and, second, when there are significant differences in material stiffness over the mesh. It is not uncommon to have differences in critical time steps as much as a hundred to one over a mesh. The consequence is that the central difference time integration must function with the smallest critical time step.

Fortunately, Courant subcycling may be introduced in order to recover much of the efficiency offered by explicit algorithms. In Courant subcycling each finite element is integrated with the largest time step permitted by the local critical time step. Thus, small, stiff elements are integrated with many small time steps, and elsewhere in the mesh large, soft elements are integrated periodically with their larger time steps.

The benefit is significant since the time to perform a calculation drops and the answers are more accurate since the central difference algorithm performs as close to the critical step as is practicable everywhere. Figure 12 shows an example of a domain in which elements are integrated with two different time steps. In this case the ratio is only 2 to 1, but the principle is demonstrated.

Clearly, software intended for a wide variety of applications should provide Courant subcycling.

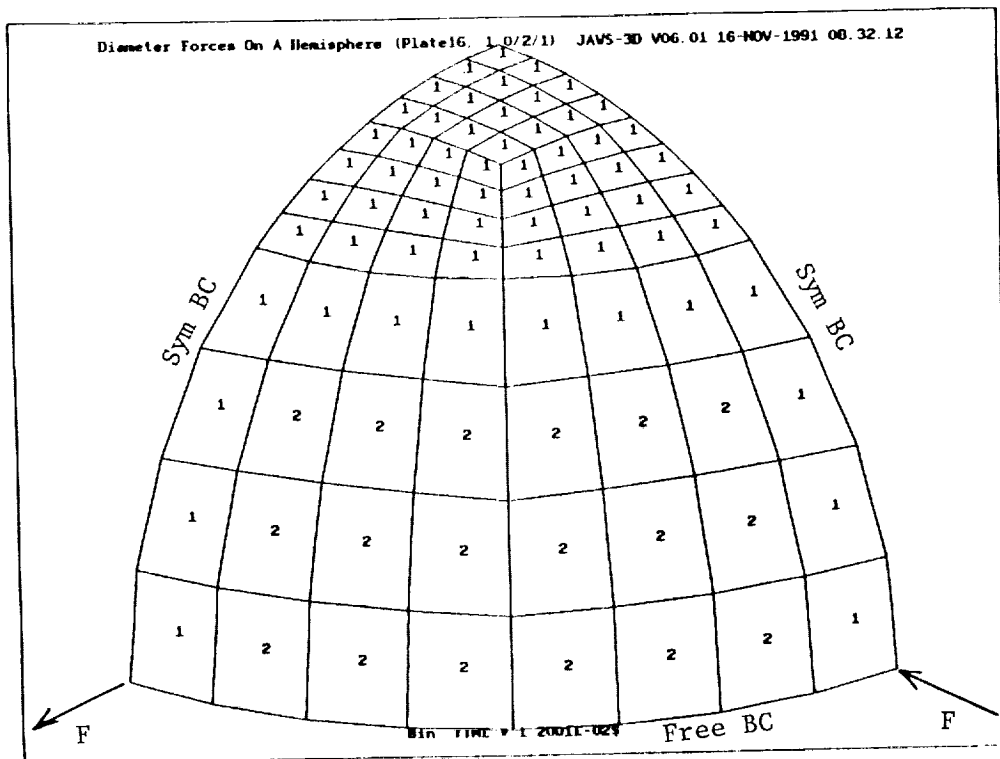


Figure 12 - Element integration bins for Courant subcycling

PLASTICITY IMPLEMENTATIONS

Traditional elastic-plastic material models are based on a linear representation of plastic hardening and radial-return numerical integration. While an exceptionally effective approach for large plastic strains, it is somewhat approximate for moderate plastic strains (plastic strains less than a ten times elastic strains). Ductile metals can exhibit a very "rounded" stress-strain curve when first yielding plastically. An elastic-linear strain hardening model with its transition from elastic to plastic response at a sharp corner does not mimic a gradual transition to large plastic strains.

One should expect a variety of material models in a crash simulation program including the basic linear strain hardening model and a model for plastic yielding that has a smooth transition from elastic to plastic response. For small plastic strains the models available should include sub-stepping where the time step within the material model is broken into smaller steps to control the numerical integration error.

SOFTWARE SURVEY

The following two tables (Tables 1 and 2) are a modest survey of the crash simulation software represented by the speakers at this NASA Workshop on Crashworthiness Technology. In brief, the software surveyed is as follows:

1. FMA-3D is a full-feature program available commercially from KEY Associates, 1851 Tramway Terrace Loop NE, Albuquerque, NM 87122 that include subcycling.
2. DYNA-3D is a full-featured program available through a technology sharing agreement from the Lawrence Livermore National Laboratory, Attn: Robert Whirley, P.O. Box 808, Livermore, CA 94550.
3. PRONTO-3D is a limited-feature program available with a license agreement from Sandia National Laboratories, Attn: Steven Attaway, Organization 1425, Albuquerque, NM 87185.
4. SUPERWHAMS is a full-featured program soon to be available commercially from KBS2, Suite 112, 455 South Frontage Road, Burr Ridge, IL 60521.
5. DYCAST is a limited-feature program based on an implicit integration algorithm available commercially from Grumman Aerospace Corporation, Attn: Allan Pifko, MS A08-35, Bethpage, NY 11714.

Table 1. Technology Availability

	FMA-3D	DYNA	PRONTO
Time Derivative			
Jaumann	Yes	Yes	No
Green-McInnis	Yes	No	Yes
Strain Increment			
Weak Objectivity	Yes	Yes	No
Strong Objectivity	Yes	No	Yes
Element Integration			
1-Point	No	Yes	No
Mean Quadrature	Yes	Yes	Yes
4-Node Shells			
BLT Quad	Yes	Yes	Yes
Improved Quad	KEY	EWQ	No
Beam Elements			
Illyshin Plasticity	(i/i)	Yes	No
Integrated	Yes	Yes	No
Plasticity			
Linear Hardening w/ Radial Return	Yes	Yes	Yes
Smooth Hardening w/ Sub-Stepping	Yes	"Yes"	No
Time Subcycling	Yes	No	No

Table 2. Technology Availability

	SUPER WHAMS	DYCAST
Time Derivative		
Jaumann	Yes	(no solid elements)
Green-McInnis	No	
Strain Increment		
Weak Objectivity	Yes	(no solid elements)
Strong Objectivity	No	
Element Integration		
1-Point	No	(no solid elements)
Mean Quadrature	Yes	
4-Node Shells		
BLT Quad	Yes	($\Delta l/d\&r$)
Improved Quad	BWCQ	(inf strain)
Beam Elements		
Illyshin Plasticity	No	No
Integrated	Yes	Yes
Plasticity		
Linear Hardening w/ Radial Return	Yes	No
Smooth Hardening w/ Sub-Stepping	No	Yes
Time Subcycling	Yes	Implicit

REFERENCES

1. Belytschko, T., Lin, J. I. and Tsay, C. S., "Explicit Algorithms for the Nonlinear Dynamics of Shells," *Computational Methods in Applied Mechanics and Engineering*, Vol. 42, 1984, pp. 225-251.
2. Belytschko, T., Wong, B. L. and Chiang, H. Y., "Improvements in Low-Order Shell Elements for Explicit Transient Analysis," in *Analytical and Computational Models for Shells*, A. K. Noor, T. Belytschko and J. C. Simo (eds.), ASME Winter Annual Meeting, San Francisco, CA, Dec. 1989, ASME, NY, CED Vol. 3, 1989, pp. 383-398.
3. Dienes, J. K., "On the Analysis of Rotation and Stress Rate in Deforming Bodies," *Acta Mechanica*, Vol. 32, 1979, pp. 217-232.
4. MacNeal, R. H. and Harder, R. L., "A Proposed Standard Set of Problems to Test Finite Element Accuracy," *Finite Elements in Analysis and Design*, Vol. 1, 1985, pp. 3-20.
5. Rashid, M. M., "Incremental Kinematics for Finite Element Applications," Sandia National Laboratories, Albuquerque, NM (to appear).

51039
187841
P-90

N94-19475

Crashdynamics with DYNA3D: Capabilities and Research Directions

Robert G. Whirley and Bruce E. Engelmann
Lawrence Livermore National Laboratory
Livermore, CA

Work performed under the auspices of the U.S. Department of Energy by the
Lawrence Livermore National Laboratory under contract W-7405-Eng-48.

CRASHDYNAMICS WITH DYNA3D: CAPABILITIES AND RESEARCH DIRECTIONS

This paper discusses the application of the explicit nonlinear finite element analysis code DYNA3D to crashworthiness problems. Emphasized in the first part of this work are the most important capabilities of an explicit code for crashworthiness analyses. The remainder of the paper discusses the areas with significant research promise for the computational simulation of crash events.

PRECEDING PAGE BLANK NOT FILMED

186
186
186

0-9

WHAT IS CRASHWORTHINESS?

In the present context, crashworthiness is defined as the study of vehicle survivability under the impact with another object. It is the focus on survivability which differentiates a crashworthiness analysis from other kinds of vehicle dynamic analysis. Crashworthiness analyses include the simulation of multi-car collisions, impacts of automobiles into highway barriers, as well as aircraft collisions with terrain or airborne objects such as birds.

The Laboratory's involvement with crashworthiness began in a passive role in the mid 1980's, when many carmakers began using our DYNA3D software for crashworthiness analysis and providing us feedback on its performance. Recently, the Laboratory has taken a more active role in crashworthiness analysis through a DOT highway project, the DOE Auto Initiative, and involvement in the Electric Vehicle Consortium.

Crashworthiness is the study of vehicle survivability under impact with another object.

- Auto/Auto
- Auto/Highway barrier
- Aircraft/Terrain
- Aircraft/Bird

LLNL's involvement in crashworthiness began with DYNA3D, and more recently:

- DOT Highway Project
- DOE Auto Initiative
- Electric Vehicle Consortium

CHARACTERIZATION OF CRASH EVENTS

Crash events are characterized by highly dynamic transient structural response of 5-100 millisecond duration. Mechanical contact conditions are almost always present. In addition, vehicle crash events frequently involve large deformations of thin structures and highly inelastic material response. These characteristics suggest explicit nonlinear finite element analysis as an effective tool for crashworthiness analysis.

Crash events usually involve:

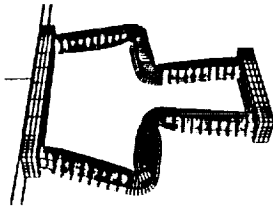
- Transient dynamic effects (5-100 ms duration)
- Mechanical contact conditions
- Large deformations of thin structures
- Inelastic material response

These characteristics often motivate the use of an explicit nonlinear finite element code for crashworthiness analysis.

CRASH STUDIES USE FINITE ELEMENT MODELS AT SEVERAL LEVELS

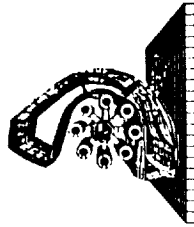
Although many people identify crashworthiness analysis with very large full-body models, effective crash analysis is often conducted with a hierarchy of models. These models range from single components to subassemblies containing a small number of components to full vehicle models. The appropriate level of model complexity is selected based on considerations of simulation accuracy versus the time required to construct the model, run the analysis, and interpret the results.

Component



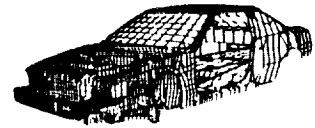
rail collapse

Subassembly



B1-B side impact

Full Vehicle



frontal impact

Tradeoff is simulation accuracy vs. time to:

- Construct model
- Run analysis
- Evaluate results

KEY DYNA3D CAPABILITIES FOR CRASHWORTHINESS MODELING

The following viewgraphs discuss some of the capabilities of DYNA3D which have been found important for crashworthiness modeling. The selection of these features as key capabilities was based on both our experience at LLNL and on extensive feedback received from the DYNA3D outside user community. Viewed collectively, this list of capabilities depicts a general computational simulation capability which is representative of the current state-of-the-art in crashworthiness software used for production analysis, including both DYNA3D and its derivatives as well as other explicit FE crash codes.

Based on our experience + feedback from user community:

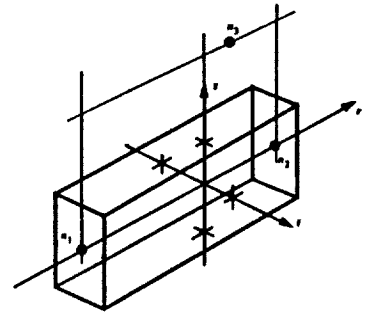
- Rigid materials/bodies
- Good structural elements (shells and beams)
- Fast unilateral contact
- Robust general contact algorithms
- Variety of constitutive models
- Failure modeling

KEY CAPABILITIES - GOOD STRUCTURAL ELEMENTS

Most large crashworthiness models use some beam elements to represent vehicle structural members. DYNA3D contains the Hughes-Liu beam element and the Belytschko-Schwer beam element. The Hughes-Liu beam uses numerical integration in the cross section and contains a moveable reference surface, and is therefore more general but also more expensive. More commonly used in crash problems is the resultant-based Belytschko-Schwer beam element.

Beams are also frequently useful in vehicle modeling.

- Beam elements:
 - Hughes-Liu
 - Belytschko-Schwer
 - Simple truss
- One point integration along the length
- Hughes-Liu uses variable-order numerical integration in the cross-section for accurate nonlinear material behavior
- Belytschko-Schwer is simple resultant formulation (much less expensive)



KEY DYNA3D CAPABILITIES FOR CRASHWORTHINESS MODELING

The following viewgraphs discuss some of the capabilities of DYNA3D which have been found important for crashworthiness modeling. The selection of these features as key capabilities was based on both our experience at LLNL and on extensive feedback received from the DYNA3D outside user community. Viewed collectively, this list of capabilities depicts a general computational simulation capability which is representative of the current state-of-the-art in crashworthiness software used for production analysis, including both DYNA3D and its derivatives as well as other explicit FE crash codes.



Based on our experience + feedback from user community:

- Rigid materials/bodies
- Good structural elements (shells and beams)
- Fast unilateral contact
- Robust general contact algorithms
- Variety of constitutive models
- Failure modeling

KEY CAPABILITIES - RIGID MATERIALS/BODIES

The capability of modeling portions of a vehicle as rigid and other portions as deformable in the same analysis is quite useful in crashworthiness analysis. So-called "rigid materials" can be used to correctly represent the mass and inertial properties of part of a vehicle which experiences little deformation at a small fraction of the cost required if all deformable materials were used. Another common application of rigid materials is the inexpensive definition of a complex curved surface for contact calculations, such as a rigid pole or partial barrier to be struck by an oncoming vehicle. Finally, rigid materials serve as a powerful model debugging feature. Portions of the model can be easily changed from deformable to rigid, thereby isolating regions of the model which may be the source of difficulties.

- Define all elements of a specified material as composing a rigid body (inertial properties automatically computed from geometry or specified by analyst)
- Greatly reduces cost compared to deformable elements
- Useful for:
 - representing mass properties for parts of vehicle experiencing little deformation
 - defining a complex rigid surface for contact
 - model debugging

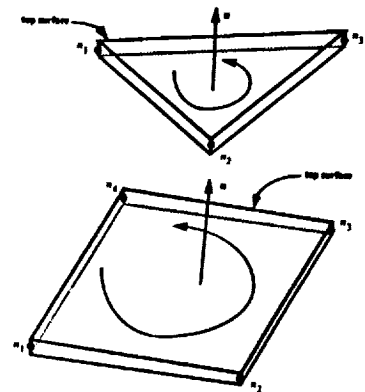


KEY CAPABILITIES - GOOD STRUCTURAL ELEMENTS

A variety of good structural elements are essential for vehicle crashworthiness analysis. DYNA3D contains a library of quadrilateral and triangular shell elements, each with unique capabilities. All elements share the common features of one-point in-plane integration with stabilization of zero-energy modes, and variable order numerical integration in the through-thickness direction.

A family of shell elements with common features gives versatility.

- One point in-plane integration with stabilization
- Variable-order numerical integration thru-thickness
- Shell elements (4-node quads and 3-node triangles):
 - Hughes-Liu
 - Belytschko-Tsay
 - C^0 triangle
 - BCIZ triangle
 - Membrane (derived from B-T)
 - YASE

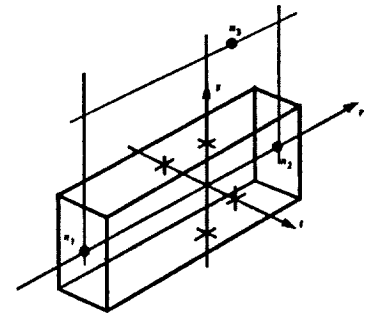


KEY CAPABILITIES - GOOD STRUCTURAL ELEMENTS

Most large crashworthiness models use some beam elements to represent vehicle structural members. DYNA3D contains the Hughes-Liu beam element and the Belytschko-Schwer beam element. The Hughes-Liu beam uses numerical integration in the cross section and contains a moveable reference surface, and is therefore more general but also more expensive. More commonly used in crash problems is the resultant-based Belytschko-Schwer beam element.

Beams are also frequently useful in vehicle modeling.

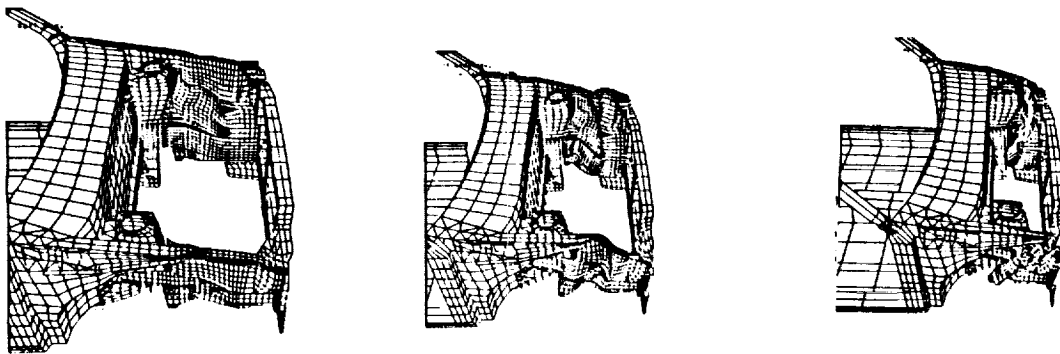
- Beam elements:
 - Hughes-Liu
 - Belytschko-Schwer
 - Simple truss
- One point integration along the length
- Hughes-Liu uses variable-order numerical integration in the cross-section for accurate nonlinear material behavior
- Belytschko-Schwer is simple resultant formulation (much less expensive)



KEY CAPABILITIES - UNILATERAL CONTACT (RIGID WALLS)

Unilateral contact, known as "rigid walls" in DYNA3D, is another widely used feature for crashworthiness analysis. This option allows a simple definition of a rigid plane for contact, and is often used to simulate vehicle barrier crash tests. Unilateral contact offers execution speed and modeling simplicity as advantages over discretizing the barrier and using general two-surface contact to treat the impact conditions.

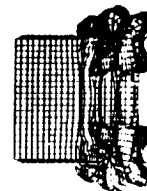
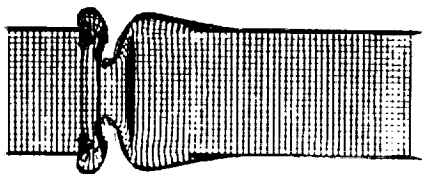
- Applicable for deformable vehicle impact onto rigid barrier
- Much less expensive than discretizing target and using general contact formulation
- Often used for auto frontal crash



KEY CAPABILITIES - ROBUST GENERAL CONTACT

Robust general contact algorithms may be the most important capability in a crashworthiness code. DYNA3D contact is based on a slave node on master segment concept, and a two-way symmetric treatment is used to eliminate any bias in the calculations. Important components of this capability are the treatment of contact between solid and shell elements, between beams and other element types, and single surface (self) contact.

- Slave node on master segment, symmetric treatment, penalty-method based
- Two-surface algorithm:
 - arbitrary interaction of rigid and deformable bodies
 - general treatment of solids and shells, beams by node only
 - incremental search
- Single-surface algorithm (self-contact) - buckling and folding



KEY CAPABILITIES - FAILURE MODELING

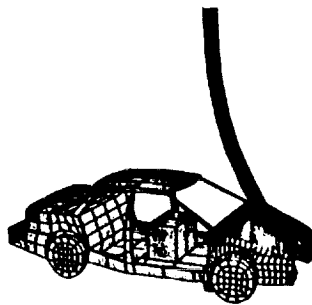
Failure modeling is evolving as a useful tool for crashworthiness modeling. Current approaches in DYNA3D include nodal constraint release options, material-based failure, and element deletion based on a failure criterion. Although these approaches have repeatedly proved their value to skilled analysts, they are somewhat ad-hoc and lack theoretical basis in general settings.

- Nodal constraint release
 - "tie-breaking shell slidelines"
 - "tied node sets with failure"
- Material-based failure - element no longer carries stress (deviatoric or total)
- These approaches are somewhat ad-hoc and may be mesh-dependent, but have proven useful to skilled analysts
- Significant improvements are needed here.

CRASHWORTHINESS SIMULATION ACTIVITIES AT LLNL

Crashworthiness efforts at LLNL include both computational methods research and applications.

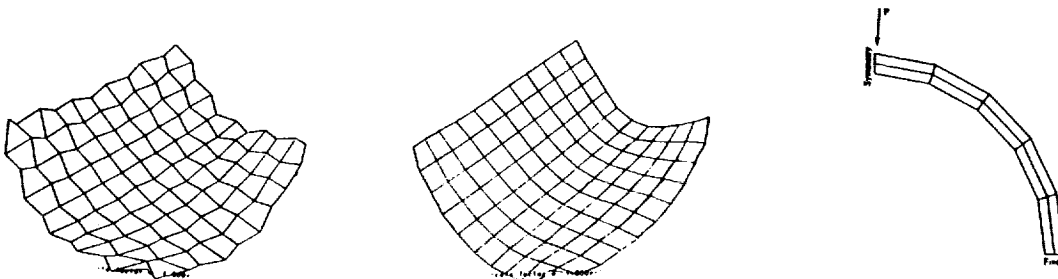
- Computational methods
 - YASE shell - resistant to hourglassing
 - SAND - adaptive slidesurfaces for failure modeling
 - Constitutive models and failure criteria - metals and composites
 - ParaDyn - massively parallel DYNA3D
- Simulation techniques



YASE SHELL ELEMENT

The YASE shell element is a recent outgrowth of research at LLNL. This element is a four-node quadrilateral which extends ideas and the coordinate system of the Belytschko-Tsay element. In the YASE shell, the stabilization evolves directly from the formulation and there are no free parameters which must be chosen by the user. This element yields improvements in accuracy over the Belytschko-Tsay element, and is comparable in performance to more recent elements developed by Belytschko and coworkers. The YASE shell as implemented in DYNA3D is within 10% of the speed of the Belytschko-Tsay element and therefore does not represent a substantial increase in analysis cost.

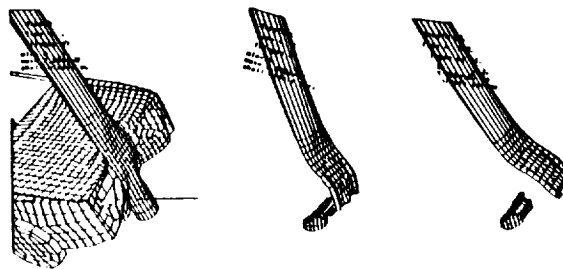
- Builds on ideas and coordinate system of Belytschko-Tsay
- Four-node quad, resultant-based, element normal
- Stabilization evolves directly from the formulation - no "tunable parameters"
- Good coarse mesh accuracy, especially for in-plane bending
- Speed competitive with Belytschko-Tsay (the fastest DYNA3D quad shell)



SAND-SLIDESURFACES WITH ADAPTIVE NEW DEFINITIONS

A recently developed DYNA3D capability for modeling material failure on contact surfaces is SAND (Slidesurfaces with Adaptive New Definitions). Engineering analysts have found SAND useful in modeling bird impacts on windshields and airframes as well as vehicle impacts on soft "frangible" roadside structures. SAND acts as an algorithmic vehicle to implement failure in an explicit finite element code; the difficult task of defining appropriate failure criteria for different problem classes remains a significant area of research.

- Models material failure on contact surfaces
- Failed elements are deleted and contact surface adapts to new outer material boundary
- Permits structural modeling using solid and shell elements
- Allows penetration and failure modeling in Lagrangian framework
- Useful for bird strikes on airframe, vehicle impacts on multiple soft barriers



PARADYN - MASSIVELY PARALLEL DYNA3D

The development of massively parallel explicit nonlinear finite element software is the goal of the LLNL ParaDyn Project. The move to massively parallel computing hardware will allow the solution of much larger problems with reduced turnaround times. It is important to realize, however, that MPP may not offer large speedups for today's small and moderate-sized problems due to difficulties with load balancing and multiprocessor overhead. The true potential of MPP-based analysis lies in the ability to incorporate levels of modeling detail which are totally infeasible with current computing hardware, and in the promise of improved price/performance across a range of machines.

Major Objectives:

- Develop a new generation of DYNA codes to take full advantage of teraflop computing platforms
- Solve significantly larger problems in times commensurate with design cycles
- Determine the architecture and parallel programming models best suited to explicit finite element methods
- Architectures: CM-5, KSR, Intel, Cray MPP0
- Programming Models: F90, HPF, Message Passing
- Establish a community of university and industrial collaborators

DYNA3D IS USED TO MODEL THE UCD/CALTRANS TEST BOGEY. PROPER MATERIAL MODEL IS NEEDED FOR AGREEMENT WITH TEST DATA

One recent LLNL crashworthiness study involved modeling a frontal crush unit tested on the UC Davis/Caltrans test bogey. The graph shows that agreement between the force-displacement curves measured in the experiment and predicted by DYNA3D was significantly improved when the forming-limit failure criterion was added into the DYNA3D model. Other LLNL crash activities include modeling the impact of the vehicles into various roadside barriers and objects such as light poles.

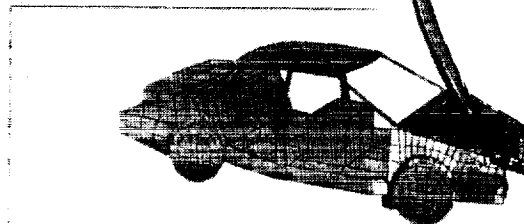
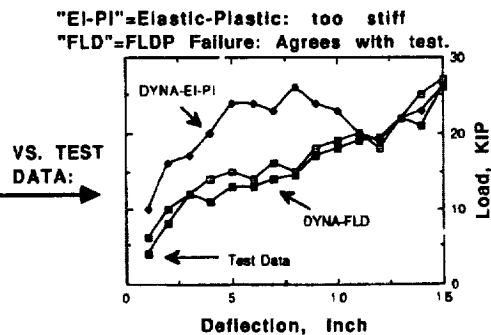
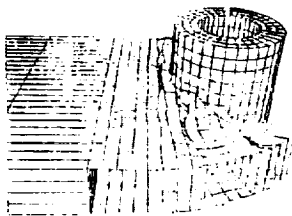


** Bogey developed and built as UCD-Caltrans collaboration

DYNA
MODEL



FRONTAL
CRUSH



WE ARE WORKING WITH FHWA AND
U. ALASKA TO DEVELOP COMPLETE
VEHICLE-BARRIER SIMULATIONS

DATA WAS SUPPLIED BY NHTSA FOR A 30 MPH FRONTAL IMPACT. THAT EVENING, WE RAN OUR SATURN MODEL "AS-IS" IN POST-PREDICTIVE MODE

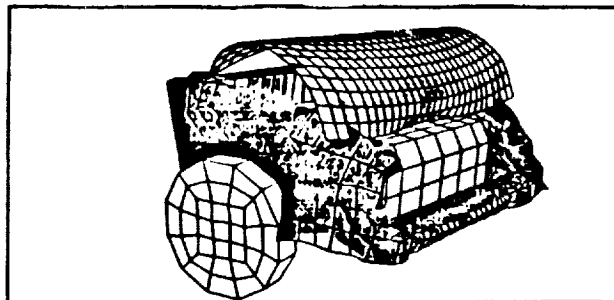
Another recent crashworthiness effort at LLNL consisted of taking our simplified Saturn model (developed in collaboration with J. Wekezer and shown on the lower right of this figure) and simulating a 30 mph frontal crash into a rigid barrier. Test data was supplied by the National Highway Traffic Safety Administration (NHTSA) at three locations: front brake caliper, engine, and rear seat. This was not intended as a detailed modeling effort, but rather an appraisal of the usefulness of our highly simplified car model for representing gross response behavior in an auto crash scenario.

**Accelerations were supplied
by NHTSA**

At three locations:

- **Wheel**
- **Engine**
- **Rear Seat**

**These were compared to the
first and only DYNA3D run**



—

—

DATA WAS SUPPLIED BY NHTSA FOR A 30 MPH FRONTAL IMPACT. THAT EVENING, WE RAN OUR SATURN MODEL "AS-IS" IN POST-PREDICTIVE MODE

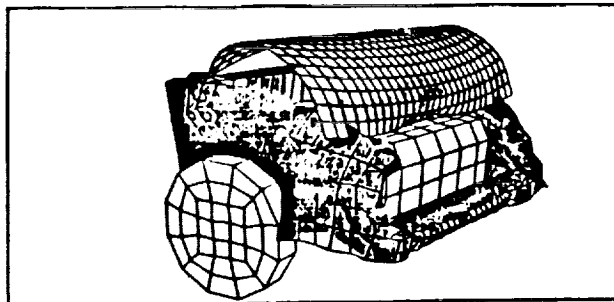
Another recent crashworthiness effort at LLNL consisted of taking our simplified Saturn model (developed in collaboration with J. Wekezer and shown on the lower right of this figure) and simulating a 30 mph frontal crash into a rigid barrier. Test data was supplied by the National Highway Traffic Safety Administration (NHTSA) at three locations: front brake caliper, engine, and rear seat. This was not intended as a detailed modeling effort, but rather an appraisal of the usefulness of our highly simplified car model for representing gross response behavior in an auto crash scenario.

**Accelerations were supplied
by NHTSA**

At three locations:

- **Wheel**
- **Engine**
- **Rear Seat**

**These were compared to the
first and only DYNA3D run**



DYNA3D ACCELERATIONS OF ENGINE AND REAR SEAT AGREE WITH TEST DATA, ALLOWING FOR BUMPER CRUSH

The simplified Saturn model was run once in DYNA3D for the 30 mph frontal crash, and the results were compared with test data for the engine block and rear seat locations. Reasonably good agreement was obtained considering that the model pre-dated the test data and was not tuned, and considering that the model was of a size and complexity to permit overnight analysis on an engineering workstation. Although clearly not a replacement for detailed full-body crashdynamics models, this does illustrate that useful results can be obtained with carefully defined simple finite element models.

At Engine Block:

- DYNA curve affect 30ms for bumper crush
- DYNA shows less rebound due to rigid motor mounts

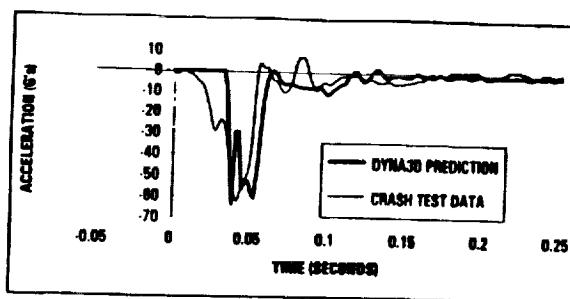
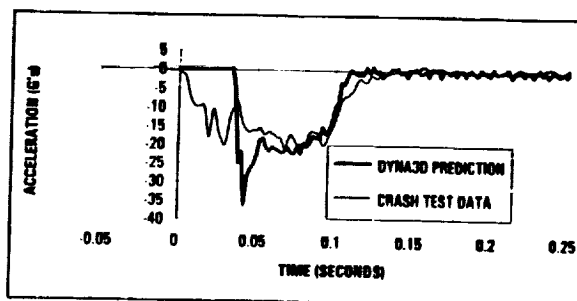


Fig. 18. Acceleration history of the engine block.

At Rear Seat:

- DYNA shows early peak due to rigid model aft of firewall
- Overall impulse and duration agrees, allowing for bumper crush



FUTURE DIRECTIONS

Although substantial progress has been made in the computational modeling of vehicle crashworthiness in recent years, clearly much remains to be done. The computational modeling of composite materials, particularly under severe dynamic axial loads, remains an area in need of additional research. The general area of failure modeling, including both metals and composites, needs a more fundamental basis and more robust computational methods. The treatment of small scale structural details such as fasteners and spotwelds in a large crashworthiness model merits examination. As in the case of failure models, ad-hoc methods exist which usually work in the hands of skilled analysts, but lack theoretical foundation and are difficult to apply in new situations without substantial reliance on small-scale experiments.

In conclusion, there is an opportunity for shared benchmark problems to be posed as a vehicle for communication among the research, code development, and engineering analysis communities in both the automotive and aerospace industries. These benchmarks could serve as illustrations of current needs in industry and as concrete objectives for researchers and code developers. These should be viewed as learning exercises and growth opportunities by all parties, however, and should not be viewed as software evaluation criteria.

- Improved constitutive models for composite structural failure, especially axial compression - need increasing with growing use of composites in aircraft and vehicles
- Improved progressive failure modeling - current procedures are ad-hoc but usually work. Need better basis and more robust methods
- Special elements for modeling spotwelds and other small-scale features. Current tied-node capability (DYNA3D) is not sufficiently general and may excite hourglassing.
- There is a strong need in both aerospace and automotive areas for shared benchmark problems of current relevance. These could be a strong vehicle for communication between crashworthiness analysis and research communities.

511-39.

187842

P-42
N94-19476

Transient Dynamics Capability at Sandia National Laboratories

S. W. Attaway, J. H. Biffle, G. D. Sjaardema,
M. W. Heinsteins and L. A. Schoof
Sandia National Laboratories
Albuquerque, New Mexico

PRECEDING PAGE BLANK NOT FILMED

207

206

INTRODUCTION

This report will present a brief overview of the transient dynamics capabilities at Sandia National Laboratories, with an emphasis on recent new developments and current research. In addition, the Sandia National Laboratories (SNL) Engineering Analysis Code Access System (SEACAS), which is a collection of structural and thermal codes and utilities used by analysts at SNL, will be described. The SEACAS system includes pre- and post-processing codes, analysis codes, database translation codes, support libraries, Unix shell scripts for execution, and an installation system.

SEACAS is used at SNL on a daily basis as a production, research and development system for the engineering analysts and code developers. Over the past year, approximately 190 days of CPU time have been used by SEACAS codes on jobs running from a few seconds up to two and one-half days of CPU time. SEACAS is running on several different systems at SNL including Cray Unicos, Hewlett Packard PH-UX, Digital Equipment Ultrix, and Sun SunOS.

An overview of SEACAS, including a short description of the codes in the system, will be presented. Abstracts and references for the codes are listed at the end of the report.

Additional information about obtaining SEACAS can be obtained by contacting:

Marilyn K. Smith
Division 1425
Sandia National Laboratories
P.O. Box 5800
Albuquerque, NM 87185-5800
(505) 844-3082; Fax (505) 844-9297

PRECEDING PAGE BLANK NOT FILMED

208

PHILOSOPHY

SEACAS is a modular system based upon a common binary datafile format called EXODUS that includes the mesh description and the timeplanes of the computed results. A subset of this format, called GENESIS, is used to refer to the mesh description portion of the EXODUS format.

All of the preprocessing, analysis, postprocessing, and translation codes can read and/or write EXODUS database files. A schematic of this is shown in Fig. 1.

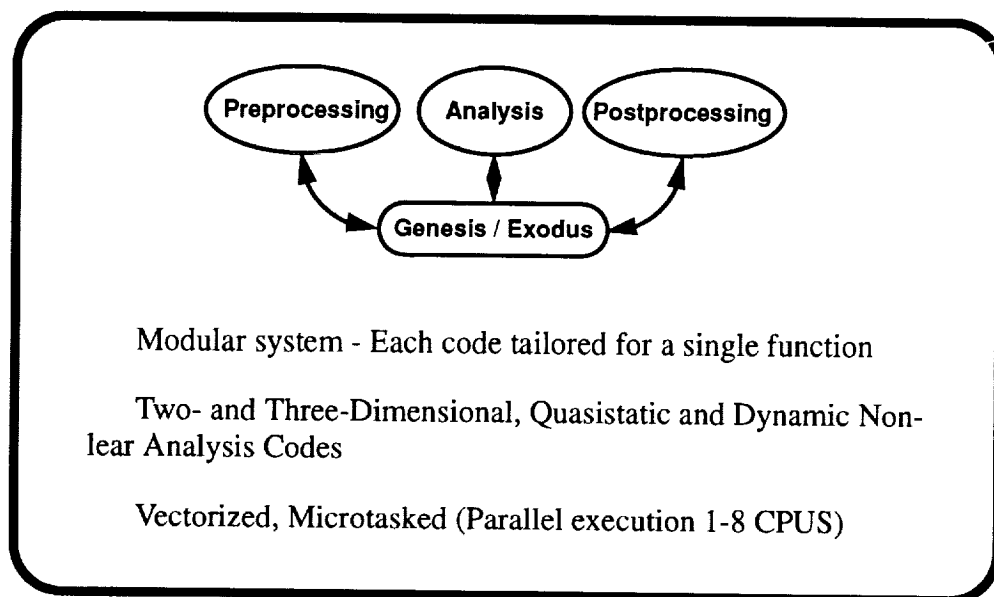


Figure 1 - Modular structure of SEACAS

With this structure, codes can be tailored for a single function. For example, an analysis code can be added to the system without writing new mesh generation and postprocessing programs. Also, code-to-code data transfers and restarts use the EXODUS format. A more complete view of this is shown in Fig. 2.

This modular concept is used extensively in the mesh generation process. Several special-purpose codes have been written that perform a certain mesh generation task. Examples of this are:

- generate two-dimensional mesh (fastq)
- transform two-dimensional mesh into a three-dimensional mesh (gen3d, genshell)
- join two or more 2D or 3D meshes into a single mesh (gjoin)
- reposition a 2D or 3D mesh (grepos).

Finite element meshes of several complicated three-dimensional geometries have been successfully generated using this system, which is built up of codes that singly provide a limited capability, but when used as a system are very powerful.

All of the codes are written in as portable a form as possible. Fortran codes are written in ANSI Standard FORTRAN-77 and C language codes are written in ANSI Standard C where possible. Machine-specific routines are limited in number and are grouped together to minimize the time required to adapt them to a new system.

A code management system is used for all of the SEACAS codes to provide traceability and retrievability for quality assurance. The change logs include who changed the code, when it was changed, what was changed, and why the change was made. If required, a previous version can be retrieved.

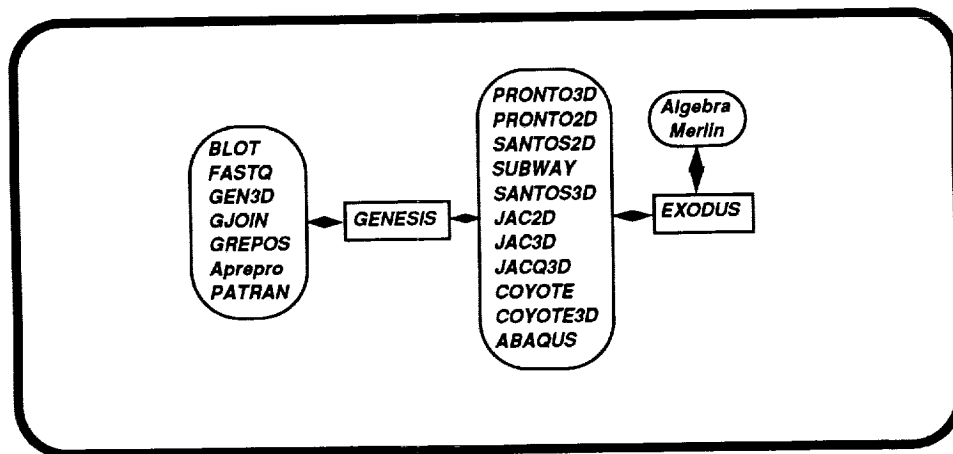


Figure 2 - Code-to-code data transfers using SEACAS

Figure 3 shows an example of a very large, complex problem solved using the codes in SEACAS.

SEACAS is divided into five broad categories of codes: prepost, analysis, translator, libraries, and scripts. The categories can be roughly defined as follows:

prepost: Pre- and postprocessing codes including mesh generation, visualization, preprocessors, and database manipulation codes.

analysis: Finite element analysis codes including quasistatic, transient dynamics, thermal, and electromechanics. Two- and three-dimensional, nonlinear, large deformation.

translators: Translation codes for editing output files (EXODUS), inter-machine translation, and exodus from/to commercial database translation.

libraries: Support libraries including database routines, common machine-specific routines, plot routines, graphics device drivers, and interactive help routines.

scripts: Unix shell scripts for executing the prepost, analysis, and translation codes. Also includes support and installation routines.

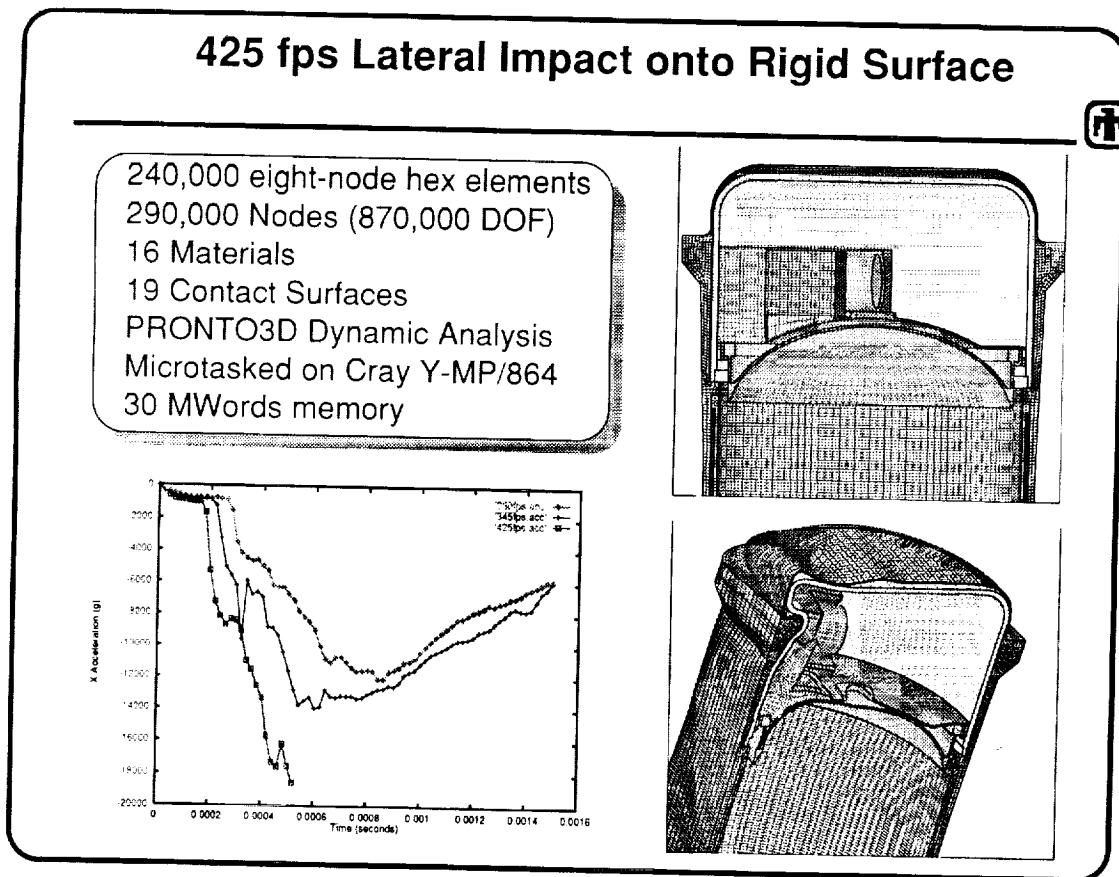


Figure 3 - Example of a complex problem solved using the codes in SEACAS

EXODUS DATA FILE

Figure 4 summarizes the features of the EXODUS data file. An EXODUS data base contains data entities used for input and output of finite element analyses. The features of this data base are:

- self-describing data file -- the file includes information that describes the contained data (dimensionality, size, type, etc.).
- random read (and write) access -- data can be written or read in an arbitrary order.
- machine-independent binary representation -- data is stored in eXternal Data Representation (XDR) format and thus can be transferred to, or accessed from, any machine without being concerned about what machine generated the data.
- FORTRAN and C subroutine interface -- application programs access the data via simple calls to a subroutine library.
- extensible -- because the file is self-describing and not just a rigid file format, new data entities and features can be added without modifying all of the application codes using the data base.
- translators -- capability to translate to/from many commercial application codes (i.e., ABAQUS, PATRAN, etc.).

Common binary datafile format

One common data file that each analysis code uses to communicate between the pre- and post-processors.

- Random read (and write) access
- Machine-independent binary representation
- Fortran and C callable subroutine interface
- Object-oriented data
- Extensible
- Translators available for PATRAN, ABAQUS, ASCII

Figure 4 - Summary of Exodus data file

The EXODUS II data model is used for transferring finite element analysis data among application codes. It includes data to define the finite element mesh and label both boundary condition and load application points. EXODUS II accommodates multiple element types and is sufficiently general to service many different analysis codes, providing a very general format for analysis results. The data is stored in a machine-independent format and is randomly accessible. A FORTRAN and C application programming interface is also specified.

Translation codes are used to convert EXODUS databases into different formats and to edit EXODUS databases.

algebra: Manipulates EXODUS finite element output data by evaluating algebraic expressions. Equation variables are dependent on the input database variable names.

seaexo: Converts SEACO files (the binary file format that preceded EXODUS) into EXODUS files.

exotxt and txtexo: Converts EXODUS to and from a specially formatted ASCII text file.

exoexo: A program which simply translates an EXODUS file to the same EXODUS file. It is used as a base program for writing new translators or database manipulation programs.

abaexo: Converts ABAQUS (commercial finite element code) results files to EXODUS.

conex: Concatenates several EXODUS files into a single EXODUS file. Used to create a single EXODUS file from analyses that have been restarted.

exoxdr and xdrexo: Converts EXODUS to and from an external data representation format (XDR) which can be transmitted between computers of different architectures, word lengths, and byte orders.

exogen: Creates a GENESIS mesh database from a specific time step of an EXODUS file. Used when an analysis of a deformed geometry is required. For example, an impact analysis followed by a thermal analysis.

merlin2: Transfers (maps) nodal data between finite element meshes. For example, thermal output from a heat conduction code to a thermal input file for a quasistatic mechanics code.

exopat and patexo: Converts EXODUS to and from PATRAN (commercial mesh generation program) neutral file format.

exo1exo2 and exo2exo1: Converts EXODUS I format files to EXODUS II format.

In addition to the translation codes listed above, the Cray Unicos system provides the capability to translate EXODUS files into a VMS and IEEE format using the exoexo code.

PREPROCESSING AND POSTPROCESSING CODES

The pre- and postprocessing codes are comprised of the following mesh generation, visualization and database manipulation codes.

gjoin: Join together two or more GENESIS databases into a single GENESIS database.

gen3d: Transform a two-dimensional GENESIS database into a three-dimensional GENESIS database. Several transformations are supported and additional transformations can be easily added.

grepos: Reposition or scale a GENESIS database.

fastq: Interactive two-dimensional finite element mesh generation program. Includes several mesh generation options including paving.

aprepro: An algebraic preprocessing program.

genshell: Transform a two-dimensional GENESIS database into a three-dimensional shell GENESIS database. Several transformations are supported and additional transformations can be easily added.

numbers: Calculates several properties of an EXODUS file, including mass properties, timesteps, condition numbers, cavity volumes, and others.

grope: Interactively examine an EXODUS database. Grope is also contained within the blot program. Grope is primarily used to validate EXODUS files.

blot: The primary graphical two-dimensional and three-dimensional postprocessing code. It includes deformed mesh plots, contour plots, shaded fringe plots, variable versus variable and time history plots, and distance versus variable plots.

Paving Technique

Figure 7 shows examples of the paving technique. The paving algorithm fills an area by first placing elements along the interior and exterior boundaries. Row endpoints are determined so that elements can be fitted into and around corners. Once the row is generated, it is smoothed. The new row can be adjusted based on curvature. Elements called wedges are inserted into rows that are being generated concave outward to keep element sizes from becoming larger. Tucks or the removal of elements are performed for rows that are concave inward to keep elements from becoming smaller. When two rows of elements overlap, the overlap is sewn together by being pushed apart and attached together. When two rows are close but not touching, they are pulled together with a process called seaming cracks. The meshing process produces nearly square elements with corners of approximately 90 degrees. Smoothing and deletions of elements are performed until each element passes a "goodness" test.

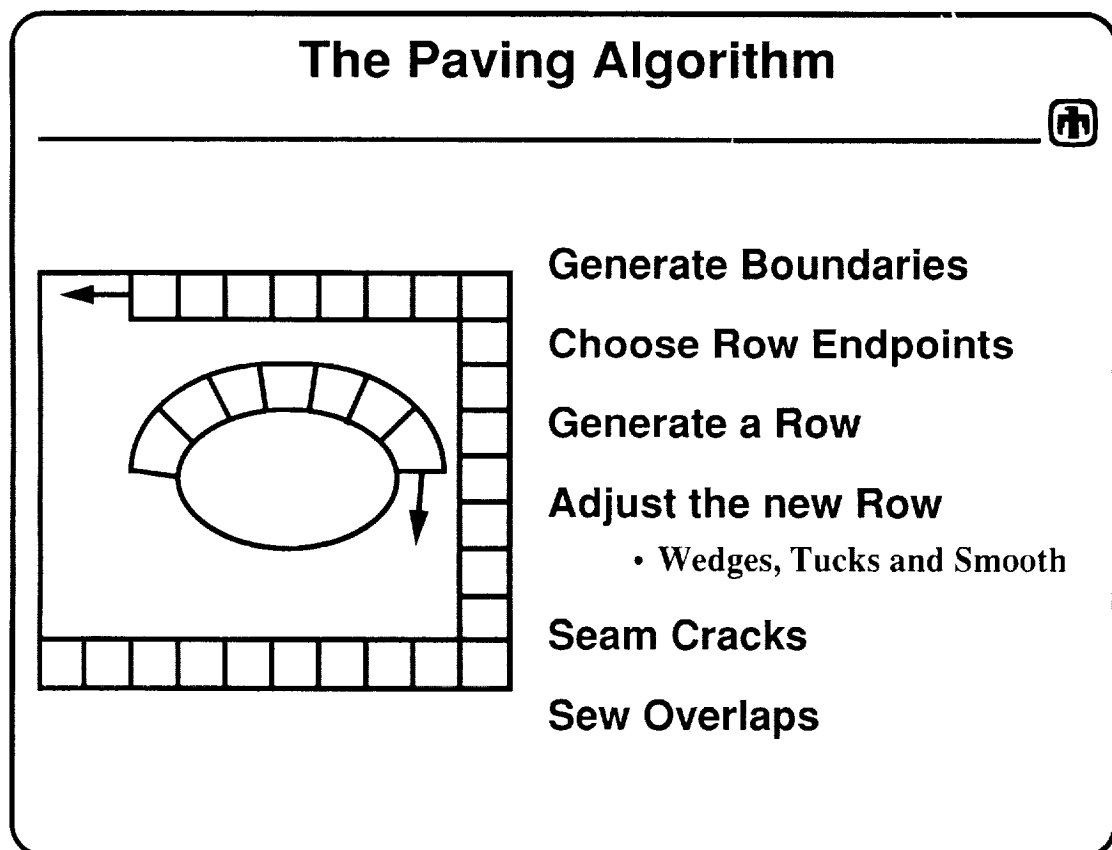


Figure 7 - Examples of the paving technique

PREPROCESSING AND POSTPROCESSING CODES

The pre- and postprocessing codes are comprised of the following mesh generation, visualization and database manipulation codes.

gjoin: Join together two or more GENESIS databases into a single GENESIS database.

gen3d: Transform a two-dimensional GENESIS database into a three-dimensional GENESIS database. Several transformations are supported and additional transformations can be easily added.

grepos: Reposition or scale a GENESIS database.

fastq: Interactive two-dimensional finite element mesh generation program. Includes several mesh generation options including paving.

aprepro: An algebraic preprocessing program.

genshell: Transform a two-dimensional GENESIS database into a three-dimensional shell GENESIS database. Several transformations are supported and additional transformations can be easily added.

numbers: Calculates several properties of an EXODUS file, including mass properties, timesteps, condition numbers, cavity volumes, and others.

grope: Interactively examine an EXODUS database. Grope is also contained within the blot program. Grope is primarily used to validate EXODUS files.

blot: The primary graphical two-dimensional and three-dimensional postprocessing code. It includes deformed mesh plots, contour plots, shaded fringe plots, variable versus variable and time history plots, and distance versus variable plots.

Figure 5 summarizes the capability the new pre-processing tool APREPRO gives a user. We have found that when APREPRO is combined with the other pre-processing tools, a great increase in productivity can be obtained. APREPRO can also be used to convert data in a variety of different units to one set of units.

APREPRO: Algebraic Preprocessor

- Define problem in terms of variables
- Global variables in one file that is *included* in all other files
- Trigonometric and algebraic functions -- C-like syntax
- Portable: versions available on Unicos/VMS/Unix/Amiga

Easily extendable (we wrote, have source)

INPUT

```
{include(one.inc)}
point 1 {x1 = rad*cosd(angle)} {y1=rad}
point 2 {x2 = x1 + rad} {y1 = y1 + 1/2}

{units(inch-lbf-sec)}
point 3 {5*m} {2.54*cm}
point 4 {1*ft} {1*ft + 1*in}
velocity = {1*mile/hour}
```

OUTPUT

```
$ Aprepro (version #) date
$ include file ONE.INC
$ rad = 1.
$ angle = 30.
point 1 0.866025 1.0
point 2 1.866025 1.5

$ units: inch-lbf-sec
point 3 196.85039 1.0
point 4 12.0 13.0
velocity = 17.6
```

- Any expression inside { } will be evaluated and printed
- Can be used with any file that does not contain { } for other reasons

Figure 5 - Aprepro: An algebraic preprocessor

MESH GENERATION

Figure 6 lists the current areas of active research on mesh generation at Sandia. The first goal of the CUBIT mesh generation project is to develop advanced meshing algorithms for meshing arbitrary three-dimensional surfaces and volumes. The paving algorithm was developed as a 2D all-quadrilateral meshing algorithm. It was recently extended to meshing general 3D trimmed surfaces. The plastering algorithm is being developed as a 3D all-hexahedral volume meshing algorithm.

The development of all of the 3D meshing algorithms cannot progress rapidly without the inclusion of a general geometry generation mechanism. A solid modeling package, ACIS, is being used for this purpose. A nonmanifold topology and meshing database was designed and coded. This database serves all the mesh generation and geometry generation tools. The database allows direct access to modeling functionality and should prove an extremely useful prototype for commercial development of a true solid-model-based meshing program.

The second goal is to develop for the first time an extremely robust adaptive finite element analysis capability for use in all fields of mechanics. The paving and plastering algorithms are very well suited for use in adaptive solution algorithms.

The mesh generation algorithms for paving and plastering are superior to any mesh generation algorithms currently available to private industry. Consequently, several software houses have entered into Cooperative Research and Development Agreements (CRADA) with Sandia.

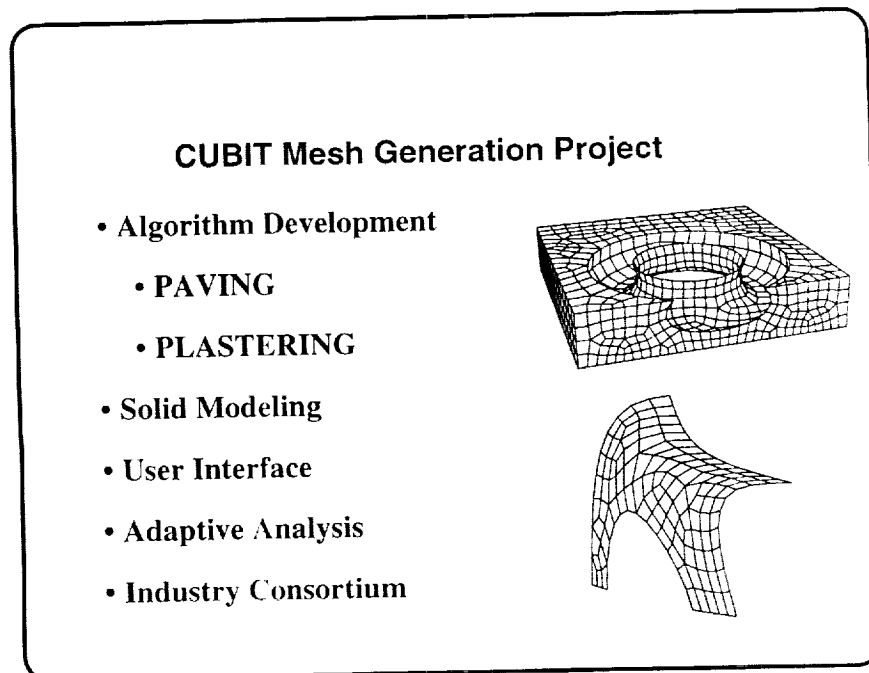


Figure 6 - Current areas of active research on mesh generation at Sandia

Paving Technique

Figure 7 shows examples of the paving technique. The paving algorithm fills an area by first placing elements along the interior and exterior boundaries. Row endpoints are determined so that elements can be fitted into and around corners. Once the row is generated, it is smoothed. The new row can be adjusted based on curvature. Elements called wedges are inserted into rows that are being generated concave outward to keep element sizes from becoming larger. Tucks or the removal of elements are performed for rows that are concave inward to keep elements from becoming smaller. When two rows of elements overlap, the overlap is sewn together by being pushed apart and attached together. When two rows are close but not touching, they are pulled together with a process called seaming cracks. The meshing process produces nearly square elements with corners of approximately 90 degrees. Smoothing and deletions of elements are performed until each element passes a "goodness" test.

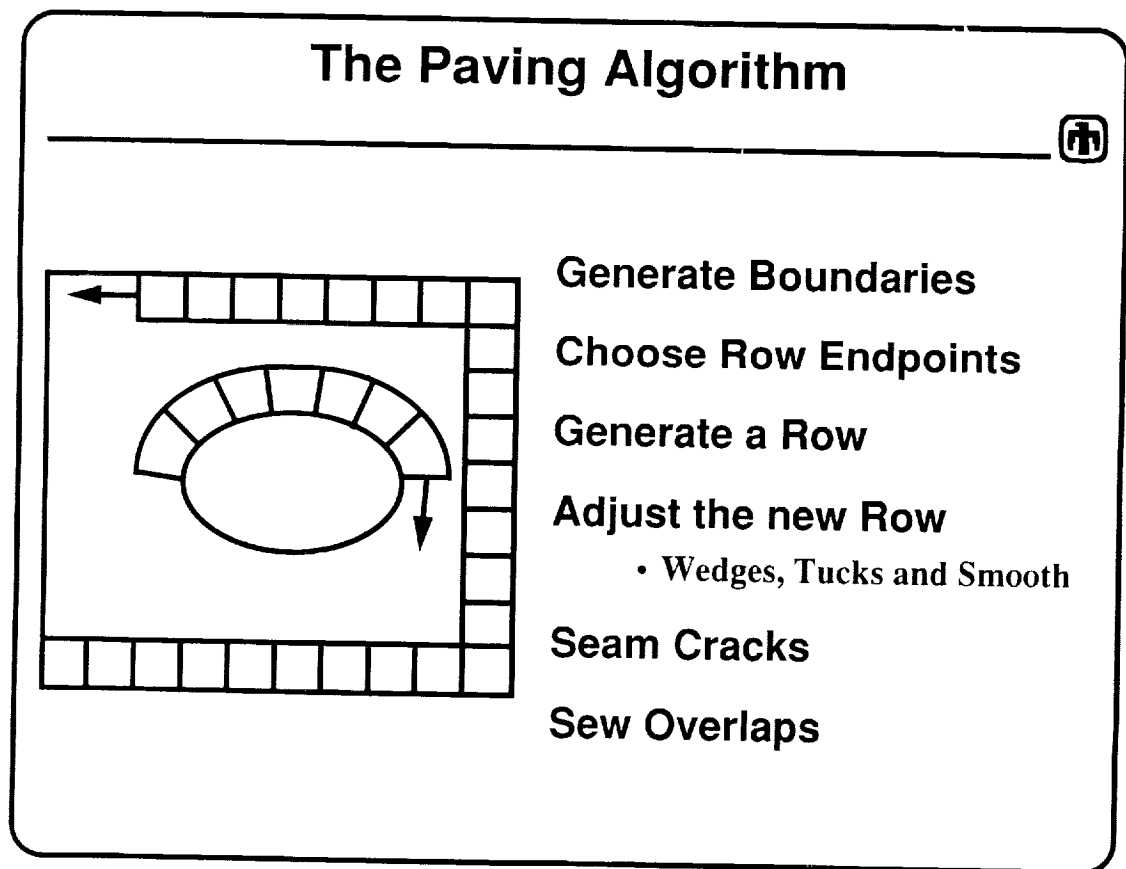


Figure 7 - Examples of the paving technique

As an example, one of the meshing tools is the sewing process. First intersections are found and then candidates for connection are chosen. Then the connections are formed between nodes that are close together. Seams are then formed by pushing rows of element edges together to remove the overlaps. The mesh is then smoothed and elements not meeting a set of "goodness" tests are deleted. Figure 8 shows how sewing can be used to mesh a part with multiple holes.

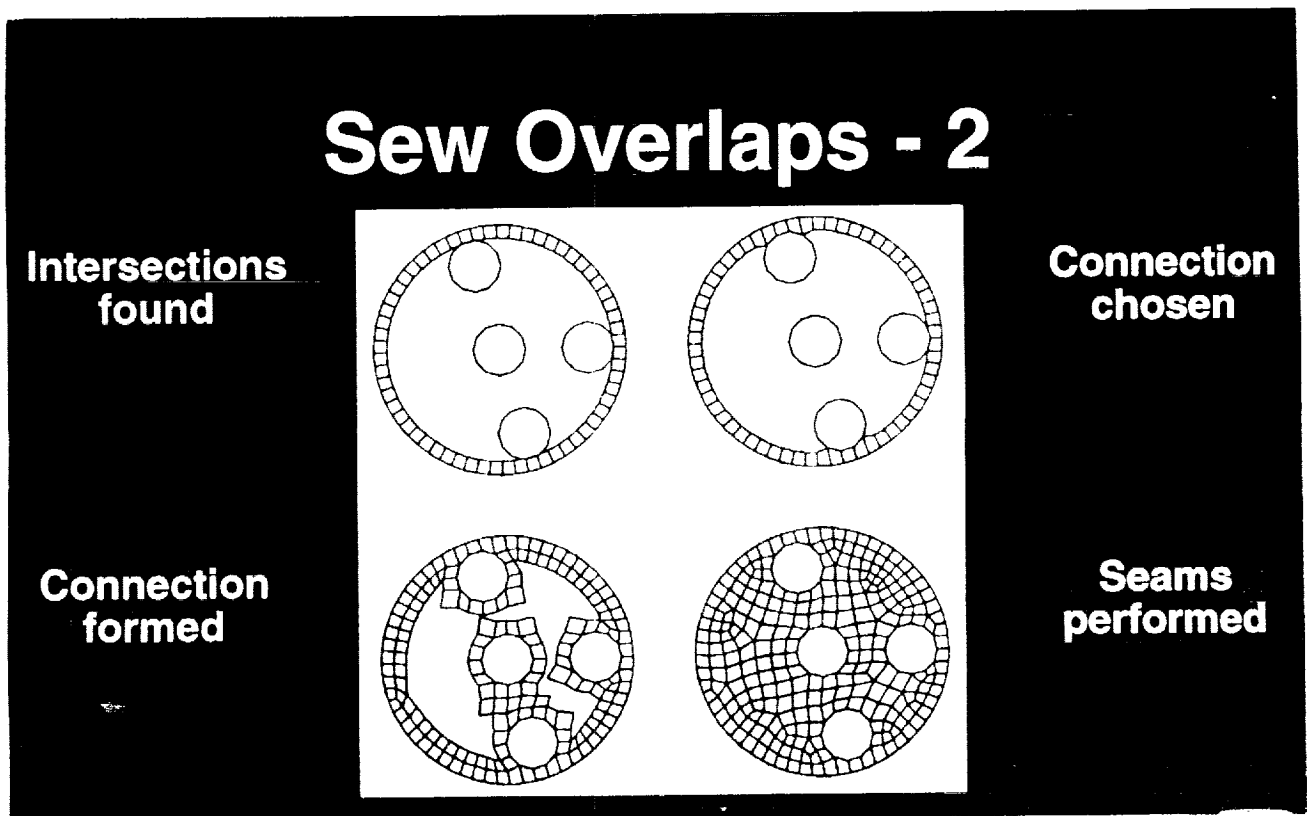


Figure 8 - Example of sewing process used in paving

Plastering Algorithm

Figure 9 shows an example of a plastered volume. The plastering algorithm will be capable of filling an arbitrary three-dimensional solid with an all-hexahedral mesh. The algorithm will first mesh the exterior and interior surfaces with the surface paving algorithm. Then the volume will be filled by projecting the surface elements toward the interior to form elements. Once this is done to all the surfaces, this will define a new volume to be meshed. The process is continued until the volume is filled. Concepts analogous to sewing, seaming, wedges and tucks for surface paving will be used to place elements on the interior of surfaces. This is an example test case for a transition from a 2×2 mesh to a 4×4 mesh with nonregular meshing of the other sides.

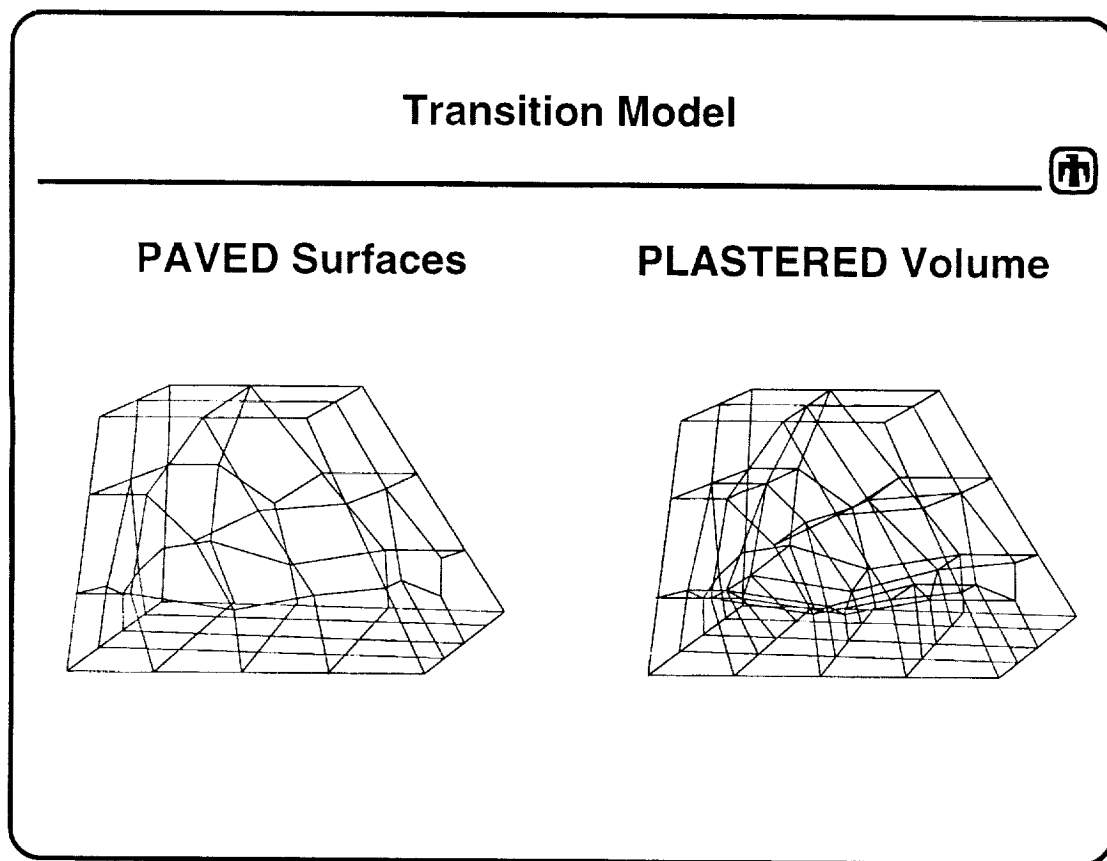


Figure 9 - Example of a plastered volume

Figure 10 shows 3D paving of a NURBS surface (nonuniform rational B-spline). The development of the surface paving algorithm has progressed to being capable of paving NURBS surfaces. This is an example of the surfaces being defined by a solid model and the paving algorithm meshing the surfaces. The example demonstrates the ability to pave arbitrary non-planar surfaces that have complex intersections with other surfaces.

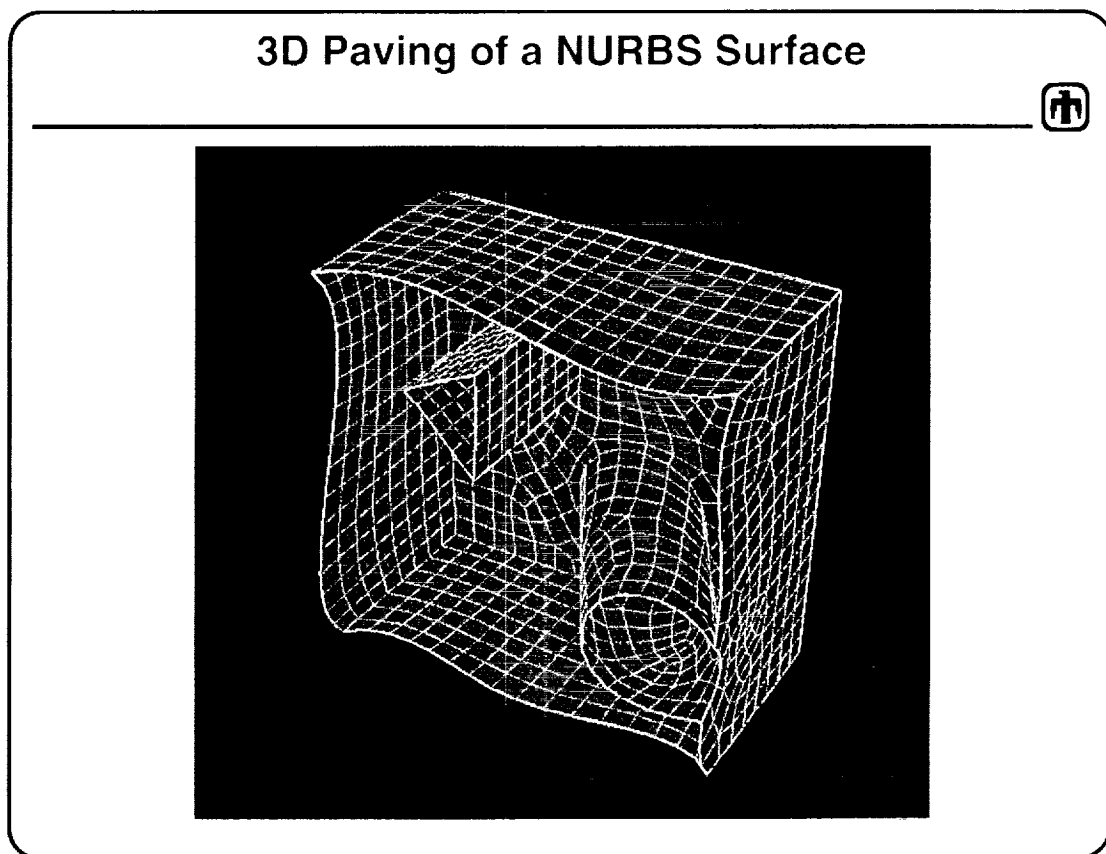


Figure 10 - Three-dimensional paving of a NURBS surface

Visualization Software

Figure 15 shows a typical screen of what an analyst might expect to see while working at his desk. Application Visualization System (AVS), a commercial scientific visualization environment, was selected as the foundation for our software development effort after an extensive survey of the market two years ago. It was chosen because of the following characteristics:

- functional -- contains a full-featured suite of modules which operate on numerous data types, including two-dimensional images and scalar and vector fields associated with structured or unstructured grids.
- extensible -- due to its modularity, functions can be readily added/customized.
- ubiquitous -- available on wide variety of hardware platforms.
- distributable -- AVS modules can execute on different machines within an application.

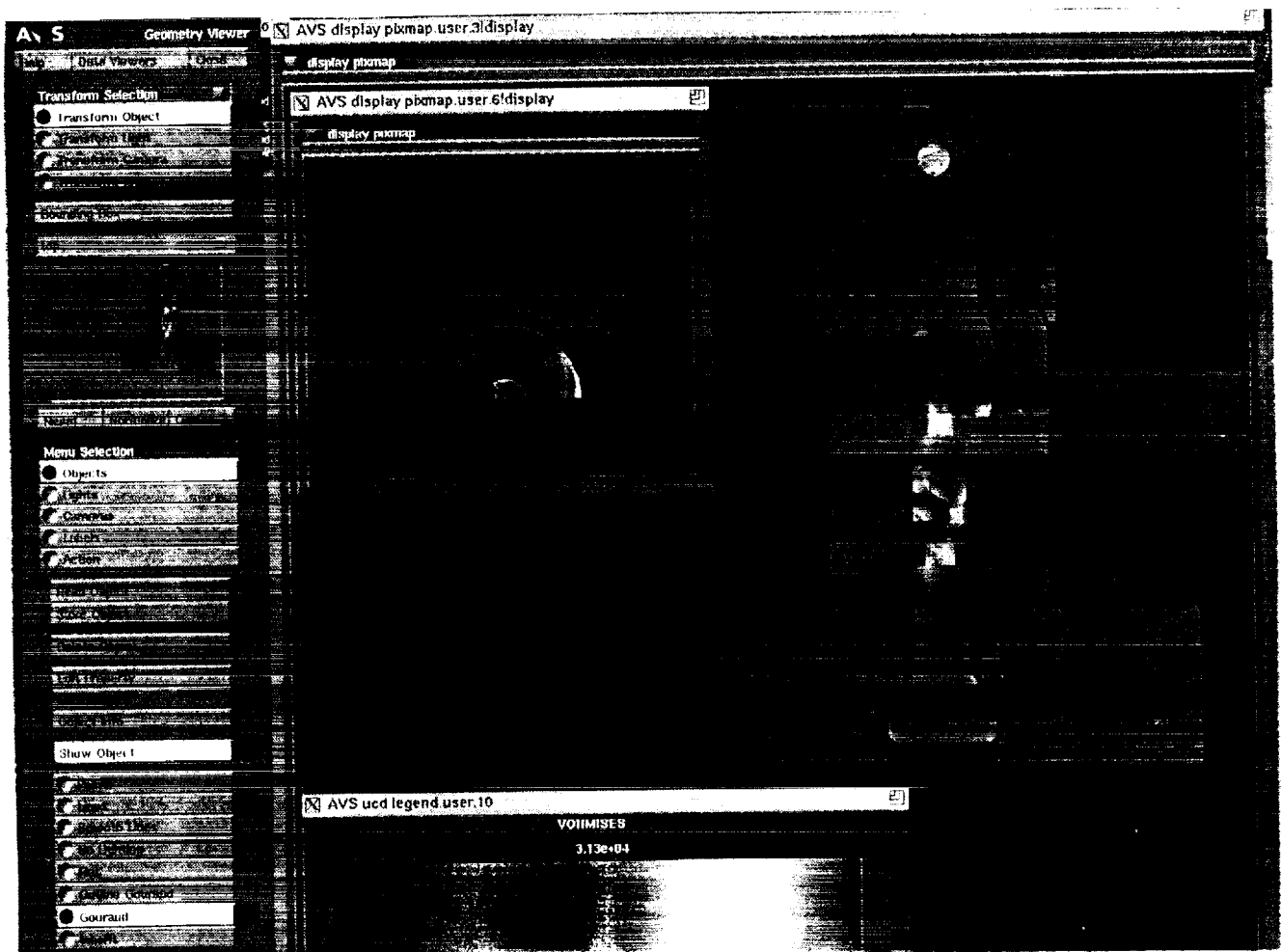


Figure 15 - Example of the AVS visualization tool

Figure 10 shows 3D paving of a NURBS surface (nonuniform rational B-spline). The development of the surface paving algorithm has progressed to being capable of paving NURBS surfaces. This is an example of the surfaces being defined by a solid model and the paving algorithm meshing the surfaces. The example demonstrates the ability to pave arbitrary non-planar surfaces that have complex intersections with other surfaces.

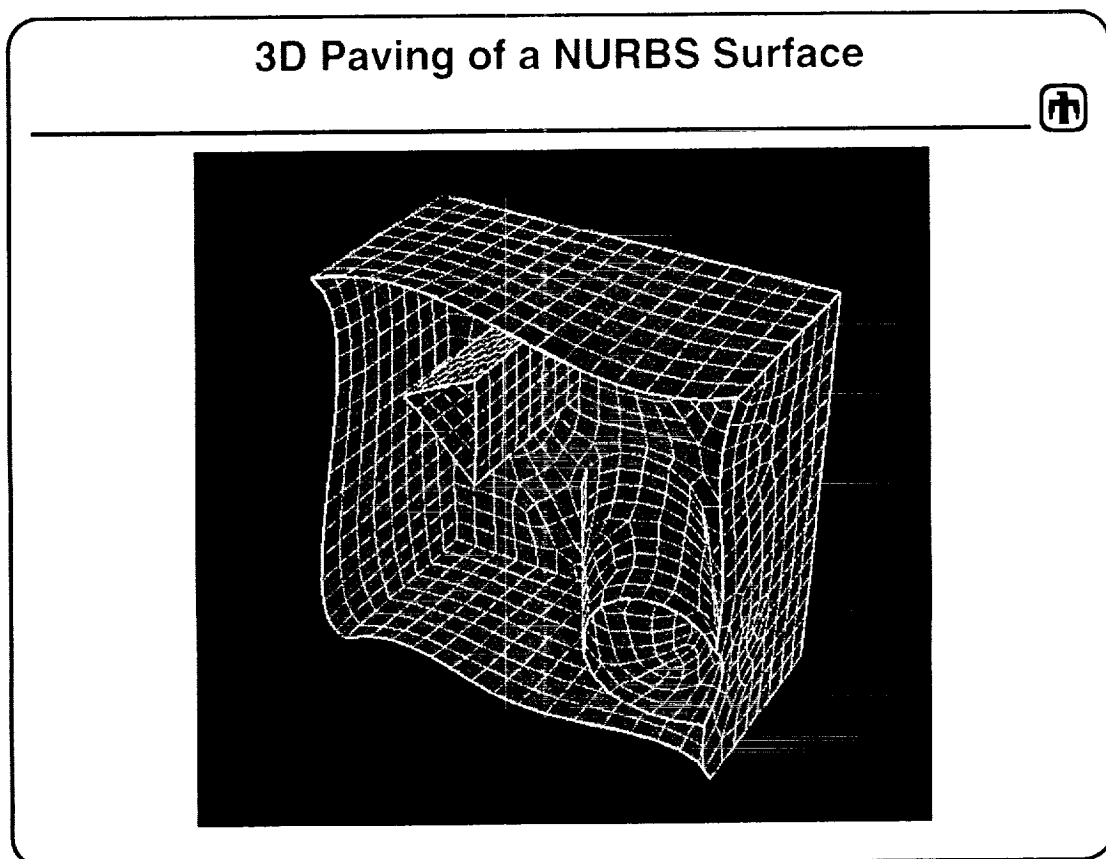


Figure 10 - Three-dimensional paving of a NURBS surface

Adaptive Analysis

The paving algorithm has been used in a proof of concept example to perform an adaptive analysis. The geometry and loads for the problem are first defined. Then an initial mesh of approximately equal size elements is generated with the paving algorithm, and a static analysis is performed. The resulting stresses are used to determine an error function at the nodes of the initial mesh. The surface is then remeshed with the paving algorithm by sizing and placing elements based on an error function. This results in smaller elements where the error is large. This process was repeated four times and the final mesh produces an accurate answer to the problem. An example of adaptive meshing using paving is shown in Fig. 11.

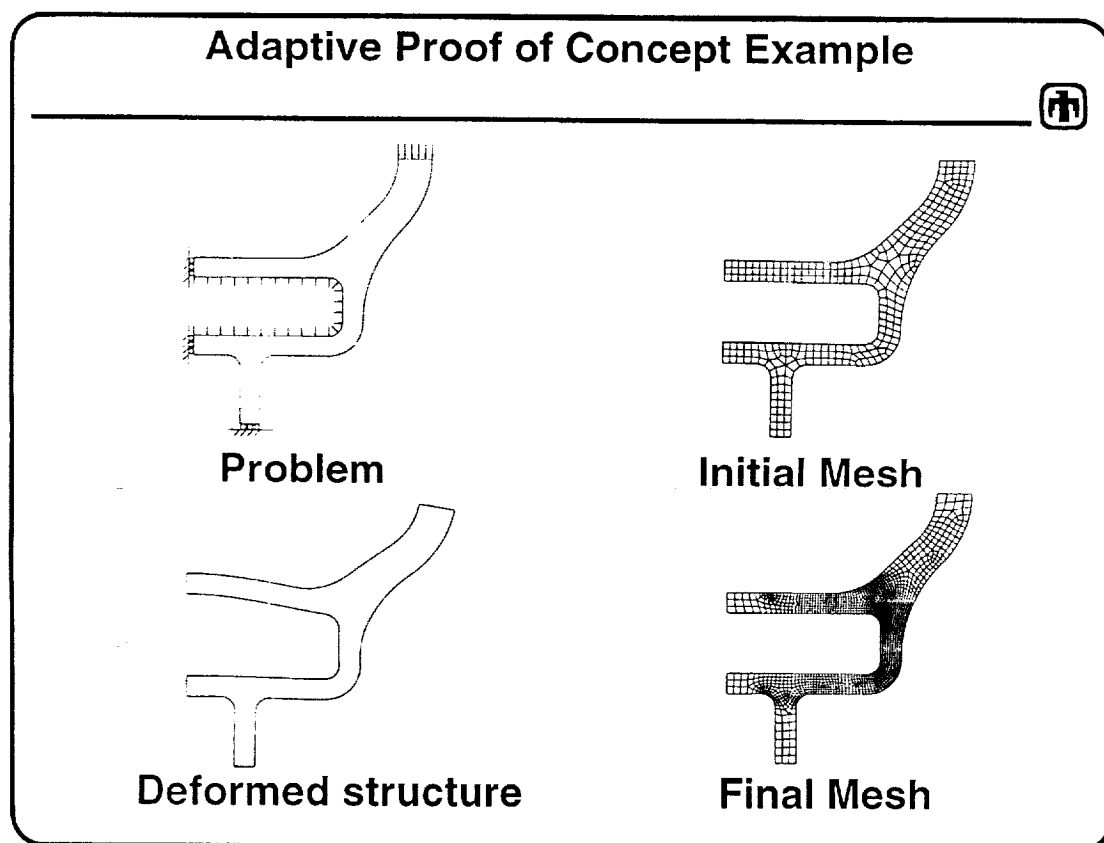


Figure 11 - Adaptive proof of concept example

Mesh Generation Consortium

Sandia has created a Mesh Generation Consortium of computer-aided software companies and Sandia National Laboratories to develop and commercialize the meshing algorithms. To date, ten companies have shown active interest and Cooperative Research and Development Agreements (CRADAs) have been completed. The work is supported with industry funds and matching Department of Energy research funds. The paving algorithm will appear in commercial software within three months. Figure 12 lists the important points of the mesh generation consortium.

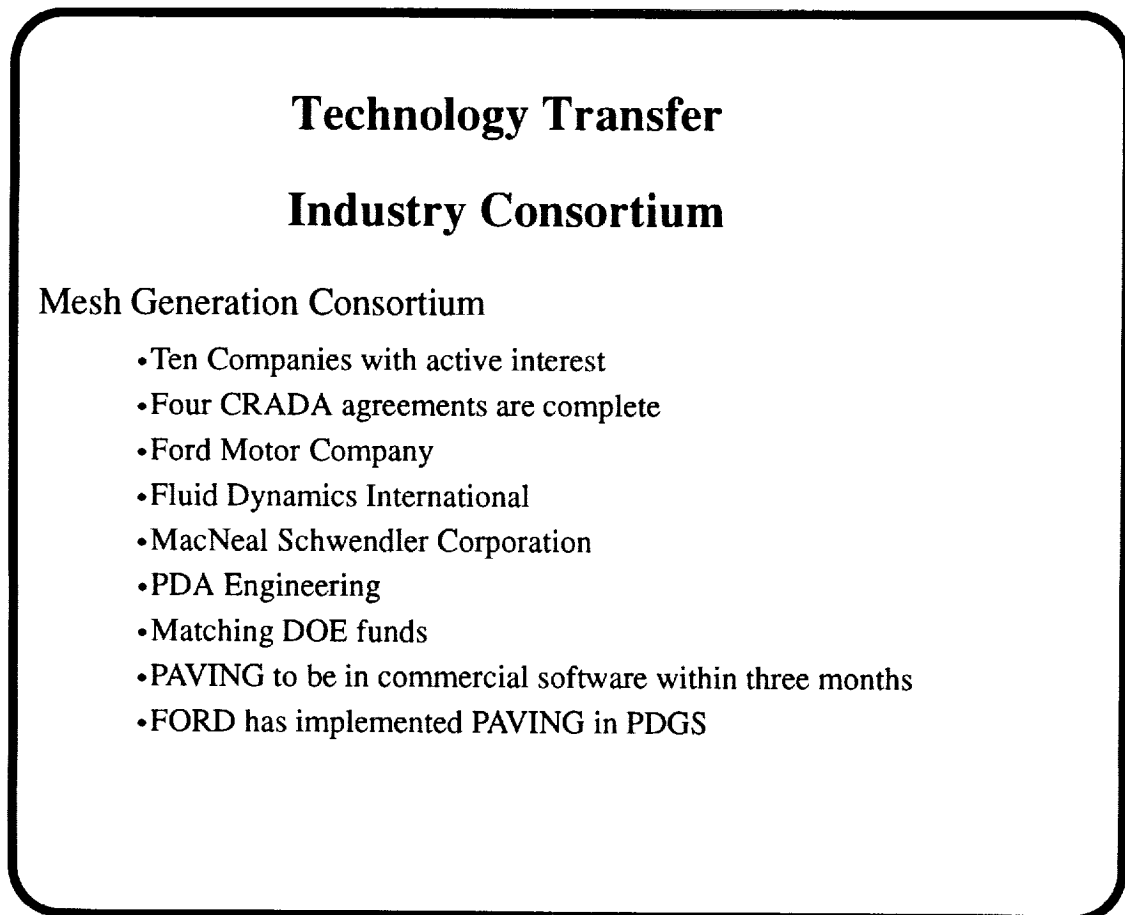


Figure 12 - Mesh generation consortium

PRODUCTION VISUALIZATION ENVIRONMENT

Applied Visualization Group

Supercomputers, both traditional and massively parallel machines, are capable of generating enormous amounts of data. Scientific visualization techniques are necessary to obtain useful information from these massive amounts of data. These techniques include responsive manipulation and animation of three-dimensional objects.

Resulting databases can be on the order of several gigabytes, so high speed access to these large remote databases is required. Another challenge is that analysts want to perform these visualization activities at their desks.

An **Applied Visualization Group (AVG)** has been established at Sandia National Laboratories to design and implement a production scientific visualization environment for use by the staff in the engineering sciences discipline. These analysts perform finite element and finite difference calculations in the areas of high velocity impact physics, shock wave physics, structural dynamics, structural mechanics, thermodynamics, and fluid mechanics. Visual results are critical in the data analysis functions performed.

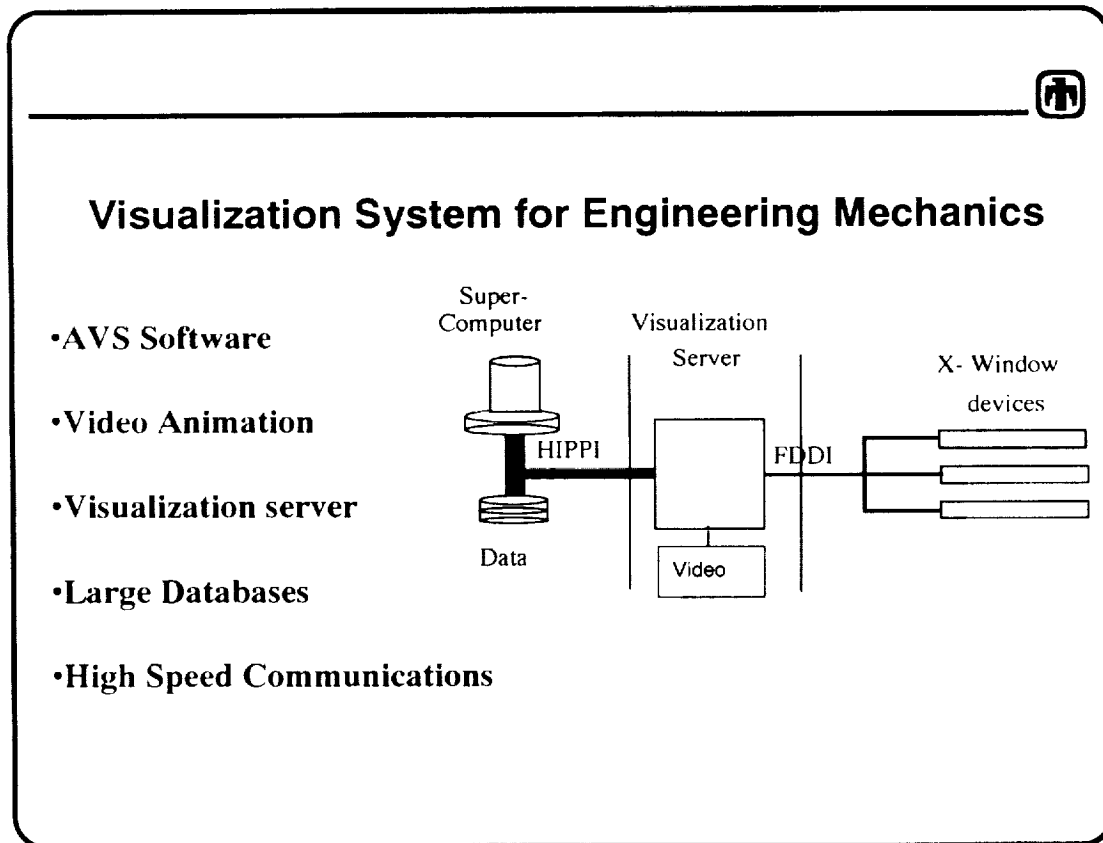


Figure 13 - Visualization system for engineering mechanics

Visualization Server

A visualization server concept is being implemented. One or several very high powered graphics machines will be used to perform the graphics manipulations, with the resulting images transmitted to an X-window display on the analyst's desk. We also expect to use PEX to distribute 3D graphics between the visualization server and the desktop display. We anticipate having a 100MByte channel connection from the visualization server to a supercomputer and network storage system, with FDDI connections from the visualization server to the offices. A block diagram of the proposed production environment consisting of hardware, software, and output capabilities integrated in an easy to use fashion is shown in Fig. 13. (See previous page.)

A video animation system, using a component video laser disk recorder, high resolution converter, video transcoder, and a workstation, allows workers to rapidly create videos of analyses. The use of component and composite video technology allows for high quality when results are played directly from the laser disc, while still allowing for VHS video tapes to be created for showing at remote locations. A block diagram of the system currently in use at Sandia is shown in Fig. 14.

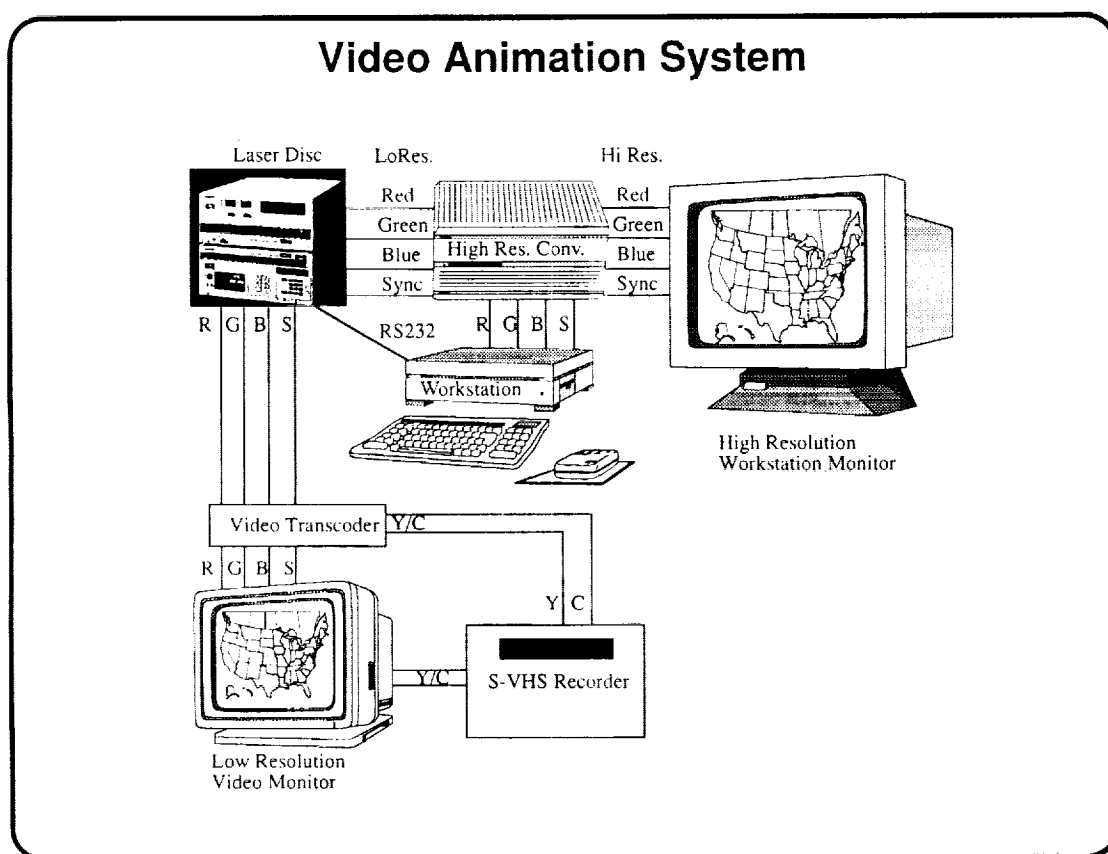


Figure 14 - Video animation system at Sandia

Visualization Software

Figure 15 shows a typical screen of what an analyst might expect to see while working at his desk. Application Visualization System (AVS), a commercial scientific visualization environment, was selected as the foundation for our software development effort after an extensive survey of the market two years ago. It was chosen because of the following characteristics:

- functional -- contains a full-featured suite of modules which operate on numerous data types, including two-dimensional images and scalar and vector fields associated with structured or unstructured grids.
- extensible -- due to its modularity, functions can be readily added/customized.
- ubiquitous -- available on wide variety of hardware platforms.
- distributable -- AVS modules can execute on different machines within an application.

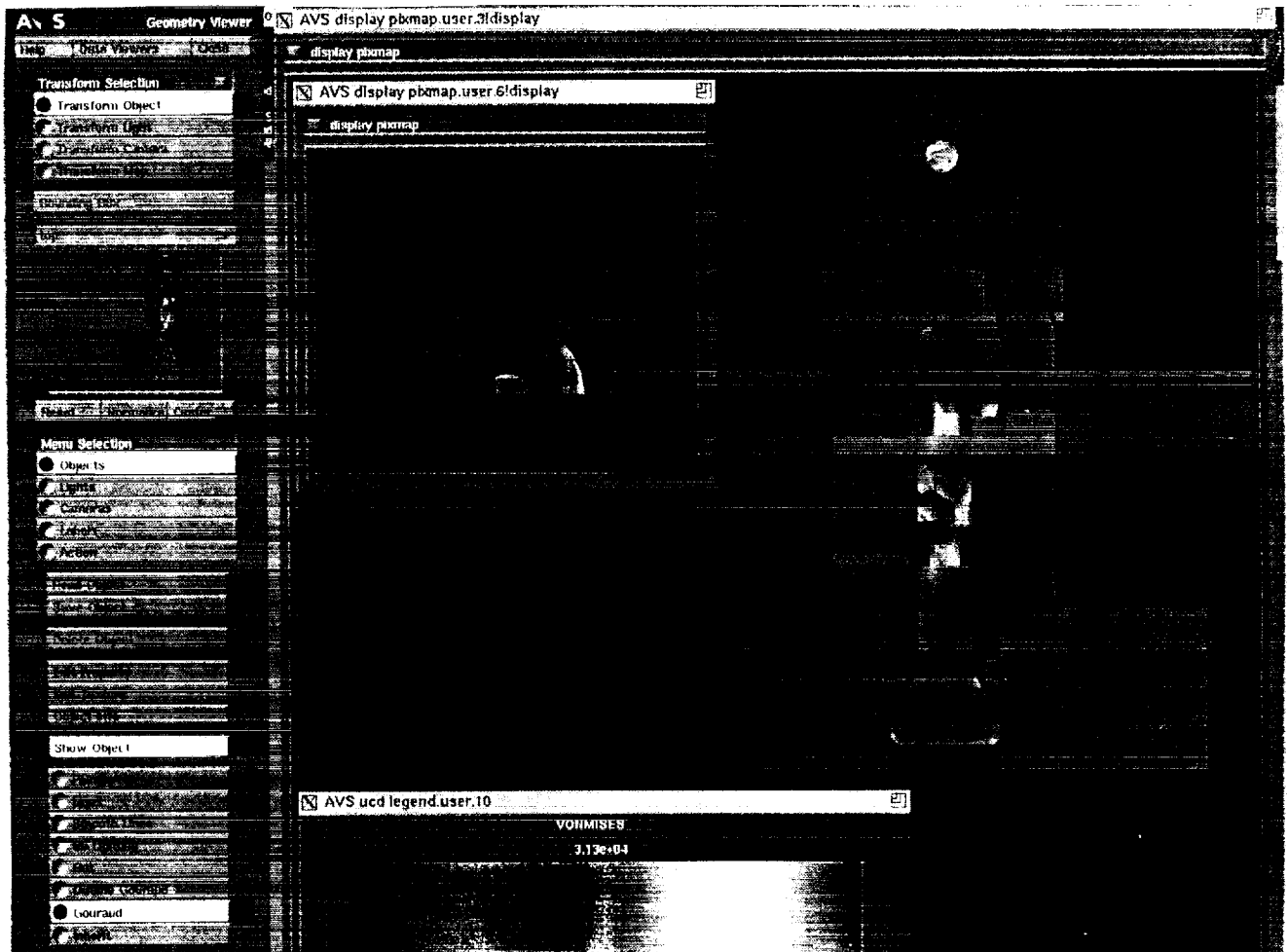


Figure 15 - Example of the AVS visualization tool

ANALYSIS PROGRAMS

The analysis codes in SEACAS include quasistatic, transient dynamics, thermal, and electromechanics codes.

jac2d: Jac2d is a finite element program which uses a nonlinear conjugate gradient technique to solve the large displacement, large strain, temperature-dependent and material nonlinear problem for two-dimensional plane or axisymmetric solids.

jac3d: Jac3d is a finite element program which uses a nonlinear conjugate gradient technique to solve the large displacement, large strain, temperature-dependent and material nonlinear problem for three-dimensional solids.

jacq3d: Jacq3d is a finite element program which uses a nonlinear conjugate gradient technique to solve the thermal conduction problem for three-dimensional solids.

pronto2d: Pronto2d is a two-dimensional (planar and axisymmetric) transient solid dynamics code. Lagrangian formulation with explicit time integration is used for analyzing large deformations of highly nonlinear materials subjected to extremely high strain rates.

pronto3d: Pronto3d is a three-dimensional transient solid dynamics code. Lagrangian formulation with explicit time integration is used for analyzing large deformations of highly nonlinear materials subjected to extremely high strain rates.

sancho: Sancho is a finite element program which uses a dynamic relaxation technique to compute the quasistatic, large deformation, temperature-dependent, inelastic response of planar or axisymmetric solids.

santos: Santos is a finite element program which uses a dynamic relaxation technique to compute the quasistatic, large deformation, temperature-dependent, inelastic response of planar or axisymmetric solids. Newer than sancho.

santos3d: Santos3d is a three-dimensional version of santos. It is currently in development.

conchas: Conchas is a linear structural analysis code for axisymmetric structures with loads that are symmetric about a plane.

subway: Subway is a three-dimensional finite element program for calculating the transient electro-mechanical response of dielectric materials.

Constitutive Models

Many constitutive models are implemented in the analysis codes.

Elastic: Typical linear elastic material using Hooke's Law.

Elastic-Plastic with Combined Hardening: Standard von Mises type yield condition with combined kinematic and isotropic linear hardening.

Viscoplastic: Simple rate-dependent plasticity.

Viscoelastic: Thermoviscoelastic model for glass solidification.

Damage: Dynamic fracture of brittle rock.

Soils and Crushable Foam: Volumetric plasticity model.

Low Density Foam: Low density polyurethane foam behavior.

Hydrodynamic: Used with Equations of State in PRONTO

Elastic-Plastic Hydrodynamic: Combination of elastic-plastic combined hardening with hydrodynamic pressure response: Mie_Gruneisen type equation of state, JWL High Explosive Equation of State.

Rate and Temperature Dependent Plasticity: Unified creep plasticity.

Secondary Creep: Power hardening steady-state creep with elastic bulk response. Isotropic Elastic/Plastic Power-Law Hardening with Luders Strain.

Johnson-Cook Strength: Rate and temperature-dependent plasticity.

Elastic Plastic Power Law Hardening with Luder's Strain: Describes post-yield strain hardening by a power law equation and includes a yield plateau.

Hyperelastic: Stress based on the principal strains.

Salt Consolidation: Power hardening steady-state creep deviatoric response with consolidation bulk response.

Not all of the constitutive models are implemented in all of the analysis codes. The quasistatic analysis codes typically implement the constitutive models using temperature-dependent properties to facilitate thermal-stress calculations.

TRANSIENT DYNAMICS DEVELOPMENT

A summary of the transient dynamics code PRONTO and the development objectives for PRONTO are shown in Fig. 16.

PRONTO Description:

A two- and three-dimensional transient solid dynamics code for analyzing large deformations of highly non-linear materials subjected to high strain rates

- Explicit mid-point time integration
- One point element integration
- 2D - four node quad
- 3D - eight node hexagon, 3D - four node shell
- Hourglass control
- Adaptive time step control
- Symmetric contact algorithm
- Objective material coordinate system

Code Development Objectives:

- Well documented and consistent
- Accurate numerical algorithms which minimize error
- Dependable and aborts executions by providing diagnostics
- Executes rapidly
- Uses existing pre- and post- processing software
- Easy to add new constitutive models

Figure 16 - PRONTO description and development objectives

New Contact Detection Algorithm

An increasingly important aspect of large-scale finite element simulations is the efficient and accurate determination of contact between deformable bodies. Generally there are several aspects of the numerical model that make contact detection difficult. This section reviews some currently used contact detection techniques and outlines some difficulties associated with these algorithms. Then, a new algorithm is proposed which circumvents these difficulties.

The key points of the new contact detection algorithm are: i) uses the existing contact penalty/kinematic constraint method (including partitioned contact); ii) easily models self-contacting surfaces; iii) automatically defines all surfaces given the mesh connectivity; iv) models tearing and eroding surfaces; v) reduces user input; vi) uses a fast, memory-efficient global search to decide what slave nodes are in proximity to a master surface; and vii) does a detailed contact check using projected movements of both the master and slave to determine the magnitude and direction of slave node penetration of the master surface. See Fig. 17.

Contact surfaces

New contact detection algorithm:

- Uses the existing contact penalty/kinematic constraint method
- Partitioned contact (both surfaces can be master and slave)
- Static and dynamic friction
- Self contacting surfaces
- Automatically defines contacting surfaces
- Allows for tearing and eroding surfaces
- Reduces user input
- Does not require slideline pairing
- Performs a global search for contact
- Efficient contact search ($k n \log n$)
- Resolves contact corner ambiguities

Figure 17 - Contact surfaces

Multibody Impact: Elastic-Plastic Bar Impacting Bricks

The following example demonstrates two features of the contact detection algorithm that are important to this particular class of problems. The example shown in Fig. 18 has an elastic-plastic bar impacting a stack of 17 elastic bricks. A stationary elastic-plastic wall is also resting against the stack of bricks.

An important feature of the contact detection algorithm is the spatial independence of the $kn \text{ Log} n$ vectorized sorting algorithm. The speed of the algorithm is independent on the location of the bricks. This becomes particularly important late in this example since the volume that the bodies occupy is increasing.

Another feature of the contact detection algorithm that is both more efficient and useful is that the surfaces are not required to be paired. In fact, the surfaces were automatically defined using a new surface definition algorithm. For problems where random contact is anticipated, as in this example, each body could potentially impact any other body. For a contact-pairing algorithm, this implies that n_i^2 contact pairs would be necessary, with each pair having $2m$ slave nodes. For the current global contact searching algorithm, it would imply one search with $n_i m$ slave nodes. Consider in this example 19^2 pairs would have to be defined since random contact is expected. Assuming that each block has $m \approx 50$ slave nodes, 19^2 pairs would require $19^2 (2m \log (2m)) = 239,843$ comparisons, whereas the current global contact searching algorithm would require only $19m \log_2(19m) = 9397$ comparisons.

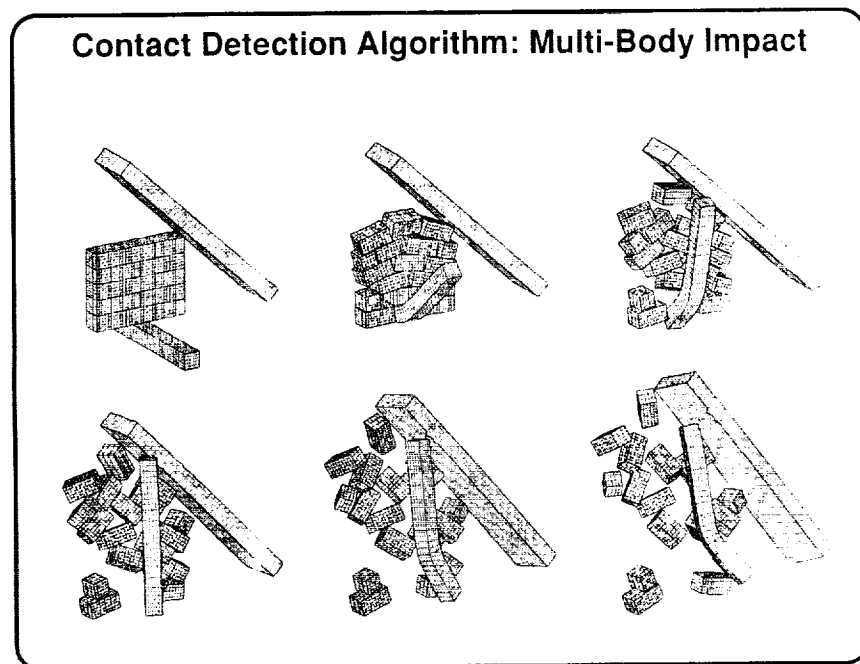


Figure 18 - Elastic-plastic bar impacting bricks

Self-Contacting Impact: Buckling of Shell-Like Structures

The following example demonstrates the self-contacting capability of the contact detection algorithm. This feature is important to modeling crash dynamics where buckling, tearing and self-contact is common. The example shown in Fig. 19 has an elastic plate impacting an elastic-plastic can (shell-like structure). The can is 0.7 inches thick and has an inside radius of 12.5 inches. After 10 milliseconds the can is nearly crushed flat with numerous folds and buckles that self contact.

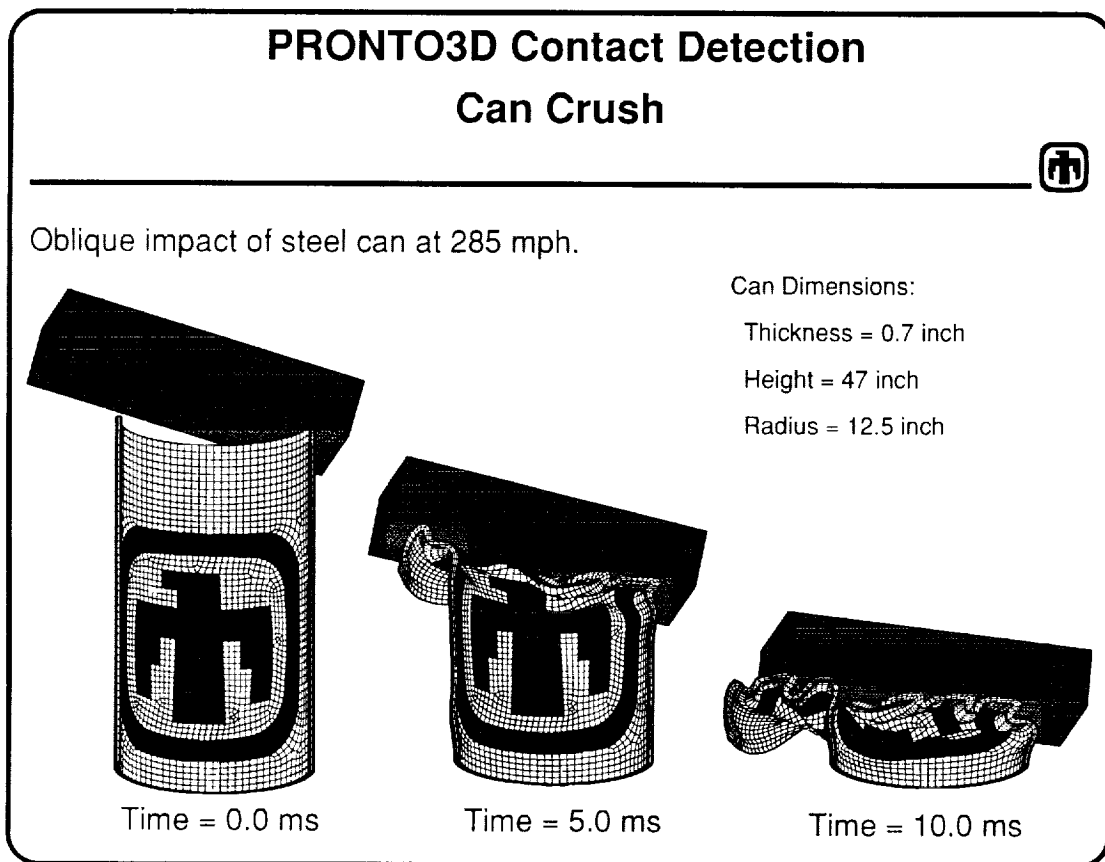


Figure 19 - Self-contacting impact of a buckling shell-like structure

Automatic Contact Surface Redefinition: Tearing/Petalling of a Plate

In the following example, the capability of automatically redefining the contact surface is essential. This feature is also important for modelling crash dynamics where buckling, tearing and self-contact is common. The example shown in Fig. 20 has a solid elastic sphere impacting a thin elastic-plastic plate. The plate is 0.25 inches thick and has an overall dimension of 12.0 inches by 14.0 inches. After a few milliseconds the plate is damaged such that two tears develop orthogonal to one another. The tears are actually a series of deleted elements where the damage has accumulated to 1.0. The newly created surface is automatically included in the contact algorithm by redefining the surface after any elements are deleted. At late time, the edges of the tears are in contact with the elastic sphere.

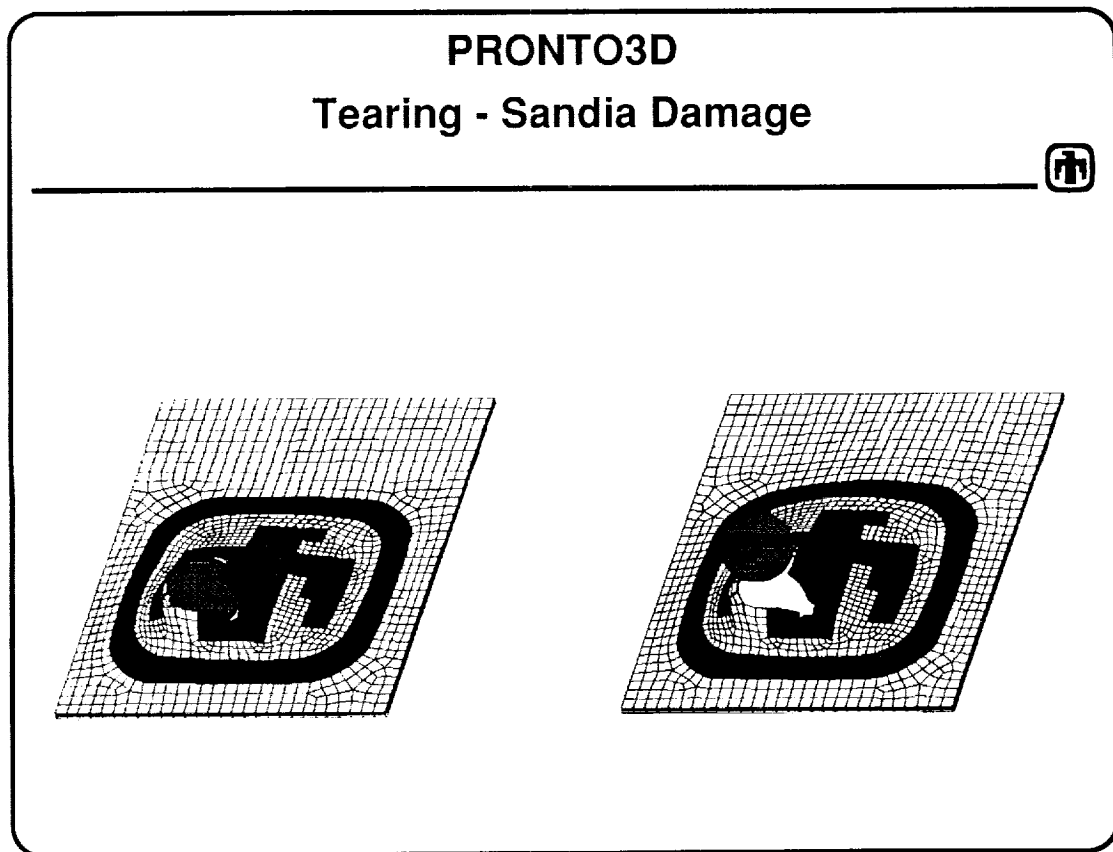


Figure 20 - Automatic contact surface redefinition: tearing/petalling of a plate

Contact Algorithm Implementation: Reduced User Input

Reduced user input is a convenience that is an outcome of the global searching and automatic surface definition capability. One can, for example, selectively include all surfaces of a body composed of a material and/or include only a subset of the surface. Figure 21 shows the typical input required for a problem. Reducing the input required from the user minimizes the number of mistakes, which minimizes cost.

Contact Surface

Reduced user input

```
contact material 1
contact material 2
contact material 5
contact surface 100
contact data material 2, material 5, friction = .1
```

Surface 100, materials 1, 2 and 5 will be globally searched for contacts. Contacts between material 2 and 5 will have a coefficient of friction equal to 0.1

Figure 21 - Reduced user input

Contact Detection Algorithm: Capturing Slave Nodes for a Master Surface

It is widely held that the location phase is the most time-consuming part of the contact detection algorithm. Obviously, the most robust approach would be to check every slave node against every master surface every time step. This exhaustive global searching approach requires nodal distance calculations on the order n^2 , where n is the number of nodes. Several algorithms have been proposed to speed up the location phase.

The proposed contact detection algorithm uses a new global search algorithm. It uses $7n$ memory locations and requires $(k n \log n)$ comparisons and depends on only the number of entities (n) to be compared. It takes advantage of the known positions of the slave nodes and master surfaces as well as the predicted positions in the next time step. After the slave nodes are sorted by x , y and z coordinate, the master surfaces are processed sequentially. This processing involves bounding the space occupied by a master surface at its known location and its predicted location. Figure 22 shows a bounding box for a master surface over one time step. Clearly, a slave node could only make contact with this master surface if it is no further from the bounding box than the distance it could move in the time step. Therefore, any slave node inside the capture box should be considered for potential contact with the master surface.

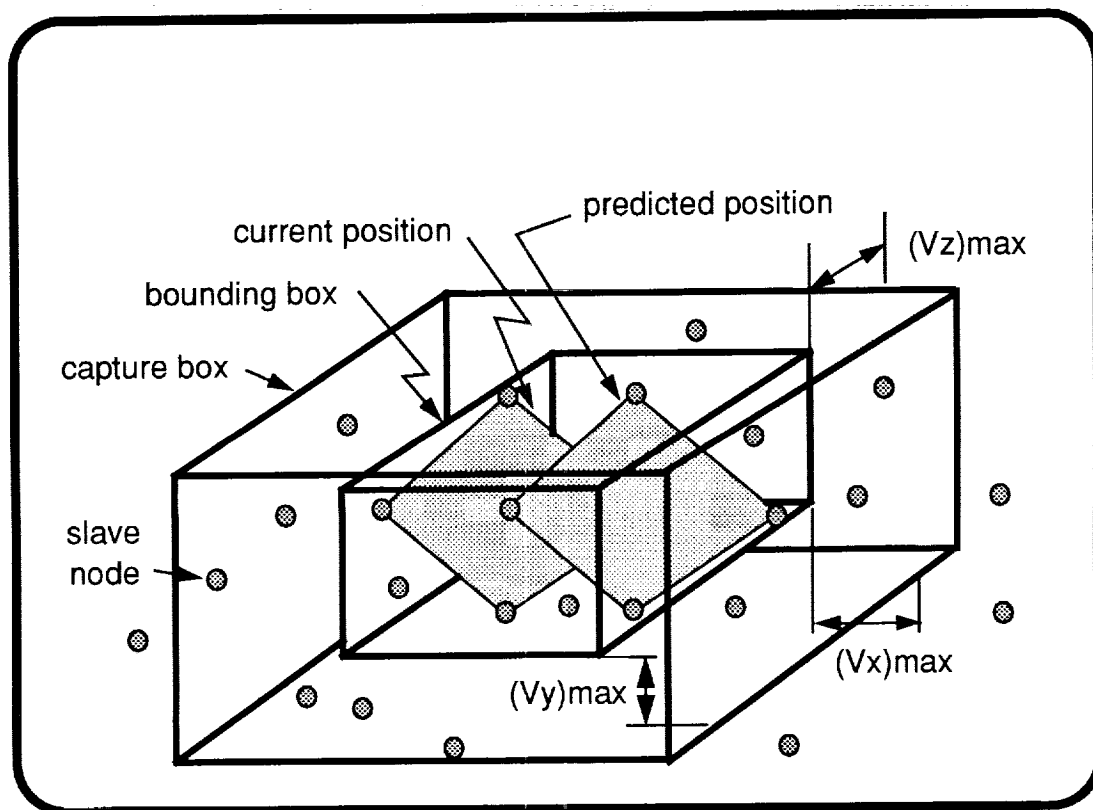


Figure 22 - Contact search bounding box

Contact Detection Algorithm: Slave Node/Master Surface Contact

Unfortunately there are many ambiguous cases when determining contact between a slave node and a master surface. One such ambiguity arises because the surface normal is not continuous. This can result in either missed contacts or multiple solutions. In the proposed algorithm, the motion of the slave node and the master surface are considered and these ambiguities are avoided. As shown in Fig. 23, the time of contact and the point of contact is determined for each possible master surface that a slave node can penetrate. The algorithm solves for the time when a slave node and master surface all lie in the same plane. When the slave node can contact more than one master surface, the minimum time to contact determines the correct master surface contact.

Further ambiguity is introduced when a contact algorithm performs detailed contact checks based only on the estimated (deformed) configuration. If an algorithm does not make use of information about how the slave node deforms to the estimated position, the algorithm must decide which contact violation to enforce. This is commonly done by determining which surface is most opposed to the slave node surface normal. When two surfaces are already in contact this so-called strength of contact check can be effective. However, when the surfaces are just coming into contact this type of static contact check cannot consistently predict the correct contact.

In the proposed algorithm, the motion of the slave node and the master surface are considered and these ambiguities are avoided. In determining the push back direction, a distinction is made between convex and concave surfaces. The push back direction for a convex surface is determined simply by the minimum distance to the master surface. The push back direction can be along the master surface normal or it may be defined by the minimum distance to a vertex. For a concave surface the push back direction is always along the normal of the master surface that the slave node was previously in contact with.

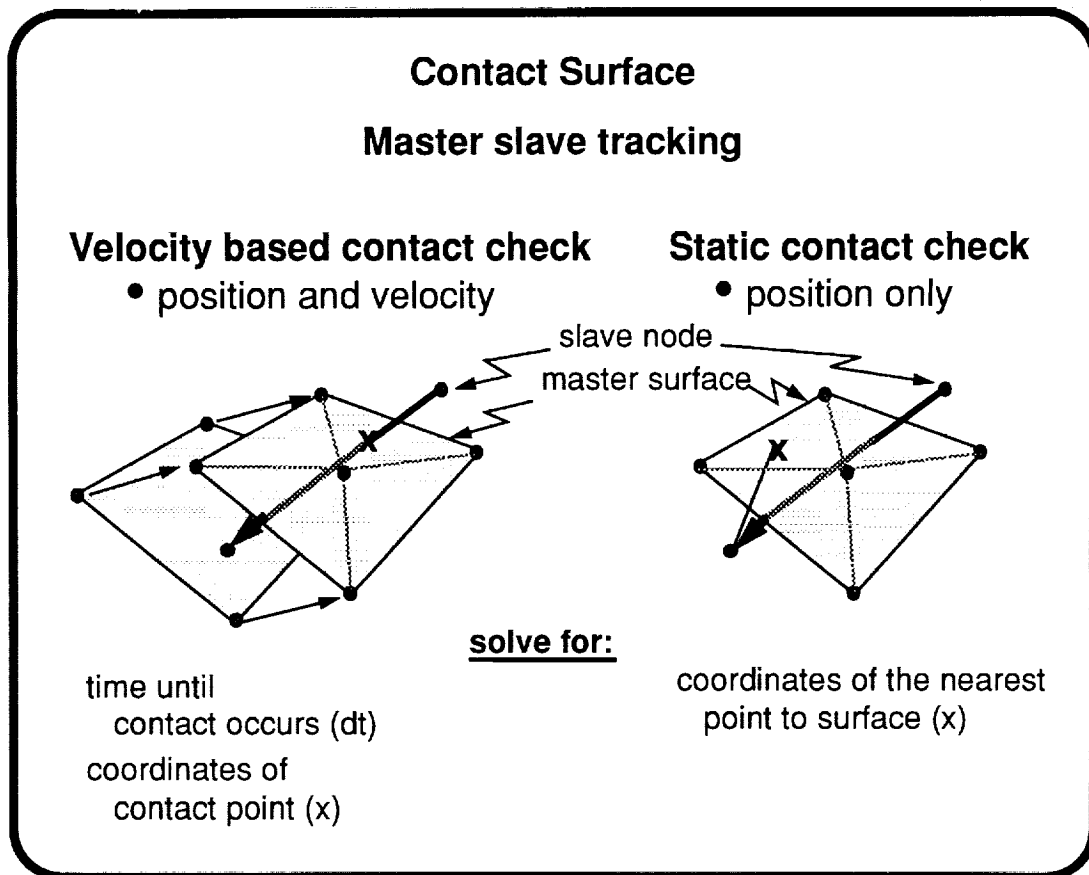


Figure 23 - Master/slave tracking

FUTURE CODE DEVELOPMENT

Figure 24 lists some of the active areas of code development and research at Sandia.

- Incorporate rezoning/remeshing algorithms
- Constitutive model development
 - Orthotropic materials
 - Damage and tearing constitutive relations
- Add Belytschko's physical hourglass control
- Add Rashid's fully objective incremental formulation
- Add rigid bodies, beams, springs and dash pots
- Couple particle hydrodynamics with structural dynamics
- C++ and Massively Parallel Computers

Figure 24 - Future code development

uniform strain hexahedral elements are used in the finite element formulation. A number of new numerical algorithms which have been developed for the code are described in this report. An adaptive time step control algorithm is described which greatly improves stability as well as performance in plasticity problems. A robust hourglass control scheme which eliminates hourglass distortions without disturbing the finite element solution is included. All constitutive models in PRONTO are cast in an unrotated configuration defined using the rotation determined from the polar decomposition of the deformation gradient. An accurate incremental algorithm was developed to determine this rotation and is described in detail. A robust contact algorithm was developed which allows for the impact and interaction of deforming contact surfaces of quite general geometry. Numerical examples are presented to demonstrate the utility of these algorithms.

L. M. Taylor and D. P. Flanagan, "PRONTO 3D, A Three-Dimensional Transient Solid Dynamics Program," SAND87-1912, Sandia National Laboratories, Albuquerque, New Mexico, March 1989.

An external code interface is defined which allows other transient applications to communicate with the PRONTO family of finite element programs. This interface is written in ANSI FORTRAN and allows an independent author to specify requirements for an external code to PRONTO. The interface is written such that updates to PRONTO will not require modifications to the external code.

L. M. Taylor and D. P. Flanagan, "An External Code Interface for the PRONTO Family of Transient Solid Dynamics Programs," SAND87-3003, Sandia National Laboratories, Albuquerque, New Mexico, September 1988.

PRONTO 2D and PRONTO 3D are two- and three-dimensional solid dynamics codes for analyzing large deformations of highly nonlinear materials subjected to high strain rates. This newsletter is issued to document changes to these codes. As of this writing, the latest version of PRONTO 2D is Version 4.5.6, and the latest version of PRONTO 3D is Version 4.5.6.

This update of the two codes discusses two major modifications to the numerical formulations, three new constitutive models, and the additions and improvements of contact surfaces. Changes in file formats, other miscellaneous revisions, and the availability of PRONTO 2D and PRONTO 3D are also discussed. In addition, updated commands for PRONTO 2D are provided in Appendix A of this newsletter.

S. W. Attaway, "Update of PRONTO 2D and PRONTO 3D Transient Solid Dynamics Program," SAND90-0102, Sandia National Laboratories, Albuquerque, New Mexico, November 1990.

PRONTO 3D is a three-dimensional transient solid dynamics code for analyzing large deformations of highly nonlinear materials subjected to high strain rates. It is a Lagrangian finite element program with explicit integration of the equations of motion through time. This report documents the implementation of a four-node quadrilateral shell element into Version 6.0 of PRONTO 3D.

This report describes the theory, implementation and use of a four-node shell element. Also described are the required architectural changes made to PRONTO 3D to allow multiple element types. Several test problems are documented for verification of the PRONTO 3D implementation and for demonstration of computational savings using shell elements for thin structures. These problems also serve as examples for the user. A complete, updated list of the PRONTO 3D input commands is also included.

V. L. Bergmann, "Transient Dynamics Analysis of Plates and Shells with PRONTO 3D," SAND91-1182, Sandia National Laboratories, Albuquerque, New Mexico, September 1991.

This update discusses modifications of PRONTO 3D tailored to the design of fast burst nuclear reactors. A thermoelastic constitutive model and spatially variant thermal history load were added for

FUTURE CODE DEVELOPMENT

Figure 24 lists some of the active areas of code development and research at Sandia.

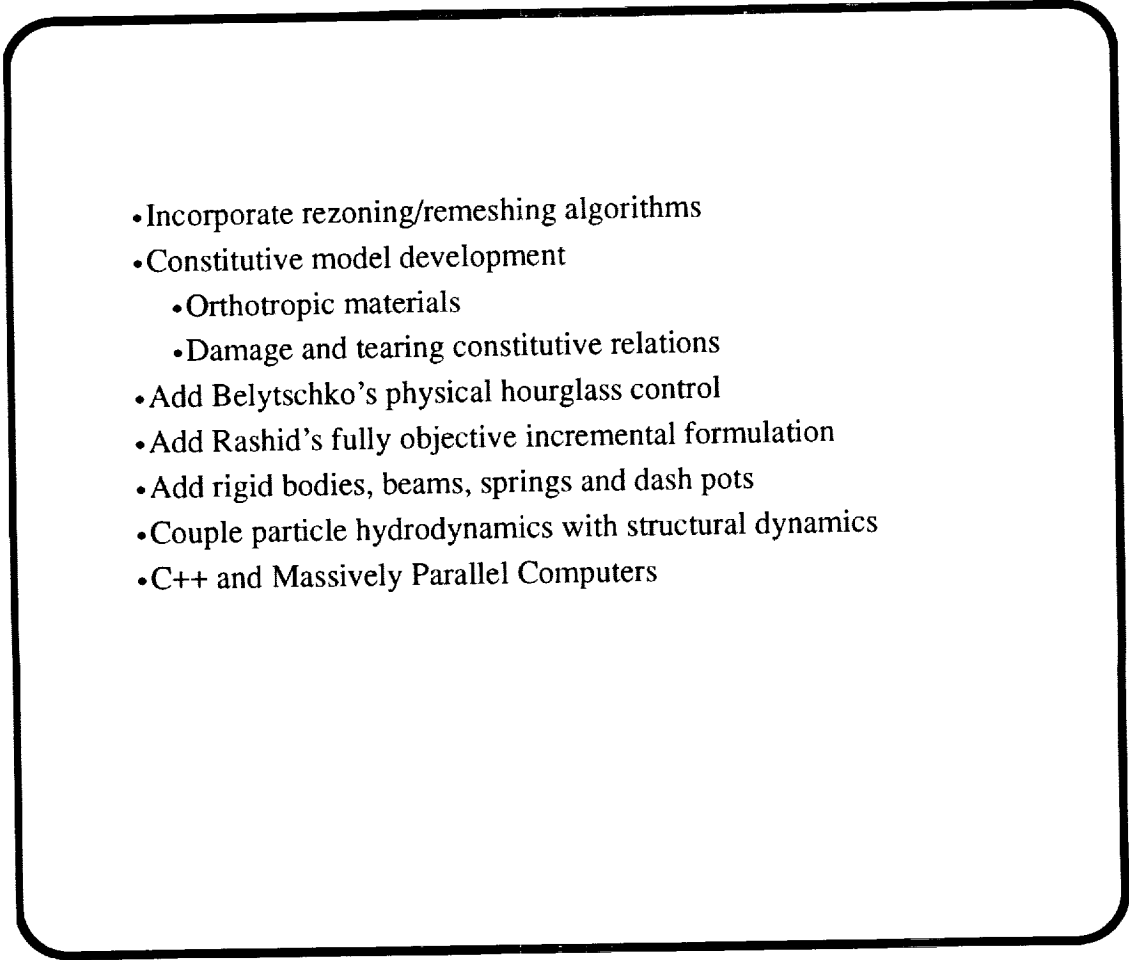
- 
- Incorporate rezoning/remeshing algorithms
 - Constitutive model development
 - Orthotropic materials
 - Damage and tearing constitutive relations
 - Add Belytschko's physical hourglass control
 - Add Rashid's fully objective incremental formulation
 - Add rigid bodies, beams, springs and dash pots
 - Couple particle hydrodynamics with structural dynamics
 - C++ and Massively Parallel Computers

Figure 24 - Future code development

Couple Particle Hydrodynamics with Structural Dynamics

Figure 25 shows an example problem using a combination of finite elements and particle elements. One major difficulty associated with the Lagrangian finite element method is modeling materials with no shear strength; for example, gases, fluids and explosives biproducts. Typically these materials can be modelled for only a short time with a Lagrangian finite element code. Tangling of the mesh will eventually lead to numerical difficulties such as negative element area or "bow tie" elements. Remeshing will allow the problem to continue for a short while, but the lack of shear strength causes instabilities that prevent a complete analysis.

Smooth particle hydrodynamics is a gridless Lagrangian hydrodynamic technique. Requiring no mesh, SPH can model material fracture, large shear flows, and penetration. SPH treats material as particles that have their masses smoothed in space. The density is computed at a point by summing the contributions of the smoothed particle masses in the vicinity of the point. SPH computes the strain rate and the stress divergence based on the nearest neighbors of a particle. The nearest neighbors are determined using an efficient particle sorting technique.

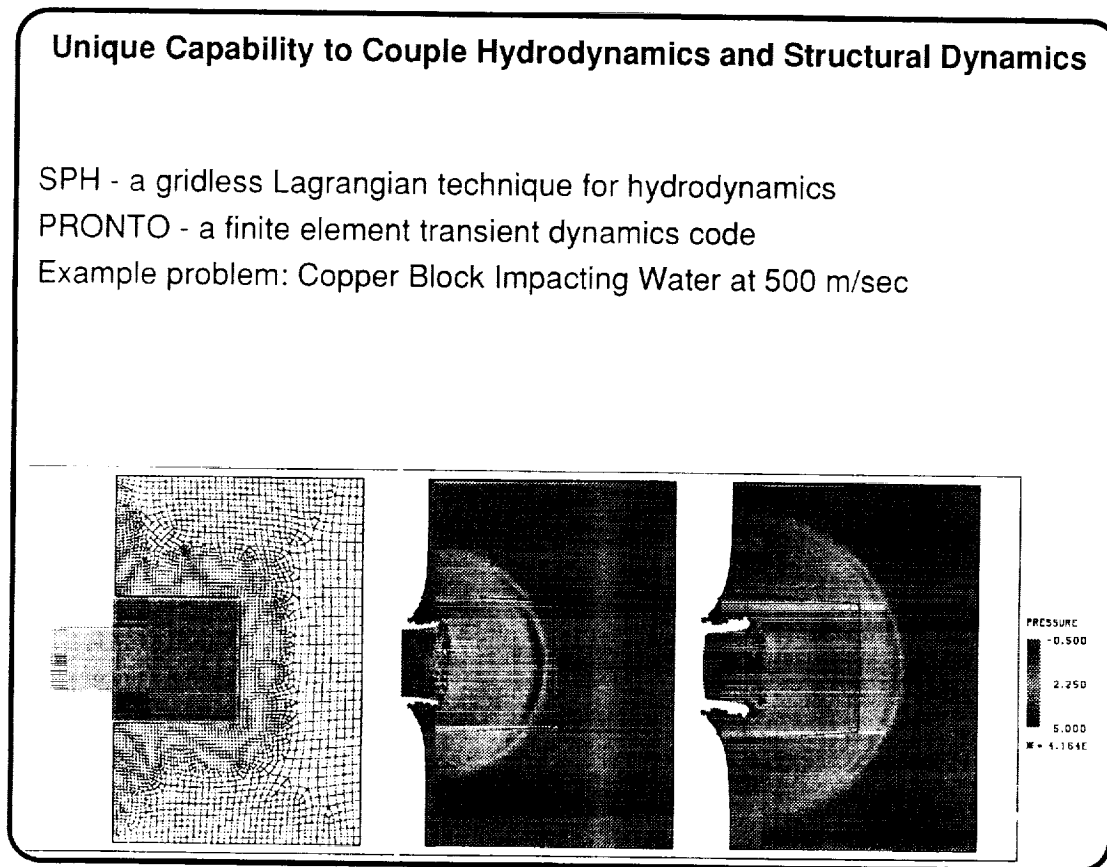


Figure 25 - Coupling particle hydrodynamics and structural dynamics

The SPH computational technique was embedded within the PRONTO computer code. SPH elements are modeled within PRONTO as elements that have only one node. Each element has the typical element variables associated with it (stress, strain, rotation, stretch, density, energy and other state variables). By using the existing PRONTO architecture, the SPH elements used the same constitutive equations as used by the quadrilateral elements in PRONTO.

The embedding of the SPH method within PRONTO allows part of the problem to be modeled with quadrilateral elements while other parts of the problem are modeled with the gridless SPH method. The quadrilateral elements are coupled to the SPH elements through a contact-like algorithm.

Object-Oriented Code

Figure 26 outlines the objectives for a new code that would combine solid, fluid and heat transfer problems into one code architecture. The goal of this effort is to apply object-oriented concepts to the design of a code architecture for solving problems in solid mechanics, fluid mechanics, and heat transfer. Consolidating these areas into a single package has the potential of reducing the time required for code maintenance and adding new features. Such an architecture should facilitate development of the capability to solve strongly coupled problems among these three areas of engineering science. The code will be implemented in the object-oriented language C++ to simplify code reuse and provide for extensibility. The code architecture will be designed to run efficiently on message passing MIMD computers and to take advantage of vector capabilities that exist on some machines in that class.

Object-Oriented Finite Element Code Architecture for Massively Parallel Computers

One code architecture for:

- Solid mechanics problems
- Fluid mechanics problems
- Heat transfer problems

C++ object-oriented architecture will:

- simplify porting to new generations of supercomputers
- ease implementation of new element types, solution algorithms
- provide environment that encourages teamwork in software development
- facilitate reuse of software
- reduce effort for software maintenance
- provide environment for solving large, strongly coupled problems

Figure 26 - Object-oriented finite element code architecture for massively parallel computers

ABSTRACTS AND REFERENCES

References and complete abstracts for selected analysis, preprocessing, postprocessing, translation, and library codes are listed in this section. The abstracts and references for translators are not listed.

Algebra

The Algebra program allows the user to manipulate data from a finite element analysis before it is plotted. The finite element output data is in the form of variable values (e.g., stress, strain, and velocity components) in an EXODUS database. The Algebra program evaluates user-supplied functions of the data and writes the results to an output EXODUS database which can be read by plot programs.

Amy P. Gilkey, "ALGEBRA - A Program that Algebraically Manipulates the Output of a Finite Element Analysis (EXODUS Version)," SAND88-1431, Sandia National Laboratories, Albuquerque, New Mexico, August 1988.

Blot

Blot is a graphics program for postprocessing of finite element analyses output in the EXODUS database format. It is command driven with free-format input and can drive any graphics device supported by the Sandia Virtual Device Interface.

Blot produces mesh plots with various representations of the analysis output variables. The major mesh plot capabilities are deformed mesh plots, line contours, filled (painted) contours, vector plots of two/three variables (e.g., velocity vectors), and symbol plots of scalar variables (e.g., discrete cracks). Pathlines of analysis variables can also be drawn on the mesh. Blot's features include element selection by material, element birth and death, multiple views for combining several displays on each plot, symmetry mirroring, and node and element numbering.

Blot can also produce X-Y curve plots of the analysis variables. Blot generates time-versus-variable plots or variable-versus-variable plots. It also generates distance-versus-variable plots at selected time steps where the distance is the accumulated distance between pairs of nodes or element centers.

Amy P. Gilkey and John H. Glick, "BLOT-A Mesh and Curve Plot Program for the Output of a Finite Element Analysis," SAND88-1432, Sandia National Laboratories, Albuquerque, New Mexico, August 1991.

R. J. Myers, "Updates to the Postprocessing Program BLOT," memo to distribution dated August 21, 1990, Sandia National Laboratories, Albuquerque, New Mexico.

Conchas

CONCHAS is a linear finite element structural analysis code which is specialized for axisymmetric structures. Loads and responses are limited to those symmetric about a plane which includes the symmetric axis of the structure. CONCHAS will perform eigenanalysis, static analysis, and dynamic analysis. The element library includes consistent-mass shell, solid, and beam elements, nonlinear springs, and concentrated masses. Pre- and postprocessing is available with the separately supported utilities BLOT, PATRAN and FASTQ.

William C. Mills-Curran and Dennis P. Flanagan, "CONCHAS Users Manual," SAND88-1006, Sandia National Laboratories, Albuquerque, New Mexico, June 1989.

Exodus and Genesis File Format

William C. Mills-Curran, Amy P. Gilkey and Dennis P. Flanagan, "EXODUS: A Finite Element File Format for Pre- and Postprocessing," SAND87-2977, Sandia National Laboratories, Albuquerque, New Mexico, September 1988.

L. M. Taylor, D. P. Flanagan and W. C. Mills-Curran, "The GENESIS Finite Element Mesh File Format," SAND86-0910, Sandia National Laboratories, Albuquerque, New Mexico, May 1986.

Fastq

The FASTQ code is an interactive two-dimensional finite element mesh generation program. It is designed to provide a powerful and efficient tool to both reduce the time required of an analyst to generate a mesh, and to improve the capacity to generate good meshes in arbitrary geometries. It is based on a mapping technique and employs a set of higher-order primitives which have been developed for automatic meshing of commonly encountered shapes (i.e., the triangle, semi-circle, etc.) and conditions (i.e., mesh transitioning from coarse to fine mesh size). FASTQ has been designed to allow user flexibility and control. The user interface is built on a layered command level structure. Multiple utilities are provided for input, manipulation, and display of the geometric information, as well as for direct control, adjustment, and display of the generated mesh. Enhanced boundary flagging has been incorporated and multiple element types and output formats are supported. FASTQ includes the paving algorithm which meshes arbitrary two-dimensional geometries with an all quadrilateral mesh.

T. D. Blacker, "FASTQ Users Manual, Version 2.1," SAND88-1326, Sandia National Laboratories, Albuquerque, New Mexico, July 1988.

This paper presents a new mesh generation technique, paving, which meshes arbitrary two-dimensional geometries with an all-quadrilateral mesh. Paving allows varying element size distributions on the boundary as well as the interior of a region. The generated mesh is well formed (i.e., nearly square elements, elements perpendicular to boundaries, etc.) and geometrically pleasing (i.e., mesh contours tend to follow geometric contours of the boundary). In this paper we describe the theory behind this algorithmic/heuristic technique, evaluate the performance of the approach and present examples of automatically generated meshes.

T. D. Blacker and M. B. Stephenson, "Paving: A New Approach to Automated Quadrilateral Mesh Generation," *International Journal for Numerical Methods in Engineering*, Vol. 32, 1991, pp. 811-847.

Grope

Grope is a program that examines the input to a finite element analysis (which is in the GENESIS database format) or the output from an analysis (in the EXODUS database format). Grope allows the user to examine any value in the database. The display can be directed to the user's terminal or to a print file.

Amy P. Gilkey, "GROPE - A GENESIS/EXODUS Database Examination Program," RS1523/88/02, Sandia National Laboratories, Albuquerque, New Mexico.

Numbers

Numbers is a program which reads and stores data from a finite element model described in the EXODUS database format. Within this program are several utility routines which generate information about the finite element model. The utilities currently implemented in Numbers allow the analyst to determine information such as (1) the volume and coordinate limits of each of the materials in the model; (2) the mass properties of the model; (3) the minimum, maximum, and average element volumes for each material; (4) the volume and change in volume of a cavity; (5) the nodes or elements that are within a specified distance from a user-defined point, line, or plane; (6) an estimate of the explicit central-difference timestep for each material; (7) the validity of contact surfaces or slidelines; that is, whether two surfaces overlap at any point; and (8) the distance between two surfaces.

G. D. Sjaardema, "NUMBERS: A Collection of Utilities for Pre- and Postprocessing Two- and Three-Dimensional EXODUS Finite Element Models," SAND88-0737, Sandia National Laboratories, Albuquerque, New Mexico, March 1989.

Plastering

This report describes the progress of the three-dimensional mesh generation research, using plastering, during the 1990 fiscal year. Plastering is a three-dimensional extension of the two-dimensional paving technique. The objective is to fill an arbitrary volume with hexahedral elements. The plastering algorithm's approach to the problem is to remove rows of elements from the exterior of the volume. Elements are removed, one level at a time, until the volume vanishes. Special closure algorithms may be necessary at the center. The report also discusses the common development environment and software management issues.

M. B. Stephenson, S. A. Canann and T. D. Blacker, "Plastering: A New Approach to Automated, Three-Dimensional Hexahedral Mesh Generation, Progress Report I," SAND89-2192, Sandia National Laboratories, Albuquerque, New Mexico, February 1992.

Pronto2D and Pronto3D

PRONTO2D is a two-dimensional transient solid dynamics code for analyzing large deformations of highly nonlinear materials subjected to extremely high strain rates. This Lagrangian finite element program uses an explicit time integration operator to integrate the equations of motion. Four node uniform strain quadrilateral elements are used in the finite element formulation. A number of new numerical algorithms which have been developed for the code are described in this report. An adaptive time step control algorithm is described which greatly improves stability as well as performance in plasticity problems. A robust hourglass control scheme which eliminates hourglass distortions without disturbing the finite element solution is included. All constitutive models in PRONTO are cast in an unrotated configuration defined using the rotation determined from the polar decomposition of the deformation gradient. An accurate incremental algorithm was developed to determine this rotation and is described in detail. A robust contact algorithm was developed which allows for the impact and interaction of deforming contact surfaces of quite general geometry. A number of numerical examples are presented to demonstrate the utility of these algorithms.

Lee M. Taylor and Dennis P. Flanagan, "PRONTO2D, A Two-Dimensional Transient Solid Dynamics Program," SAND86-0594, Sandia National Laboratories, Albuquerque, New Mexico, March 1987.

PRONTO3D is a three-dimensional transient solid dynamics code for analyzing large deformations of highly nonlinear materials subjected to extremely high strain rates. This Lagrangian finite element program uses an explicit time integration operator to integrate the equations of motion. Eight-node

uniform strain hexahedral elements are used in the finite element formulation. A number of new numerical algorithms which have been developed for the code are described in this report. An adaptive time step control algorithm is described which greatly improves stability as well as performance in plasticity problems. A robust hourglass control scheme which eliminates hourglass distortions without disturbing the finite element solution is included. All constitutive models in PRONTO are cast in an unrotated configuration defined using the rotation determined from the polar decomposition of the deformation gradient. An accurate incremental algorithm was developed to determine this rotation and is described in detail. A robust contact algorithm was developed which allows for the impact and interaction of deforming contact surfaces of quite general geometry. Numerical examples are presented to demonstrate the utility of these algorithms.

L. M. Taylor and D. P. Flanagan, "PRONTO 3D, A Three-Dimensional Transient Solid Dynamics Program," SAND87-1912, Sandia National Laboratories, Albuquerque, New Mexico, March 1989.

An external code interface is defined which allows other transient applications to communicate with the PRONTO family of finite element programs. This interface is written in ANSI FORTRAN and allows an independent author to specify requirements for an external code to PRONTO. The interface is written such that updates to PRONTO will not require modifications to the external code.

L. M. Taylor and D. P. Flanagan, "An External Code Interface for the PRONTO Family of Transient Solid Dynamics Programs," SAND87-3003, Sandia National Laboratories, Albuquerque, New Mexico, September 1988.

PRONTO 2D and PRONTO 3D are two- and three-dimensional solid dynamics codes for analyzing large deformations of highly nonlinear materials subjected to high strain rates. This newsletter is issued to document changes to these codes. As of this writing, the latest version of PRONTO 2D is Version 4.5.6, and the latest version of PRONTO 3D is Version 4.5.6.

This update of the two codes discusses two major modifications to the numerical formulations, three new constitutive models, and the additions and improvements of contact surfaces. Changes in file formats, other miscellaneous revisions, and the availability of PRONTO 2D and PRONTO 3D are also discussed. In addition, updated commands for PRONTO 2D are provided in Appendix A of this newsletter.

S. W. Attaway, "Update of PRONTO 2D and PRONTO 3D Transient Solid Dynamics Program," SAND90-0102, Sandia National Laboratories, Albuquerque, New Mexico, November 1990.

PRONTO 3D is a three-dimensional transient solid dynamics code for analyzing large deformations of highly nonlinear materials subjected to high strain rates. It is a Lagrangian finite element program with explicit integration of the equations of motion through time. This report documents the implementation of a four-node quadrilateral shell element into Version 6.0 of PRONTO 3D.

This report describes the theory, implementation and use of a four-node shell element. Also described are the required architectural changes made to PRONTO 3D to allow multiple element types. Several test problems are documented for verification of the PRONTO 3D implementation and for demonstration of computational savings using shell elements for thin structures. These problems also serve as examples for the user. A complete, updated list of the PRONTO 3D input commands is also included.

V. L. Bergmann, "Transient Dynamics Analysis of Plates and Shells with PRONTO 3D," SAND91-1182, Sandia National Laboratories, Albuquerque, New Mexico, September 1991.

This update discusses modifications of PRONTO 3D tailored to the design of fast burst nuclear reactors. A thermoelastic constitutive model and spatially variant thermal history load were added for

this special application. Included are descriptions of the thermoelastic constitutive model and the thermal loading algorithm, two example problems used to benchmark the new capability, a user's guide and PRONTO 3D input files for the example programs. The results from PRONTO 3D thermoelastic finite element analysis are benchmarked against measured data and finite difference calculations.

PRONTO 3D is a three-dimensional transient solid dynamics code for analyzing large deformations of highly nonlinear materials subjected to high strain rates. The code modifications are implemented in PRONTO 3D Version 5.3.3.

D. S. Oscar, S. W. Attaway and J. D. Miller, "Modifications of the PRONTO 3D Finite Element Program Tailored to Fast Burst Nuclear Reactor Design," SAND91-0959, Sandia National Laboratories, Albuquerque, New Mexico, August 1991.

Subway 3D

SUBWAY 3D is a three-dimensional finite element code for numerical simulation of the transient electromechanical response of dielectric materials. The code uses a preconditioned conjugate gradient method to solve Poisson's equation governing the electric potential in the dielectrics. This field solver is embedded in a modified version of the finite element transient dynamics code PRONTO 3D and allows solution for the electric response at each time step used in the explicit integration of the equations of motion. The code is structured to allow flexibility in formulation of initial-boundary value problems by permitting specification of electrical conductors and allowing these conductors to be connected to electrical circuits isolated from the mechanical deformations. An algorithm for solution of these initial-boundary value problems is incorporated into the code with special material models to represent the response of ordinary dielectrics and electromechanically active dielectrics like piezoelectric and ferroelectric ceramics. The code has a wide range of applications and, in particular, can be used to calculate responses of shock activated power supplies, impact gages, and the change in electrical capacitance due to deformations.

S. T. Montgomery - documentation not yet available.

Sancho

SANCHO is a finite element computer program designed to compute the quasistatic, large deformation, inelastic response of planar or axisymmetric solids. Finite strain constitutive theories for plasticity, volumetric plasticity, and metallic creep behavior are included. A constant bulk strain, bilinear displacement isoparametric finite element is employed for the spatial discretization. The solution strategy used to generate the sequence of equilibrium solutions is a self-adaptive dynamic relaxation scheme which is based on explicit central difference pseudo-time integration and artificial damping. A master-slave algorithm for sliding interfaces is also implemented. A theoretical development of the appropriate governing equations and a description of the numerical algorithms are presented along with a user's guide which includes several sample problems and their solution.

Charles M. Stone, Raymond D. Krieg and Zelma E. Beisinger, "SANCHO, A Finite Element Computer Program for the Quasistatic, Large Deformation, Inelastic Response of Two-Dimensional Solids," SAND84-2618, Sandia National Laboratories, Albuquerque, New Mexico, April 1985.

Santos and Santos3D

SANTOS is a finite element computer program designed to compute the quasistatic, large deformation, inelastic response of planar or axisymmetric solids. SANTOS is based on the dynamics program PRONTO2D by L. M. Taylor and D. P. Flanagan. SANTOS utilizes a self-adaptive dynamic relaxation algorithm to achieve a quasistatic solution. The efficiency, speed, through vectorization, and state-of-the-art algorithms that Taylor and Flanagan built into PRONTO2D are maintained in SANTOS. The architecture of the code as well as the user interface is similar for both codes which improves code reliability and encourages the use of both codes by analysts. By utilizing the same material interface, the same constitutive models may be utilized by both codes which allows for coupling of the two codes.

C. M. Stone - documentation not yet available.

Jac2D, Jac3D and Jacq3D

The nonlinear conjugate gradient procedure is employed in the computer program JAC2D to solve quasi-static nonlinear mechanics problems. A set of continuum equations which describe accurately nonlinear mechanics involving large rotation and strain are very conveniently used with the conjugate gradient method to solve the nonlinear problem. The method is exploited in a two-dimensional setting while using various methods for accelerating convergence. Sliding interface conditions are also implemented. A four-node Lagrangian uniform strain element is used with hourglass stiffness to control the zero energy modes. Materials which can be modeled are elastic and isothermal elastic-plastic with combined kinematic and isotropic hardening. The program is vectorized to perform very efficiently on CRAY computers. Sample problems described are the bending of a thin beam, the rotation of a unit cube, and a pressurized and thermally-loaded sphere and cylinder.

J. H. Biffle, "A Two-Dimensional Finite Element Computer Program for the Nonlinear Quasistatic Response of Solids with the Conjugate Gradient Method," SAND81-0998, Sandia National Laboratories, Albuquerque, New Mexico, April 1984.

JAC3D is a three-dimensional finite element program designed to solve quasi-static nonlinear mechanics problems. A set of continuum equations, which describe nonlinear mechanics involving large rotation and strain, is used. A nonlinear conjugate gradient method is used to solve the nonlinear equations. The method is implemented in a three-dimensional setting with various methods for accelerating convergence. Sliding interface conditions are also implemented. An eight-node Lagrangian uniform strain element is used with hourglass stiffness to control the zero energy modes. This release of the code contains elastic and isothermal elastic-plastic material models. Other material models can be added relatively easily. The program is vectorized to perform very efficiently on CRAY computers. Sample problems described are the bending of a thin beam, the rotation of a unit cube, and a pressurized and thermally loaded sphere.

J. H. Biffle, "JAC3D - A Three-Dimensional Finite Element Computer Program for the Nonlinear Quasistatic Response of Solids with the Conjugate Gradient Method," in preparation.

The nonlinear conjugate gradient procedure is employed in the computer program JAC3D to solve the steady-state and transient nonlinear heat conduction problem for solids in three dimensions. The program can also be used for other types of diffusion problems. The problem is formulated with the finite element method and employs an eight-node uniform gradient element with hourglass stiffness to control the zero energy modes. JACQ3D is highly vectorized to perform efficiently on the CRAY computer. Sample problems are included to verify the code and to provide examples of the use of the code.

J. H. Biffle, "JAC3D - A Three-Dimensional Finite Element Computer Program for Nonlinear Heat Conduction Problems with the Conjugate Gradient Method," in preparation.

Merlin II

The MERLIN II program is designed to transfer data between finite element meshes of arbitrary geometry. The program is structured to accurately interpolate previously computed solutions onto a given mesh and format the resulting data for immediate use in another analysis program. Data from either two-dimensional or three-dimensional meshes may be considered. The theoretical basis and computational algorithms used in the program are described and complete user instructions are presented. Several example problems are included to demonstrate program usage.

D. K. Gartling, "MERLIN II - A Computer Program to Transfer Solution Data Between Finite Element Meshes," SAND89-2989, Sandia National Laboratories, Albuquerque, New Mexico, July 1991.

Supes Library

The Software Utilities Package for the Engineering Sciences (SUPES) is a collection of subprograms which perform frequently used non-numerical services for the engineering applications programmer. The three functional categories of SUPES are: (1) input command parsing, (2) dynamic memory management, and (3) system dependent utilities. The subprograms in categories one and two are written in standard FORTRAN-77, while the subprograms in category three are written to provide a standardized FORTRAN interface to several system dependent features.

J. H. Red-Horse, W. C. Mills-Curran and D. P. Flanagan, "SUPES Version 2.1, A Software Utilities Package for the Engineering Sciences," SAND90-0247, Sandia National Laboratories, Albuquerque, New Mexico, May 1990.

Gen3D

GEN3D is a three-dimensional mesh generation program. The three-dimensional mesh is generated by mapping a two-dimensional mesh into three-dimensions according to one of four types of transformations: translating, rotating, mapping onto a spherical surface, and mapping onto a cylindrical surface. The generated three-dimensional mesh can then be reoriented by offsetting, reflecting about an axis, and revolving about an axis. GEN3D can be used to mesh geometries that are axisymmetric or planar, but, due to three-dimensional loading or boundary conditions, require a three-dimensional finite element mesh and analysis. More importantly, it can be used to mesh complex three-dimensional geometries composed of several sections when the sections can be defined in terms of transformations of two-dimensional geometries. The code GJOIN is then used to join the separate sections into a single body. GEN3D reads and writes two-dimensional and three-dimensional mesh databases in the GENESIS database format; therefore, it is compatible with the preprocessing, postprocessing, and analysis codes used by the Engineering Analysis Department at Sandia National Laboratories, Albuquerque, New Mexico.

Amy P. Gilkey and Gregory D. Sjaardema, "GEN3D: A GENESIS Database 2D to 3D Transformation Program," SAND89-0485, Sandia National Laboratories, Albuquerque, New Mexico, March 1989.

This memo describes the changes that have been made to the GEN3D program since the manual (SAND89-0485) was published. The changes include: (1) new mesh generation options: spline, project, twist, interval, and rotcen transformations; (2) new mesh modification options: change

J. H. Biffle, "JAC3D - A Three-Dimensional Finite Element Computer Program for Nonlinear Heat Conduction Problems with the Conjugate Gradient Method," in preparation.

Merlin II

The MERLIN II program is designed to transfer data between finite element meshes of arbitrary geometry. The program is structured to accurately interpolate previously computed solutions onto a given mesh and format the resulting data for immediate use in another analysis program. Data from either two-dimensional or three-dimensional meshes may be considered. The theoretical basis and computational algorithms used in the program are described and complete user instructions are presented. Several example problems are included to demonstrate program usage.

D. K. Gartling, "MERLIN II - A Computer Program to Transfer Solution Data Between Finite Element Meshes," SAND89-2989, Sandia National Laboratories, Albuquerque, New Mexico, July 1991.

Supes Library

The Software Utilities Package for the Engineering Sciences (SUPES) is a collection of subprograms which perform frequently used non-numerical services for the engineering applications programmer. The three functional categories of SUPES are: (1) input command parsing, (2) dynamic memory management, and (3) system dependent utilities. The subprograms in categories one and two are written in standard FORTRAN-77, while the subprograms in category three are written to provide a standardized FORTRAN interface to several system dependent features.

J. H. Red-Horse, W. C. Mills-Curran and D. P. Flanagan, "SUPES Version 2.1, A Software Utilities Package for the Engineering Sciences," SAND90-0247, Sandia National Laboratories, Albuquerque, New Mexico, May 1990.

Gen3D

GEN3D is a three-dimensional mesh generation program. The three-dimensional mesh is generated by mapping a two-dimensional mesh into three-dimensions according to one of four types of transformations: translating, rotating, mapping onto a spherical surface, and mapping onto a cylindrical surface. The generated three-dimensional mesh can then be reoriented by offsetting, reflecting about an axis, and revolving about an axis. GEN3D can be used to mesh geometries that are axisymmetric or planar, but, due to three-dimensional loading or boundary conditions, require a three-dimensional finite element mesh and analysis. More importantly, it can be used to mesh complex three-dimensional geometries composed of several sections when the sections can be defined in terms of transformations of two-dimensional geometries. The code GJOIN is then used to join the separate sections into a single body. GEN3D reads and writes two-dimensional and three-dimensional mesh databases in the GENESIS database format; therefore, it is compatible with the preprocessing, postprocessing, and analysis codes used by the Engineering Analysis Department at Sandia National Laboratories, Albuquerque, New Mexico.

Amy P. Gilkey and Gregory D. Sjaardema, "GEN3D: A GENESIS Database 2D to 3D Transformation Program," SAND89-0485, Sandia National Laboratories, Albuquerque, New Mexico, March 1989.

This memo describes the changes that have been made to the GEN3D program since the manual (SAND89-0485) was published. The changes include: (1) new mesh generation options: spline, project, twist, interval, and rotcen transformations; (2) new mesh modification options: change

material, change sideset, and change nodeset; (3) new mesh orientation option: scale; and (4) miscellaneous changes.

G. D. Sjaardema, "Updates to the mesh generation program GEN3D," memo to distribution dated April 11, 1990, Sandia National Laboratories, Albuquerque, New Mexico.

Gjoin

Gjoin is a computer program which is used to merge two or more GENESIS databases into a single GENESIS database.

G. D. Sjaardema, "GJOIN: A Program for Merging Two or More GENESIS Databases," (memo to distribution dated June 19, 1991), Sandia National Laboratories, Albuquerque, New Mexico.

Grepas

GREPOS is a mesh utility program that repositions or modifies the configuration of a 2D or 3D mesh. Grepas can be used to change the orientation and size of a 2D or 3D mesh; change the material block, nodeset, and sideset IDs; or "explode" the mesh to facilitate viewing of the various parts of the model. Grepas also updates the EXODUS QA and information records to help track the codes and files used to generate the mesh. GREPOS reads and writes 2D and 3D mesh databases in the GENESIS database format; therefore, it is compatible with the preprocessing, postprocessing, and analysis codes in SEACAS.

G. D. Sjaardema, "GREPOS: A GENESIS Database Repositioning Program," SAND90-0566, Sandia National Laboratories, Albuquerque, New Mexico, April 1990.

Aprepro

APREPRO is a translator that reads a text file containing both general text and algebraic expressions. It echoes the general text to the output file, along with the results of the algebraic expressions. The syntax used in APREPRO is such that all expressions between the delimiters '{' and '}' are evaluated and all other text is simply echoed to the output file.

G. D. Sjaardema, "Aprepro: An Algebraic Preprocessor for Input Files," memo to distributed dated May 18, 1990, Sandia National Laboratories, Albuquerque, New Mexico.

The initial implementation of a units conversion capability in Aprepro has been completed. The units conversion is a very useful capability for analysts and it is required for the implementation of the MATS material database system.

G. D. Sjaardema, "Implementation of Units Conversion in Aprepro," memo to distribution dated April 24, 1992, Sandia National Laboratories, Albuquerque, New Mexico.

Constitutive Models

B. J. Thorne, "A Damage Model for Rock Fragmentation and Comparison of Calculations with Blasting Experiments in Granite," SAND90-1389, Sandia National Laboratories, Albuquerque, New Mexico, October 1990.

E. P. Chen, "A Computational Model for Jointed Media with Orthogonal Sets of Joints," SAND86-1122, Sandia National Laboratories, Albuquerque, New Mexico, March 1987.

M. K. Neilsen, H. S. Morgan, R. D. Krieg, "A Phenomenological Constitutive Model for Low Density Polyurethane Foams," SAND86-2927, Sandia National Laboratories, Albuquerque, New Mexico, April 1987.

R. S. Chambers, "A Viscoelastic Material Model for Computing Stresses in Glass," SAND90-0645, Sandia National Laboratories, Albuquerque, New Mexico, July 1990.

G. D. Sjaardema and R. D. Krieg, "A Constitutive Model for the Consolidation of WIPP Crushed Salt and Its Use in Analyses of Backfilled Shaft and Drift Configurations," SAND87-1977, Sandia National Laboratories, Albuquerque, New Mexico, October 1987.

C. M. Stone, G. W. Wellman and R. D. Krieg, "A Vectorized Elastic/Plastic Power Law Hardening Material Model Including Luders Strain," SAND90-0153, Sandia National Laboratories, Albuquerque, New Mexico, March 1990.

J. R. Weatherby, R. D. Krieg and C. M. Stone, "Incorporation of Surface Tension into the Structural Finite Element Code SANCHO," SAND89-0509, Sandia National Laboratories, Albuquerque, New Mexico, March 1989.

S. W. Attaway, "A Local Isotropic/Global Orthotropic Finite Element Technique for Modeling the Crush of Wood," SAND88-1449, Sandia National Laboratories, Albuquerque, New Mexico, September 1988.

R. D. Krieg, "A Simple Constitutive Description for Soils and Crushable Foams," SC-DR-72-0883, Sandia National Laboratories, Albuquerque, New Mexico, 1987.

D. J. Bammann, "An Internal Variable Model of Viscoplasticity," International Journal of Engineering Science, Vol. 22, 1984, pp. 1041-1053.

OMIT
TO
END

**LIST OF BOOKS, MONOGRAPHS, SPECIAL ISSUES OF JOURNALS,
SURVEY PAPERS AND REPORTS ON
COMPUTATIONAL TECHNIQUES FOR SIMULATING CRASH**

Howard S. Levine
Weidlinger Associates, Los Altos, CA
and
Ahmed K. Noor
University of Virginia, Hampton, VA

Several books, monographs, conference proceedings and research reports have been published on the subject of crash dynamics. For the benefit of the readers of the proceedings, all the literature known to the compilers is listed subsequently. The literature is divided into five categories: books, monographs and special issues of journals; survey papers; reports; research papers; and commercial software systems. The references within each category are listed alphabetically.

I. Books, Monographs and Special Issues of Journals

1. Davies, G. A. O., ed.: *Proceedings of the International Conference on Structural Impact and Crashworthiness*. vol. 1, Keynote Lectures, Elsevier, London, 1984.
2. International Symposium on Structural Crashworthiness and Failure. Special issue of *International Journal of Mechanical Sciences*, Vol. 35, Nos. 3/4, 1993.
3. Johnson, W.; and Mamalis, A. G., eds.: *Crashworthiness of Vehicles*. Mechanical Engineering Publications, Ltd., London, 1978.
4. Jones, N.; and Wierzbicki, T., eds.: *Structural Crashworthiness*. Butterworths, London, 1983.
5. Jones, N., ed.: *Structural Failure Symposium, June 6-8, 1988*. Int. J. Impact Eng., special issue, vol. 7, no. 2, 1988.
6. Jones, N., ed.: Symposium on Structural Crashworthiness and Failure. Special issue of *International Journal of Impact Engineering*, Vol. 13, No. 2, May 1993.
7. Jones, N.; and Wierzbicki, T., eds.: *Structural Crashworthiness and Failure*. Elsevier Science Publishers, London, 1993.
8. Khalil, T. B.; Ne, C. M.; Mahmood, H. F.; and King, A. I., eds.: *Crashworthiness and Occupant Protection in Transportation Systems - 1991*. AMD Vol. 126/BED Vol. 19, ASME Winter Annual Meeting, Atlanta, GA, 1991.
9. King, A.; and Khalil, T., eds.: *Crashworthiness and Occupant Protection*. AMD Vol. 106, BED Vol. 13, American Society of Mechanical Engineers, NY, 1989.
10. Macauley, M.: *Introduction to Impact Engineering*. Chapman & Hall, London, 1987.
11. Morton, J., ed.: *Proceedings of the International Conference on Structural Impact and Crashworthiness*. vol. 2, Conference Papers, Elsevier, London, 1984.
12. Reid, S. R., ed.: *Structural Failure Symposium, June 6-8, 1988*, Int. J. Mech. Sci., special issue, vol. 30, nos. 3/4, 1988.
13. Sabir, A. B.; and Niku-Lari, A., eds.: *CRASH-93: Numerical Methods in Crash Simulation*. IITT International, Gournay-sur-Marne, France.

250
INTENTIONALLY BLANK

14. Saczalski, K.: *Aircraft Crashworthiness*. Univ. Press of Virginia, Charlottesville, VA, 1975.
15. Schwer, L. E.; Salamon, L. E.; and Liu, W., eds.: *Computational Techniques for Contact, Impact, Penetration and Perforation of Solids*. AMD Vol. 103, ASME Winter Annual Meeting, San Francisco, CA, Dec. 10-15, 1989, American Society of Mechanical Engineers, NY, 1989.
16. Tong, P., Ni, C. M., King, A. and Lantz, S., eds.: *Symposium on Vehicle Crashworthiness Including Impact Biomechanics*. AMD Vol. 79, BED Vol. 1, American Society of Mechanical Engineers, NY, 1986.
17. Wierzbicki, T.; and Jones, N., eds.: *Structural Failures*. John Wiley & Sons, NY, 1989.

II. Survey Papers

1. Anderson, C. E.; and Bodner, S. R.: The Status of Ballistic Impact Modeling. *Int. J. Impact Eng.*, vol. 7, 1988, pp. 9-35.
2. Belytschko, T.: On Computational Methods for Crashworthiness. *Comput. & Struct.*, vol. 42, no. 2, 1992, pp. 271-279.
3. Campbell, G. S.; and Lahey, R. T. C.: *A Survey of Serious Aircraft Accidents Involving Fatigue Fracture. vol. 2. Rotary-Wing Aircraft*. National Aeronautical Establishment, Ottawa, Ontario, NRC 21277, April 1983. (See also vol. 1, AD-A137-254.)
4. Campbell, G. S. and Lahey, R. T. C.: *A Survey of Serious Aircraft Accidents Involving Fatigue Fracture. Vol. 1. Fixed-Wing Aircraft*. National Aeronautical Establishment, Ottawa, Ontario, NRC 21276, April 1983. (See also vol. 2, AD-A137-255.)
5. Carden, H. D.: *Impact Dynamics Research on Composite Transport Structures*. NASA TM-83691, March 1985.
6. Dallard, P. R. B.; and Miles, J. C.: Design Tools for Impact Engineers. *Proceedings of the International Conference on Structural Impact and Crashworthiness*. G. A. O. Davies, ed., vol. 1, 1984, pp. 369-382.
7. Farley, G. L.; Boitnott, R. L.; and Carden, H. D.: *Helicopter Crashworthiness Research Program*. NASA CP-2495, 1987.
8. Fasanella, E. L.; Carden, H. D.; Boitnott, R. L.; and Hayduk, R. J.: *A Review of the Analytical Simulation of Aircraft Crash Dynamics*. NASA TM-102595, Jan. 1990.
9. Hayduk, R. J.; Thomson, R. G.; and Carden, H. D.: NASA/FAA General Aviation Crash Dynamics Program - An Update. *Forum*, vol. 12, no. 3, 1979, pp. 147-156.
10. Hayduk, R. J.; Carden, H. D.; Fasanella, E. L.; and Boitnott, R. L.: Status of Analytical Simulation of Aircraft Crash Dynamics. *66th AGARD Structures and Materials Panel Meeting*, Luxembourg, May 1988.
11. Huculak, P.: A Review of Research and Development in Crashworthiness of General Aviation Aircraft: Seats, Restraints and Floor Structures. Aeronautical Note NAE-AN-64. NRC No. 31334, Ottawa, National Research Council of Canada, Feb. 1990.

12. Hui, D.; and Jones, N.: *Recent Advances in Impact Dynamics of Engineering Structures - 1989*. Winter Annual Meeting, American Society of Mechanical Engineers, Dec. 10-15, 1989, San Francisco, CA, AMD-vol. 105, AD-vol. 17, ASME, NY, 1989.
13. Jarzab, W.; and Schwarz, R.: Crashworthiness of Aircraft Structures (U). Advisory Group for Aerospace Research and Development, Neuilly-Sur-Seine, France. Conference Proceedings of Energy Absorption of Aircraft Structures as an Aspect of Crashworthiness (66th), Luxembourg, May 1-6, 1988. Report AD-A212-606, Dec. 1988, pp. 17.1-17.13.
14. McComb, Jr., H.; Thomson, R. G.; and Hayduk, R. J.: Structural Dynamics Research in a Full-Scale Transport Aircraft Crash Test. *J. Aircraft*, vol. 24, no. 7, July 1987.
15. Poon, C.: A Review of Crashworthiness of Composite Aircraft Structures. Aeronautical Note NAE-AN-63. NRC No. 31276, Ottawa, National Research Council of Canada, Feb. 1990.
16. Saczalski, K. J.; Singley III, G. T.; Pilkey, W. D.; and Huston, R. L.: *Aircraft Crashworthiness*. University Press of Virginia, Charlottesville, VA, 1975.
17. Thomson, R. G.; and Goetz, R. C.: NASA/FAA General Aviation Crash Dynamics Program - A Status Report. *J. Aircraft*, vol. 17, no. 8, Aug. 1980, p. 584.
18. Thomson, R. G.; Carden, H. D.; and Hayduk, R. J.: *Survey of NASA Research on Crash Dynamics*. NASA TP-2298, April 1984.
19. Thomson, R. G.; Carden, H. D.; and Hayduk, R. J.: *Research at NASA on Crash Dynamics, Structural Impact and Crashworthiness*. vol. 1, Keynote Lectures, G. A. O. Davies, ed., Elsevier Applied Science Publishers, London, July 1984, pp. 1-43.
20. Thornton, P. M.; Mahmood, H. F.; and Magee, C. L.: Energy Absorption by Structural Collapse. *Proc. of the International Conference on Structural Impact and Crashworthiness*, G. A. O. Davies, ed., vol. 1, 1984, pp. 96-117.
21. Widmayer, E.: A Structural Survey of Classes of Vehicles for Crashworthiness. Boeing Vertol Co. Report No. FRA/ORD-79-13, U.S. Dept. of Transportation, 1979.
22. Wittlin, G.; and Gamon, M. A.: A Literature Survey of Airborne Vehicles Impacting with Water and Soil; Head Injury Criteria and Severity Index Development of Computer Program KRASH. DOT/FAA/CT-90/24, July 1992.

III. Reports

1. *A Study of U.S. Air Carrier Accidents 1964-1969*. NTSB Report No. PB-211-054, 1972.
2. Advisory Group for Aerospace Research and Development, Neuilly-Sur-Seine, France. Conference Proceedings of Energy Absorption of Aircraft Structures as an Aspect Crashworthiness (66th) held in Luxembourg, May 1-6, 1988 (U). Report AGARD-CP-443.
3. Advisory Group for Aerospace Research and Development, Neuilly-Sur-Seine, France. Crashworthiness of Airframes (U). Presented at the 61st Meeting of the Structures and Materials Panel of AGARD, Oberammergau, Germany, Sept. 8-13, 1985.
4. Ahlers, R. H.: Full-Scale Aircraft Crash Tests of Modified Jet Fuel. U.S. Dept. of Transportation, Federal Aviation Administration, Systems Research and Development Service. Final Report No. FAA-RD-77-13, covering period July 1972-May 1974; July 1977.

33. Johnson, D.; and Garodz, L.: Crashworthiness Experiment Summary - Full-Scale Transport Controlled Impact Demonstration Program (U). Federal Aviation Administration Technical Center, Atlantic City, NJ. Final Report for June 1981-Dec. 1985, DOT/FAA/CT-85/20, June 1986.
34. Johnson, N. B.; Robertson, S. H.; and Hall, D.S.: Aircraft Crash Survival Design Guide, vol. 5, Aircraft Postcrash Survival (U). Simula, Inc., Phoenix, AZ, Final Report, Sept. 1986-Aug. 1989, DTIC, USAAVSCOM, TR-89-D-22E, Dec. 1989. (See also vol. 1, AD-A218-434, Revision of Aircraft Crash Survival Design Guide, 1980, vol. 5, AD-A082-513.)
35. Johnson, R.; and Wade, B.: Longitudinal Impact Test of a Transport Airframe Section. Federal Aviation Administration Technical Center, Atlantic City, NJ. Final Report, Feb.-Oct. 1987, DOT/FAA/CT-87/26, July 1988.
36. Kevlin, S. G.: Full-Scale Crash Tests of A-3 and RB-66 Aircraft Conducted for the FAA to Evaluate Use of Gelled Fuel. Dept. of the Navy, Naval Air Test Facility, Lakehurst, NJ. NAVAIRTESTFAC Letter Report No. NATF-R136, Aug. 1973.
37. Kot, C. A.; Lin, H. C.; van Erp, J. B.; Eichler, T. V.; and Wiedermann: Evaluation of Aircraft Crash Hazards Analyses for Nuclear Power Plants. Nuclear Regulatory Commission, Washington, D.C. NUREG/CR-2859, June 1982.
38. Laananen, D., et al: Computer Simulation of an Aircraft Seat and Occupant in a Crash Environment. Vol. I - Technical Report. Vol. II - Program SOM-LA User's Manual. DOT/FAA/CT-82/33-1 and 33-11, March 1983.
39. Laananen, D. H.: Computer Simulation of an Aircraft Seat and Occupant(s) in a Crash Environment - Program SOM-LA/SOM-TA (User Manual) (U). Arizona State University, Tempe Dept. of Mechanical and Aerospace Engineering. Final Report No. CR-R-90026, July 1989-Feb. 1990, DOT/FAA/CT, XF; 90/4, DOT/FAA/CT, May 1991.
40. Lindsey, G. D.: Analysis of FY79 Army Aircraft Accidents. Army Safety Center, Fort Rucker, AL. Technical Report USASC-TR-80-2, April 1980.
41. Lucha, G. B.; Robertson, M. A.; and Schooley, F. A.: *An Analysis of Aircraft Accidents Involving Fires*. Stanford Research Institute for Ames Research Center. NASA CR-137690, May 1975.
42. McGuire, R.; Nissley, W.; and Wilson, A.: Drop Test -- Cessna Golden Eagle 421B (U). Federal Aviation Administration Technical Center, Atlantic City, NJ. Technical Note, Feb.-Nov. 1990, U.S. Department of Transportation, DOT/FAA/CT-TN91/32, May 1992.
43. Mikkola, M.; and Tuomala, M.: Mechanics of Impact Energy Absorption. Dept. of Structural Engineering, Helsinki University of Technology. Julkaisu Report 104, Espoo 1989.
44. Military Standard, System Safety Program Requirements. Depart. of Defense, reproduced by NTIS, U.S. Department of Commerce, MIL-STD-882B, March 30, 1984, superseding MIL-STD-882A, June 28, 1977, AMSC No. F3329, FSC SAFT, 98 pp., March 30, 1984.
45. Muehlbauer, J. C.; Bronn, C. E.; and Sturgeon, R. F.: Large Military Aircraft Accident Statistics and Analysis. Lockheed-Georgia Company, Nov. 1971.

12. Hui, D.; and Jones, N.: *Recent Advances in Impact Dynamics of Engineering Structures - 1989*. Winter Annual Meeting, American Society of Mechanical Engineers, Dec. 10-15, 1989, San Francisco, CA, AMD-vol. 105, AD-vol. 17, ASME, NY, 1989.
13. Jarzab, W.; and Schwarz, R.: *Crashworthiness of Aircraft Structures (U)*. Advisory Group for Aerospace Research and Development, Neuilly-Sur-Seine, France. Conference Proceedings of Energy Absorption of Aircraft Structures as an Aspect of Crashworthiness (66th), Luxembourg, May 1-6, 1988. Report AD-A212-606, Dec. 1988, pp. 17.1-17.13.
14. McComb, Jr., H.; Thomson, R. G.; and Hayduk, R. J.: Structural Dynamics Research in a Full-Scale Transport Aircraft Crash Test. *J. Aircraft*, vol. 24, no. 7, July 1987.
15. Poon, C.: A Review of Crashworthiness of Composite Aircraft Structures. Aeronautical Note NAE-AN-63. NRC No. 31276, Ottawa, National Research Council of Canada, Feb. 1990.
16. Saczalski, K. J.; Singley III, G. T.; Pilkey, W. D.; and Huston, R. L.: *Aircraft Crashworthiness*. University Press of Virginia, Charlottesville, VA, 1975.
17. Thomson, R. G.; and Goetz, R. C.: NASA/FAA General Aviation Crash Dynamics Program - A Status Report. *J. Aircraft*, vol. 17, no. 8, Aug. 1980, p. 584.
18. Thomson, R. G.; Carden, H. D.; and Hayduk, R. J.: *Survey of NASA Research on Crash Dynamics*. NASA TP-2298, April 1984.
19. Thomson, R. G.; Carden, H. D.; and Hayduk, R. J.: *Research at NASA on Crash Dynamics, Structural Impact and Crashworthiness*. vol. 1, Keynote Lectures, G. A. O. Davies, ed., Elsevier Applied Science Publishers, London, July 1984, pp. 1-43.
20. Thornton, P. M.; Mahmood, H. F.; and Magee, C. L.: Energy Absorption by Structural Collapse. *Proc. of the International Conference on Structural Impact and Crashworthiness*, G. A. O. Davies, ed., vol. 1, 1984, pp. 96-117.
21. Widmayer, E.: A Structural Survey of Classes of Vehicles for Crashworthiness. Boeing Vertol Co. Report No. FRA/ORD-79-13, U.S. Dept. of Transportation, 1979.
22. Wittlin, G.; and Gamon, M. A.: A Literature Survey of Airborne Vehicles Impacting with Water and Soil; Head Injury Criteria and Severity Index Development of Computer Program KRASH. DOT/FAA/CT-90/24, July 1992.

III. Reports

1. *A Study of U.S. Air Carrier Accidents 1964-1969*. NTSB Report No. PB-211-054, 1972.
2. Advisory Group for Aerospace Research and Development, Neuilly-Sur-Seine, France. Conference Proceedings of Energy Absorption of Aircraft Structures as an Aspect Crashworthiness (66th) held in Luxembourg, May 1-6, 1988 (U). Report AGARD-CP-443.
3. Advisory Group for Aerospace Research and Development, Neuilly-Sur-Seine, France. *Crashworthiness of Airframes (U)*. Presented at the 61st Meeting of the Structures and Materials Panel of AGARD, Oberammergau, Germany, Sept. 8-13, 1985.
4. Ahlers, R. H.: Full-Scale Aircraft Crash Tests of Modified Jet Fuel. U.S. Dept. of Transportation, Federal Aviation Administration, Systems Research and Development Service. Final Report No. FAA-RD-77-13, covering period July 1972-May 1974; July 1977.

5. Badrinath, Y.: Simulation, Correlation and Analysis of the Structural Response of a CH-47A to Crash Impact. USARTL-TR-78-24, Aug. 1978.
6. Bark, L.; Lou, K.: Comparison of SOM-LA and ATB Programs for Prediction of Occupant Motions in Energy Absorbing Seating Systems. TR-91020, American Helicopter Society, May 1991.
7. Berry, V.; Cronkhite, J.: YAH-63 Helicopter Crashworthiness Simulation and Analysis. USAAVRADCOM-TR-82-D-34, Feb. 1983.
8. Burrows, L.; Lane, R.; and McElhenny, J.: CH-47 Crash Test (T-40) Structural, Cargo Restraint, and Aircrew Inflatable Restraint Experiments. USARTL-TR-78-22, April 1978.
9. Cannon, M. R.; and Zimmermann, R. E.: Seat Experiments for the Full-Scale Transport Aircraft Controlled Impact Demonstration. RMS Technologies, Inc., Trevese, PA. Final Report DOT/FAA/CT 84/10, March 1985.
10. Cannon, M. R.; and Zimmermann, R. E.: Crash Dynamics Program Transport Seat Performance and Cost Study Benefit Study (U). RMS Technologies, Inc., Trevese, PA. Final Report for March 1984-Oct. 1985. Report No. TR-85433, DOT/FAA/CT 85/36, Oct. 1986.
11. Cannon, M. R.; and Zimmermann, R. E.: Seat Experiment Results of Full-Scale Transport Aircraft Controlled Impact Demonstration (U). RMS Technologies, Inc., Trevese, PA. Final Report for Jan.-July 1985, Report No. TR-85413, DOT/FAA/CT 85/25, July 1986. (See also AD-A155 024.)
12. Clarke, R. K.; Foley, J. T.; Hartman, W. F.; and Larson, D. W.: Accident Environments Expected in Air Force C-5, C-141 and C-130 Aircraft Accidents. Sandia Report SAND-75-0231, Aug. 1975.
13. Clarke, R. K.; Foley, J. T.; Hartman, W. F.; and Larson, D. W.: Severities of Transportation Accidents - vol. I, Summary and Vol. II, Cargo Aircraft. Sandia Laboratories, Sandia Report SLA-74-0001, vols. I and II, Sept. 1976.
14. Coltman, J. W.: Development of Categorized Crashworthiness Design Criteria for U.S. Army Aircraft (U). Final Report. Simula, Inc., Phoenix, AZ, USAAVSCOM TR-89-D-16, May 1990.
15. Coltman, J. W.; Van Ingen, C.; Johnson, N. B.; and Zimmerman, R. E.: Aircraft Crash Survival Design Guide, vol. II, Aircraft Design Crash Impact Conditions and Human Tolerance: Vol. II of five volume report. Defense Technical Information Center. USAAVSCOM TR-89-D-22B, Aircraft Crash Survival Design Guide, Dec. 1989.
16. Cominsky, A.: *Transport Aircraft Accident Dynamics*. Douglas Aircraft Company, Long Beach, CA, Final Report for Feb. 1980-March 1982. NASA CR-165850, FAA-RD-74-12, March 1982.
17. Cronkhite, J., et al: Investigation of the Crash Impact Characteristics of Advanced Airframe Structures. USARTL-TR-79-11, Sept. 1979.
18. Cronkhite, J.; Berry, V.: Investigation of the Crash Impact Characteristics of Helicopter Composite Structures. USAAVRADCOM-TR-82-D-14, Feb. 1983.

19. Cronkhite, J., et al: Crashworthy Composite Structures. USAAVSCOM TR-87-D-10, Dec. 1987.
20. Del Gandio, F.: Full-Scale Transport Controlled Impact Demonstration Program - Aircraft Accident Investigation Experiment and Report of Investigation. U.S. Dept. of Transportation. DOT/FAA/ASF-86-001, Dec. 1984.
21. Desjardins, S. P.; Laananen, D. H.; and Singley, G. T., III: Aircraft Crash Survival Design Guide. Vol. I - Design Criteria and Check Lists. Report USARTL-TR-79-22A. Applied Technology Lab., U.S. Army Research and Technology Labs. (AVRADCOM), Ft. Eustis, VA 23604, Dec. 1980.
22. Desjardins, S. P.; Zimmerman, R. E.; Bolukbasi, A. O.; and Merritt, N. A.: Aircraft Crash Survival Design Guide, vol. 4, Aircraft Seats, Restraints, Litters, and Cockpit/Cabin Delethalization (U). Simula, Inc., Phoenix, AZ. Final Report for Sept. 1986-Aug. 1989. USAAVSCOM, TR-89-D-22D, Dec. 1989.
23. Desjardins, S. P., et al: Aircraft Crash Survival Design Guide. USAAVSCOM TR-89-D-22A through E, 5 volumes, Dec. 1989.
24. Finnegan, P. M.; Puthoff, R. L.; and Turnbow, J. W.: *Preliminary Impact Speed and Angle Criteria for Design of a Nuclear Airplane Fission Product Containment Vessel*. NASA TM X-2245, May 1971.
25. Fitzgibbon, D. P.: Crash Loads Environment Study. Federal Aviation Administration Report, Feb. 1967.
26. Flight Safety Foundation, Inc., Arlington, VA: International Aircraft Occupant Safety Conference and Workshop, Arlington, VA, Oct. 31-Nov. 3, 1988 (U). Final Report, Proceedings containing formal conference presentations and summaries of informal workshop discussions. DOT/FAA/OV 89-2, Nov. 1988.
27. Gatlin, C., et al: Analysis of Helicopter Structural Crashworthiness. Vol. I - Mathematical Simulation and Experimentation Verification for Helicopter Crashworthiness. Vol. II - User's Manual for "Crash," A Computer Program for the Response of a Spring-Mass System Subjected to One-Dimensional Impact Loading (UH-1D/H Helicopter Application), USAAVLABS TR 70-71A and 71B, Jan. 1971.
28. Gowdy, V.: Development of a Crashworthy Seat for Commuter Aircraft (U). Federal Aviation Administration, Washington, D.C., Office of Aviation Medicine. Final Report DOT/FAA/AM-90/11, Sept. 1990.
29. Greer, D. L.: Design Study and Model Structures Test Program to Improve Fuselage Crashworthiness. General Dynamics/Convair, FAA Technical Report DS-67-20, Oct. 1967.
30. Greer, D. L.; Breedon, J. S.; and Heid, T. L.: Crashworthy Design Principles. Federal Aviation Administration Report No. ADS-24, Sept. 1964.
31. Haley, J. L.; Turnbow, J. W.; and Walhout, G. J.: Floor Accelerations and Passenger Injuries in Transport Accidents. U.S. Army Aviation Materials Laboratory Technical Report 67-16, May 1967.
32. Hayduk, R. J.; Thomson, R. G.; Wittlin, G.; and Kamat, M. P.: Nonlinear Structural Crash Dynamics Analyses. SAE Paper 790588, April 1979.

33. Johnson, D.; and Garodz, L.: Crashworthiness Experiment Summary - Full-Scale Transport Controlled Impact Demonstration Program (U). Federal Aviation Administration Technical Center, Atlantic City, NJ. Final Report for June 1981-Dec. 1985, DOT/FAA/CT-85/20, June 1986.
34. Johnson, N. B.; Robertson, S. H.; and Hall, D.S.: Aircraft Crash Survival Design Guide, vol. 5, Aircraft Postcrash Survival (U). Simula, Inc., Phoenix, AZ, Final Report, Sept. 1986-Aug. 1989, DTIC, USAAVSCOM, TR-89-D-22E, Dec. 1989. (See also vol. 1, AD-A218-434, Revision of Aircraft Crash Survival Design Guide, 1980, vol. 5, AD-A082-513.)
35. Johnson, R.; and Wade, B.: Longitudinal Impact Test of a Transport Airframe Section. Federal Aviation Administration Technical Center, Atlantic City, NJ. Final Report, Feb.-Oct. 1987, DOT/FAA/CT-87/26, July 1988.
36. Kevlin, S. G.: Full-Scale Crash Tests of A-3 and RB-66 Aircraft Conducted for the FAA to Evaluate Use of Gelled Fuel. Dept. of the Navy, Naval Air Test Facility, Lakehurst, NJ. NAVAIRTESTFAC Letter Report No. NATF-R136, Aug. 1973.
37. Kot, C. A.; Lin, H. C.; van Erp, J. B.; Eichler, T. V.; and Wiedermann: Evaluation of Aircraft Crash Hazards Analyses for Nuclear Power Plants. Nuclear Regulatory Commission, Washington, D.C. NUREG/CR-2859, June 1982.
38. Laananen, D., et al: Computer Simulation of an Aircraft Seat and Occupant in a Crash Environment. Vol. I - Technical Report. Vol. II - Program SOM-LA User's Manual. DOT/FAA/CT-82/33-1 and 33-11, March 1983.
39. Laananen, D. H.: Computer Simulation of an Aircraft Seat and Occupant(s) in a Crash Environment - Program SOM-LA/SOM-TA (User Manual) (U). Arizona State University, Tempe Dept. of Mechanical and Aerospace Engineering. Final Report No. CR-R-90026, July 1989-Feb. 1990, DOT/FAA/CT, XF; 90/4, DOT/FAA/CT, May 1991.
40. Lindsey, G. D.: Analysis of FY79 Army Aircraft Accidents. Army Safety Center, Fort Rucker, AL. Technical Report USASC-TR-80-2, April 1980.
41. Lucha, G. B.; Robertson, M. A.; and Schooley, F. A.: *An Analysis of Aircraft Accidents Involving Fires*. Stanford Research Institute for Ames Research Center. NASA CR-137690, May 1975.
42. McGuire, R.; Nissley, W.; and Wilson, A.: Drop Test -- Cessna Golden Eagle 421B (U). Federal Aviation Administration Technical Center, Atlantic City, NJ. Technical Note, Feb.-Nov. 1990, U.S. Department of Transportation, DOT/FAA/CT-TN91/32, May 1992.
43. Mikkola, M.; and Tuomala, M.: Mechanics of Impact Energy Absorption. Dept. of Structural Engineering, Helsinki University of Technology. Julkaisu Report 104, Espoo 1989.
44. Military Standard, System Safety Program Requirements. Depart. of Defense, reproduced by NTIS, U.S. Department of Commerce, MIL-STD-882B, March 30, 1984, superseding MIL-STD-882A, June 28, 1977, AMSC No. F3329, FSC SAFT, 98 pp., March 30, 1984.
45. Muehlbauer, J. C.; Bronn, C. E.; and Sturgeon, R. F.: Large Military Aircraft Accident Statistics and Analysis. Lockheed-Georgia Company, Nov. 1971.

46. NACA Conference on Airplane Crash-Impact Loads: Crash Injuries and Principles of Seat Design for Crashworthiness, April 1956.
47. NHTSA, SB-27: Crashworthiness of Motor Vehicles. National Technical Information Service, Springfield, VA, 1978.
48. Preston, G. M.; and Pesman, G. J.: Accelerations in Transport-Airplane Crashes. National Advisory Committee for Aeronautics, Technical Note 4158, Feb. 1958.
49. Quintiere, J. G.; and Tanaka, T.: An Assessment of Correlations Between Laboratory and Full-Scale Experiments for the FAA Aircraft Fire Safety Program, Part 5: Some Analyses of the Post Crash. U.S. Dept. of Commerce, National Bureau of Standards, National Engineering Laboratory, Center for Fire Research, Washington, D.C., NBSIR 82-2537, DOT/FAA/CT-82/107, July 1982.
50. Reed, W. H.; and Avery, J. P.: Principles for Improving Structural Crashworthiness for STOL and CTOL Aircraft. Defense Technical Information Center, USSAVLABS TR-66-39, Technical Report AVSER 65-18, June 1966.
51. Reed, W. H.; Robertson, S. H.; Weinberg, L. W. T.; and Tyndall, L. H.: Full-Scale Dynamic Crash Test of a Lockheed Constellation Model 1649 Aircraft. Federal Aviation Administration Technical Report ADS-38, Oct. 1965.
52. Reed, W. H.; Robertson, S. H.; Weinberg, L. W. T.; and Tyndall, L. H.: Full-Scale Dynamic Crash Test of a Douglas DC-7 Aircraft. Federal Aviation Administration Technical Report ADS-37, April 1965.
53. Safety Report: General Aviation Crashworthiness Project, Phase One. National Transportation Safety Board, Bureau of Technology, Report No. NTSB/SR-83/01, Government Accession No. PB83-917004, covering period 1972-1981, June 27, 1983.
54. Schaible, J. J.: Large-Scale Aircraft Crash Tests of Anti-Misting Kerosene. Dept. of the Navy, Naval Air Engineering Center, Lakehurst, NJ. Final Report NAEC-TR-190, May 21, 1982.
55. Schaible, J. J.: Crash Test of an RB-66 Aircraft Fueled with Anti-Misting Kerosene FM-9. Dept. of the Navy, Naval Air Engineering Center, Lakehurst, NJ. NAEC-TR-198, Sept. 9, 1983.
56. Sen, J.: Advanced Technology Landing Gear. USAAVSCOM TR-89-D-13A and 13B, Aug. 1990.
57. Shane, J. S.: *Design and Testing of an Energy-Absorbing Crewseat for the F/FB-111 Aircraft, vol. I.* Final Report, NASA CR-3916, Aug. 1985.
58. Shane, J. S.: *Design and Testing of an Energy-Absorbing Crewseat for the F/FB-111 Aircraft, vol. II.* Data From Seat Testing, NASA CR-3917, Sept. 1985.
59. Shane, J. S.: *Design and Testing of an Energy-Absorbing Crewseat for the F/FB-111 Aircraft, Vol. III.* Data From Crew Module Testing, NASA CR-3918, Aug. 1985.

60. Solomon, K. A.: Analysis of Ground Hazards Due to Aircrafts and Missiles (U). Rand Corporation, Santa Monica, CA, Report No. RAND/P-7459, June 1988.
61. Statistical Summary of Commercial Jet Aircraft Accidents: Worldwide Operations, 1959-1991. Boeing Commercial Airplane Group, Boeing Document No. D6-53810-90, N30225R4-1b, June 1992.
62. Weinberg, L. W. T.; and Carroll, D. F.: Three Full-Scale Dynamic Crash Tests of a CNV-103/C Shipping Container. Report to AVSER 66-23, revised April 11, 1967.
63. Welch, R. E.; Bruce, R. W.; and Belytschko, T.: Finite Element Analysis of Automotive Structures Under Crash Loadings. IIT Research Institute Report DOT-HS-801-847. U.S. Dept. of Transportation, Washington, D.C., March 1976.
64. Widmayer, E.; and Brende, O. B.: *Commercial Jet Transport Crashworthiness*. Boeing Commercial Airplane Company, Seattle, WA, NASA CR-165849, DOT/FAA/CT 82-68, April 1982.
65. Wittlin, G.; Gammon, M.: Experimental Program for the Development of Improved Helicopter Structural Crashworthiness Analytical and Design Techniques. Vol. I - Computerized Unsymmetrical Mathematical Simulation and Experimental Verification for Helicopter Crashworthiness in which Multidirectional Impact Forces are Present. Vol. II - Test Data and Description of an Unsymmetrical Crash Analysis Computer Program, Including a User's Guide and Sample Case. USAAMRDL TR-72-72A and 72B, May 1973.
66. Wittlin, G.; Park, K.: Development and Experimental Verification of Procedures to Determine Nonlinear Load-Deflection Characteristics of Helicopter Substructures Subjected to Crash Forces. Vol. I - Development of Simplified Analytical Techniques to Predict Typical Helicopter Airframe Crushing Characteristics and the Formulation of Design Procedures. Vol. II - Test Data and Description of Refined Program "KRASH" Including a User's Guide and a Sample Case. USAAMRDL TR-74-12A and 12B, May 1974.
67. Wittlin, G.; Gammon, M.; and Shycoff, D.: Transport Aircraft Crash Dynamics. NASA CR-16585; Federal Aviation Administration Technical Center, U.S. Dept. of Transportation. FAA Report DOT/FAA/CT-82/69, March 1982.
68. Wittlin, G.; and Lackey, D.: *Analytical Modeling of Transport Aircraft Crash Scenarios to Obtain Floor Pulses*. NASA CR-166089, April 1983; Lockheed-California Co., Burbank, CA, U.S. Dept. of Transportation, Report for Nov. 1981-July 1982, FAA Report DOT/FAA/CT-83/23, April 1983.
69. Wittlin, G.: KRASH Analysis Correlation, Transport Airplane Controlled Impact Demonstration Test (U). Lockheed-California Co., Burbank, CA. Final Report for Feb-Aug. 1985, Report No. LR-30916, DOT/FAA/CT 86-13, Dec. 1986.
70. Wittlin, G.; and LaBarge, W. L.: KRASH Parametric Sensitivity Study-Transport Category Airplanes (U). Lockheed-California Co., Burbank, CA. Final Report for Oct. 1985-June 1986, DOT/FAA/CT 87/13, Dec. 1987 (see also Report Nos. DOT/FAA/CT-85/9 and DOT/FAA/CT-86/13).
71. Wittlin, G.; and LaBarge, W. L.: KRASH Dynamics Analysis Modeling - Transport Airplane Controlled Impact Demonstration Test, Revision (U). Lockheed-California Co., Burbank, CA. Final Report for Jan.-Sept. 1984, Report No. LR-30776, DOT/FAA/CT-85/9, March 1986 (revision to report, May 1985).

72. Wittlin, G.: Investigation of Transport Airplane Fuselage Fuel Tank Installations Under Crash Conditions. DOT/FAA/CT-88/24, July 1989.
73. Yeung, K. S.; and Welch, R. E.: Refinement of Finite Element Analysis of Automobile Structures Under Crash Loading. Final Report, Vol. II, DOT, NHTA Con. DOT-HS-6-01364, 1977.
74. Zagarella, A.: Full-Scale Aircraft Crash Tests of Anti-Misting Kerosene. Dept. of the Navy, Naval Air Engineering Center, Lakehurst, NJ. Interim Report NAEC-TR-183, Aug. 4, 1980.
75. Zimmerman, R. E.; and Merritt, N. A.: Aircraft Crash Survival Design Guide, vol. I - Design Criteria and Checklists, vol. 1 of five-volume Report. Defense Technical Information Center, USAAVSCOM TR-89-D-22A, Aircraft Crash Survival Design Guide, Dec. 1989.
76. Zimmerman, R. E.; Warrick, J. C.; Lane, A. D.; Merritt, N. A.; Bolukbasi, A. O.: Aircraft Crash Survival Design Guide, vol. 3, Aircraft Structural Crash Resistance (U). Simula, Inc., Phoenix, AZ, Final Report for Sept. 1986-Aug. 1989, DTIC, USAAVSCOM, TR-89-D-22C, Dec. 1989 (see also vol. 4, AD-A218 437). Revision of Aircraft Crash Survival Design Guide, 1980, vol. 3, AD-A089 104.

IV. Research Papers

1. Alfaro-Bou, E.; Hayduk, R. J.; Thomson, R. G.; and Vaughan, V. L., Jr.: Simulation of Aircraft Crash and Its Validation. *Aircraft Crashworthiness*, K. Siczalski, G. T. Singley III, W. D. Pilkey and R. L. Huston, eds., University Press of Virginia, Charlottesville, 1975, pp. 485-497.
2. Alfaro-Bou, E.; and Vaughan, V. L., Jr.: *Light Airplane Crash Tests at Impact Velocities of 13 and 27 m/sec.* NASA TP 1042, Nov. 1977.
3. Alfaro-Bou, E.; Williams, M. S.; and Fasanella, E. L.: Determination of Crash Test Pulses and Their Application to Aircraft Seat Analysis. SAE Paper 810611, April 1981.
4. Alfaro-Bou, E.; Fasanella, E. L.; and Williams, M. S.: Crashworthy Design Considerations for General Aviation Seats. SAE Paper 850855, April 1985.
5. Armen, H.; Pifko, A. B.; and Levine, H. S.: Nonlinear Finite Element Techniques for Aircraft Crash Analysis. *Aircraft Crashworthiness*, University Press of Virginia, Charlottesville, 1975, pp. 517-548.
6. Berry, V. L.; and Cronkhite, J. D.: KRASH Analysis Correlation with Full-Scale YAH-63 Helicopter Crash Test. AHS National Specialists' Meeting on Crashworthy Design of Rotorcraft, Georgia Institute of Technology, Atlanta, GA, April 7-9, 1986.
7. Boitnott, R. L.; Fasanella, E. L.; Carden, H. D.; and Calton, L. E.: Impact Response of Composite Fuselage Frames. *General Aviation Aircraft Crash Dynamics*, SAE Publication SP-716, 1987. Also available as SAE Paper 871009, April 1987.
8. Boitnott, R. L.; and Kindervater, C.: Crashworthy Design of Helicopter Composite Airframe Structure. Paper No. 93, Fifteenth European Rotorcraft Forum, Amsterdam, Sept. 12-15, 1989.

67. Thompson, D. E.; Braisted, W. R.; Brockman, R. A.: Foreign Object Impact Assessment of a High-Mach Engine Inlet. Proceedings of the AIAA/ASME/ASCE/AHS 34th Structures, Structural Dynamics and Materials Conference, La Jolla, CA, April 19-21, 1993.
68. Bouchard, M. P.; and Davisson, J. C.: Advanced Transparency Development for USAF Aircraft. Proceedings of the AIAA/ASME/ASCE/AHS 34th Structures, Structural Dynamics and Materials Conference, La Jolla, CA, April 19-21, 1993.
69. Thomson, R. G.; and Caiafa, C.: Designing for Aircraft Structural Crashworthiness. *J. Aircraft*, vol. 19, no. 10, Oct. 1982, pp. 868-874.
70. Thomson, R. G.; and Caiafa, C.: Structural Response of Transport Airplanes in Crash Situations. NASA TM 85654, June 1983; Federal Aviation Administration Technical Center, U.S. Dept. of Transportation, DOT/FAA/CT-83/42, Final Report, Nov. 1983.
71. Thomson, R. G.; Cardin, H. A.; and Hayduk, R. J.: *Survey of NASA Research on Crash Dynamics*. NASA TP-2298, 1984.
72. Tong, P.; Ni, C. M.; King, A.; and Lantz, S.: *Symposium on Vehicle Crashworthiness Including Impact Biomechanics*. ASME Winter Annual Meeting, Anaheim, CA, Dec. 7-12, 1986, AMD Vol. 79, BED vol. 1, American Society of Mechanical Engineers, NY, 1986.
73. Turnbow, J. W.: A Dynamic Crash Test of the H25 Helicopter. SAE Paper 517A, National Aeronautics Meeting, April 3-6, 1962.
74. Tuttle, W. D.: United States Air Force (USAF) Experience in Aircraft Accident Survivability. Directorate of Aerospace Safety, Norton Air Force Base, CA, Aircraft Crashworthiness Symposium, Oct. 6, 1975, Cincinnati, OH, Oct. 1975.
75. Tuttle, W. D.: United States Air Force (USAF) Experience in Aircraft Accident Survivability. Directorate of Aerospace Safety, Norton Air Force Base, CA, Aerospace Medical Association Scientific Meeting, Bel Harbour, FL, May 10-13, 1976, April 1976.
76. Ulrich, D. and Pickett, A. K.: Crash Simulation and Verification for Metallic, Sandwich and Laminate Structures (U). Advisory Group for Aerospace Research and Development, Neuilly-sur-Seine, France. Conference Proceedings of Energy Absorption of Aircraft Structures as an Aspect of Crashworthiness (66th), Luxembourg, May 1-6, 1988, Report AD-A212 606, Dec. 1988, pp. 18-1 thru 18-18.
77. Vaughan, V. L., Jr.; and Alfaro-Bou, E.: *Light Airplane Crash Tests at Three Pitch Angles*. NASA TP 1481, Nov. 1979.
78. Vaughan, V. L., Jr.; and Hayduk, R. J.: *Crash Tests of Four Identical High-Wing Single-Engine Airplanes*. NASA TP 1699, Aug. 1980.
79. Von Gierke, H., E.; and Brinkley, J. W.: Human Crashworthiness and Crash Load Limits (U). Harry G. Armstrong Aerospace Medical Research Lab, Wright-Patterson Air Force Base, OH. Conference Proceedings of Energy Absorption of Aircraft Structures as an Aspect of Crashworthiness (66th), Luxembourg, May 1-6, 1988, Report AD-A212 606, Dec. 1988, pp. 22-1 thru 22-15.
80. Walker, B. D.; and Dallard, P. R. B.: An Integrated Approach to the Simulation of Vehicle Crashworthiness and Occupant Protection Systems. Int. Congress and Exposition, Detroit, MI, Feb. 25-March 1, 1991. SAE Technical Paper Series 910148.

72. Wittlin, G.: Investigation of Transport Airplane Fuselage Fuel Tank Installations Under Crash Conditions. DOT/FAA/CT-88/24, July 1989.
73. Yeung, K. S.; and Welch, R. E.: Refinement of Finite Element Analysis of Automobile Structures Under Crash Loading. Final Report, Vol. II, DOT, NHTA Con. DOT-HS-6-01364, 1977.
74. Zagarella, A.: Full-Scale Aircraft Crash Tests of Anti-Misting Kerosene. Dept. of the Navy, Naval Air Engineering Center, Lakehurst, NJ. Interim Report NAEC-TR-183, Aug. 4, 1980.
75. Zimmerman, R. E.; and Merritt, N. A.: Aircraft Crash Survival Design Guide, vol. I - Design Criteria and Checklists, vol. 1 of five-volume Report. Defense Technical Information Center, USAAVSCOM TR-89-D-22A, Aircraft Crash Survival Design Guide, Dec. 1989.
76. Zimmerman, R. E.; Warrick, J. C.; Lane, A. D.; Merritt, N. A.; Bolukbasi, A. O.: Aircraft Crash Survival Design Guide, vol. 3, Aircraft Structural Crash Resistance (U). Simula, Inc., Phoenix, AZ, Final Report for Sept. 1986-Aug. 1989, DTIC, USAAVSCOM, TR-89-D-22C, Dec. 1989 (see also vol. 4, AD-A218 437). Revision of Aircraft Crash Survival Design Guide, 1980, vol. 3, AD-A089 104.

IV. Research Papers

1. Alfaro-Bou, E.; Hayduk, R. J.; Thomson, R. G.; and Vaughan, V. L., Jr.: Simulation of Aircraft Crash and Its Validation. *Aircraft Crashworthiness*, K. Saczalski, G. T. Singley III, W. D. Pilkey and R. L. Huston, eds., University Press of Virginia, Charlottesville, 1975, pp. 485-497.
2. Alfaro-Bou, E.; and Vaughan, V. L., Jr.: *Light Airplane Crash Tests at Impact Velocities of 13 and 27 m/sec.* NASA TP 1042, Nov. 1977.
3. Alfaro-Bou, E.; Williams, M. S.; and Fasanella, E. L.: Determination of Crash Test Pulses and Their Application to Aircraft Seat Analysis. SAE Paper 810611, April 1981.
4. Alfaro-Bou, E.; Fasanella, E. L.; and Williams, M. S.: Crashworthy Design Considerations for General Aviation Seats. SAE Paper 850855, April 1985.
5. Armen, H.; Pifko, A. B.; and Levine, H. S.: Nonlinear Finite Element Techniques for Aircraft Crash Analysis. *Aircraft Crashworthiness*, University Press of Virginia, Charlottesville, 1975, pp. 517-548.
6. Berry, V. L.; and Cronkhite, J. D.: KRASH Analysis Correlation with Full-Scale YAH-63 Helicopter Crash Test. AHS National Specialists' Meeting on Crashworthy Design of Rotorcraft, Georgia Institute of Technology, Atlanta, GA, April 7-9, 1986.
7. Boitnott, R. L.; Fasanella, E. L.; Carden, H. D.; and Calton, L. E.: Impact Response of Composite Fuselage Frames. *General Aviation Aircraft Crash Dynamics*, SAE Publication SP-716, 1987. Also available as SAE Paper 871009, April 1987.
8. Boitnott, R. L.; and Kindervater, C.: Crashworthy Design of Helicopter Composite Airframe Structure. Paper No. 93, Fifteenth European Rotorcraft Forum, Amsterdam, Sept. 12-15, 1989.

9. Boitnott, R. L.; and Fasanella, E. L.: Crashworthiness of Composite Floor Sections. *Aerospace Engineering*, Dec. 1989, pp. 9-12.
10. Bolukbasi, A. O.; and Laananen, D. H.: Computer Simulation of a Transport Aircraft Seat and Occupant(s) in a Crash Environment, vol. 2, Program SOM-TA (Seat/Occupant Simulation Model for Transport Aircraft). Users Manual (U). Simula, Inc., Phoenix, AZ. Final Report for June 1983-March 1986, Report No. TR-84429, Report No. DOT/FAA/CT 86/25-2, Aug. 1986. (See also vol. 1, AD-A175-953.)
11. Bolukbasi, A. O.; and Laananen, D. H.: Computer Simulation of a Transport Aircraft Seat and Occupant(s) in a Crash Environment, vol. 1, Technical Report (U). Simula, Inc., Phoenix, AZ, Final Report for June 1983-March 1986, Report No. TR-84430, DOT/FAA/CT 86/25, Aug. 1986. (See also vol. 2, AD-A176-074.)
12. Brockman, R. A.; Held, T. W.: X3D User's Manual. University of Dayton Research Institute Report No. UDR-TR-92-59, April 1992.
13. Brockman, R. A.; Held, T. W.: Explicit Finite Element Analysis Techniques for Transparency Impact Analysis. Proceedings of the Conference on Aerospace Transparent Materials and Enclosures. Monterey, CA, Jan. 16-20, 1989.
14. Carden, H. D.; and Hayduk, R. J.: Aircraft Subfloor Response to Crash Loadings. SAE Paper 810614, April 1981.
15. Carden, H. D.: *Correlation and Assessment of Structural Airplane Crash Data with Flight Parameters at Impact*. NASA TP-2083, Nov. 1982.
16. Carden, H. D.: Impulse Analysis of Airplane Crash Data with Consideration Given to Human Tolerance. SAE Paper 830748, April 1983.
17. Carden, H. D.: *Full-Scale Crash Test Evaluation of Two Load-Limiting Subfloors for General Aviation Airframes*. NASA TP-2380, Dec. 1984.
18. Carden, H. D.: Unique Failure Behavior of Metal/Composite Aircraft Structural Components Under Crash Type Loads. Proceedings of the 1990 Aircraft Interiors Conference, Wichita, KS, April 24-25, 1990.
19. Carden, H. D.: *Unique Failure Behavior of Metal/Composite Aircraft Structural Components Under Crash Type Loads*. NASA TM-102679, May 1990.
20. Carden, H. D.; Boitnott, R. L.; and Fasanella, E. L.: *Behavior of Composite/Metal Aircraft Structural Elements and Components Under Crash Type Loads -- What are They Telling Us?* NASA TM-102681 and USAAVSCOM TR-90-B-003, May 1990; also Paper No. 90-1.7.1, Proceedings of 17th ICAS Congress, Stockholm, Sweden, Sept. 9-14, 1990.
21. Carden, H. D.; and Robinson, M. P.: *Failure Behavior of Generic Metallic and Composite Aircraft Structural Components Under Crash Loads*. NASA RP-1239, Nov. 1990.
22. Carden, H. D.; Boitnott, R. L.; Fasanella, E. L.; and Jones, L. E.: *An Overview of the Crash Dynamics Failure Behavior of Metal/Composite Aircraft Structures*. NASA CP-3104, Part 2, Jan. 1991, pp. 1005-1035.

23. Castle, C. B.: *Full-Scale Crash Test of a CH-47C Helicopter*. NASA TM X-3412, 1976.
24. Castle, C. B.; and Alfaro-Bou, E.: *Light Airplane Crash Tests at Three Flight-Path Angles*. NASA TP 1210, June 1978.
25. Castle, C. B.; and Alfaro-Bou, E.: *Light Airplane Crash Tests at Three Roll Angles*. NASA TP 1477, Oct. 1979.
26. Castle, C. B.; and Alfaro-Bou, E.: *Crash Tests of Three Identical Low-Wing Single-Engine Airplanes*. NASA TP 2190, Sept. 1983.
27. Cronkhite, J. D.; and Berry, V. L.: *Crashworthy Airframe Design Concepts - Fabrication and Testing*. NASA CR-3603, Sept. 1982.
28. Cronkhite, J. D.; and Mazza, L. T.: *KRASH Analysis Correlation with the Bell ACAP Full-Scale Aircraft Crash Test*. American Helicopter Society, National Technical Specialists' Meeting on Advanced Rotorcraft Structures, Williamsburg, VA, Oct. 25-27, 1988.
29. Cronkhite, J. D.; and Mazza, L. T.: *Bell ACAP Full-Scale Aircraft Crash Test and KRASH Correlation*. American Helicopter Society, 44th Annual Forum and Technology Display, Washington, D.C., June 16-18, 1989.
30. Eiband, A. M., et al: *Accelerations and Passenger Harness Loads Measured in Full-Scale Light Airplane Crashes*. NACA TN-2991, Aug. 1953.
31. Eichelberger, C. P.; Alfaro-Bou, E.; and Fasanella, E. L.: *Development of an Energy Absorbing Passenger Seat for a Transport Aircraft*. NASA CP-2371, 1985.
32. Fasanella, E. L. and Alfaro-Bou, E.: *NASA General Aviation Crashworthiness Seat Development (Technical Paper Series)*, Vought Corporation, and NASA Langley Research Center. Presented at Business Aircraft Meeting and Exposition, Century II, Wichita, KS, Society of Automotive Engineers, Inc., April 3-6, 1979.
33. Fasanella, E. L.; and Alfaro-Bou, E.: *Vertical Drop Test of a Transport Fuselage Section Located Aft of the Wing*. NASA TM 89025, Sept. 1986.
34. Fasanella, E. L.; Alfaro-Bou, E.; and Hayduk, R. J.: *Impact Data From a Transport Aircraft During a Controlled Impact Demonstration*. NASA TP-2589, Sept. 1986.
35. Fasanella, E. L.; Hayduk, R. J.; Robinson, M. P.; and Widmayer, E.: *Analysis of a Transport Fuselage Section Drop Test*. NASA CP-2335, 1984, pp. 347-368.
36. Fasanella, E. L.; Alfaro-Bou, E.; and Hayduk, R. J.: *Impact Data From a Transport Aircraft During a Controlled Impact Demonstration*. NASA TP-2589, Sept. 1986.
37. Fasanella, E. L.; Widmayer, E.; and Robinson, M. P.: *Structural Analysis of the Controlled Impact Demonstration of a Jet Transport Airplane*. *J. Aircraft*, vol. 24, no. 4, April 1987, pp. 274-280.
38. Fasanella, E. L.; Jones, L. E.; and Carden, H. D.: *Interim Transportation Overpack Container (ITOC) Experiments and Analysis*. NASA TM-101510, Oct. 1988.
39. Fasanella, E. L.; Carden, H. D.; Boitnott, R. L.; and Hayduk, R. J.: *A Review of the Analytical Simulation of Aircraft Crash Dynamics*. NASA TM-102595, Jan. 1990.

40. Frese, J.; and Nitschke, D.: Crushing Behavior of Helicopter Subfloor Structures (U). Advisory Group for Aerospace Research and Development, Neuilly-Sur-Seine, France. Conference Proceedings of Energy Absorption of Aircraft Structures as an Aspect of Crashworthiness (66th), Luxembourg, May 1-6, 1988, Report AD-A212-606, Dec. 1988, pp. 10.1-10.23.
41. Hayduk, R. J.: *Comparative Analysis of PA-31-350 Chieftain (N44LV) Accident and NASA Crash Test Data*. NASA TM 80102, Oct. 1979.
42. Hayduk, R.; and Williams, S.: *Vertical Drop Test of a Transport Fuselage Section Located Forward of the Wing*. NASA TM-85679, Aug. 1983.
43. Hayduk, R. J.; Winter, R.; Pifko, A. B.; and Fasanella, E. L.: Application of the Nonlinear Finite Element Computer Program 'DYCAST' to Aircraft Crash Analysis. *Structural Crashworthiness*, J. Jones and T. Wierzcicki, eds., Butterworths, 1983, pp. 283-307.
44. Hayduk, R. J.; Fasanella, E. L.; and Alfaro-Bou, E.: Full-Scale Transport Controlled Impact Demonstration Preliminary NASA Structural Data. AIAA Paper 85-0712, April 1985.
45. Hayduk, R. J.; Fasanella, E. L.; and Alfaro-Bou, E.: Structural Crashworthiness Experiments of the Controlled Impact Demonstration. Int. Society of Air Safety Investigators, Stirling, VA. Special edition FAA/NASA Controlled Impact Demonstration. *Forum*, Vol. 18, No. 4, 1986, pp. 33-43.
46. Hayduk, R. J.; Fasanella, E. L.; and Alfaro-Bou, E.: NASA Experiments Onboard the Controlled Impact Demonstration. SAE Paper 851885, Oct. 1985.
47. Hayduk, R. J., ed.: *Full-Scale Transport Controlled Impact Demonstration*. NASA CP-2395, 1986.
48. Human Tolerance Related to Impact Conditions as Related to Motor Vehicle Design. SAE J885, Society of Automotive Engineers, Warrendale, PA, 1988.
49. Kaiser, A.: Some Examples of Numerical Simulation in Vehicle Safety Development. *Proceedings of the Sixth International Conference on Vehicle Structural Mechanics*. SAE, 1992, pp. 107-117.
50. Khalil, T. B.; and Bennett, J. A.: Nonlinear Finite Element Analysis in Crashworthiness of Automotive Shell Structures - An Overview. Analytical and Computational Models of Shells, Proceedings of the Symposium, CED-vol. 3, ASME Winter Annual Meeting, San Francisco, CA, Dec. 10-15, 1989, pp. 569.
51. Khalil, T. B.; and Vander Lugt, D. A.: Identification of Vehicle Front Structure Crashworthiness by Experiment and Finite Element Analysis. Crashworthiness and Occupant Protection, A. King and T. Khalil, eds., AMD vol. 106, BED Vol. 13, American Society of Mechanical Engineers, NY, 1989, pp. 41-51.
52. Khalil, T. B.; Ni, C. B.; Mahmood, H. F.; and King, A. I., eds, Crashworthiness and Occupant Protection in Transportation Systems - 1991. ASME Winter Annual Meeting, Atlanta, GA, Dec. 1-6, 1991. AMD Vol. 126, BED vol. 19, American Society of Mechanical Engineers, NY, 1991.

53. Kindervater, Ch.; Georgi, H.; and Koerber, U.: Crashworthy Design of Aircraft Subfloor Structural Components (U). Advisory Group for Aerospace Research and Development. Neuilly-Sur-Seine, France. Conference Proceedings of Energy Absorption of Aircraft Structures as an Aspect of Crashworthiness (66th), held in Luxembourg, May 1-6, 1988, Report AD-A212 606, Dec. 1988, pp. 12-1 thru 12-24.
54. Hill, R. G. et al.: *Post Crash Fuel Fire Hazard Measurements in a Wide-Body Aircraft Cabin*. FAA-NA-79-42, Dec. 1979.
55. Hill, R. G. et al.: *Aircraft Interior Panel Test Criteria Derived From Full-Scale Fire Tests*. DOT/FAA/CT-85/23, Sept. 1985.
56. Holland, H.; and Smith, K. F.: Full-Scale Helicopter Crash Testing (U). Army Aviation Research and Technology Activity. Conference Proceedings of Energy Absorption of Aircraft Structures as an Aspect of Crashworthiness (66th), Luxembourg, May 1-6, 1988. Report AD-A212-606, Dec. 1988, pp. 9.1-9.7.
57. Horton, T. W.; and Kempel, R. W.: *Flight Test Experience and Controlled Impact of a Remotely Piloted Jet Transport Aircraft*. NASA TM-4084, 1988.
58. McComb, H. G.; Thomson, R. G.; and Hayduk, R. J.: *Structural Dynamics Research in a Full-Scale Transport Aircraft Crash Test*. Fifteenth Congress International Council of Aeronautical Sciences, London, Sept. 1986.
59. Morton, J.: Scaling of Impact Loaded Carbon Fiber Composites. 28th Structural Dynamics Conference, Monterey, CA, April 6-8, 1987.
60. Parsons, D.; and Belfield, A.: Predicting Crash Performance (U). Advisory Group for Aerospace Research and Development, Neuilly-sur-Seine, France. Conference Proceedings of Energy Absorption of Aircraft Structures as an Aspect of Crashworthiness (66th), held in Luxembourg, May 1-6, 1988, Report AD-A212 606, Dec. 1988, pp. 20-1 thru 20-13.
61. Pifko, A. B.; and Winter, R.: *Theory and Application of Finite Element Analysis to Structural Crash Simulation*. Pergamon Press, 1981; *Computers and Structures*, vol. 13, 1981, pp. 277-285.
62. Saczalski, K. J.; and Pilkey, W. D.: Techniques for Predicting Vehicle Structure Crash Impact Response. *Aircraft Crashworthiness*. University Press of Virginia, Charlottesville, VA, 1975, pp. 467-484.
63. Saczalski, K. J.; and Park, K. C.: An Interactive Hybrid Technique for Crashworthy Design of Complex Vehicular Systems. *Proceedings of the SAE International Conference on Vehicle Structural Mechanics*, March 26-28, 1974, SAE Paper No. 740327.
64. Smith, K. F.: Full-Scale Crash Test (T-41) of YAH-63 Attack Helicopter. USAAVSCOM TR-86-D-2, Aviation Applied Technology Directorate, U.S. Army Research and Technology Laboratory, Fort Eustis, VA, April 1986.
65. Soltis, S.; Caiafa, C.; and Wittlin, G.: FAA Structural Crash Dynamics Program Update - Transport Category Aircraft. SAE Paper 851887, Oct. 1985.
66. Sturt, R. M. V.; Walker, B. D.; Miles, J. C.; Giles, A.; and Grew, N.: Modeling the Occupant in a Vehicle Context - An Integrated Approach. 91-S9-0-19, Oct. 1991.

67. Thompson, D. E.; Braisted, W. R.; Brockman, R. A.: Foreign Object Impact Assessment of a High-Mach Engine Inlet. Proceedings of the AIAA/ASME/ASCE/AHS 34th Structures, Structural Dynamics and Materials Conference, La Jolla, CA, April 19-21, 1993.
68. Bouchard, M. P.; and Davisson, J. C.: Advanced Transparency Development for USAF Aircraft. Proceedings of the AIAA/ASME/ASCE/AHS 34th Structures, Structural Dynamics and Materials Conference, La Jolla, CA, April 19-21, 1993.
69. Thomson, R. G.; and Caiafa, C.: Designing for Aircraft Structural Crashworthiness. *J. Aircraft*, vol. 19, no. 10, Oct. 1982, pp. 868-874.
70. Thomson, R. G.; and Caiafa, C.: Structural Response of Transport Airplanes in Crash Situations. NASA TM 85654, June 1983; Federal Aviation Administration Technical Center, U.S. Dept. of Transportation, DOT/FAA/CT-83/42, Final Report, Nov. 1983.
71. Thomson, R. G.; Cardin, H. A.; and Hayduk, R. J.: *Survey of NASA Research on Crash Dynamics*. NASA TP-2298, 1984.
72. Tong, P.; Ni, C. M.; King, A.; and Lantz, S.: *Symposium on Vehicle Crashworthiness Including Impact Biomechanics*. ASME Winter Annual Meeting, Anaheim, CA, Dec. 7-12, 1986, AMD Vol. 79, BED vol. 1, American Society of Mechanical Engineers, NY, 1986.
73. Turnbow, J. W.: A Dynamic Crash Test of the H25 Helicopter. SAE Paper 517A, National Aeronautics Meeting, April 3-6, 1962.
74. Tuttle, W. D.: United States Air Force (USAF) Experience in Aircraft Accident Survivability. Directorate of Aerospace Safety, Norton Air Force Base, CA, Aircraft Crashworthiness Symposium, Oct. 6, 1975, Cincinnati, OH, Oct. 1975.
75. Tuttle, W. D.: United States Air Force (USAF) Experience in Aircraft Accident Survivability. Directorate of Aerospace Safety, Norton Air Force Base, CA, Aerospace Medical Association Scientific Meeting, Bel Harbour, FL, May 10-13, 1976, April 1976.
76. Ulrich, D. and Pickett, A. K.: Crash Simulation and Verification for Metallic, Sandwich and Laminate Structures (U). Advisory Group for Aerospace Research and Development, Neuilly-sur-Seine, France. Conference Proceedings of Energy Absorption of Aircraft Structures as an Aspect of Crashworthiness (66th), Luxembourg, May 1-6, 1988, Report AD-A212 606, Dec. 1988, pp. 18-1 thru 18-18.
77. Vaughan, V. L., Jr.; and Alfaro-Bou, E.: *Light Airplane Crash Tests at Three Pitch Angles*. NASA TP 1481, Nov. 1979.
78. Vaughan, V. L., Jr.; and Hayduk, R. J.: *Crash Tests of Four Identical High-Wing Single-Engine Airplanes*. NASA TP 1699, Aug. 1980.
79. Von Gierke, H., E.; and Brinkley, J. W.: Human Crashworthiness and Crash Load Limits (U). Harry G. Armstrong Aerospace Medical Research Lab, Wright-Patterson Air Force Base, OH. Conference Proceedings of Energy Absorption of Aircraft Structures as an Aspect of Crashworthiness (66th), Luxembourg, May 1-6, 1988, Report AD-A212 606, Dec. 1988, pp. 22-1 thru 22-15.
80. Walker, B. D.; and Dallard, P. R. B.: An Integrated Approach to the Simulation of Vehicle Crashworthiness and Occupant Protection Systems. Int. Congress and Exposition, Detroit, MI, Feb. 25-March 1, 1991. SAE Technical Paper Series 910148.

81. Widmayer, E.; and Brende, O. B.: *Commercial Jet Transport Crashworthiness*. NASA CR-165849, March 1982.
82. Williams, M. S.; and Fasanella, E. L.: *Results From Tests of Three Prototype General Aviation Seats*. NASA TM 84533, August 1982.
83. Williams, M. S.; and Fasanella, E. L.: *Crash Tests of Four Low-Wing Twin-Engine Airplanes with Truss-Reinforced Fuselage Structure*. NASA TP-2070, Sept. 1982.
84. Williams, M. S.; and Hayduk, R. J.: *Vertical Drop Test of a Transport Fuselage Section Located Forward of the Wing*. NASA TM-85679, August 1983.
85. Williams, M. S.; and Hayduk, R. J.: *Vertical Drop Test of a Transport Fuselage Center Section Including the Wheel Wells*. NASA TM-85706, Oct. 1983.
86. Winter, R.; Pifko, A. B.; and Armen, H.: *Crash Simulation of Skin Frame Structures Using a Finite Element Code*. SAE Paper 770484, presented at Business Aircraft Meeting, Society of Automotive Engineers, Inc., New York, March 29-April 1, 1977.
87. Winter, R.; Pifko, A. B.; and Cronkhite, J. D.: *Crash Simulation of Composite and Aluminum Helicopter Fuselages Using a Finite Element Program*. AIAA Paper 79-0781, presented at AIAA/ASME/ASCE/AHS 20th Structures, Structural Dynamics and Materials Conference, St. Louis, MO, 4-6 April 1979.
88. Wittlin, G.; and Gamon, M. A.: *A Method of Analysis for General Aviation Airplane Structural Crashworthiness. Measurement and Prediction of Structural and Biodynamic Crash Impact*. Salczalski, K. J. and Pilkey, W. D., eds, American Society of Mechanical Engineers, NY, 1976, pp. 63-82.
89. Wittlin, G.; Gamon, M.; and Shycoff, D.: *Transport Aircraft Crash Dynamics*. NASA CR-165851, March 1982.
90. Wittlin, G.; and Caiafa, C.: *Transport Airplane Crash Simulation, Validation and Application to Crash Design Criteria (U)*. Lockheed Aeronautical Systems, Burbank, CA. Conference Proceedings of Energy Absorption of Aircraft Structures as an Aspect of Crashworthiness (66th), Luxembourg, May 1-6, 1988, Report AD-A212 606, Dec. 1988, pp. 1-16 thru 16-23.
91. Yeung, K. S.; and Hollowell, T.: *Large Displacement, Nonlinear Static and Dynamic Analysis of Automobile Sheet Metal Structure*. SAE Paper 780367, presented at 1978 Congress and Exposition, Society of Automotive Engineers, Detroit, MI, March 1978.

V. Commerical Software Systems

1. ABAQUS Reference: Hibbitt, Karlson and Sorensen (West), 3900 Newpart Mall Road, Suite 205, Newark, CA 94560.
2. Bathe, K.: *ADINA User's Manual -- ADINA, A Finite Element Program for Automatic Dynamic Incremental Nonlinear Analysis*. Massachusetts Institute of Technology Report No. 82448-1, Sept. 1975 (some recent revisions).
3. Belytschko, T.; and Kennedy, J. M.: *WHAMS-3D, An Explicit Three-Dimensional Finite Element Program*. KBS2, Inc., P.O. Box 453, Willow Springs, IL 60480, 1986.

4. Gamon, M. A.; Wittlin, G.; and LaBarge, B.: *KRASH 85 User's Guide - Input/Output Format (U)*. Lockheed-California Company, Burbank, CA. Final Report for Jan.-Sept. 1984, Report No. LR-30777, DOT/FAA/CT 85-10, July 1985.
5. Hallquist, J. O.; and Whirley, R. G.: *DYNA3D User's Manual*. UCID-19592, Rev. 5, Lawrence Livermore National Laboratory, May 1989.
6. Miles, J. C.; Sturt, R. M. V.; and Leach, J. H.: *Practical Tools for Vehicle Impact Simulation, Part 2: An Integrated Approach Using OASYS DYNA3D*. Proc. Inst. Mech. Engrs, vol. 205, June 1991, p. 95
7. *PAM-CRASH User's Manual*. Engineering System International, 20 Rue Saarinen, Silic 2700, 64578 Rungis, Cedex, France, 1985.
8. Pifko, A. B.; Winter, R.; and Ogilvie, P. L.: *DYCAST - A Finite Element Program for the Crash Analysis of Structures*. NASA CR-4040, Jan. 1987.
9. Taylor, L. M.; and Flanagan, D. P.: *PRONTO 2D - A Two-Dimensional Transient Solid Dynamics Program*. SAND86-0594, Sandia National Laboratories, Albuquerque, NM, March 1987.
10. Taylor, L. M.; and Flanagan, D. P.: *PRONTO 3D - A Three-Dimensional Transient Solid Dynamics Program*. SAND87-1912, Sandia National Laboratories, Albuquerque, NM, March 1989.
11. Vaughan, D. K.: *FLEX User's Guide*. Report UG8298, Weidlinger Associates, Palo Alto, CA, May 1983.

REPORT DOCUMENTATION PAGE			Form Approved OMB No. 0704-0188	
Public reporting burden for this collection of information is estimated to average 1 hour per response, including the time for reviewing instructions, searching existing data sources, gathering and maintaining the data needed, and completing and reviewing the collection of information. Send comments regarding this burden estimate or any other aspect of this collection of information, including suggestions for reducing this burden, to Washington Headquarters Services, Directorate for Information Operations and Reports, 1215 Jefferson Davis Highway, Suite 1204, Arlington, VA 22202-4302, and to the Office of Management and Budget, Paperwork Reduction Project (0704-0188), Washington, DC 20503.				
1. AGENCY USE ONLY (Leave blank)	2. REPORT DATE August 1993	3. REPORT TYPE AND DATES COVERED Conference Publication		
4. TITLE AND SUBTITLE Computational Methods for Crashworthiness		5. FUNDING NUMBERS 505-63-50-09		
6. AUTHOR(S) Ahmed K. Noor and Huey D. Carden, Compilers				
7. PERFORMING ORGANIZATION NAME(S) AND ADDRESS(ES) NASA Langley Research Center Hampton, VA 23681-0001 University of Virginia Center for Computational Structures Technology Hampton, VA 23681-0001		8. PERFORMING ORGANIZATION REPORT NUMBER L-17284		
9. SPONSORING/MONITORING AGENCY NAME(S) AND ADDRESS(ES) National Aeronautics and Space Administration Washington, DC 20546-0001		10. SPONSORING/MONITORING AGENCY REPORT NUMBER NASA CP-3223		
11. SUPPLEMENTARY NOTES Proceedings of a workshop sponsored by the National Aeronautics and Space Administration and the University of Virginia Center for Computational Structures Technology, Hampton, VA, and held at NASA Langley Research Center on September 2-3, 1992.				
12a. DISTRIBUTION/AVAILABILITY STATEMENT Unclassified-Unlimited Subject Category 39		12b. DISTRIBUTION CODE		
13. ABSTRACT (Maximum 200 words) This document contains presentations and discussions from the joint UVA/NASA Workshop on Computational Methods for Crashworthiness held at Langley Research Center on September 2-3, 1992. The presentations addressed activities in the area of impact dynamics. Workshop attendees represented NASA, the Army and Air Force, the Lawrence Livermore and Sandia National Laboratories, the aircraft and automotive industries, and academia. The workshop objectives were to assess the state-of-technology in the numerical simulation of crash and to provide guidelines for future research.				
14. SUBJECT TERMS Crashworthiness; Computational methods; Impact analysis; Software systems		15. NUMBER OF PAGES 281		
		16. PRICE CODE A13		
17. SECURITY CLASSIFICATION OF REPORT Unclassified	18. SECURITY CLASSIFICATION OF THIS PAGE Unclassified	19. SECURITY CLASSIFICATION OF ABSTRACT Unclassified	20. LIMITATION OF ABSTRACT	